Tracing soil carbon and nitrogen cycling in arbuscular and ectomycorrhizal systems

Dissertation

Saskia Klink

Tracing soil carbon and nitrogen cycling in arbuscular and ectomycorrhizal systems

Dissertation

Saskia Klink

Tracing soil carbon and nitrogen cycling in arbuscular and ectomycorrhizal systems

Dissertation

Zur Erlangung des akademischen Grades

einer Doktorin der Naturwissenschaften (Dr. rer. nat.)

an der Fakultät für Biologie, Chemie und Geowissenschaften

der Universität Bayreuth

vorgelegt von

Saskia Klink

Aus Essen (Nordrhein-Westfalen)

Bayreuth, 2021

Die vorliegende Arbeit wurde in der Zeit von Januar 2018 bis Dezember 2021 in Bayreuth am Lehrstuhl Agrarökologie unter der Betreuung von Frau Junior-Professorin Dr. Johanna Pausch angefertigt.

Die Dissertation wurde von Juli 2018 bis September 2021 über ein Projekt (PA 2377/2-1) der Deutschen Forschungsgemeinschaft (DFG) gefördert.

Einreichung der Dissertation am: **20.12.2021**

Zulassung durch die Promotionskommission am: **26.01.2022**

Wissenschaftliches Kolloquium am: **05.08.2022**

Amtierender Dekan: Prof. Dr. Benedikt Westermann

Prüfungsausschuss:

JProf. Dr. Johanna Pausch (Gutachterin)

Prof. Dr. Tillmann Lüders (Gutachter)

Prof. Dr. Eva Lehndorff (Vorsitz)

Prof. Dr. Gerhard Gebauer

The illustrations given on the cover page and throughout this thesis are by Katrin Giesemann.

List of Content

List of Figures

Acknowledgements

First, I want to thank my supervisor *Johanna Pausch* for supporting my scientific career and the chance to work at her lab at the DFG funded project 'Towards a predictive understanding of how mycorrhizal types influence the decomposition of soil organic matter'. I'm grateful for the opportunity to establish a mycorrhizal analysis section at the department of Agroecology, the traveling to our partners in Bloomington and conferences.

Special thanks to *Philipp Giesemann*, whose professional expertise helped a lot in making sample management, data analysis, and manuscript writing successful, and to keep up my motivation during hard times. I'm grateful for the mental support and cheer-up activities that helped me stay on track!
I thank the members of the department of Agroecology for scientific exchange, and particularly *Ilse Thaufelder*, *Liu Qiong, Manal Dafalla,* and *Andreas Wild* for helping with technical challenges, experiment set-up, and analytical discussions.
Warm thanks to the team of the BayCEER Laboratory of Isotope Biogeochemistry, especially *Gerhard Gebauer*, *Carina Bauer*, *Petra Eckert*, *Christine Tiroch*, who not only provided technical expertise but were always a place to come down, find support and have a nice coffee break. I want to thank *Stefan Bindereif* and *Franziska Zahn* for long discussions on scientific practice, statistics, but also career plans and leisure time events.

Big thanks to our collaborators at Phillips lab at Indiana University, in particular *Rich Phillips*, *Adrienne Keller*, *Elizabeth Huenupi Pena*, *Matthew Craig,* and *Katie Beidler*. I felt welcome from the first moment we met, and I enjoyed my time in Bloomington so much! I highly appreciate all your technical and scientific support, the farmers' market visits, and the soup and Thanksgiving parties! Special thank you to Adrienne – you have become such a good friend, and I don't want to miss you in my life! I thank the students *Timo Hubmann*, *Cara Meyer*, *Tina Köhler* for their help extracting hyphae, growing fungi in microcosms, watering plants, and preparing samples for analyses.

Further, I'm happy for the support of *Mechthild Kredler* for helping with staining approaches, *Laura Skates* for proofreading, native speaker expertise and mental support, *Sofia Gomes* for DNA analyses and outlooks to new approaches, *Oliver Otti* for instruction to the autoclave and laminar flow at the department of animal ecology, *Merissa Saric* and *Alexander Guhr* for working with me through the first trial for the microcosms. I'm grateful to the team of the mycology department of the Université Louvain la Neuve for the opportunity to get a person-to-person training on AM culture, *Ronald Kerner,* and *Stephen Russell* for help with the identification of the fungi sampled in the USA, and to *Mark Brundrett* for feedback on fungal hyphae figures and methodological proceedings.

Finally, I thank the DFG for funding the project I worked on and the University of Bayreuth Graduate School for offering financial support and advanced training opportunities. For anyone I forgot to mention here, thank you for your support during this journey.

Big thank you to my dad, who always supported me and is always there for me!

"*I thought a forest was made up entirely of trees, but now I know that the foundation lies below ground, in the fungi*"

Derrick Jensen

Summary

The plant-soil-microbe system trades carbon (C) and nutrients and drives the storage or release of these compounds. The intimacy of mycorrhizal fungi with plants supports plant nutrient supply, contributes to soil organic matter (SOM) decomposition and formation. Dominant fungal guilds in temperate systems are arbuscular mycorrhizal (AM), ectomycorrhizal (ECM), and saprotrophic (SAP) fungi. While their disparate nutrient acquisition strategies affect nutrient cycling, SOM formation, and C and nutrient storage of the system, impacts of different fungal guilds on these processes remain obscure.

Climate change will greatly affect plant-soil-microbe interactions. Increasing atmospheric carbon dioxide (CO_2) enhances photosynthesis, simultaneously aggravating nutrient limitation and competition. Subsequently, changed environmental conditions favor invasive species spread, with unknown consequences for nutrient cycling dynamics.

This thesis investigates (i) the role of different fungal guilds on C and nutrient cycling and SOM formation, (ii) the potential of different fungi for nutrient acquisition, and (iii) how impacts of climate change like elevated CO_2 levels or plant invasion affect the plant-microbe-soil systems' C and nutrient cycling dynamics.

Stable isotopes possess source and process information, allowing to trace the origin and the fate of compounds in a system. This information was unknown for AM hyphae, thus in **manuscript 1** a method to determine AM hyphal isotopic signatures was developed. AM hyphal ^{13}C and ^{15}N separated them from plant tissues and soil. A mixed C source of plant carbohydrates and lipids was deciphered, contrasting with current knowledge on the C-source of ECM fungi.

Manuscript 2 used the application of manuscript 1 to analyze the contribution of fungal inputs to specific SOM fractions. Forest plots with dominant tree species associated with ECM or AM fungi were chosen. Main contributions of ECM fungi to stable SOM were predicted in ECM systems, and SAP fungi as major contributors in AM systems, the latter due to activation *via* AM exudates. The combination of a Bayesian Inference Stable Isotope Mixing model with amino sugar analyzes showed that particulate organic matter fractions were dominated by plant and SAP inputs for both tree species. More stable mineral-associated organic matter was dominated by SAP followed by ECM inputs irrespective of tree species. These findings highlight fungal inputs as dominant source of stable organic matter and a need to consider fungal communities for efforts to increase long-term soil C storage.

Manuscript 3 investigated the degradative and nutrient trading potential of ECM fungi and sought to determine nitrogen (N) fractionations in the mycorrhizal nutrient trading. In microcosms, the trading of soil N to *Pinus sylvestris* was investigated for *Paxillus involutus* and *Pisolithus arhizus* with greater enzymatic repertoire relative to *Laccaria laccata* and *Laccaria bicolor* with lower degradative capability. Plant biomass was increased due to colonization by *P. involutus*, *P. arhizus,* and *L. laccata* but not by *L. bicolor*. Under N-limited conditions, *P. involutus* and *P. arhizus* tended to trade ^{15}N-enriched N. *Laccaria* species differed in degradative capabilities and plant benefit. The results highlight the impact of disparate fungal species on SOM decomposition and a need to consider fungal community composition to predict nutrient cycling dynamics. Thus, manuscript 3 supports different ECM fungi varying in their efficiency in accessing nutrients *via* SOM decomposition and contributing to stable SOM *via* fungal inputs.

Climate change impacts may affect the dynamics of plant-soil-microbe systems' C and nutrient trading and storage. Invasive plant species benefit from conditions allowing spread and reproduction, dominating over native species. Despite threats by increased litter input rates and a preference to invade AM-associated systems, the magnitude and direction of invasive plant effects on AM- or ECM-systems are obscure. **Manuscript 4** investigated the effect of invasive C_4 grass *Microstegium vimineum* on SOM turnover in tree stands with AM- or ECM-association. Invasion by *M. vimineum* increased decomposition of SOM under ECM-associated trees but decreased decomposition under AM-associated trees. These results highlight the potential of invasive plant species to modify SOM decomposition and that despite more SOC in ECM topsoils, this C is more easily lost under changing environmental conditions.

Impacts of nutrient limitation and plant-microbe competition under elevated CO_2 were analyzed in **manuscript 5**. Elevated CO_2 often results in growth benefits of plants and microbes but simultaneously aggravates nutrient limitation. Plants with varying microbial interactions to acquire nutrients were grown at ambient *vs.* elevated CO_2 to evaluate trading of N from ^{15}N labeled litter. Despite different microbial interactions to acquire nutrients, plants equally benefitted more from soil nutrients than soil microbes under elevated CO_2. These results highlight the need to consider ecosystem constituents as interwoven when discussing measures to decelerate the impacts of climate change.

Overall, this thesis highlights the need to consider mycorrhizal fungi for predicting ecosystems' C and N cycling and storage patterns, and for developing plans to adapt environments for changing conditions.

Zusammenfassung

Das Pflanze-Mikroben-Boden-System zirkuliert Kohlenstoff (C) und Nährstoffe und beeinflusst die Speicherung oder Freisetzung dieser Stoffe. Die Verbindung mit Mykorrhizapilzen verbessert den pflanzlichen Nährstoffbezug und trägt zu Abbau und Bildung organischer Bodensubstanz (OBS) bei. Dominate Pilzgruppen in temperaten Zonen sind arbuskuläre (AM) und ekto-Mykorrhiza (ECM) sowie saprotrophe (SAP) Pilze. Obwohl deren unterschiedliche Strategien zum Nährstoffgewinn Nährstoffkreislauf, -speicherung und OBS-Bildung beeinflussen, ist der Einfluss einzelner Pilzgruppen auf diese Prozesse unklar.

Der Klimawandel hat großen Einfluss auf Pflanze-Mikroben-Boden-Interaktionen. Steigendes atmosphärisches Kohlendioxid (CO_2) verbessert die Photosynthese, verstärkt dabei aber Nährstofflimitierung und Konkurrenz. Veränderte Umweltbedingungen fördern die Ausbreitung invasiver Arten mit unbekannten Folgen für Dynamiken des Nährstoffkreislaufes.

Diese Arbeit untersucht (i) die Rolle unterschiedlicher Pilzgruppen für den C und Nährstoffkreislauf und die Bildung von OBS, (ii) das Nährstoffbezugspotenzial verschiedener Pilze, und (iii) wie Klimawandelfolgen, wie erhöhtes CO_2 oder Pflanzeninvasionen, die Dynamiken von C und Nährstoffkreislaufen beeinflussen.

Stabile Isotope beinhalten Quellen- und Prozessinformationen, womit der Ursprung und der Verbleib von Komponenten in einem System verfolgt werden kann. Diese Informationen waren für AM-Hyphen unbekannt, sodass in **Manuskript 1** eine Methode zur Bestimmung der Isotopensignatur von AM-Hyphen entwickelt wurde. Die ^{13}C- und ^{15}N-Signatur der AM-Hyphen trennte diese von Pflanzen und Boden. Es wurde eine gemischte C-Quelle aus pflanzlichen Kohlenhydraten und Lipiden entschlüsselt, die im Gegensatz zum derzeitigen Wissen über die C-Quelle von ECM-Pilzen steht.

Manuskript 2 nutzte die Anwendung aus Manuskript 1 zur Analyse der Beiträge pilzlicher Einträge zu spezifischen OBS-Fraktionen. Für Plots mit ECM-assoziierten Bäumen wurde ein dominanter Beitrag von ECM-Pilzen zur stabilen OBS vorhergesagt, für AM-assoziierte ein dominanter Beitrag von SAP-Pilzen, aktiviert durch Exsudate von AM-Pilzen. Die Kombination eines Bayes'schen Mischungsmodells für stabile Isotope mit Aminozuckeranalysen zeigte dominante Einträge von Pflanze und SAP-Pilzen zur partikulären OBS für beide Bäume. Stabilere, mineralassoziierte OBS war für beide Bäume von SAP- und ECM-Pilzeinträgen bedingt. Dies zeigt die Bedeutung pilzlicher Quellen für stabile OBS und die Notwendigkeit Pilzgemeinschaften für Langzeitkohlenstoffspeicherung in Boden zu berücksichtigen.

Manuskript 3 untersuchte das Abbau- und Nährstofftransferpotenzial von ECM-Pilzen, sowie Stickstoff (N-)Fraktionierungen im Mykorrhiza-Nährstofftransfer. Der Transfer von Boden-N zu *Pinus sylvestris* wurde für *Paxillus involutus* und *Pisolithus arhizus* mit größerer Abbaukapazität relativ zu *Laccaria laccata* und *Laccaria bicolor* mit geringerer Abbaufähigkeit untersucht. Pflanzenbiomasse nahm unter *P. involutus*, *P. arhizus* und *L. laccata* zu, nicht aber mit *L. bicolor*. Unter N-limitierten Bedingungen nutzten *P. involutus* und *P. arhizus* ^{15}N-angereicherten N. Die *Laccaria*-Arten unterschieden sich in Abbaufähigkeiten und Pflanzenvorteilen. Die Ergebnisse verdeutlichen den Einfluss unterschiedlicher Pilze auf den OBS-Abbau und die Notwendigkeit, Pilzgemeinschaften für Vorhersagen zu Nährstoffdynamiken zu berücksichtigen. Somit bestätigt Manuskript 3, dass unterschiedliche ECM-Pilze in ihrer Effizienz Nährstoffe aus OBS Abbau zu beziehen und mit Einträgen zu stabiler OBS beizutragen variieren.

Klimawandelfolgen beeinflussen die Nährstofftransfer- und Speicherungsdynamiken in Pflanze-Mikroben-Boden-Systemen. Invasive Pflanzen nutzen vorteilhafte Bedingungen zur Ausbreitung. Trotz Einflüssen durch erhöhten Streueintrag oder die vermehrte Invasion in AM-Systeme ist das Ausmaß der Effekte invasiver Pflanzen auf AM- und ECM-Systeme unklar. **Manuskript 4** untersuchte Effekte des invasiven C_4 Grases *Microstegium vimineum* auf AM- oder ECM-Bäume. Die Invasion mit *M. vimineum* erhöhte den OBS-Abbau bei ECM-Bäumen, verminderte ihn aber bei AM-Bäumen. Diese Ergebnisse zeigen das Potenzial invasiver Arten den OBS-Abbau zu beeinflussen, und dass trotz eines höheren Boden-C-Gehaltes in ECM Oberböden dieses C leichter bei veränderten Umweltbedingungen verloren geht.

Der Einfluss von Nährstoffmangel und Konkurrenz zwischen Pflanze und Mikrobe unter erhöhtem CO_2 wurde in **Manuskript 5** untersucht. Erhöhtes CO_2 führt oft zu Wachstumsvorteilen von Pflanzen und Mikroben, gleichzeitig aber auch zu Nährstoffmangel. Pflanzen mit unterschiedlichen mikrobiellen Interaktionen zum Nährstoffgewinn wuchsen unter unverändertem und erhöhtem CO_2, um den Transfer von N aus ^{15}N-angereicherter Streu zu verfolgen. Trotz unterschiedlicher Interaktionen profitierten die Pflanzen unter erhöhtem CO_2 mehr von Bodennährstoffen als die Bodenmikroben. Diese Ergebnisse zeigen, dass die Vernetzung in Ökosystemen bei Maßnahmen zur Verringerung von Klimawandelfolgen berücksichtigt werden muss.

Zusammenfassend unterstreicht diese Arbeit die Notwendigkeit, Mykorrhizapilze für Vorhersagen zum Umsatz und zur Speicherung von C und N in Ökosystemen, als auch für die Entwicklung von Plänen zur Steigerung der Ökosystemresilienz gegenüber veränderten Bedingungen, zu berücksichtigen.

Outline

Chapter 1 introduces

- The plant-fungi-soil system & the role of fungi
- Stable isotopes and fungi
- Carbon and nutrient fluxes in the plant-fungi-soil system
- Impact of the plant-fungi-association on soil organic matter
- Impacts of climate change on nutrient cycling and soil organic matter dynamics
- Tracing carbon and nutrient fluxes and estimating inputs
- Objectives of this thesis

Chapter 2 presents the

- Main results
- Author contributions
- List of further publications
- References

Chapter 3 displays the

- Manuscripts of this thesis
- Declaration

Chapter 1

1 Introduction

1.1 The plant-fungi-soil system

An organism or a compartment such as the soil can never function and thrive entirely as a separate entity but is in an interplay with other partners and effectors (e.g., abiotic conditions) in its immediate environment. Consequently, a typical terrestrial ecosystem can be described as the coexistence of plants and microorganisms living in the soil, connected above it, and interacting in biotically and abiotically processes (Chapin *et al.*, 2002; Wittig & Streit, 2004; Sadava *et al.*, 2011). The close relationship and interdependence of plants, microorganisms, and the soil demand the consideration of all three actors if ecosystem processes and mechanisms are to be understood (Deyn *et al.*, 2008).

Plants rely on different strategies to acquire nutrients from the soil. A plant-own strategy is the establishment of a root system allowing for efficient nutrient uptake e.g., increased fine root production (Yanai *et al.*, 1995; Jackson *et al.*, 2009; Nie *et al.*, 2013; Piñeiro *et al.*, 2017) and exuding organic acids to access soil nutrients (Dakora & Phillips, 2002). Further, root exudation can **prime** soil microorganisms to mine for soil nutrients that can be taken up by the plant (Dakora & Phillips, 2002; Verbruggen *et al.*, 2017; Frey, 2019) or undergo a symbiotic association with microorganisms, e.g., rhizobia bacteria, mycorrhizal or endophytic fungi (Arnone & Gordon, 1990; Jumpponen, 2001; Temperton *et al.*, 2003; Smith & Read, 2008). The mycorrhizal association is common among the majority of vascular land plant species (Brundrett & Tedersoo, 2018).

Priming. Alteration of soil organic matter decomposition due to higher substrate availability for heterotrophic organisms.
A mechanism described for plant roots (root exudates) and root fungi (fungal exudates) attracting other organisms that mine for nutrients.

A mycorrhiza (Greek for *myces* – fungus and *rhiza* – root, first described by Frank (1885)) is the association of a plant root and a symbiotic fungus with the aim of a mutually beneficial cooperation (Smith & Read, 2008). Therefore, the plant partner shares up to 35% (Hobbie, 2006; Allen & Kitajima, 2014; Kaiser *et al.*, 2015; Ouimette *et al.*, 2020) of the photosynthetically derived carbohydrates with the symbiotic fungi living in and around its root system. The fungi can use this energy for growth, but also for scavenging and mining for nutrients displayed in scattered patches in the soil (Smith & Read, 2008). As hyphae are thinner (diameter ~3×10^{-4} cm; mostly 2-4 μm diameter) than roots (~200 times larger diameter, most delicate roots <0.5 mm diameter, root hairs 10 μm diameter) (Gashaw Deressa & Schenk, 2008; Smith & Read, 2008) they can access nutrients embedded in fine soil pores which would otherwise be inaccessible to the plant (Schack-Kirchner

et al., 2000; Ritz & Young, 2004). The nutrients are then shared with the plant partner in exchange for carbohydrates (Smith & Read, 2008). The mycorrhizal association allows the fungus to be independent from fixing its own carbon (C), while the plant is less limited in nutrient acquisition (Smith & Read, 2008; Brundrett & Tedersoo, 2018; Tedersoo *et al.*, 2020). Depending on the saprotrophic capabilities of the fungal partner and the soil nutrient availability, the plant may receive low molecular weight organic nutrients (e.g., amino acids) in addition to inorganic nutrients (Abuzinadah & Read, 1989; Marschner & Dell, 1994; Talbot *et al.*, 2008; Whiteside *et al.*, 2012; Hodge & Storer, 2015).

Four primary forms of mycorrhizal associations are known: (i) the arbuscular mycorrhiza (AM), the ectomycorrhiza (ECM), the ericoid mycorrhiza (ERM), and the orchid mycorrhiza (OrM) (Smith & Read, 2008; Brundrett & Tedersoo, 2018; Tedersoo *et al.*, 2020). While OrM is restricted to the plant partner from the Orchidaceae (Tedersoo *et al.*, 2020) and ErM to Ericaceae and Diaspensiaceae (Tedersoo *et al.*, 2020), ECM and AM are usually found in a broader variety of plant families (Brundrett & Tedersoo, 2018).

Ectomycorrhiza is common among woody plants and trees (Smith & Read, 2008; Brundrett & Tedersoo, 2018). Typical morphological features of ECM fungi include a hyphal sheath (mantle) around the plant root and a labyrinth-like hyphal structure in the root cortex, the Hartig net (**Figure 1**), which supports nutrient exchange with the plant partner (Berndt *et al.*, 1990; Smith & Read, 2008). ECM fungi can establish various types of hyphal exploration, from short to medium to long-distance exploration (Agerer, 2001; Peay *et al.*, 2011), and hyphal surfaces can be hydrophobic or hydrophilic (Lilleskov *et al.*, 2011; Chen *et al.*, 2019). These morphological features are linked to saprotrophic capabilities, such that hydrophilic, short-distance exploration types have lower saprotrophic capabilities and utilize labile C and nitrogen (N) compounds, while hydrophobic, longer distance exploration types have greater degradative capabilities allowing access to older, more stable soil organic matter (SOM) (Hobbie *et al.*, 2012; Chen *et al.*, 2019). Having ancestors with highly saprotrophic capabilities, many ECM fungi possess the ability for enzymatic decay of organic material, though they are beyond the degradative capabilities of saprotrophic fungi (Lindahl & Tunlid, 2015; Martin *et al.*, 2016; Shah *et al.*, 2016). Saprotrophic ability varies across ECM fungal genera and species (e.g., Lindahl & Tunlid, 2015; Martin *et al.*, 2016; Shah *et al.*, 2016). Still, the extent to which these different saprotrophic abilities control patterns of nutrient cycling, decomposition and C and N storage remains largely obscure.

The arbuscular mycorrhiza is the most common mycorrhizal type with an association to ~72 to 78% of land plant species (Brundrett & Tedersoo, 2018; Tedersoo *et al.*, 2020), most of which are vascular (Brundrett & Tedersoo, 2018; Tedersoo *et al.*, 2020). Typical morphological characteristics of AM fungi are vesicles and branching hyphae, the arbuscules, and hyaline hyphae without septa (Smith & Read, 2008). The AM fungi penetrate the plant root cells **(Figure 1)**, and the arbuscules in the plant root cell are the location of most efficient C for nutrient exchange (Smith & Read, 2008). The degradative capabilities of AM fungi are considered limited (e.g., Read & Perez-Moreno, 2003; Hodge & Fitter, 2010; Welc *et al.* 2014; **Box 1**). The extraradical mycelium of AM fungi often has lower biomass than that of ECM fungi, although there is considerable variation between different genera and species of AM fungal mycelium biomass (Read & Perez-Moreno, 2003; Leigh *et al.*, 2009; Chen *et al.*, 2016; Cheng *et al.*, 2016). The most notable difference to ECM fungi is the absence of easily visible, aboveground sporocarps for AM fungi. Sporocarps of AM fungi grow hypogaeic (= below ground) and have rarely been analyzed (Jobim *et al.*, 2019). Instead, spores, specific biomarkers (e.g., phospholipid/neutral lipid fatty acids (PLFAs/NLFAs), or hyphae may serve as surrogates for AM fungal tissues (Allen & Allen, 1990; Nakano *et al.*, 1999; Courty *et al.*, 2011; Walder *et al.*, 2012; Walder *et al.*, 2013; Courty *et al.*, 2015; Suetsugu *et al.*, 2020).

Box 1: Saprotrophic capabilities of AM fungi

The potential of AM fungi to saprotrophically access nutrients from organic matter is primarily considered to be very limited (Read & Perez-Moreno, 2003; Hodge & Fitter, 2010; Welc *et al.*, 2014). This assumption results in particular from the absence of genes necessary for the production of cell wall-degrading enzymes in *Rhizophagus irregularis* (Tisserant *et al.*, 2013). Still, genes for reduction and uptake of nitrite and sulfite were preserved in the genome, allowing for accessing and utilizing mineral soil nutrients (Tisserant *et al.*, 2013).

While the primary function of AM fungi in a mycorrhiza has been seen in the provision of immobile phosphate from areas to which the plant has limited uptake efficiency (root depletion zone), an increase in SOM decomposition in the presence of AM fungi was documented (Hodge *et al.*, 2001). At patches of organic material AM hyphae activate, prime, saprotrophic organisms *via* exudation to decompose SOM, providing a nutritional benefit to the associated plant partner (*cf.* Hodge *et al.*, 2001; Leigh *et al.*, 2009).

Nevertheless, studies that uncovered hydrolytic capabilities of AM fungi in terms of accessing organic phosphorous (Joner & Johansen, 2000; Koide & Kabir, 2000) encourage a closer look at the saprotrophic capabilities of AM fungi also in relation to other nutrients such as N from soil (*cf.* Burke *et al.*, 2011).

1.2 The role of fungi in ecosystems

The biomass produced by plants and animals contains energy and nutrients which are recycled through the soil after the senescence or death. Alongside microorganisms such as bacteria, many fungi fulfill a fundamental function as nutrient recyclers in ecosystems (Kjoller & Struwe, 2002; Leake *et al.*, 2003; Boer *et al.*, 2005; Lindahl & Tunlid, 2015; Martin *et al.*, 2016). To degrade and decompose organic material, fungi employ a variety of mechanisms, such as **Fenton chemistry**, **enzymatic oxidation**, or the activation of **saprotrophic** microorganisms (priming) (Kjoller & Struwe, 2002; Lindahl & Tunlid, 2015; Verbruggen *et al.*, 2017; Frey, 2019). Roughly, terrestrial fungi can be divided into plant-associated mycorrhizal fungi and free-living saprotrophic (SAP) fungi (Lindahl & Tunlid, 2015). These groups vary in their relationship to neighboring plants, C and nutrient acquisition strategies, and degradative capabilities (Lindahl & Tunlid, 2015; Martin *et al.*, 2016; Brundrett & Tedersoo, 2018; Tedersoo & Bahram, 2019).

Fenton chemistry. Non-enzymatic reaction in e.g. *Paxillus involutus* fungi involving ferrous ions (Fe^{2+}) and hydrogen peroxide. Radicals formed introduce the depolymerization of lignocellulose.

Enzymatic oxidation. Enzyme reaction enabling molecules to increase their oxidative state through the loss of electrons of the ions or atoms involved. The chemical reaction is typical for white-rot fungi.

Saprotroph. A heterotrophic organism utilizing dead organic material as a nutrient source.

In contrast to mycorrhizal fungi, SAP fungi are independent of a plant partner and access both C and nutrients *via* their own degradative capabilities (Eichlerová *et al.*, 2015; Martin *et al.*, 2016). They possess a broad spectrum of enzymes and degrade complex compounds such as lignin, chitin, or cellulose (Grinhut *et al.*, 2007; Baldrian, 2008). The extensive mycelium often follows a niche separation with ECM fungi to reduce competition for the same nutrients. Therefore, SAP fungi predominate in the upper soil layer, while ECM fungi occupy a predominant niche in deeper mineral soil layers (Lindahl *et al.*, 2007; Clemmensen *et al.*, 2013). Similar to ECM fungi, SAP fungi produce sporocarps (mostly epigaeic, above ground) for reproduction. Since SAP fungi are a broad group that includes parasitic fungi, sporocarps and mycelium can be found on different substrates, for example soil, litter, leaves, and wood tissues of dead and living plants (Lewis, 1973; Gebauer & Taylor, 1999).

Depending on the biome the actors of the plant-microorganism-soil system occur in, the plant and fungal members can vary greatly. In boreal forests, typically conifers associate with ECM or ericoid mycorrhizal fungi (Read, 1991; Soudzilovskaia *et al.*, 2019; Tedersoo *et al.*, 2020). In temperate zones coniferous and/or deciduous, broadleaf trees associated with ectomycorrhizal or arbuscular mycorrhizal fungi (**Figure 1**) predominate (Read, 1991; Chapman *et al.*, 2006; Phillips *et al.*, 2013; Soudzilovskaia *et al.*, 2019; Tedersoo *et al.*, 2020). Trees associated with AM fungi are dominant in tropical forests, promoting presence of soils with high inorganic nutrients (Waring *et al.*, 2016; Soudzilovskaia *et al.*, 2019; Tedersoo *et al.*, 2020). Accordingly, different processes and

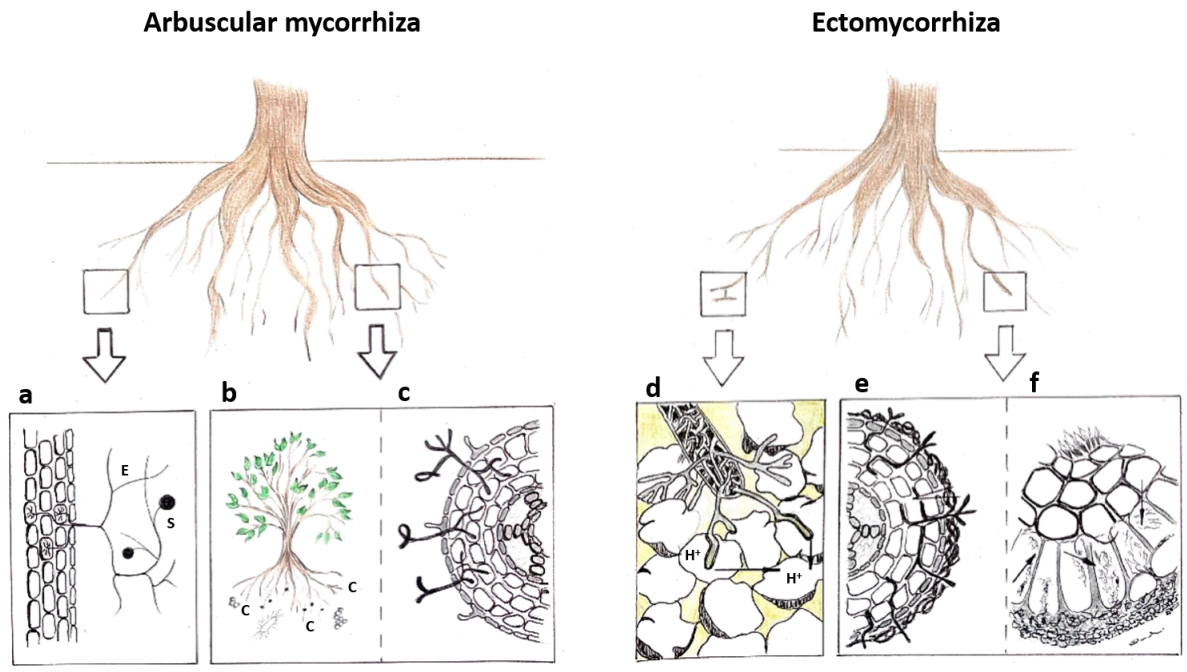

Figure 1: Characteristic features of arbuscular and ectomycorrhiza. (a) Arbuscules in the plant root cells and extraradical mycelium (E) with spore (S). (b) Plant-derived C is channeled to AM fungi which activate saprotrophs via priming. (c) AM hyphae penetrate plant root cells. (d) Hyphal sheath around root tips and hyphae release acids and enzymes for decomposition of OM. (e) Hyphal sheath around root and hyphae do not penetrate plant root cells. (f) Hartig net (arrows). Drawings c, d and e modified and aligned from Landeweert et al. (2001). Drawing by Katrin Giesemann.

mechanisms of C and nutrient cycling prevail in each of these plant-microorganism-soil systems (Waring *et al.*, 2016; Soudzilovskaia *et al.*, 2019).

Even within a given biome, different plant types and their association with certain fungi influence patterns of nutrient cycling and soil C storage (Chapman *et al.*, 2006; Phillips *et al.*, 2013; Goodale, 2017; Craig *et al.*, 2018; Zhang *et al.*, 2018). These different plant-fungi-associations often result in distinct nutrient cycling economies based on the type of mycorrhizal interaction, framed as Mycorrhizal-Associated-Nutrient-Economy (MANE) by Phillips *et al.* (2013) (**Figure 2**, **Box 2**). Based on longitudinal studies and regular analyses of a wide range of ecosystem parameters, such as leaf litter quality, enzyme activities, or patterns of root exudates (Midgley & Phillips, 2014; Midgley *et al.*, 2015; Midgley & Phillips, 2016; Cheeke *et al.*, 2017; Keller *et al.*, 2021), an organic nutrient economy has been described and supported for ECM-associated systems. In contrast, AM-associated systems exhibit an inorganic nutrient economy (Chapman *et al.*, 2006; Phillips *et al.*, 2013) (**Box 2**) and high rates of mineralization and leaching (Phillips *et al.*, 2013). Given predicted future climate change impacts, a shift towards a dominance of AM-associated trees in temperate zones is likely (Jo *et al.*, 2019), with far-reaching consequences for nutrient cycling processes and soil C storage (Phillips *et al.*, 2012; Phillips *et al.*, 2013; Jo *et al.*, 2019).

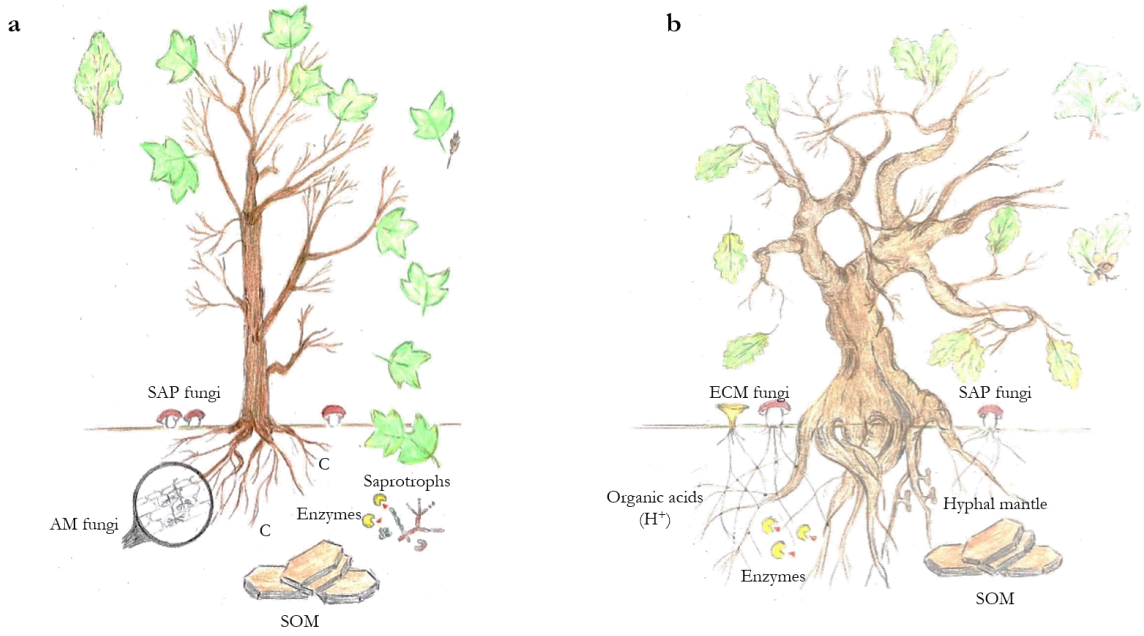

Figure 2: MANE framework (cf. Phillips et al. 2013) illustrated for Liriodendron tulipifera (a, AM-associated tree) and Quercus alba (b, ECM-associated tree). In the AM-system, an open, inorganic nutrient cycling occurs due to the presence of high quality leaf litters and the priming of saprotrophic organisms via AM fungi to degrade SOM. A rapid transformation of organic N to inorganic N by saprotrophs, accompanied by high rates of mineralization, nitrification and N leaching occurs. In the ECM-system, a closed, organic nutrient cycle occurs, with ECM and SAP fungi decomposing SOM and competing for nutrients. The release of enzymes and organic acids favours decomposition, but also competitive potential. Drawing by Katrin Giesemann.

1.3 Stable isotopes and fungi

Isotopic fractionation. The isotopic fractionation is given as α, i.e., the difference of the isotope ratio between the product and the educt.

An isotope (Greek *isos* = equal, *topos* = place) is an element/atom with an equal number of protons but an unequal number of neutrons in its atomic core (Fry, 2006). Thus, the element has different masses and accordingly can be lighter or heavier. The chemical behavior of the different isotopes is, nevertheless, almost similar (Fry, 2006). Around 283 isotopes are stable (Fry, 2006), and do not undergo radioactive decay, in contrast to radioactive isotopes. The most common isotopes used in ecology are those of carbon (^{13}C, ^{12}C, ^{14}C as radioactive variant), nitrogen (^{15}N, ^{14}N), hydrogen (^{2}H, ^{1}H), oxygen (^{18}O, ^{16}O,^{17}O), and sulfur (^{32}S, ^{33}S, ^{34}S, ^{36}S) (Fry, 2006).

Though being the same element with similar chemical properties, the light isotopes, those with a smaller number of neutrons, tend to differ from the heavy isotopes, those with a higher number of neutrons, in their reaction time. Lighter isotopes and those with an equal number of neutrons mostly have a shorter reaction time than the heavier isotopes and those with an unequal number of neutrons (Fry, 2006). This results in a shift of the naturally occurring equilibrium between the ratio of heavy and light isotopes during reactions (Fry, 2006). The light isotopes react faster so that

the heavy isotopes remain in the educt due to their slower reaction time. Depending on the system, this **isotopic fractionation** results in a different ratio of light to heavy isotopes in the product compared to the educt (open system) or equilibrates with time of the process (closed system) (Fry, 2006). Specific processes in nature result in an enrichment with heavy isotopes, like a heterotrophic mode of nutrition (**Box 3**) (DeNiro & Epstein, 1978, 1981).

The stable isotope signature of a fungus results from its source of C and nutrient supply (= source information) and the process for using these C and nutrient sources (= process information) (Fry, 2006) (**Box 4**). For mycorrhizal fungi, such as AM or ECM fungi, C supply is guaranteed by the associated plant partner (Smith & Read, 2008; Veresoglou *et al.*, 2012). Photosynthetically produced carbohydrates are transported to the fungus, where they are more ^{13}C enriched compared to those found inside plant leaves (Gleixner *et al.*, 1993; Kohzu *et al.*, 1999). In addition, the form of C further determines the ^{13}C enrichment. Carbohydrates are more ^{13}C enriched than lipids (Gleixner *et al.*, 1993) so that the gain of a mixture of carbohydrates and lipids by AM fungi (Jiang *et al.*, 2017; Keymer *et al.*, 2017; Luginbuehl *et al.*, 2017; Rich *et al.*, 2017) results in their more depleted ^{13}C signature relative to ECM fungi (Klink *et al.*, 2020). Saprotrophic fungi on the other hand, independent from plant photosynthates, gain their C from the decay of e.g., wood or litter rich in ^{13}C enriched cellulose (Gleixner *et al.*, 1993; Kohzu *et al.*, 1999; Chen *et al.*, 2019).

The nitrogen isotopic signature is, in large part, determined by the nutrient source of the fungus, its foraging niche, and whether it shares the nitrogen with a plant partner or not (Gebauer & Taylor, 1999; Lindahl *et al.*, 2007; Hobbie & Högberg, 2012; Högberg *et al.*, 2020). Fungi with saprotrophic capabilities such as SAP fungi and many ECM fungi can access ^{15}N enriched N *via* enzymatic and oxidative decay (Hobbie & Högberg, 2012; Frey, 2019). In contrast, AM fungi are thought to largely lack saprotrophic capabilities and thus rely on the same ^{15}N depleted N sources as many plants (Read & Perez-Moreno, 2003; Field & Pressel, 2018). Plant-associated fungi share the N scavenged with their plant partner. The fungi tend to keep the majority of the organic, ^{15}N enriched N necessary for growth and biomass preservation, while the cheaper ^{15}N depleted N is transported to the plant partner (Gebauer & Dietrich, 1993; Hobbie & Högberg, 2012). This leads to ECM fungi often being more ^{15}N enriched than SAP fungi, though both can saprotrophically access ^{15}N enriched N sources. Niche separation of ECM (deeper soil layers) and SAP fungi (upper soil layers) further drives ^{15}N patterns (Lindahl et al., 2007; Clemmensen et al., 2013).

Box 2: MANE framework & implications on SOM decomposition

The capability of ECM and AM fungi to decompose leaf litter and provide nutrients impacts the forms of nutrients cycled in the associated systems, conceptualized in the Mycorrhiza-Associated Nutrient Economy (MANE) framework (Phillips *et al.*, 2013). ECM fungi can access both an inorganic and organic nutrient pool *via* hydrolytic and oxidative exo-enzymes. *Via* these enzymes, ECM fungi can further contribute to mineral weathering (e.g., Jongmans *et al.*, 1997; van Schöll *et al.*, 2008) and access mineral-associated organic matter (OM). Conversely, AM fungi with little saprotrophic capabilities mainly take up inorganic nutrients released by saprotrophic organisms that they activate *via* C-rich exudates (Kohzu *et al.*, 1999; Read & Perez-Moreno, 2003; Cheng *et al.*, 2012; Tisserant *et al.*, 2013; Kaiser *et al.*, 2015; Verbruggen *et al.*, 2017).

These distinct nutrient acquisitions of ECM and AM fungi have consequences for the system's entire nutrient cycling and economy. Leaf litters of AM-associated plants tend to possess a lower C:N ratio (Phillips *et al.*, 2013; Midgley *et al.*, 2015) and to decompose faster compared to ECM-plant leaf litters with a higher C:N ratio and slower decomposition (e.g., Cornelissen *et al.*, 2001; Read & Perez-Moreno, 2003; Midgley *et al.*, 2015). The presence of a thick organic layer in ECM-associated systems combined with higher soil acidity in the surface layer contributes to higher dissolved organic C and organic N to inorganic N ratios (Phillips *et al.*, 2013).

Based on these processes and mechanisms, an inorganic nutrient economy is described for AM-associated systems, while for ECM-associated systems an organic nutrient economy occurs (Figure 2). The AM-inorganic nutrient economy is represented by the litter (leaves, roots, hyphae) of high quality (Phillips *et al.*, 2013), allowing the saprotrophic community to convert organic to inorganic N rapidly and promote nitrification and leaching (Phillips *et al.*, 2013). In ECM-associated systems the slower turnover of the litter, competition between ECM and SAP fungi for nutrients, and the acidification potential of plant litter (Finzi *et al.*, 1998; Reich *et al.*, 2005) support the presence of organic nutrients (Phillips *et al.*, 2013).

As litter quality is a controlling factor of the formation of SOM and SOM fractions, the fast turnover, high-quality litter of AM-associated plants favors the creation of mineral-associated organic matter (MAOM) over particulate organic matter (POM) (Cotrufo *et al.*, 2013; Cotrufo *et al.*, 2019; Lavallee *et al.*, 2020) in topsoils due to increased production of microbial residues. Conversely, ECM-associated systems favor the formation of POM over MAOM (Cotrufo *et al.*, 2013; Cotrufo *et al.*, 2019) in topsoils. Craig *et al.* (2018) could further show a depth influence in the amount of SOM for ECM- and AM-associated systems. While more SOM was present in ECM-topsoils relative to AM-topsoils, more SOM occurred in AM soils to a depth of 1 m relative to ECM soils (Craig *et al.*, 2018).

1.4 Carbon and nutrient fluxes in the plant-fungi-soil system

Within the plant-fungi-soil system, roots and hyphae are major routes for the transfer of carbon and nutrients from one member of the system to another (Gill & Finzi, 2016; Frey, 2019; Vidal *et al.*, 2021). One route by which C enters the system is when atmospheric CO_2 is utilized by plants during photosynthesis and transformed into compounds for nutrition (e.g., sugars), storage (e.g., lipids) or tissue construction (e.g., cellulose) (Gleixner *et al.*, 1993). Metabolized carbohydrates are transported to the roots, where they can enter the **rhizosphere** and soil (Kuzyakov *et al.*, 2000; Cheng & Kuzyakov, 2005; Keiluweit *et al.*, 2015) or to hyphae of mycorrhizal fungi which serve as transport pathways for the carbohydrates to more distant soil regions and into fine soil pores (Frey, 2019). Apart from utilizing the C for growth and production of metabolites (e.g., enzymes), fungi can release a certain proportion of C into the soil, aiming to facilitate the activation of saprotrophic soil organisms (Toljander *et al.*, 2007; Verbruggen *et al.*, 2017; Frey, 2019). This priming can support microbial activity and thus the scavenging for and mobilization of nutrients in the soil, which in turn can be taken up by mycorrhizal fungi and plant species in the system (Hodge *et al.*, 2001; Toljander *et al.*, 2007; Leigh *et al.*, 2009).

Rhizosphere. The zone impacted by a living plant root through chemical, physical, or biological processes in soil. It represents an interaction zone of plants, microorganisms, and soil. The environmental conditions can differ from the surroundings. Organisms are primarily attracted by easily available carbon in this zone.

Box 3: Heterotrophy

Heterotrophy (greek *heteros* = different and *trophé* = nutrition) describes the nutrition of an organism from existing organic compounds by the breakdown of these compounds for their energy supply and the creation of tissues or endogenous substances (Sadava *et al.*, 2011; Wittig & Streit, 2004).

Members of heterotrophic organisms are animals, fungi, most bacteria, archaea, and certain plant species. Ecologically, heterotrophs are consumers in contrast to autotrophs as producers (Sadava *et al.*, 2011; Wittig & Streit, 2004). The nutrition of heterotrophs can be plant-based, carnivorous, or omnivorous. Particularly many fungi occupy an important ecological role as decomposers serving as sanitary police.

Producers and consumers form a nutritional network of different trophic levels depending on their nutrient sources. Stable isotope patterns of ^{13}C and ^{15}N have been shown to demonstrate the nutritional mode and trophic level of organisms (DeNiro & Epstein, 1978, 1981), and with the availability of a lower and an upper end member, the percentual nutrient gain of an organism can be calculated (Marshall & Ehleringer, 1990). Producers are the most depleted organisms in the trophic chain, and with each new trophic level a trophic enrichment of approximately 3 ‰ in ^{15}N and approximately 1.5 ‰ in ^{13}C occurs (DeNiro & Epstein, 1978, 1981; Post, 2002). That way, nutrition from sources of different trophic levels can be evaluated.

Initially originated from plant leaves, the leaf litter represents another pathway by which C and nutrients can enter the soil system (*cf.* Deyn *et al.*, 2008; Mikutta *et al.*, 2019; Frey, 2019). Leachates of dissolved organic matter (DOM) (Mikutta *et al.*, 2019; Frey, 2019) represent a valuable C source for microbes. The litter quality of leaves can be variable depending on the plant species it originated from, and degradability depends on the C:N and lignin:N ratio of the leaf tissues (Cornelissen *et al.*, 2001; Deyn *et al.*, 2008; Phillips *et al.*, 2013; Midgley *et al.*, 2015).

Brown rot fungi. A group of saprotrophic fungi capable to degrade plant cellulose using cellulase enzymes. The remaining lignin shapes cube-like textures and is responsible for the brown color of degraded plant tissue.

Similar to fungal-originated compounds, root exudates and residues can contribute to soil C inputs and storage while also solubilizing and mobilizing C and N bound to mineral surfaces *via* e.g., organic acids or hydrolytic enzymes (Jilling *et al.*, 2018; Angst *et al.*, 2021). Thus, stabilized SOM can hold two functions: (i) serving as an essential sink capturing large amounts of atmospheric CO_2 belowground, contributing a positive effect on climate change conditions, and (ii) acting as a source for C and N when being solubilized, remobilized and mineralized (Jilling *et al.*, 2018; Daly *et al.*, 2021).

White rot fungi. A group of saprotrophic agaricomycete fungi capable to degrade plant lignin using laccase enzymes alongside the degradation of cellulose and hemicellulose. Residuals shape defibrillated and white plant tissue.

Particularly SAP fungi are capable of releasing C and N from complex and recalcitrant plant tissues such as wood (Baldrian, 2008; Martin *et al.*, 2016). Typical wood decomposing fungi are **brown rot** and **white rot fungi** whose ability to access C from cellulose *via* enzymatic decay also largely impacts their stable isotope signature towards the ^{13}C enriched signature of the cellulose (Gleixner *et al.*, 1993). It has been suggested that some ectomycorrhizal fungi possess the ability to obtain some C from the decomposition of wood or litter as well (Zeller *et al.*, 2007). Still, it remains widely presumed that the dominant C source for mycorrhizal fungi derived from the plant partner (*cf.* Lindahl & Tunlid, 2015; Zak *et al.*, 2019).

1.5 Impact of the plant-fungi-association on soil organic matter

Organic material in soils, the SOM, represents the most extensive depository for C and N on earth (Batjes, 1996). SOM is composed of myriad organic compounds, which range in level of decay from largely undecomposed fresh plant litter to highly converted organic matter (Schmidt *et al.*, 2011; Lehmann & Kleber, 2015). In the progression of decay and the formation of SOM, organic components of different size, intricacy, and biodegradability are formed (Lützow *et al.*, 2007; Lehmann *et al.*, 2020; Angst *et al.*, 2021), and can exist as free particles or attach with mineral surfaces (*cf.* Lehmann & Kleber, 2015). Thus, the different genesis, chemical formulation, persistence, and function of these compounds lead to the emergence of distinct pools and fractions of organic matter (Golchin *et al.*, 1994; Lavallee *et al.*, 2020).

To evaluate the fate of C and N within the complex continuum of SOM, a separation of SOM into measurable fractions is required (Poeplau *et al.*, 2018). The distinction between particulate organic matter (POM) and mineral-associated organic matter (MAOM) is a valuable way to analyze differences in the storing of C and N and to draw comparisons of SOM dynamics between different systems and studies (Golchin *et al.*, 1994; Lavallee *et al.*, 2020).

Particulate OM is predominated by inputs of plant-originated, complex structural C compounds (Baldock & Skjemstad, 2000; Lavallee *et al.*, 2020; Angst *et al.*, 2021). Although a majority of POM is susceptible to degradation (Christensen, 2001; Lützow *et al.*, 2007; Cotrufo *et al.*, 2019), incorporation within aggregates and high chemical complexity (e.g., aromaticity, aliphaticity) of specific constituents can lead to high persistence of parts of POM (Mueller & Koegel-Knabner, 2009). Compared to POM, the MAOM fraction is primarily driven by microbial inputs (Kopittke *et al.*, 2018; Kopittke *et al.*, 2020), whose association to mineral surfaces reduces vulnerability to decay (Lützow *et al.*, 2007; Kögel-Knabner *et al.*, 2008; Poeplau *et al.*, 2018; Lavallee *et al.*, 2020). Nonetheless, plant-originated biomolecules such as litter leachates also add to MAOM (Mikutta *et al.*, 2019; Sokol & Bradford, 2019). As a result, recent studies point to a stronger consideration of plant contributions complementing microbial contributions to MAOM (e.g. Angst *et al.*, 2021).

Box 4: Source and process information

Stable isotope signatures possess information about the sources and processes of an organism or system. Changes in the isotopic composition can be predicted and used to identify mechanisms and the fate of compounds.

Process information is generated when physical or chemical reactions cause an isotopic fractionation (Fry, 2006). The difference in the frequency of isotopes between the substrate of the reaction and the product of the reaction provides information about the conditions of the reaction. Examples for process information gained by stable isotope applications are the different forms of plant photosynthesis, C_3, C_4, or CAM photosynthesis, where the activity of various enzymes results in different carbon isotopic signatures (Dawson *et al.*, 2002; Fry, 2006).

Source information allows drawing interferences from different isotopic frequencies of single ecosystem compartments or substrate classes about the origin (source) of single substances (Fry, 2006). This allows determining which substance is derived from which ecosystem compartment. An example of source information is the N signature of legumes derived from N fixation from the air in nodules compared to N sources from soil (Dawson *et al.*, 2002; Peoples *et al.*, 2015).

Despite distinct chemical and physical attributes, POM and MAOM fractions represent dynamic systems and are interconnected e.g., *via* fungal hyphae that serve as vectors for C and N transfers (*cf.* Vidal *et al.*, 2021). Plant-originated compounds can act as a starting point for MAOM formation (Witzgall *et al.*, 2021), and fungi active in POM fractions can contribute to the generation of MAOM with microbially converted products and fungal residues (e.g., Gleixner, 2013). Consequential, MAOM fractions are not as insusceptible to remobilization and mining attacks then could be assumed. Roots and the rhizosphere can remobilize and detach organic material from MAOM *via* exudate excretion (organic acids) and microbial priming, while fungi can liberate N from MAOM *via* enzymes (Jilling *et al.*, 2018; Daly *et al.*, 2021).

For this reason, MAOM can be both a sink for C and N through mineral associations and shielding of organic matter from microbial processing, as well as a source of C and N through remobilization processes. Owing to the low C:N ratio of MAOM (Lützow *et al.*, 2007; Cotrufo *et al.*, 2019) and a prevalence of microbial inputs, MAOM can be a valuable source of organic N for plants and microorganisms. It should be emphasized that the rate of mobilization and solubility is a function of the properties of minerals and soil, coupled with their interaction with microbes and MAOM at the respective site (Jilling *et al.*, 2018).

1.6 Impacts of climate change on nutrient cycling and SOM dynamics

The functioning and interplay of the plant-microbe-soil system is affected and threatened by changing conditions in conjunction with climate change, such as increasing atmospheric CO_2 levels, rising temperatures and resulting invasion by non-native plant species (e.g., Treseder, 2004; Cheng *et al.*, 2012; Liu *et al.*, 2017; Kuzyakov *et al.*, 2019). Both aboveground vegetation and belowground soil pools can remove and store CO_2 from the atmosphere, and particularly soils are a significant sink for C (Dixon *et al.*, 1994; Ainsworth & Long, 2005; Kuzyakov *et al.*, 2019). Whether this C remains stored in soil or is released to the atmosphere depends on the balance between C inputs from primary production and the outputs by SOM decomposition (Phillips *et al.*, 2012). Notably, the potential of C release from SOM *via* microbial decomposition depends not only on the level of atmospheric CO_2 but also on the system's nutrient availability (Treseder, 2004). While most often an increase in plant and fungal biomass in response to increasing concentrations of atmospheric CO_2 were observed (Sanders *et al.*, 1998; Treseder & Allen, 2000; Treseder, 2004; Alberton *et al.*, 2005; Drigo *et al.*, 2010), increased atmospheric CO_2 levels frequently cause a nutrient limitation on the plants' site (Oren *et al.*, 2001; Schlesinger & Lichter, 2001; Finzi *et al.*, 2002). This might become aggravating when the increased C supply from plants' site transferred to the fungal partner does not pay back in an increased nutrient transfer from fungi to plant, but the fungi become a sink for nutrients (Progressive Nutrient Limitation hypothesis, PNL) (Luo *et al.*, 2004; Johnson,

2006). However, several studies reported an increased N uptake with increasing CO_2 (summarized in Johnson, 2006), suggesting for N acquisition strategies supporting the N uptake under elevated CO_2 conditions.

A plant group often greatly benefitting from globalization and climate change conditions are invasive plant species (Liu *et al.*, 2017). Invasive or alien plant species are non-native plants introduced to habitats they did not occur in originally (Callaway & Aschehoug, 2000). In their new habitat, invasive plant species often occupy a growth and/or reproduction benefit over the native plant species, increasing the risk of out-competition of native plant species and related organisms (Callaway & Aschehoug, 2000). Moreover, due to their dominance in many habitats and often a production of fast decaying litter (Jo *et al.*, 2017) and exudate-accelerated SOM decomposition (Bradford *et al.*, 2012; Morris *et al.*, 2016), invasive plants can impact the soil microbial community (Sokol *et al.*, 2019), SOM C and N cycling and turnover processes (Liao *et al.*, 2008; Craig *et al.*, 2019).

With respect to contrasting mycorrhizal associations with ECM or AM fungi, it was shown that AM-associated systems tend to be more vulnerable to the invasion by non-native species relative to ECM-associated systems (Jo *et al.*, 2018). The facilitated spread of invasive plant species may be attributed to the higher litter quality and nutrient availability in AM-associated systems combined with a more favorable soil pH than in ECM-associated systems (Phillips *et al.*, 2013). Given the differences in plant invasion depending on the mycorrhizal-association of native plants and the effect of invasive plants on SOM dynamics, understanding the mechanisms and processes ongoing with plant invasion in systems with contrasting mycorrhizal association is indispensable.

2 Objectives of this thesis

This thesis aims to span a comprehensive perspective on the role of mycorrhizal fungi for C and nutrient trading in the plant-microbe-soil system. The role of plant and microbial inputs to SOM in systems with a distinct mycorrhizal association was investigated.

Therefore, **(1)** the stable isotope signature of AM hyphae as an active transfer site between plant and soil will be compared to frequently applied analyses of PLFAs/NLFAs (Manuscript 1). Hence, methods to isolate AM hyphae from roots and soil will be established or modified.

This information will **(2)** provide a vital missing data link of AM fungal tissue in a temperate deciduous forest in the USA, where C and N inputs from various sources to SOM fractions will be deciphered *via* a combined approach of stable isotope and amino sugar analyses (Manuscript 2). A Bayesian Inference Isotope Mixing Model will determine probabilities of the contributions of plant- and microorganism-derived inputs to SOM fractions.

Besides the effect of AM fungi on SOM, **(3)** the contribution of ECM fungi to SOM decomposition and nutrient provision will be revealed by analyzing the degradative capabilities of different ECM fungal species in a microcosm study (Manuscript 3). Further, the microcosm study aims to decipher N-fractionations between plant, fungi, and soil hardly measurable in the field, but essential for understanding N-cycling patterns in mycorrhizal fungi-associated systems on a detailed basis.

As the functioning and storage patterns of native AM *vs.* ECM systems can be affected when invasive species are introduced **(4)**, a CO_2 analysis priming study analyzed the vulnerability of SOM in AM *vs.* ECM systems to changing conditions due to the invasion by a non-native grass (Manuscript 4).

Elevated CO_2 levels due to climate change further affect the functioning of plant-microbe-soil systems **(5)** by impacting nutrient availability, cycling and decomposition. *Via* a climate control chamber experiment, the response of plants with different microbial interactions to acquire soil nutrients to elevated CO_2 conditions will provide insights into the profiteers and losers of climate change within the plant-microbe-soil system (Manuscript 5).

The manuscripts that this thesis comprises and their main aims are the following:

- **Manuscript 1** identifies the ^{13}C and ^{15}N stable isotope signatures of AM hyphae. It shows the necessity of stable isotope data of AM fungi, and relates the method of hyphae isolation to commonly applied estimates of spores, PLFAs and NLFAs.

- **Manuscript 2** adds the information on AM fungal isotopic signatures to identify the inputs from plant tissues and different microbial groups (AM and ECM fungi, SAP fungi, bacteria) to various SOM fractions. The combination of stable isotope data in a Bayesian Inference Isotope Mixing Model with amino sugar data provides insights into the fate of C and N from different sources to various POM and MAOM fractions.

- **Manuscript 3** takes a closer look at the capabilities of four different ECM fungi to degrade SOM using a disparate repertoire of enzymes and investigates isotopic N fractionation in the plant-fungi-soil system in detail. This will imply if the frequency of distinct fungal species can essentially control SOM decay but also favors fungal inputs to SOM *via* extensive mycelial growth.

- **Manuscript 4** analyses the impact of an invasive plant species on SOM decomposition in systems with AM- *vs*. ECM-association. The response of the invasive species to the distinct nutrient economies per mycorrhizal association may provide management strategies for invasive plant species along with a predicted shift in plant community composition from ECM to AM tree species under climate change.

- **Manuscript 5** focuses on the response of plant species with different microbial interactions to acquire soil nutrients to elevated CO_2 and how nutrient limitation is alleviated or aggravated on plant and microbial sites. This will allow drawing predictions on how these plant and microbial species may cope with climate change and establish strategies to manage their thriving and minimize undesired effects of climate change.

3 Methodological approaches

3.1 Tracing carbon and nutrient fluxes and estimating inputs

Different methods have been used to trace and estimate C and N fluxes within the plant-microbe-soil system, all with distinct advantages and disadvantages. The combination of several of these specific methods is a reliable way to minimize weaknesses of single methods and to enhance scientific understanding of C and nutrient fluxes in the complex plant-microbe-soil system.

As stable isotope applications bear source and process information of the system (**Box 4**), they represent a reliable tool to trace inputs and fluxes (Fry, 2006; Hobbie & Högberg, 2012; methods applied in manuscripts 1-5). Two applications are primarily utilized: (i) natural abundances of stable isotopes of both bulk samples, or component-specific (Gleixner, 2013) and (ii) labeling approaches, for which a distinct component or compartment of the system gets artificially enriched in heavy isotopes to trace its fate in the system (Fry, 2006). While labeling approaches facilitate the follow-up of distinct compounds and allow for a clear statement about the fate of the labelled substance, they are often limited by snapshot results and the artificial enrichment which may not represent natural conditions (Fry, 2006). Conversely, natural abundances of stable isotopes are not limited by those artificial conditions but interpreting their patterns requires sound knowledge of fractionation processes during modification steps within the system (Fry, 2006; Hobbie & Högberg, 2012).

The utilization of stable isotopes to trace C and N fluxes in the plant-microbe-soil system demands knowledge of the isotopic patterns of the respective constituents (e.g., leaves, soil, fungi). While sporocarps of ECM and SAP fungi are easily collectible and thus measurable (e.g., Gebauer & Taylor, 1999; Kohzu *et al.*, 1999; Hobbie *et al.*, 2012; Chen *et al.*, 2019), the hypogaeic sporocarps of AM fungi (Jobim *et al.* 2019) aggravated their analysis. The analysis of extra- and intraradical AM hyphae following modified methods by Brundrett *et al.* (1994) and Saito (1995) allows gaining information on the hyphae as nutrient trading organ (method applied in manuscript 1; plus development of mechanical isolation approach). The interpretation of the data demands the consideration of other accompanying fungal hyphae (e.g., soil fungal community in field samples, endophytic root fungi) or bacterial biofilms on the hyphal surface. Moreover, a trade-off between avoiding isotopic fractionation by excluding the application of digestive enzymes (*cf.* Saito, 1995) *vs.* the risk of causing cytoplasm loss by breaking fine hyphae needs to be evaluated.

Bayesian Inference Isotope Mixing models (Parnell *et al.*, 2010; Parnell & Jackson, 2013) can aid deciphering the contribution of various inputs to a specific source (e.g., POM, MAOM; method applied in manuscript 2). Informed with the isotopic data and prior information such as C- or N-contents, trophic enrichment, or fractionation factors, this model uses Bayesian statistics to

calculate probabilities for each input group to contribute to the respective source (Parnell *et al.*, 2010; Bond & Diamond, 2011). Sound knowledge of the system analyzed, and its constituents is necessary and basic requirements need to be fulfilled (e.g., data within the mixing polygon) (Phillips & Gregg, 2003; Parnell *et al.*, 2010; Bond & Diamond, 2011).

Amino sugars, cell wall components of bacteria and fungi (Amelung, 2001), are a tool to identify the contribution of microbial tissues to SOM (method applied in manuscript 2). Typically, the four amino sugars muramine, glucosamine, mannosamine, and galactosamine are measured. Bacterial tissues can be related to muramic acid, while fungal tissues are related to glucosamine (Amelung, 2001; Joergensen, 2018). With the application of conversion factors determined by Appuhn & Joergensen (2006) and Engelking *et al.* (2007) the contribution of bacterial and fungal C and N to SOM can be calculated. While amino sugars do not allow for an itemization of microbial groups (e.g., mycorrhizal *vs.* saprotrophic fungi), their combination with stable isotope analyses provides more detailed differentiation of microbial groups (Joergensen, 2018).

Analyzing PLFAs or NLFAs is widely applied to estimate the amount of bacterial and fungal tissue contributions to a (soil) system (Olsson, 1999; Joergensen & Wichern, 2008; Wallander *et al.*, 2009; Walder *et al.*, 2012, 2013; Paterson *et al.*, 2016; Suetsugu *et al.*, 2020; methods discussed in manuscript 1). This method allows for the separation of microbial groups, with specific fatty acids for Gram-positive or Gram-negative bacteria, saprotrophic, ectomycorrhizal, or arbuscular mycorrhizal fungi (Olsson, 1999; Balser *et al.*, 2005; Paterson *et al.*, 2016). However, PLFA and NLFA analyses are limited by the overlap of specific fatty acids with other compounds, e.g., C16:1ω5 for AM fungi is also present in some Gram-negative bacteria and degrading spores (Nichols *et al.*, 1986; Joergensen & Wichern, 2008; Ngosong *et al.*, 2012; Paterson *et al.*, 2016). Despite their higher specificity, NLFAs suffer from interferences with distinct NLFAs in spores or dead biomass with long residence time (Paterson *et al.*, 2016). Currently the lack of an AM fungi-specific fatty acid hampers precise statements for AM fungi (*cf.* Olsson, 1999).

Analyses of CO_2 concentrations and isotopic signatures *via* e.g., soil cores allow for identifying shifts in microbial respiration (Werth & Kuzyakov, 2010) with e.g., different mycorrhizal association or presence of an invasive plant species (method applied in manuscript 4). This method particularly aims to estimate the priming effect, *ergo* the activation of microorganisms *via* C inputs to soil (e.g., Werth & Kuzyakov, 2010; Pausch *et al.*, 2013; Chao *et al.*, 2019). Utilizing the distinct isotopic signatures of soils from **C_3** or **C_4 plant** cover allows separating CO_2 fluxes into different sources (e.g., native SOM-derived *vs.* invasive plant-derived) *via* two-source isotopic mixing models. The

C_3 plant. A plant that conducts C_3 pathway of photosynthesis with Ribulose-1,5-biphosphate-Carboxylase/-Oxigenase (RuBisCO) as a key enzyme. C_3 plants are best adapted to temperate regions. The ^{13}C isotopic signature of C_3 plants is *app.* –28 ‰.

application of Miller/Tans models is considered to account for impacts caused by atmospheric CO_2 (Miller & Tans, 2003; Pausch & Kuzyakov, 2012). The difference between the invasive plant-derived CO_2 and the native SOM-derived CO_2 depicts the priming effect.

C_4 plant. A plant that conducts C_4 pathway of photosynthesis with pre-fixation of CO_2 to oxal-acetate. Prefixation and Calvin cycle occurs under spatial separation, allowing for a higher rate of photo-synthesis and a superiority of C_4 plants relative to C_3 plants in arid regions. The ^{13}C isotopic signature of C_4 plants is *app.* –14 ‰.

SOM describes the entirety of organic matter found in soil. SOM comprises living organic matter, the edaphon, dead organic matter, and substances exuded by plants and the edaphon (Sadava *et al.*, 2011; Wittig & Streit, 2004). SOM occurs in various stages of decomposition, with different complexities of compounds being present. Resulting from the continuum of decomposition present for SOM, separation into different fractions of SOM aids in identifying processes and mechanisms coupled to SOM dynamics (Golchin *et al.*, 1994; Lavallee *et al.*, 2020). While a variety of methods to separate SOM into fractions occurs, a most recommended approach is the separation into POM and MAOM (Lavallee *et al.*, 2020; **Figure 3**). This separation is conducted *via* solubilizing SOM in a mixture of sodium-hexametaphosphate and water and separating fractions *via* a 53 µm sieve. The fraction on top of the sieve (> 53 µm) then represents the POM fraction, and the fraction washed through the sieve (< 53 µm) represents the MAOM fraction. A finer separation of POM and MAOM fractions can be performed, for example, *via* a particle size and density separation (Amelung & Zech, 1999; Mueller *et al.*, 2014), whereby SOM is washed through different sieve sizes and further separated according to its density in sodium polytungstate (SPT; method applied in manuscript 2). Finer separation enables to follow the process of SOM decomposition concerning the fate of particular substances and compounds, e.g., from leaf litter to large or small POM particles, or to compare processes in systems with distinct mycorrhizal association.

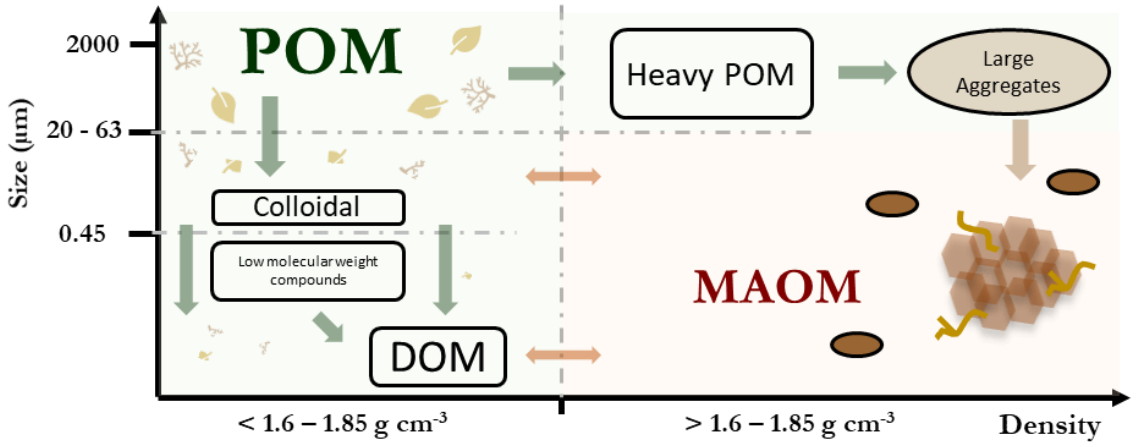

Figure 3: Fractions resulting from particle size and density fractionation (modified from Lavallee et al., 2020). Arrows indicate SOM formation pathways. POM = Particulate Organic Matter; MAOM = Mineral-Associated Organic Matter; DOM = Dissolved Organic Matter

3.2 Field site Moore's Creek Research and Teaching Preserve

The field site Moore's Creek Research and Teaching Preserve in Bloomington, Indiana, USA (Figure 4) was selected for the analysis of plant- or microbial-derived contributions to different SOM fractions under AM- or ECM-associated tree species (*cf.* Manuscript 2) and the effect of an invasive grass species on SOM dynamics in AM- or ECM-associated systems (*cf.* Manuscript 4). The field site comprises a mixed, temperate deciduous forest of around 80 years age, with a characteristic ridge-ravine topography (39°05′ N, 86°28′ W, *cf.* Midgley & Phillips, 2016). The soils are sandstone-, siltstone- and shale-derived unglaciated Inceptisols; the mean annual temperature is about 11.6 °C, and the site experiences about 1200 mm mean annual precipitation (Midgley & Phillips, 2016).

Dominant ECM-associated tree species are *Quercus alba* L., *Quercus rubra* L., *Quercus velutina* LAM., *Fagus grandifolia* EHRH. and *Carya glabra* MILL.; dominant AM-associated tree species are *Liriodendron tulipifera* L., *Sassafras albidum* NUTT, *Acer saccharum* MARSHALL and *Prunus serotina* EHRH. (Phillips *et al.*, 2013; Midgley & Phillips, 2016). To avoid impacts caused by topography of Moore's Creek forest (Figure 4c), the analyses and sampling was restricted to trees growing on the upper third of north-facing ridges (*cf.* Manuscript 2).

Figure 4: Field site Moore's Creek forest with its ridge-ravine topography (c). Mycelium of saprotrophic fungi (a) and sporocarps of mycorrhizal Cortinarius sp., saprobic Laetiporus sulphureus (d) and mycorrhizal Inocybe sp. (e).

"*The world depends on fungi, because they are major players in the cycling of materials and energy around the world*"
E. O. Wilson

Chapter 1 introduces

- The plant-fungi-soil system
- The role of fungi in ecosystems
- Stable isotopes and fungi
- Carbon and nutrient fluxes in the plant-fungi-soil system
- Impact of the plant-fungi-association on soil organic matter
- Tracing carbon and nutrient fluxes and estimating inputs
- Impacts of climate change on nutrient cycling and SOM dynamics
- Objectives of this thesis

Chapter 2 presents the

- Main results
- Author contributions
- List of further publications
- References

Chapter 3 displays the

- Manuscripts of this thesis
- Declaration

Chapter 2

4 Synopsis

4.1 Manuscript 1: Stable C and N isotope natural abundance of intraradical hyphae of arbuscular mycorrhizal fungi

Though stable isotope natural abundance patterns represent an effective tool to trace C and nutrient shifts in plant-microbe-soil systems, for mycorrhizal systems they are limited due to the lack of a quantifiable way of arbuscular mycorrhizal fungi in the ecosystems. This results from the hypogaeic growth of AM fungal sporocarps, causing challenges for collection and analysis (Jobim *et al.*, 2019). While specific compounds like lipids associated to membranes or storage structures, fungal spores, or soil hyphae served as a surrogate for AM fungi stable isotope signatures, the isotopic patterns of intraradical hyphae as functional nutrient trading organ remain largely obscure. Therefore, methods to determine the isotopic signatures of intra- and extraradical hyphae were developed or existing procedures modified. In a split-microcosm experiment, AM fungus *Rhizophagus irregularis* was inoculated to the grass *Festuca ovina* or the legume *Medicago sativa* grown in a sterile soil-sand-mixture. Intraradical hyphae were isolated from plant roots *via* a developed mechanical or an enzymatic approach (modified from Saito, 1995). Additionally, soil hyphae were extracted *via* a modified approach by Brundrett *et al.* (1994) to compare isotopic signatures of intraradical and extraradical hyphae. Independent of the plant partner, hyphae of *R. irregularis* were enriched in ^{13}C and ^{15}N relative to plant tissues and enriched in ^{15}N relative to the soil (**Figure 5**). Our results indicate the potential of AM fungi to gain low molecular weight organic N compounds, resulting in a ^{15}N enrichment of AM hyphae. The ^{13}C isotopic patterns underline the C gain from the plant partner, most likely a combination of carbohydrates and lipids (*cf.* Jiang *et al.*, 2017; Keymer *et al.*, 2017; Luginbuehl *et al.*, 2017; Rich *et al.*, 2017). The consistency of an enrichment in ^{13}C and ^{15}N for AM hyphae needs to be evaluated for further species and genera, as variability occurs for e.g., AM spores (Courty *et al.*, 2015). Our data supplement existing data on membrane biomarkers and spores of AM fungi by the hyphae as the functional nutrient trading organ. The transferability to field studies likely will be limited by the presence of a diverse fungal community that needs to be separated from AM fungi. However, if technical possibilities for this separation are available stable isotope natural abundances of AM hyphae will support the understanding of C and nutrient trading in plant-microbe-soil systems.

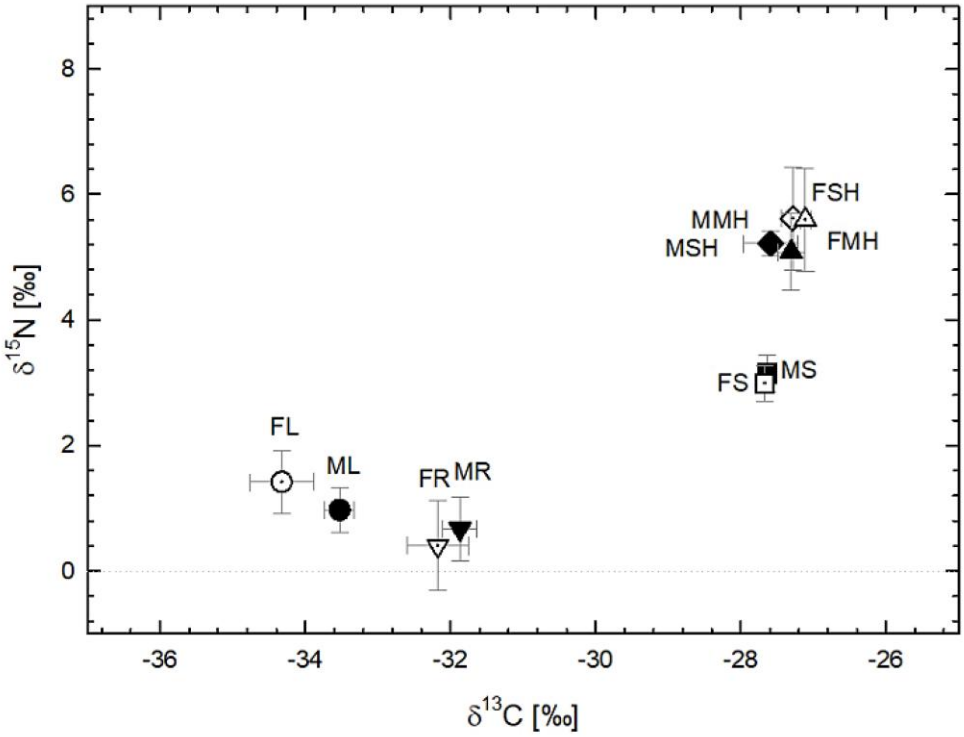

Figure 5: Dual isotope scatter plot of δ¹⁵N and δ¹³C isotopic values of leaves, roots, soil, and AM hyphae of Festuca ovina and Medicago sativa inoculated with Rhizophagus irregularis (Figure taken from manuscript 1). AM hyphae from both soil and mechanical isolation were more δ¹⁵N- and δ¹³C-enriched than plant tissues, and more δ¹⁵N-enriched than soil. FL = Festuca leaves, ML = Medicago leaves, FR = Festuca roots, MR = Medicago roots, FS = Festuca soil, MS = Medicago soil, FSH = Festuca soil hyphae, MSH = Medicago soil hyphae; FMH = Festuca hyphae from mechanical isolation, MMH = Medicago hyphae from mechanical isolation.

4.2 Manuscript 2: Plant and fungal contributions to C and N in soil organic matter fractions

Applying the established method for isolating of AM hyphae from roots developed in manuscript 1, we aimed to trace C and N trading from plants *via* fungi and microbes to soil and various fractions of SOM. Currently, our knowledge of the contributions of C and N inputs from plant and microbial residues to SOM fractions remains somewhat limited, and particularly the contribution of different fungal groups like ECM, AM, or SAP fungi is almost unknown. Transferring the Bayesian Inference Isotope Mixing Model frequently applied in food web studies (e.g., Parnell *et al.*, 2010) to plant-microbe-soil systems with distinct mycorrhizal association (AM- or ECM-associated) sought to partition inputs from plants (leaves, roots) and microbes (mycorrhizal fungi, saprotrophs) to SOM sources. The concomitant analysis of amino sugars supplemented information on microbial residues. The study was conducted around trees with either AM-association (*Liriodendron tulipifera*) or ECM-association (*Quercus alba*), aiming to evaluate distinct contributions depending on leaf litter quality differences and nutrient cycling patterns

(*cf.* MANE framework; Phillips *et al.*, 2013). Soil OM was separated into POM and MAOM fractions of large (> 63 μm), medium (> 20 μm), and small (< 20 μm) size according to a modified method from Amelung & Zech (1999) and Müller *et al.* (2014). A shift from ^{13}C and ^{15}N depleted POM fractions resembling plant tissues to enriched MAOM fractions resembling fungal tissues was discovered for both mycorrhizal associations. For POM fractions, a dominant contribution of plant tissues was calculated for both tree species, followed by SAP and then ECM fungal inputs (**Figure 6**). MAOM fractions were dominated by fungal inputs, with SAP fungi dominating over ECM fungi (**Figure 6**). While AM fungal residues contributed little to SOM fractions, their activation and fueling of saprotrophic organisms with plant-derived C likely resulted in the high presence of SAP fungi in the AM tree system. Microbial residues (as fungal and bacterial amino sugars) supported a significant role of ECM and SAP fungal residues for SOC storage in both POM and MAOM fractions. Fungal C contributed most to POM fractions, while both fungal and bacterial C contributed to MAOM fractions. Agreeing with recent literature by Angst *et al.* (2021), around 40% of plant-derived C contributed to MAOM fractions. Therein, root-derived inputs were most important, while 60% microbial-derived C highlight the dominance of microbial inputs to stable SOM. This aligns with plant-derived POM acting as a starting point for the microbially-driven mineral association of OM as described by Witzgall *et al.* (2021). The lack of differences between tulip poplar and white oak systems in isotopic and amino sugar patterns is likely attributed to the co-existence and mixing of mycorrhizal types in our mixed forest. Analyses in mono-dominated stands could aid to overcome this issue. Concluding, our results highlight the importance of different microbial inputs for C and N storage in SOM fractions and that fungal communities should be considered for supporting long-term soil C storage. Further studies should aim at a better understanding of the accessibility of N sources and N fractionation processes to further improve the accuracy of the mixing model predictions. This will help to predict the effects of divergent actors in the plant-microbe-soil systems, e.g. through different ECM fungi with different degradation potential and thus accessibility to N sources.

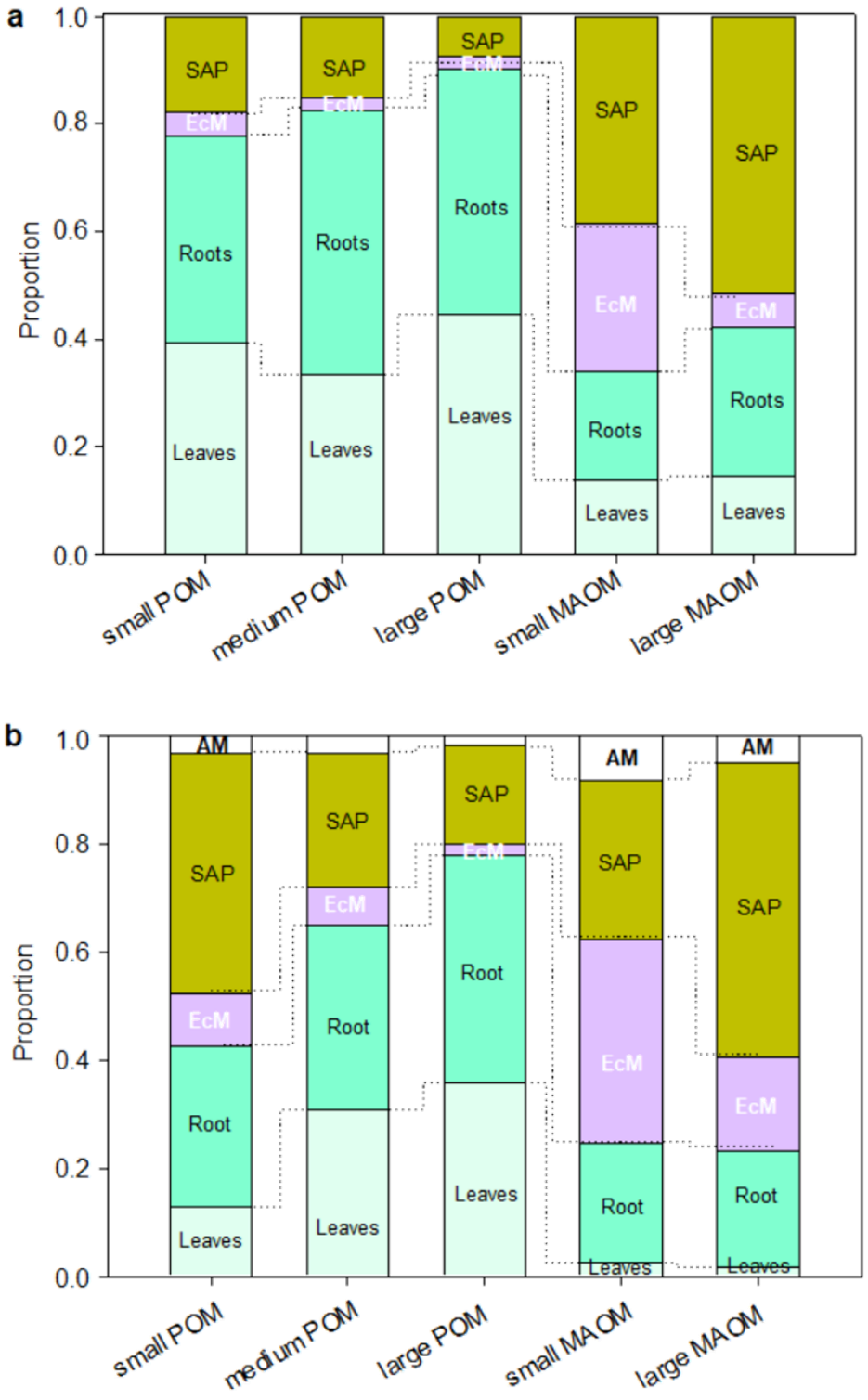

Figure 6: Stacked bar plots of the contributions of inputs from plant leaves (light green), roots (turquoise), ECM (purple), SAP (olive) and AM fungi (white) to POM (small, medium, and large size) and MAOM fractions (small and large size) of (a) white oak and (b) tulip poplar (figure taken from manuscript 2 with colour modifications). Plant inputs contributed most to POM fractions for both tree species, while SAP and ECM fungal inputs contributed most to MAOM fractions.

4.3 Manuscript 3: Nitrogen fluxes between Pinus sylvestris and ectomycorrhizal fungi with different decomposition abilities – an in vitro stable isotope approach

Despite the identification of fungal guild-specific inputs to stable SOM in the field in manuscript 2 it remained unclear, whether the N isotopy is determined solely by soil N sources, or if it is additionally impacted by fractionation processes within the plant-fungi association. Therefore, detailed microcosm studies with different ECM fungi were conducted, in order to decipher the effects of fungi on N isotopy and how different fungal enzymatic repertoires affect the C and N trading within the mycorrhizal association. Certain types of mycorrhizal fungi, such as ericoid or ECM fungi, have the ability to mobilize organic N (and thus C) from SOM. As ECM fungi, typical for temperate and boreal forests, derived from multiple independent evolutionary lineages, different ECM fungi have varying capabilities for SOM breakdown (*cf.* Martin *et al.* 2016; Shah *et al.*, 2016). In a microcosm study, we sought to investigate the various capabilities of four ECM fungi, *Laccaria laccata*, *Laccaria bicolor*, *Pisolithus arhizus,* and *Paxillus involutus*, to access different N forms from SOM, how this is related to the association to their plant partner *Pinus sylvestris* (**Figure 7**) and whether N isotopy is determined by soil N sources or additional isotopic fractionation processes.

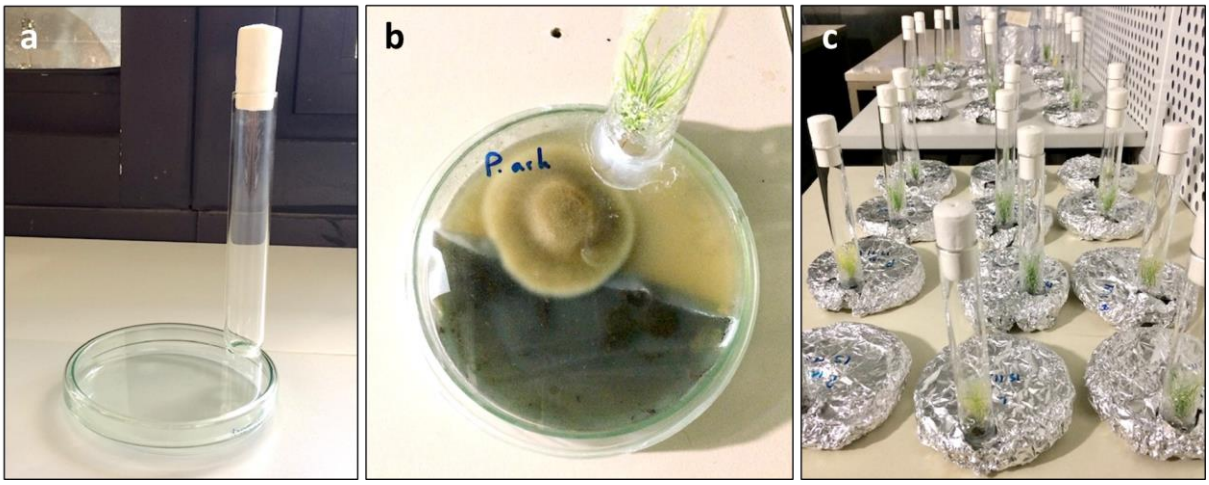

Figure 7: Depiction of the microcosms utilized in manuscript 3. A glass tube was fixated to the lid of a glass Petri dish and sealed with a cotton plug (a). The Petri dish was separated into an agar-only compartment and a soil-agar compartment with a 30 µm mesh barrier. A sapling of Pinus sylvestris was placed into the glass tube and roots were inserted into the agar. A plug of fungal mycelium was placed in close proximity to plant roots on the agar-only compartment (b). The Petri plate representing the belowground soil part was wrapped in aluminium foil. Microcosms were places in a climate control chamber during the duration of the experiment (c).

Fluxes of C and N between plant, fungi, and soil were analyzed as shifts in the natural abundances of stable isotopes of C and N. At the same time, changes in root morphology, e.g. branching patterns, were accessed *via* root scanning analyses. The association with ECM fungi had a positive effect on plant biomass, likely due to a CO_2-fertilization effect within the microcosms, except for the association with *L. bicolor*. The fact that %N in roots and shoots decreased with fungal

association (except *L. bicolor*), but biomass-related N-content remained constant indicates a dilution effect due to increased biomass and/or increasing N-limitation. Nitrogen limitation as a reason was further supported by an increased occurrence of more delicate roots for plants associated with *P. arhizus*, *P. involutus,* and *L. laccata*. Although belonging to the same genus, *L. laccata,* and *L. bicolor* appeared to possess different enzymatic repertoires, as the association with *L. bicolor* seldom differed from the plant alone treatment. All ECM fungi were more ^{15}N-depleted than the soil, indicating a primary reliance on inorganic N sources. Nevertheless, *P. arhizus,* and *P. involutus* had greater access to ^{15}N-enriched N sources due to their higher degradative capabilities relative to *Laccaria* species (**Figure 8**).

Root morphology changed to an increase in finer roots and higher branching with plant association for all fungal associations allowing for an enhanced nutrient uptake, except for the association with *L. bicolor*. These results indicate that apart from the enzymatic repertoire of an ECM fungus, the symbiosis with a plant and/or the N availability in the system dictates the capacity of ECM fungi to benefit from organic N sources. Thus, in ECM-associated systems, the fungal community, its degradative capabilities, and its response to changes in e.g. N-availability likely affect nutrient cycling and storage, SOM decomposition and the vulnerability of SOM to changing environmental conditions.

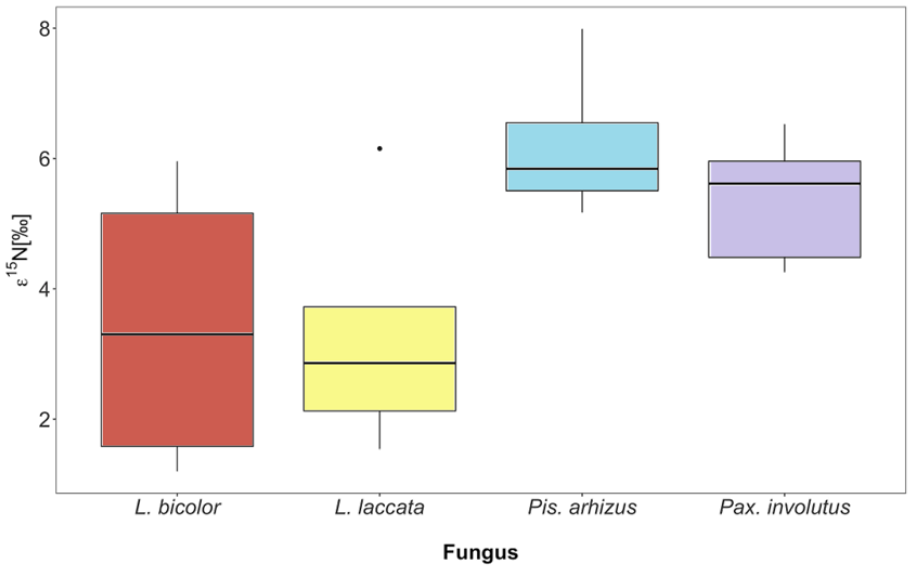

Figure 8: Boxplots of enrichment factor ε^{15}N values of ECM fungi Laccaria bicolor (red), Laccaria laccata (yellow), Pisolithus arhizus (blue) and Paxillus involutus (purple) grown in microcosms associated to Pinus sylvestris (Figure taken from manuscript 3 with colour modifications). The median is represented by the black line in the middle of the box, the box margins represent the 25th and the 75th percentile. The interquartile range (IQR) is represented by the box length. Whiskers state the minimum (25th percentile – 1.5 x IQR) or the maximum (75th percentile + 1.5 x IQR) and outliers are given as black dots. Higher ε^{15}N-enrichment indicates for access to ^{15}N-enriched compounds. Pisolithus arhizus and P. involutus had higher ε^{15}N values than Laccaria bicolor and Laccaria laccata.

4.4 Manuscript 4: Organic matter priming by invasive plants depends on dominant mycorrhizal association

Despite the presence of more SOM (in form of POM) in the topsoils of ECM systems relative to AM systems (Craig *et al.* 2018) it remained unclear how vulnerable this SOM is to changing conditions. As pressure by e.g., alien species invasion is predicted to increase in the future, impacting N-mineralization rates (Craig *et al.*, 2019) and ultimately affecting the competition between mycorrhizal and SAP fungi, we investigated AM- and ECM-systems prone to plant invasion for the speed of SOM decomposition. Promoted by favorable environmental conditions, through e.g., climate change conditions or competitive advantages, invasive plants can invade ecosystems and modify processes of nutrient cycling and SOM formation/stabilization, e.g., *via* increased litter or exudate inputs (Jo *et al.*, 2017; Bradford *et al.*, 2012; Morris *et al.*, 2016). However, *in situ* measurements of the severity of these effects in terms of magnitude and direction have rarely been investigated. In a temperate, deciduous forest in the USA, we analyzed the effect of the invasive C_4 grass *Microstegium vimineum* on decomposition under C_3 trees with either AM- or ECM-association. Effects on decomposition were measured as CO_2 fluxes from soil cores and used to calculate priming effects depending on plant invasion and differences by mycorrhizal-association-induced soil properties (*cf.* MANE-framework; Phillips *et al.*, 2013). Invasion by *M. vimineum* increased decomposition by 58 % around ECM trees (**Figure 9**, positive priming effect) with soils low in N and POM as a dominant form of SOM.

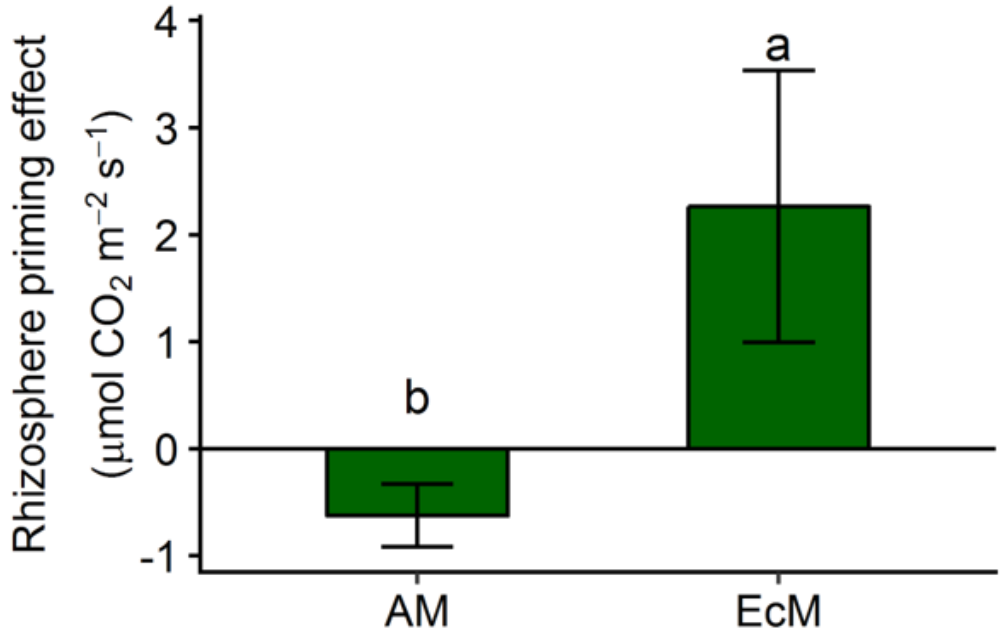

Figure 9: Rhizosphere priming effect (µmol CO2 m^{-2} s^{-1}) for AM-associated systems vs. ECM-associated systems (Figure taken from manuscript 4). Error bars indicate standard error (SE); different small superscripted letters indicate significant differences between the mycorrhizal associations. While for AM-associated systems negative priming effects occurred, priming effects were positive for ECM-associated systems.

Conversely, around AM trees with high soil N and MAOM as a dominant form of SOM decomposition was decreased by 14 % with *M. vimineum* invasion (**Figure 9**, negative priming effect). Our results underpin the ability of invasive plant species to modify SOM decomposition. While ECM-systems contain higher amounts of SOM in topsoils than AM-systems, our results show that this SOM is more vulnerable to changing conditions and C and nutrient losses. Apart from the impact of invasive species, the functioning and interaction of the plant-microbe-soil system is vulnerable to further changing conditions such as the climate change-driven increase in atmospheric CO_2 concentration, that might modify processes of nutrient cycling and storage.

4.5 Manuscript 5: Plants benefit more from elevated CO_2 in terms of nutrient acquisition than microbes despite different plant-microbial interactions

Not just invasive plant species impact SOM turnover processes but increased atmospheric CO_2 concentrations due to climate change and the associated changes in nutrient availability. The atmospheric CO_2 concentration as a significant threat related to climate change is predicted to double until 2100. While increased CO_2 concentrations were often found beneficial for C_3-plants and microbes in terms of growth and biomass production, elevated CO_2 concomitantly causes competition for soil nutrients. Many plants associate with microbes to promote nutrient supply, though plants were primarily considered to be out-competed by soil microbes in a plant *vs.* soil microbe competition for nutrients. As microbes and soil pools become sinks for nutrients, increased photosynthesis and belowground C supply are not rewarded by increased nutrient transfer, as stated in the progressive nutrient limitation (PNL) hypothesis (Luo *et al.*, 2004). However, Johnson (2006) summarized several studies showing an increased N uptake with elevated CO_2, demanding for a closer look at different plant nutrient acquisition strategies and their competitive potential relative to microbes. In a climate control chamber experiment, we investigated the responses of three plant species in a gradient of mycorrhizal dependency to ambient (400 ppm) and elevated (700 ppm) atmospheric CO_2 levels. The plants, weakly mycorrhizal *Silene acaulis*, legume *Medicago sativa,* and mycorrhizal *Festuca ovina* grew in mesocosms with a native microbial community and were inoculated with AM fungus *Rhizophagus irregularis*. Responses to changes in CO_2 concentrations were analyzed in terms of changes in the amount of ^{15}N label obtained from ^{15}N-labelled leaf litter and transferred to fungal and plant tissues. Responses of microbes were investigated *via* microbial biomass measures and stable isotope abundances. Despite occupying different microbial interactions to acquire soil nutrients, our results show that the plants benefitted more from soil nutrients than soil microbes. Nutrient cycling was decelerated under elevated CO_2, as visualized by a widening of the microbial biomass C:N ratio and more ^{15}N remaining in the mesh bag. Contrary to decreasing MBN, the N-content of AM hyphae increased under elevated CO_2, indicating that plant-associated intraradical mycorrhizal

hyphae were not affected by nutrient limitation. Nutrient acquisition differed between plant species as shown by differences in N budget (**Figure 10**), with more total N in shoot or root tissues of *Festuca* and *Silene* under elevated CO_2 but less in *Medicago* shoot and root tissues. These results highlight the competitive potential of plants relative to microbes in terms of N acquisition and the need to consider the responses of all members of the plant-microbe-soil system to elevated CO_2 conditions for developing strategies related to climate change.

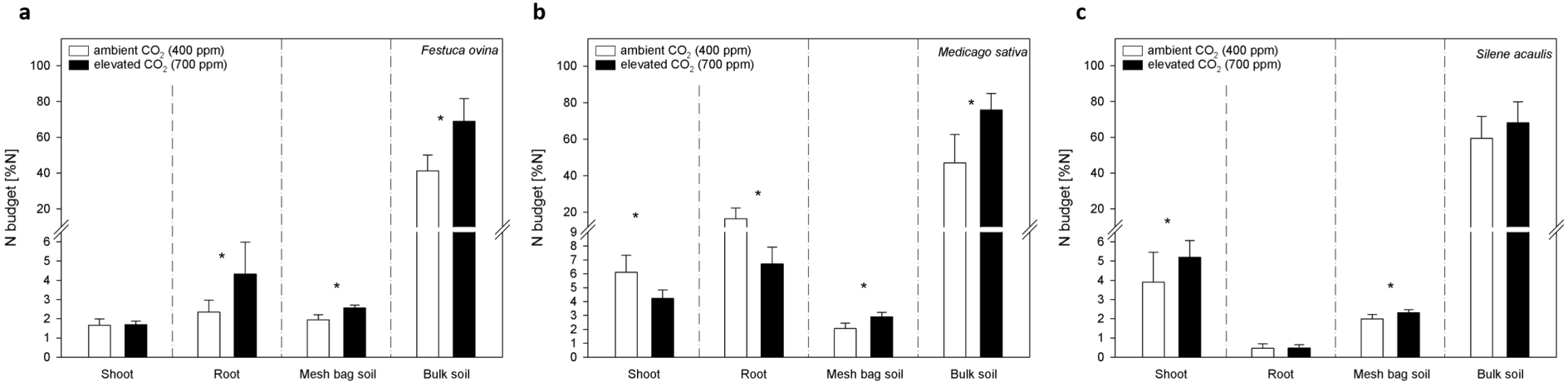

*Figure 10: N budget [% total N] for shoots, roots, mesh bag soil, and bulk soil of Festuca ovina (a), Medicago sativa (b), and Silene acaulis (c) related to unplanted controls. Error bars are given as standard deviation. The ambient CO_2 treatment is given in white, the elevated CO_2 treatment is given in black bars, and significant differences are indicated by an asterisk *.*

5 Main conclusions and outlook

The work in this thesis could identify **(1)** the stable isotope signature of AM fungus *Rhizophagus irregularis*, and support that AM hyphae gain a mixed C source of carbohydrates and lipids and likely some low molecular weight organic N. It was evident that **(2)** different fungal guilds are essential contributors to MAOM fractions, irrespective of AM- or ECM- association, and that **(3)** within fungal guilds different fungi possess distinct capabilities to access N-forms from SOM. Finally, impacts of changing conditions, like **(4)** plant invasion or **(5)** elevated CO_2 concentrations, affect C and N cycling and storage dynamics, resulting in shifts in the stocks of POM and MAOM or of competitive relationships.

Building on these findings, the following points could be investigated in the future:

- Whether the stable isotope patterns of *R. irregularis* are constantly found among AM fungi
- Analyze the contribution of fungal guilds in monodominant AM- and ECM-stands
- Including further input sources into the mixing model
- Determining the stable isotope signature of amino sugars in POM and MAOM fractions
- Evaluating the N-sources available and isotopic fractionations occurring in the field
- How management strategies to reduce impacts of changing conditions affect observed patterns of POM losses in ECM-systems and competition between plants and microbes

6 Author contributions to the manuscripts

Author contributions to the individual manuscripts in percent (%). Lowercase letters indicate contributions to a = experimental concept and study design, b = conduction of field and/or laboratory work, c = evaluation of data and statistical analyses, d = preparation of manuscript.

Manuscript 1: Stable C and N isotope natural abundance of intraradical hyphae of arbuscular mycorrhizal fungi, *Mycorrhiza*, 2020

Authors	a	b	c	d
Saskia Klink	45	50	80	60
Philipp Giesemann	45	30	20	20
Timo Hubmann	-	20	-	5
Johanna Pausch	10	-	-	15

Manuscript 2: Plant and fungal contributions to C and N in soil organic matter fractions, submitted to *Soil Biology and Biochemistry*, 2021

Authors	a	b	c	d
Saskia Klink	80	50	90	50
Adrienne B. Keller	-	10	-	5
Andreas J. Wild	-	30	-	5
Vera L. Baumert	-	-	-	5
Matthias Gube	-	-	-	5
Eva Lehndorff	-	-	-	5
Nele Meyer	-	10	10	5
Carsten W. Mueller	-	-	-	5
Richard P. Phillips	5	-	-	5
Johanna Pausch	15	-	-	10

Manuscript 3: Nitrogen fluxes between *Pinus sylvestris* and ectomycorrhizal fungi with different decomposition abilities – an *in vitro* stable isotope approach, in preparation

Authors	a	b	c	d
Cara I. Meyer	-	65	80	55
Saskia Klink	45	30	20	25
Matthias Gube	10	-	-	10
Johanna Pausch	45	5	-	10

Manuscript 4: Organic matter priming by invasive plants depends on dominant mycorrhizal association, *Soil Biology and Biochemistry*, 2020

Authors	a	b	c	d
Amit Kumar	65	75	85	30
Richard P. Phillips	20	-	-	20
Andrea Scheibe	5	15	10	15
Saskia Klink	-	10	5	15
Johanna Pausch	10	-	-	20

Manuscript 5: Plants benefit more from elevated CO_2 in terms of nutrient acquisition than microbes despite different plant-microbial interactions, in preparation

Authors	a	b	c	d
Saskia Klink	60	100	85	50
Adrienne B. Keller	-	-	5	10
Matthias Gube	5	-	-	10
Richard P. Phillips	-	-	-	10
Johanna Pausch	35	-	10	20

7 List of publications

7.1 Publications of this thesis

- **Klink, S**; Giesemann, P; Hubmann, T; Pausch, J: Stable C and N isotope natural abundances of intraradical hyphae of arbuscular mycorrhizal fungi, Mycorrhiza, ***30***(6), 773-780 (2020), doi:10.1007/s00572-020-00981-9

- Kumar, A; Phillips, R; Scheibe, A; **Klink, S**; Pausch, J: Organic matter priming by invasive plants depends on dominant mycorrhizal association, Soil Biology and Biochemistry, ***140***, 107645 (2020), doi:10.1016/j.soilbio.2019.

7.2 Further publications

- Bock C, Zimmermann S, Beisser D, Dinglinger SM, Engelskirchen S, Giesemann P, **Klink S**, Olefeld JL, Rahmann S, Vos M, Boenigk J, Sures B. 2019. Silver stress differentially affects growth of phototrophic and heterotrophic chrysomonad flagellate populations. *Environmental Pollution* **244**: 314-322, doi:10.1016/j.envpol.2018.09.146.

- **Klink S**, Giesemann P, Gebauer G. 2019. Picky carnivorous plants? Investigating preferences for preys´ trophic levels - a stable isotope natural abundance approach with two terrestrial and two aquatic Lentibulariaceae tested in Central Europe, *Annals of Botany* **123**: 1167-1177, doi:10.1093/aob/mcz022.

- Imhof HK, Sigl R, Brauer E, Feyl S, Giesemann P, **Klink S**, Leupolz K, Löder MGJ, Löschel L, Missun J, Muszynski S, Ramsperger AFRM, Schrank I, Speck S, Steibl S, Trotter B, Winter I, Laforsch C. 2017. Spatial and temporal variation of macro-, meso- and microplastic abundance on a remote coral island of the Maldives, Indian Ocean. *Marine Pollution Bulletin* **116**: 340-347, doi:10.1016/j.marpolbul.2017.01.010.

8 References

Abuzinadah RA, Read DJ. 1989. The role of proteins in the nitrogen nutrition of ectomycorrhizal plants. V. Nitrogen transfer in birch (*Betula pendula*) grown in association with mycorrhizal and non-mycorrhizal fungi. *New Phytologist* **112**: 61–68.

Agerer R. 2001. Exploration types of ectomycorrhizae. *Mycorrhiza* **11**: 107–114.

Ainsworth EA, Long SP. 2005. What have we learned from 15 years of free-air CO_2 enrichment (FACE)? A meta-analytic review of the responses of photosynthesis, canopy properties and plant production to rising CO_2. *New Phytologist* **165**: 351–371.

Alberton O, Kuyper TW, Gorissen A. 2005. Taking mycocentrism seriously: mycorrhizal fungal and plant responses to elevated CO_2. *New Phytologist* **167**: 859–868.

Allen EB, Allen MF. 1990. The mediation of competition by mycorrhizae in successional and patchy environments. In: Grace JB, ed. *Perspectives on plant competition*. San Diego: Academic Press, 367–389.

Allen MF, Kitajima K. 2014. Net primary production of ectomycorrhizas in a California forest. *Fungal Ecology* **10**: 81–90.

Amelung W, Zech W. 1999. Minimisation of organic matter disruption during particle-size fractionation of grassland epipedons. *Geoderma* **92**: 73–85.

Amelung W. 2001. Methods using amino sugars as markers for microbial residues in soil. Assessment methods for soil carbon. Boca Raton: Lewis Publishers.

Angst G, Mueller KE, Nierop KGJ, Simpson MJ. 2021. Plant- or microbial-derived? A review on the molecular composition of stabilized soil organic matter. *Soil Biology and Biochemistry* **156**: 108189.

Appuhn A, Joergensen R. 2006. Microbial colonisation of roots as a function of plant species. *Soil Biology and Biochemistry* **38**: 1040–1051.

Arnone JA, Gordon JC. 1990. Effect of nodulation, nitrogen fixation and CO_2 enrichment on the physiology, growth and dry mass allocation of seedlings of *Alnus rubra* Bong. *New Phytologist* **116**: 55–66.

Baldock JA, Skjemstad JO. 2000. Role of the soil matrix and minerals in protecting natural organic materials against biological attack. *Organic Geochemistry* **31**: 697–710.

Baldrian P. 2008. Enzymes of saprotrophic basidiomycetes. In: Boddy L, Frankland JC, van West British P, eds. *Mycological Society symposia series volume* **28**. Amsterdam, the Netherlands: Elsevier, 19–41.

Balser TC, Treseder KK, Ekenler M. 2005. Using lipid analysis and hyphal length to quantify AM and saprotrophic fungal abundance along a soil chronosequence. *Soil Biology and Biochemistry* **37**: 601–604.

Batjes NH. 1996. Total carbon and nitrogen in the soils of the world. *European Journal of Soil Science* **47**: 151–163.

Berndt R, Kottke I, Oberwinkler F. 1990. Ascomycete mycorrhizas from pot-grown silver-fir seedlings (*Abies alba* Mill.). *New Phytologist* **115**: 471–482.

Boer W de, **Folman LB, Summerbell RC, Boddy L. 2005.** Living in a fungal world: impact of fungi on soil bacterial niche development. *FEMS Microbiology Reviews* **29**: 795–811.

Bond AL, Diamond AW. 2011. Recent Bayesian stable-isotope mixing models are highly sensitive to variation in discrimination factors. *Ecological applications : a publication of the Ecological Society of America* **21**: 1017–1023.

Bradford MA, Strickland MS, DeVore JL, Maerz JC. 2012. Root carbon flow from an invasive plant to belowground foodwebs. *Plant and Soil* **359**: 233–244.

Brundrett M, Addy H, McGonigle T. 1994. Extraction and staining of hyphae from soil. In: Brundrett M, Melville L, Peterson L (eds) . *Mycologue Publications*, Guelph, pp. 24–34

Brundrett MC, Tedersoo L. 2018. Evolutionary history of mycorrhizal symbioses and global host plant diversity. *New Phytologist* **220**: 1108–1115.

Burke DJ, Weintraub MN, Hewins CR, Kalisz S. 2011. Relationship between soil enzyme activities, nutrient cycling and soil fungal communities in a northern hardwood forest. *Soil Biology and Biochemistry* **43**: 795–803.

Callaway RM, Aschehoug ET. 2000. Invasive plants versus their new and old neighbors: a mechanism for exotic invasion. *Science* **290**: 521–523.

Chao L, Liu Y, Freschet GT, Zhang W, Yu X, Zheng W, Guan X, Yang Q, Chen L, Dijkstra FA *et al.* 2019. Litter carbon and nutrient chemistry control the magnitude of soil priming effect. *Functional Ecology* **33**: 876–888.

Chapin F, Matson PA, Mooney HA. 2002. Principles of Terrestrial Ecosystem Ecology. Springer.

Chapman SK, Langley JA, Hart SC, Koch GW. 2006. Plants actively control nitrogen cycling: uncorking the microbial bottleneck. *New Phytologist* **169**: 27–34.

Cheeke TE, Phillips RP, Brzostek ER, Rosling A, Bever JD, Fransson P. 2017. Dominant mycorrhizal association of trees alters carbon and nutrient cycling by selecting for microbial groups with distinct enzyme function. *New Phytologist* **214**: 432–442.

Chen J, Heikkinen J, Hobbie EA, Rinne-Garmston KT, Penttilä R, Mäkipää R. 2019. Strategies of carbon and nitrogen acquisition by saprotrophic and ectomycorrhizal fungi in Finnish boreal *Picea abies*-dominated forests. *Fungal Biology* **123**: 456–464.

Chen W, Koide RT, Adams TS, DeForest JL, Cheng L, Eissenstat DM. 2016. Root morphology and mycorrhizal symbioses together shape nutrient foraging strategies of temperate trees. *Proceedings of the National Academy of Sciences* **113**: 8741–8746.

Cheng L, Booker FL, Tu C, Burkey KO, Zhou L, Shew HD, Rufty TW, Hu S. 2012. Arbuscular mycorrhizal fungi increase organic carbon decomposition under elevated CO_2. *Science (New York, N.Y.)* **337**: 1084–1087.

Cheng L, Chen W, Adams TS, Wei X, Le Li, McCormack ML, DeForest JL, Koide RT, Eissenstat DM. 2016. Mycorrhizal fungi and roots are complementary in foraging within nutrient patches. *Ecology* **97**: 2815–2823.

Cheng W, Kuzyakov Y. 2005. Root Effects on Soil Organic Matter Decomposition. In: Zobel RW, Wright SF, eds. *Roots and Soil Management: Interactions between Roots and the Soil*. Madison, WI, USA: American Society of Agronomy, Crop Science Society of America, Soil Science Society of America, 119–143.

Christensen BT. 2001. Physical fractionation of soil and structural and functional complexity in organic matter turnover. *European Journal of Soil Science* **52**: 345–353.

Clemmensen KE, Bahr A, Ovaskainen O, Dahlberg A, Ekblad A, Wallander H, Stenlid J, Finlay RD, Wardle DA, Lindahl BD. 2013. Roots and associated fungi drive long-term carbon sequestration in boreal forest. *Science* **339**: 1615–1618.

Cornelissen J, Aerts R, Cerabolini B, Werger M, van der Heijden M. 2001. Carbon cycling traits of plant species are linked with mycorrhizal strategy. *Oecologia* **129**: 611–619.

Cotrufo MF, Wallenstein MD, Boot CM, Denef K, Paul E. 2013. The Microbial Efficiency-Matrix Stabilization (MEMS) framework integrates plant litter decomposition with soil organic matter stabilization: do labile plant inputs form stable soil organic matter? *Global Change Biology* **19**: 988–995.

Cotrufo MF, Ranalli MG, Haddix ML, Six J, Lugato E. 2019. Soil carbon storage informed by particulate and mineral-associated organic matter. *Nature Geoscience* **12**: 989–994.

Courty P-E, Doubková P, Calabrese S, Niemann H, Lehmann MF, Vosátka M, Selosse M-A. 2015. Species-dependent partitioning of C and N stable isotopes between arbuscular mycorrhizal fungi and their C3 and C4 hosts. *Soil Biology and Biochemistry* **82**: 52–61.

Courty P-E, Walder F, Boller T, Ineichen K, Wiemken A, Rousteau A, Selosse M-A. 2011. Carbon and nitrogen metabolism in mycorrhizal networks and mycoheterotrophic plants of tropical forests: a stable isotope analysis. *Plant physiology* **156**: 952–961.

Craig ME, Lovko N, Flory SL, Wright JP, Phillips RP. 2019. Impacts of an invasive grass on soil organic matter pools vary across a tree-mycorrhizal gradient. *Biogeochemistry* **144**: 149–164.

Craig ME, Turner BL, Liang C, Clay K, Johnson DJ, Phillips RP. 2018. Tree mycorrhizal type predicts within-site variability in the storage and distribution of soil organic matter. *Global Change Biology* **24**: 3317–3330.

Dakora FD, Phillips DA. 2002. Root exudates as mediators of mineral acquisition in low-nutrient environments. In: Adu-Gyamfi JJ, ed. *Food Security in Nutrient-Stressed Environments: Exploiting Plants' Genetic Capabilities*. Dordrecht: Springer Netherlands, 201–213.

Daly AB, Jilling A, Bowles TM, Buchkowski RW, Frey SD, Kallenbach CM, Keiluweit M, Mooshammer M, Schimel JP, Grandy AS. 2021. A holistic framework integrating plant-microbe-mineral regulation of soil bioavailable nitrogen. *Biogeochemistry* **154**: 211–229.

Dawson TE, Mambelli S, Plamboeck AH, Templer PH, Tu KP. 2002. Stable Isotopes in Plant Ecology. *Annual Review of Ecology and Systematics* **33**: 507–559.

DeNiro MJ, Epstein S. 1978. Influence of diet on the distribution of carbon isotopes in animals. *Geochimica et Cosmochimica Acta* **42**: 495–506.

DeNiro MJ, Epstein S. 1981. Influence of diet on the distribution of nitrogen isotopes in animals. *Geochimica et Cosmochimica Acta* **45**: 341–351.

Deyn GB de, **Cornelissen JHC, Bardgett RD. 2008.** Plant functional traits and soil carbon sequestration in contrasting biomes. *Ecology letters* **11**: 516–531.

Dixon RK, am Solomon, Brown S, Houghton RA, Trexier MC, Wisniewski J. 1994. Erratum: Carbon Pools and Flux of Global Forest Ecosystems. *Science* **265**: 171.

Drigo B, Pijl AS, Duyts H, Kielak AM, Gamper HA, Houtekamer MJ, Boschker HTS, Bodelier PLE, Whiteley AS, van Veen JA *et al.* 2010. Shifting carbon flow from roots into associated microbial communities in response to elevated atmospheric CO_2. *Proceedings of the National Academy of Sciences* **107**: 10938–10942.

Eichlerová I, Homolka L, Žifčáková L, Lisá L, Dobiášová P, Baldrian P. 2015. Enzymatic systems involved in decomposition reflects the ecology and taxonomy of saprotrophic fungi. *Fungal Ecology* **13**: 10–22.

Engelking B, Flessa H, Joergensen RG. 2007. Shifts in amino sugar and ergosterol contents after addition of sucrose and cellulose to soil. *Soil Biology and Biochemistry* **39**: 2111–2118.

Field KJ, Pressel S. 2018. Unity in diversity: structural and functional insights into the ancient partnerships between plants and fungi. *The New phytologist* **220**: 996–1011.

Finzi AC, Canham CD, van Breemen N. 1998. Canopy tree-soil interactions within temperate forests: species effects on pH and cations. *Ecological Applications* **8**: 447–454.

Finzi AC, DeLucia EH, Hamilton JG, Richter DD, Schlesinger WH. 2002. The nitrogen budget of a pine forest under free air CO_2 enrichment. *Oecologia* **132**: 567–578.

Frank, AB. 1885. Über die auf Wurzelsymbiose beruhende Ernährung gewisser Bäume durch unterirdische Pilze. Ber. Deut. Bot. Ges.

Frey SD. 2019. Mycorrhizal Fungi as Mediators of Soil Organic Matter Dynamics. *Annual Review of Ecology, Evolution, and Systematics* **50**: 237–259.

Fry B. 2006. Stable Isotope Ecology. New York: Springer.

Gashaw Deressa T, Schenk MK. 2008. Contribution of roots and hyphae to phosphorus uptake of mycorrhizal onion (*Allium cepa* L.)-A mechanistic modeling approach. *Journal of Plant Nutrition and Soil Science* **171**: 810–820.

Gebauer G, Dietrich P. 1993. Nitrogen Isotope Ratios in Different Compartments of a Mixed Stand of Spruce, Larch and Beech Trees and of Understorey Vegetation Including Fungi. *Isotopenpraxis Isotopes in Environmental and Health Studies* **29**: 35–44.

Gebauer G, Taylor AF. 1999. ^{15}N natural abundance in fruit bodies of different functional groups of fungi in relation to substrate utilization. *New Phytologist* **142**: 93–101.

Gill AL, Finzi AC. 2016. Belowground carbon flux links biogeochemical cycles and resource-use efficiency at the global scale. *Ecology Letters* **19**: 1419–1428.

Gleixner G. 2013. Soil organic matter dynamics: a biological perspective derived from the use of compound-specific isotopes studies. *Ecological Research* **28**: 683–695.

Gleixner G, Danier HJ, Werner RA, Schmidt HL. 1993. Correlations between the ^{13}C Content of Primary and Secondary Plant Products in Different Cell Compartments and That in Decomposing Basidiomycetes. *Plant physiology* **102**: 1287–1290.

Golchin A, Oades JM, Skjemstad JO, Clarke P. 1994. Soil structure and carbon cycling. *Soil Research* **32**: 1043.

Goodale CL. 2017. Multiyear fate of a ^{15}N tracer in a mixed deciduous forest: retention, redistribution, and differences by mycorrhizal association. *Global Change Biology* **23**: 867–880.

Grinhut T, Hadar Y, Chen Y. 2007. Degradation and transformation of humic substances by saprotrophic fungi: processes and mechanisms. *Fungal Biology Reviews* **21**: 179–189.

Hobbie EA. 2006. Carbon allocation to ectomycorrhizal fungi correlates with belowground allocation in culture studies. *Ecology* **87**: 563–569.

Hobbie EA, Högberg P. 2012. Nitrogen isotopes link mycorrhizal fungi and plants to nitrogen dynamics. *The New phytologist* **196**: 367–382.

Hobbie EA, Sánchez FS, Rygiewicz PT. 2012. Controls of isotopic patterns in saprotrophic and ectomycorrhizal fungi. *Soil Biology and Biochemistry* **48**: 60–68.

Hodge A, Campbell CD, Fitter AH. 2001. An arbuscular mycorrhizal fungus accelerates decomposition and acquires nitrogen directly from organic material. *Nature* **413**: 297–299.

Hodge A, Fitter AH. 2010. Substantial nitrogen acquisition by arbuscular mycorrhizal fungi from organic material has implications for N cycling. *Proceedings of the National Academy of Sciences* **107**: 13754–13759.

Hodge A, Storer K. 2015. Arbuscular mycorrhiza and nitrogen: implications for individual plants through to ecosystems. *Plant and Soil* **386**: 1–19.

Högberg MN, Skyllberg U, Högberg P, Knicker H. 2020. Does ectomycorrhiza have a universal key role in the formation of soil organic matter in boreal forests? *Soil Biology and Biochemistry* **140**: 107635.

Jackson RB, Cook CW, Pippen JS, Palmer SM. 2009. Increased belowground biomass and soil CO_2 fluxes after a decade of carbon dioxide enrichment in a warm-temperate forest. *Ecology* **90**: 3352–3366.

Jiang Y, Wang W, Xie Q, Liu N, Liu L, Wang D, Zhang X, Yang C, Chen X, Tang D *et al.* 2017. Plants transfer lipids to sustain colonization by mutualistic mycorrhizal and parasitic fungi. *Science (New York, N.Y.)* **356**: 1172–1175.

Jilling A, Keiluweit M, Contosta AR, Frey S, Schimel J, Schnecker J, Smith RG, Tiemann L, Grandy AS. 2018. Minerals in the rhizosphere: overlooked mediators of soil nitrogen availability to plants and microbes. *Biogeochemistry* **139**: 103–122.

Jo I, Fei S, Oswalt CM, Domke GM, Phillips RP. 2019. Shifts in dominant tree mycorrhizal associations in response to anthropogenic impacts. *Science Advances* **5**: eaav6358.

Jo I, Fridley JD, Frank DA. 2017. Invasive plants accelerate nitrogen cycling: evidence from experimental woody monocultures. *Journal of Ecology* **105**: 1105–1110.

Jo I, Potter KM, Domke GM, Fei S. 2018. Dominant forest tree mycorrhizal type mediates understory plant invasions. *Ecology Letters* **21**: 217–224.

Jobim K, Błaszkowski J, Niezgoda P, Kozłowska A, Zubek S, Mleczko P, Chachuła P, Ishikawa NK, Goto BT. 2019. New sporocarpic taxa in the phylum Glomeromycota: *Sclerocarpum amazonicum* gen. et sp. nov. in the family Glomeraceae (Glomerales) and *Diversispora sporocarpia* sp. nov. in the Diversisporaceae (Diversisporales). *Mycological Progress* **18**: 369–384.

Joergensen R, Wichern F. 2008. Quantitative assessment of the fungal contribution to microbial tissue in soil. *Soil Biology and Biochemistry* **40**: 2977–2991.

Joergensen RG. 2018. Amino sugars as specific indices for fungal and bacterial residues in soil. *Biology and Fertility of Soils* **54**: 559–568.

Johnson DW. 2006. Progressive N limitation in forests: review and implications for long-term responses to elevated CO_2. *Ecology* **87**: 64–75.

Joner EJ, Johansen A. 2000. Phosphatase activity of external hyphae of two arbuscular mycorrhizal fungi. *Mycological Research* **104**: 81–86.

Jongmans AG, van Breemen N, Lundström U, van Hees PAW, Finlay RD, Srinivasan M, Unestam T, Giesler R, Melkerud P-A, Olsson M. 1997. Rock-eating fungi. *Nature* **389**: 682–683.

Jumpponen A. 2001. Dark septate endophytes - are they mycorrhizal? *Mycorrhiza* **11**: 207–211.

Kaiser C, Kilburn MR, Clode PL, Fuchslueger L, Koranda M, Cliff JB, Solaiman ZM, Murphy DV. 2015. Exploring the transfer of recent plant photosynthates to soil microbes: mycorrhizal pathway *vs* direct root exudation. *New Phytologist* **205**: 1537–1551.

Keiluweit M, Bougoure JJ, Nico PS, Pett-Ridge J, Weber PK, Kleber M. 2015. Mineral protection of soil carbon counteracted by root exudates. *Nature Climate Change* **5**: 588–595.

Keller AB, Brzostek ER, Craig ME, Fisher JB, Phillips RP. 2021. Root-derived inputs are major contributors to soil carbon in temperate forests, but vary by mycorrhizal type. *Ecology letters* **24**: 626–635.

Keymer A, Pimprikar P, Wewer V, Huber C, Brands M, Bucerius SL, Delaux P-M, Klingl V, Röpenack-Lahaye E von, **Wang TL *et al.* 2017.** Lipid transfer from plants to arbuscular mycorrhiza fungi. *eLife* **6**.

Kjoller A, Struwe S. 2002. Fungal communities, succession, enzymes, and decomposition. In: Burns RG, Dick RP, eds. *Enzymes in the Environment: Activity, Ecology and Applications*. New York: Marcel Dekker, 267–284.

Klink S, Giesemann P, Hubmann T, Pausch J. 2020. Stable C and N isotope natural abundances of intraradical hyphae of arbuscular mycorrhizal fungi. *Mycorrhiza* **30**(6): 773-780

Kögel-Knabner I, Guggenberger G, Kleber M, Kandeler E, Kalbitz K, Scheu S, Eusterhues K, Leinweber P. 2008. Organo-mineral associations in temperate soils: Integrating biology, mineralogy, and organic matter chemistry. *Journal of Plant Nutrition and Soil Science* **171**: 61–82.

Kohzu A, Yoshioka T, Ando T, Takahashi M, Koba K, Wada E. 1999. Natural ^{13}C and ^{15}N abundance of field-collected fungi and their ecological implications. *New Phytologist* **144**: 323–330.

Koide RT, Kabir Z. 2000. Extraradical hyphae of the mycorrhizal fungus *Glomus intraradices* can hydrolyse organic phosphate. *New Phytologist* **148**: 511–517.

Kopittke PM, Dalal RC, Hoeschen C, Li C, Menzies NW, Mueller CW. 2020. Soil organic matter is stabilized by organo-mineral associations through two key processes: The role of the carbon to nitrogen ratio. *Geoderma* **357**: 113974.

Kopittke PM, Hernandez-Soriano MC, Dalal RC, Finn D, Menzies NW, Hoeschen C, Mueller CW. 2018. Nitrogen-rich microbial products provide new organo-mineral associations for the stabilization of soil organic matter. *Global Change Biology* **24**: 1762–1770.

Kuzyakov Y, Friedel JK, Stahr K. 2000. Review of mechanisms and quantification of priming effects. *Soil Biology and Biochemistry* **32**: 1485–1498.

Kuzyakov Y, Horwath WR, Dorodnikov M, Blagodatskaya E. 2019. Review and synthesis of the effects of elevated atmospheric CO_2 on soil processes: No changes in pools, but increased fluxes and accelerated cycles. *Soil Biology and Biochemistry* **128**: 66–78.

Landeweert R, Hoffland E, Finlay RD, Kuyper TW & van Breemen N. 2001. Linking plants to rocks: ectomycorrhizal fungi mobilize nutrients from minerals. *Trends in ecology & evolution* **16**(5): 248-254.

Lavallee JM, Soong JL, Cotrufo MF. 2020. Conceptualizing soil organic matter into particulate and mineral-associated forms to address global change in the 21st century. *Global Change Biology* **26**: 261–273.

Leake JR, Donnelly DP, Boddy L. 2003. Interactions Between Ectomycorrhizal and Saprotrophic Fungi. In: Baldwin IT, Caldwell MM, Heldmaier G, Lange OL, Mooney HA, Schulze E-D, Sommer U, van der Heijden MGA, Sanders IR, eds. *Mycorrhizal Ecology*. Berlin, Heidelberg: Springer Berlin Heidelberg, 345–372.

Lehmann J, Hansel CM, Kaiser C, Kleber M, Maher K, Manzoni S, Nunan N, Reichstein M, Schimel JP, Torn MS *et al.* 2020. Persistence of soil organic carbon caused by functional complexity. *Nature Geoscience* **13**: 529–534.

Lehmann J, Kleber M. 2015. The contentious nature of soil organic matter. *Nature* **528**: 60–68.

Leigh J, Hodge A, Fitter AH. 2009. Arbuscular mycorrhizal fungi can transfer substantial amounts of nitrogen to their host plant from organic material. *New Phytologist* **181**: 199–207.

Lewis DH. 1973. Concepts in fungal nutrition and the origin of biotrophy. *Biological Reviews* **48**: 261–277.

Liao C, Peng R, Luo Y, Zhou X, Wu X, Fang C, Chen J, Li B. 2008. Altered ecosystem carbon and nitrogen cycles by plant invasion: a meta-analysis. *New Phytologist* **177**: 706–714.

Lilleskov EA, Hobbie EA, Horton TR. 2011. Conservation of ectomycorrhizal fungi: exploring the linkages between functional and taxonomic responses to anthropogenic N deposition. *Fungal Ecology* **4**: 174–183.

Lindahl BD, Ihrmark K, Boberg J, Trumbore SE, Högberg P, Stenlid J, Finlay RD. 2007. Spatial separation of litter decomposition and mycorrhizal nitrogen uptake in a boreal forest. *New Phytologist* **173**: 611–620.

Lindahl BD, Tunlid A. 2015. Ectomycorrhizal fungi - potential organic matter decomposers, yet not saprotrophs. *New Phytologist* **205**: 1443–1447.

Liu Y, Oduor AMO, Zhang Z, Manea A, Tooth IM, Leishman MR, Xu X, van Kleunen M. 2017. Do invasive alien plants benefit more from global environmental change than native plants? *Global Change Biology* **23**: 3363–3370.

Luginbuehl LH, Menard GN, Kurup S, van Erp H, Radhakrishnan GV, Breakspear A, Oldroyd GED, Eastmond PJ. 2017. Fatty acids in arbuscular mycorrhizal fungi are synthesized by the host plant. *Science (New York, N.Y.)* **356**: 1175–1178.

Luo Y, Su B, Currie WS, Dukes JS, Finzi A, Hartwig U, Hungate B, McMurtie RE, Oren R, Parton WJ *et al.* 2004. Progressive Nitrogen Limitation of Ecosystem Responses to Rising Atmospheric Carbon Dioxide. *BioScience* **54**: 731.

Lützow M von, **Kögel-Knabner I, Ekschmitt K, Flessa H, Guggenberger G, Matzner E, Marschner B. 2007.** SOM fractionation methods: Relevance to functional pools and to stabilization mechanisms. *Soil Biology and Biochemistry* **39**: 2183–2207.

Marshall JD, Ehleringer JR. (1990). Are xylem-tapping mistletoes partially heterotrophic?. *Oecologia* **84**(2): 244-248.

Marschner H, Dell B. 1994. Nutrient uptake in mycorrhizal symbiosis. *Plant and Soil* **159**: 89–102.

Martin F, Kohler A, Murat C, Veneault-Fourrey C, Hibbett DS. 2016. Unearthing the roots of ectomycorrhizal symbioses. *Nature reviews. Microbiology* **14**: 760–773.

Midgley MG, Brzostek E, Phillips RP. 2015. Decay rates of leaf litters from arbuscular mycorrhizal trees are more sensitive to soil effects than litters from ectomycorrhizal trees. *Journal of Ecology* **103**: 1454–1463.

Midgley MG, Phillips RP. 2014. Mycorrhizal associations of dominant trees influence nitrate leaching responses to N deposition. *Biogeochemistry* **117**: 241–253.

Midgley MG, Phillips RP. 2016. Resource stoichiometry and the biogeochemical consequences of nitrogen deposition in a mixed deciduous forest. *Ecology* **97**: 3369–3378.

Mikutta R, Turner S, Schippers A, Gentsch N, Meyer-Stüve S, Condron LM, Peltzer DA, Richardson SJ, Eger A, Hempel G *et al.* 2019. Microbial and abiotic controls on mineral-associated organic matter in soil profiles along an ecosystem gradient. *Scientific Reports* **9**: 10294.

Miller JB, Tans PP. 2003. Calculating isotopic fractionation from atmospheric measurements at various scales. *Tellus* **55B**: 207–214.

Morris KA, Stark JM, Bugbee B, Norton JM. 2016. The invasive annual cheatgrass releases more nitrogen than crested wheatgrass through root exudation and senescence. *Oecologia* **181**: 971–983.

Mueller CW, Koegel-Knabner I. 2009. Soil organic carbon stocks, distribution, and composition affected by historic land use changes on adjacent sites. *Biology and Fertility of Soils* **45**: 347–359.

Mueller CW, Gutsch M, Kothieringer K, Leifeld J, Rethemeyer J, Brueggemann N, Kögel-Knabner I. 2014. Bioavailability and isotopic composition of CO_2 released from incubated soil organic matter fractions. *Soil Biology and Biochemistry* **69**: 168–178.

Nakano A, Takahashi K, Kimura M. 1999. The carbon origin of arbuscular mycorrhizal fungi estimated from $\delta^{13}C$ values of individual spores. *Mycorrhiza*.

Ngosong C, Gabriel E, Ruess L. 2012. Use of the signature Fatty Acid 16:1ω5 as a tool to determine the distribution of arbuscular mycorrhizal fungi in soil. *Journal of Lipids* **2012**: 236807.

Nichols P, Stulp BK, Jones JG, White DC. 1986. Comparison of fatty acid content and DNA homology of the filamentous gliding bacteriaVitreoscilla, Flexibacter, Filibacter. *Archives of Microbiology* **146**: 1–6.

Nie M, Lu M, Bell J, Raut S, Pendall E. 2013. Altered root traits due to elevated CO_2 : a meta-analysis. *Global Ecology and Biogeography* **22**: 1095–1105.

Olsson PA. 1999. Signature fatty acids provide tools for determination of the distribution and interactions of mycorrhizal fungi in soil. *FEMS Microbiology Ecology* **29**: 303–310.

Oren R, Ellsworth DS, Johnsen KH, Phillips N, Ewers BE, Maier C, Schäfer KV, McCarthy H, Hendrey G, McNulty SG *et al.* 2001. Soil fertility limits carbon sequestration by forest ecosystems in a CO_2-enriched atmosphere. *Nature* **411**: 469–472.

Ouimette AP, Ollinger SV, Lepine LC, Stephens RB, Rowe RJ, Vadeboncoeur MA, Tumber-Davila SJ, Hobbie EA. 2020. Accounting for Carbon Flux to Mycorrhizal Fungi May Resolve Discrepancies in Forest Carbon Budgets. *Ecosystems* **23**: 715–729.

Parnell AC, Jackson A. 2013. siar: Stable Isotope Analysis in R.

Parnell AC, Inger R, Bearhop S, Jackson AL. 2010. Source partitioning using stable isotopes: coping with too much variation. *PloS one* **5**: e9672.

Paterson E, Sim A, Davidson J, Daniell TJ. 2016. Arbuscular mycorrhizal hyphae promote priming of native soil organic matter mineralisation. *Plant and Soil* **408**: 243–254.

Pausch J, Kuzyakov Y. 2012. Soil organic carbon decomposition from recently added and older sources estimated by $\delta^{13}C$ values of CO_2 and organic matter. *Soil Biology and Biochemistry* **55**: 40–47.

Pausch J, Zhu B, Kuzyakov Y, Cheng W. 2013. Plant inter-species effects on rhizosphere priming of soil organic matter decomposition. *Soil Biology and Biochemistry* **57**: 91–99.

Peay KG, Kennedy PG, Bruns TD. 2011. Rethinking ectomycorrhizal succession: are root density and hyphal exploration types drivers of spatial and temporal zonation? *Fungal Ecology* **4**: 233–240.

Peoples MB, Chalk PM, Unkovich MJ, Boddey RM. 2015. Can differences in ^{15}N natural abundance be used to quantify the transfer of nitrogen from legumes to neighbouring non-legume plant species? *Soil Biology and Biochemistry* **87**: 97–109.

Phillips DL, Gregg JW. 2003. Source partitioning using stable isotopes: coping with too many sources. *Oecologia* **136**(2): 261-269.

Phillips RP, Brzostek E, Midgley MG. 2013. The mycorrhizal-associated nutrient economy: a new framework for predicting carbon-nutrient couplings in temperate forests. *New Phytologist* **199**: 41–51.

Phillips RP, Meier IC, Bernhardt ES, Grandy AS, Wickings K, Finzi AC. 2012. Roots and fungi accelerate carbon and nitrogen cycling in forests exposed to elevated CO_2. *Ecology Letters* **15**: 1042–1049.

Piñeiro J, Ochoa-Hueso R, Delgado-Baquerizo M, Dobrick S, Reich PB, Pendall E, Power SA. 2017. Effects of elevated CO2 on fine root biomass are reduced by aridity but enhanced by soil nitrogen: A global assessment. *Scientific Reports* **7**: 15355.

Poeplau C, Don A, Six J, Kaiser M, Benbi D, Chenu C, Cotrufo MF, Derrien D, Gioacchini P, Grand S *et al.* 2018. Isolating organic carbon fractions with varying turnover rates in temperate agricultural soils – A comprehensive method comparison. *Soil Biology and Biochemistry* **125**: 10–26.

Post DM. 2002. Using stable isotopes to estimate trophic position: models, methods, and assumptions. *Ecology* **83**: 703–718.

Read DJ. 1991. Mycorrhizas in ecosystems. *Experientia* **47**: 376–391.

Read DJ, Perez-Moreno J. 2003. Mycorrhizas and nutrient cycling in ecosystems - a journey towards relevance? *New Phytologist* **157**: 475–492.

Reich PB, Oleksyn J, Modrzynski J, Mrozinski P, Hobbie SE, Eissenstat DM, Chorover J, Chadwick OA, Hale CM, Tjoelker MG. 2005. Linking litter calcium, earthworms and soil properties: a common garden test with 14 tree species. *Ecology Letters* **8**: 811–818.

Rich MK, Nouri E, Courty P-E, Reinhardt D. 2017. Diet of Arbuscular Mycorrhizal Fungi: Bread and Butter? *Trends in plant science* **22**: 652–660.

Ritz K, Young IM. 2004. Interactions between soil structure and fungi. *Mycologist* **18**: 52–59.

Sadava D, Hillis DM, Heller HC, Berenbaum. 2011. Purves Biologie. Heidelberg: Spektrum.

Saito M. 1995. Enzyme activities of the internal hyphae and germinated spores of an arbuscular mycorrhizal fungus, *Gigaspora margarita* Becker & Hall. *New Phytol* **129**: 425–431

Sanders IR, Streitwolf-Engel R, van der Heijden MGA, Boller T, Wiemken A. 1998. Increased allocation to external hyphae of arbuscular mycorrhizal fungi under CO_2 enrichment. *Oecologia*: 117: 496-503.

Schack-Kirchner H, Wilpert KV, Hildebrand EE. 2000. The spatial distribution of soil hyphae in structured spruce-forest soils. *Plant and Soil*: 195–205.

Schlesinger WH, Lichter J. 2001. Limited carbon storage in soil and litter of experimental forest plots under increased atmospheric CO_2. *Nature* **411**: 466–469.

Schmidt MWI, Torn MS, Abiven S, Dittmar T, Guggenberger G, Janssens IA, Kleber M, Kögel-Knabner I, Lehmann J, Manning DAC *et al.* 2011. Persistence of soil organic matter as an ecosystem property. *Nature* **478**: 49–56.

Shah F, Nicolás C, Bentzer J, Ellström M, Smits M, Rineau F, Canbäck B, Floudas D, Carleer R, Lackner G *et al.* 2016. Ectomycorrhizal fungi decompose soil organic matter using oxidative mechanisms adapted from saprotrophic ancestors. *New Phytologist* **209**: 1705–1719.

Smith SE, Read DJ. 2008. Mycorrhizal Symbiosis. New York: Elsevier.

Sokol NW, Bradford MA. 2019. Microbial formation of stable soil carbon is more efficient from belowground than aboveground input. *Nature Geoscience* **12**: 46–53.

Sokol NW, Kuebbing SE, Karlsen-Ayala E, Bradford MA. 2019. Evidence for the primacy of living root inputs, not root or shoot litter, in forming soil organic carbon. *The New phytologist* **221**: 233–246.

Soudzilovskaia NA, van Bodegom PM, Terrer C, Zelfde MV't, McCallum I, Luke McCormack M, Fisher JB, Brundrett MC, Sá NC de, **Tedersoo L. 2019.** Global mycorrhizal plant distribution linked to terrestrial carbon stocks. *Nature communications* **10**: 5077.

Suetsugu K, Matsubayashi J, Ogawa NO, Murata S, Sato R, Tomimatsu H. 2020. Isotopic evidence of arbuscular mycorrhizal cheating in a grassland gentian species. *Oecologia* **192**: 929–937.

Talbot JM, Allison SD, Treseder KK. 2008. Decomposers in disguise: mycorrhizal fungi as regulators of soil C dynamics in ecosystems under global change. *Functional Ecology* **22**: 955–963.

Tedersoo L, Bahram M. 2019. Mycorrhizal types differ in ecophysiology and alter plant nutrition and soil processes. *Biological Reviews* **94**: 1857–1880.

Tedersoo L, Bahram M, Zobel M. 2020. How mycorrhizal associations drive plant population and community biology. *Science (New York, N.Y.)* **367**.

Temperton VM, Grayston SJ, Jackson G, Barton CVM, Millard P, Jarvis PG. 2003. Effects of elevated carbon dioxide concentration on growth and nitrogen fixation in *Alnus glutinosa* in a long-term field experiment. *Tree Physiology* **23**: 1051–1059.

Tisserant E, Malbreil M, Kuo A, Kohler A, Symeonidi A, Balestrini R, Charron P, Duensing N, Frei dit Frey N, Gianinazzi-Pearson V *et al.* 2013. Genome of an arbuscular mycorrhizal fungus provides insight into the oldest plant symbiosis. *Proceedings of the National Academy of Sciences* **110**: 20117–20122.

Toljander JF, Lindahl BD, Paul LR, Elfstrand M, Finlay RD. 2007. Influence of arbuscular mycorrhizal mycelial exudates on soil bacterial growth and community structure. *FEMS Microbiology Ecology* **61**: 295–304.

Treseder KK. 2004. A meta-analysis of mycorrhizal responses to nitrogen, phosphorus, and atmospheric CO_2 in field studies. *The New Phytologist* **164**: 347–355.

Treseder KK, Allen MF. 2000. Mycorrhizal fungi have a potential role in soil carbon storage under elevated CO_2 and nitrogen deposition. *The New Phytologist* **147**: 189–200.

van Schöll L, Kuyper TW, Smits MM, Landeweert R, Hoffland E, van Breemen N. 2008. Rock-eating mycorrhizas: their role in plant nutrition and biogeochemical cycles. *Plant and Soil* **303**: 35–47.

Verbruggen E, Pena R, Fernandez CW, Soong JL. 2017. Mycorrhizal Interactions With Saprotrophs and Impact on Soil Carbon Storage. In: *Mycorrhizal Mediation of Soil*. Elsevier, 441–460.

Veresoglou SD, Chen B, Rillig MC. 2012. Arbuscular mycorrhiza and soil nitrogen cycling. *Soil Biology and Biochemistry* **46**: 53–62.

Vidal A, Klöffel T, Guigue J, Angst G, Steffens M, Hoeschen C, Mueller CW. 2021. Visualizing the transfer of organic matter from decaying plant residues to soil mineral surfaces controlled by microorganisms. *Soil Biology and Biochemistry* **160**: 108347.

Walder F, Niemann H, Lehmann MF, Boller T, Wiemken A, Courty P-E. 2013. Tracking the carbon source of arbuscular mycorrhizal fungi colonizing C3 and C4 plants using carbon isotope ratios ($\delta^{13}C$). *Soil Biology and Biochemistry* **58**: 341–344.

Walder F, Niemann H, Natarajan M, Lehmann MF, Boller T, Wiemken A. 2012. Mycorrhizal networks: common goods of plants shared under unequal terms of trade. *Plant physiology* **159**: 789–797.

Wallander H, Mörth C-M, Giesler R. 2009. Increasing abundance of soil fungi is a driver for (^{15})N enrichment in soil profiles along a chronosequence undergoing isostatic rebound in northern Sweden. *Oecologia* **160**: 87–96.

Waring BG, Adams R, Branco S, Powers JS. 2016. Scale-dependent variation in nitrogen cycling and soil fungal communities along gradients of forest composition and age in regenerating tropical dry forests. *New Phytologist* **209**: 845–854.

Welc M, Frossard E, Egli S, Bünemann EK, Jansa J. 2014. Rhizosphere fungal assemblages and soil enzymatic activities in a 110-years alpine chronosequence. *Soil Biology and Biochemistry* **74**: 21–30.

Werth M, Kuzyakov Y. 2010. ^{13}C fractionation at the root–microorganisms–soil interface: A review and outlook for partitioning studies. *Soil Biology and Biochemistry* **42**: 1372–1384.

Whiteside MD, Garcia MO, Treseder KK. 2012. Amino acid uptake in arbuscular mycorrhizal plants. *PloS one* **7**: e47643.

Wittig R, Streit B. 2004. Ökologie. Stuttgart: Eugen Ulmer.

Witzgall K, Vidal A, Schubert DI, Höschen C, Schweizer SA, Buegger F, Pouteau V, Chenu C, Mueller CW. 2021. Particulate organic matter as a functional soil component for persistent soil organic carbon. *Nature Communications* **12**: 4115.

Yanai RD, Fahey TJ, Miller SL. 1995. Efficiency of Nutrient Acquisition by Fine Roots and Mycorrhizae. In: *Resource Physiology of Conifers*. Elsevier, 75–103.

Zak DR, Pellitier PT, Argiroff W, Castillo B, James TY, Nave LE, Averill C, Beidler KV, Bhatnagar J, Blesh J, Classen AT, Craig M, Fernandez CW, Gundersen P, Johansen R, Koide RT, Lilleskov EA, Lindahl BD, Nadelhoffer KJ, Phillips RP, Tunlid A. 2019. Exploring the role of ectomycorrhizal fungi in soil carbon dynamics. *New Phytologist* **223**(1): 33-39.

Zeller B, Brechet C, Maurice J-P, Le Tacon F. 2007. ^{13}C and ^{15}N isotopic fractionation in trees, soils and fungi in a natural forest stand and a Norway spruce plantation. *Annals of Forest Science* **64**: 419–429.

Zhang H-Y, Lü X-T, Hartmann H, Keller A, Han X-G, Trumbore S, Phillips RP, Xu X. 2018. Foliar nutrient resorption differs between arbuscular mycorrhizal and ectomycorrhizal trees at local and global scales. *Global Ecology and Biogeography* **27**: 875–885.

"*If a healthy soil is full of death, it is also full of life: worms, fungi, microorganisms of all kinds…Given only the health of the soil, nothing that dies is dead for very long*"

Unknown

Chapter 1 introduces

- The plant-fungi-soil system
- The role of fungi in ecosystems
- Stable isotopes and fungi
- Carbon and nutrient fluxes in the plant-fungi-soil system
- Impact of the plant-fungi-association on soil organic matter
- Tracing carbon and nutrient fluxes and estimating inputs
- Impacts of climate change on nutrient cycling and SOM dynamics
- Objectives of this thesis

Chapter 2 presents the

- Main results
- Author contributions
- List of further publications
- References

Chapter 3 displays the

- Manuscripts of this thesis
- Declaration

Chapter 3

9 Manuscripts of this thesis

Manuscript 1

Stable C and N isotope natural abundances of intraradical hyphae of arbuscular mycorrhizal fungi

Saskia Klink[1], Philipp Giesemann[2], Timo Hubmann[1], Johanna Pausch[1]

Mycorrhiza 30(6): 773-780 (2020), doi: 10.1007/s00572-020-00981-9

[1]Department of Agroecology, Bayreuth Center of Ecology and Environmental Research (BayCEER), University of Bayreuth, 95440 Bayreuth, Germany

[2]Laboratory of Isotope Biogeochemistry, Bayreuth Center of Ecology and Environmental Research (BayCEER), University of Bayreuth, 95440 Bayreuth, Germany

Key words: Mycorrhiza, Hyphae, $\delta^{13}C$, $\delta^{15}N$, Nitrogen acquisition, Plant carbon

Received: 2 June 2020; Accepted: 11 August 2020; Published online: 25 August 2020

Mycorrhiza
https://doi.org/10.1007/s00572-020-00981-9

SHORT NOTE

Stable C and N isotope natural abundances of intraradical hyphae of arbuscular mycorrhizal fungi

Saskia Klink[1] · Philipp Giesemann[2] · Timo Hubmann[1] · Johanna Pausch[1]

Received: 2 June 2020 / Accepted: 11 August 2020

Abstract
Data for stable C and N isotope natural abundances of arbuscular mycorrhizal (AM) fungi are currently sparse, as fungal material is difficult to access for analysis. So far, isotope analyses have been limited to lipid compounds associated with fungal membranes or storage structures (biomarkers), fungal spores and soil hyphae. However, it remains unclear whether any of these components are an ideal substitute for intraradical AM hyphae as the functional nutrient trading organ. Thus, we isolated intraradical hyphae of the AM fungus *Rhizophagus irregularis* from roots of the grass *Festuca ovina* and the legume *Medicago sativa* via an enzymatic and a mechanical approach. In addition, extraradical hyphae were isolated from a sand-soil mix associated with each plant. All three approaches revealed comparable isotope signatures of *R. irregularis* hyphae. The hyphae were ^{13}C- and ^{15}N-enriched relative to leaves and roots irrespective of the plant partner, while they were enriched only in ^{15}N compared with soil. The ^{13}C enrichment of AM hyphae implies a plant carbohydrate source, whereby the enrichment was likely reduced by an additional plant lipid source. The ^{15}N enrichment indicates the potential of AM fungi to gain nitrogen from an organic source. Our isotope signatures of the investigated AM fungus support recent findings for mycoheterotrophic plants which are suggested to mirror the associated AM fungi isotope composition. Stable isotope natural abundances of intraradical AM hyphae as the functional trading organ for bi-directional carbon-for-mineral nutrient exchanges complement data on spores and membrane biomarkers.

Keywords Mycorrhiza · Hyphae · $\delta^{13}C$ · $\delta^{15}N$ · Nitrogen acquisition · Plant carbon

Introduction

Natural abundances of stable isotopes are used to trace carbon and both inorganic and organic nitrogen fluxes within plants, fungi and their associations (e.g. Gleixner et al. 1993; Gebauer and Dietrich 1993; Courty et al. 2015; Chen et al. 2019; Giesemann et al. 2020; Suetsugu et al. 2020). While profound isotopic data exist for ectomycorrhizal and saprotrophic fungi, information on arbuscular mycorrhizal (AM) fungi remain sparse due to the limited accessibility of sporocarps and the fragile nature of hyphae.

Nevertheless, a few data on isotope natural abundances are available from spores, soil hyphae and biomarkers such as phospholipid fatty acids (PLFAs) or neutral lipid fatty acids (NLFAs) (Allen and Allen 1990; Nakano et al. 1999; Courty et al. 2011, 2015; Walder et al. 2012, 2013; Suetsugu et al. 2020). Still, it is unclear whether spores and PLFA/NLFA biomarkers mirror intraradical hyphae, the functional trading organ. For instance, Courty et al. (2015) assumed the carbon (^{13}C) isotopic signature of spores might be variable because of variable lipid storage and therefore that spores may not represent an ideal substitute for AM hyphal tissue.

Mycorrhizal fungi are supplied with ^{13}C-enriched carbon from their plant partner (Gleixner et al. 1993; Gebauer et al. 2016). Thus, we expect a ^{13}C enrichment for AM hyphae relative to plant bulk material. Such ^{13}C enrichment for AM

Saskia Klink and Philipp Giesemann have shared first authorship.

Electronic supplementary material The online version of this article (https://doi.org/10.1007/s00572-020-00981-9) contains supplementary material, which is available to authorized users.

✉ Johanna Pausch
johanna.pausch@uni-bayreuth.de

[1] Department of Agroecology, Bayreuth Center of Ecology and Environmental Research (BayCEER), University of Bayreuth, 95440 Bayreuth, Germany

[2] Laboratory of Isotope Biogeochemistry, Bayreuth Center of Ecology and Environmental Research (BayCEER), University of Bayreuth, 95440 Bayreuth, Germany

Published online: 25 August 2020

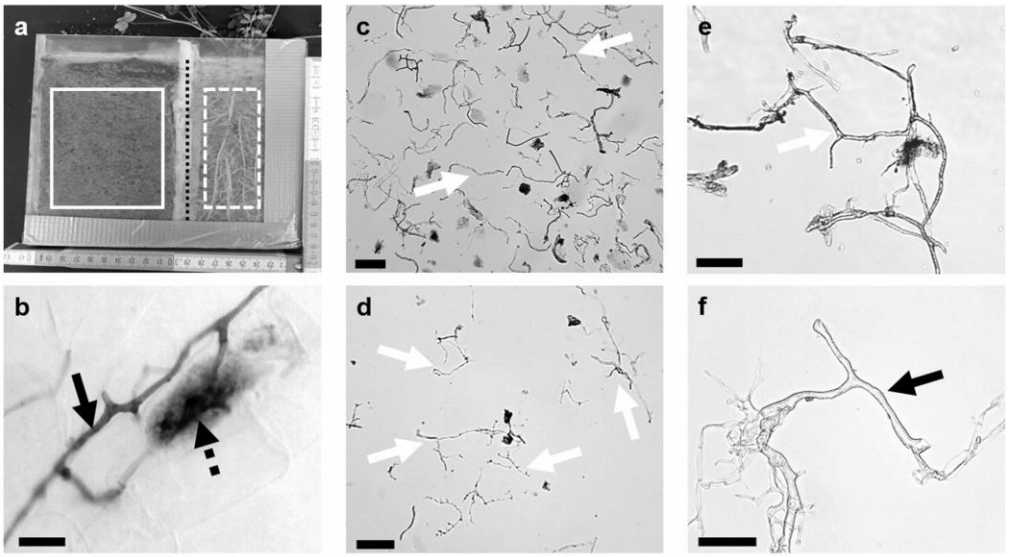

Fig. 1 Collage of split rhizoboxes and AM hyphae isolation procedure. (**a**) Side view of *Medicago sativa* planted in a split rhizobox. The white box illustrates the hyphae-only compartment (HC), the white dashed box the plant root compartment (PC), both separated by a 30 μm pore size mesh (dashed black line). (**b**) Hyphae of AMF (black arrow) and arbuscule (dashed arrow) within root cells. (**c**) Soil hyphae (white arrows) and organic material after suspending in sodium-hexametaphosphate, (**d**) soil hyphae (white arrows) after cleaning and sieving steps. (**e**) AMF hyphae (white arrow) from soil, (**f**) AMF hyphae (black arrow) from root extraction. Scale **b**, **f** 10 μm; **c**–**e** 100 μm

novel mechanical approach which aimed to avoid chemical-induced isotopic fractionation. Microscopic observation (Motic BA210; Fig. 1b–f) of aseptate, hyaline hyphae, seldom accompanied by arbuscules, vesicles and spores between the procedures was always a key step to evaluate the success of hyphal isolation.

According to our alteration from Saito (1995), roots cut into 5 mm segments and washed with deionized water were sonicated (35 kHz; Bandelin, Sonorex RK100H, Berlin, Germany) to remove soil residues and external hyphae. Constituents of the enzyme solution were 20 g L^{-1} Cellulase 'Onozuka' RS (SERVA Electrophoresis GmbH, Heidelberg, Germany), 1 g L^{-1} Pectolyase 'Y23' (Sigma-Aldrich, Darmstadt, Germany) in 0.01 M MES-KOH pH 5.5 buffer (Carl Roth, Karlsruhe, Germany). The penetration rate of the enzyme solution was increased by sonication (10 min at 20 °C) instead of using an aspirator. If not mentioned otherwise, all steps were performed at 4 °C. For the mechanical isolation, 5 mm root segments were washed with deionized water; root cell layers opened with scalpels by slicing sagittally while holding with tweezers, followed by sonication (30 min at 20 °C) in deionized water to release hyphae from the sliced roots into the water column. To compare intraradical and extraradical AM hyphae, soil hyphae (HC) were isolated according to Brundrett et al. (1994), using the whole sample (5 g soil) instead of an aliquot to increase the recovery of hyphae in a suitable amount for isotopic measurement.

Cleaning steps were identical for all samples of intraradical and soil hyphae. A combination of stacked 500 μm, 250 μm, 90 μm, 63 μm, and 20 μm sieves (Retsch test sieve, stainless steel, DIN/ISO 3310-1, Germany) separated hyphae from coarse roots, plant residues and soil particles, whereby sodium-hexametaphosphate and enzyme solution remains were washed out. To ensure a high recovery of hyphae, the sieve surface was gently sprayed and rinsed with deionized water several times. Here, most hyphae were recovered from the 20 μm sieve. It is to be noted that when isolating hyphae of different morphologies, e.g. coils or pelotons, these large structures may necessitate a greater mesh size. Cleaned hyphae (Fig. 1d) were washed from the sieve into Eppendorf tubes and centrifuged (5 s at 1306×*g*, Eppendorf Centrifuge 5415 C, Eppendorf AG, Hamburg, Germany). Microscopic observation showed that both the supernatant and the pellet contained hyphae. Because the supernatant comprised clean hyphae, while the pellet was a mixture of hyphae and organic residue, hyphae were collected from the supernatant. This collection of hyphae had to be done quickly to recover hyphae before they settled to the bottom of the tube with the soil residues. The pellet was resuspended, and the centrifugation step repeated 4–5 times until no appreciable number of

hyphae were microscopically observable either in the supernatant or in the pellet. A hyphal pellet then was produced by centrifugation (20 min at 3220×*g*, Centrifuge 5810R, Eppendorf AG, Hamburg, Germany) and dried at 60 °C for 72 h. Storage was in desiccators with silica gel until stable isotope analysis.

As an additional test for chemical-induced isotopic fractionation on fungal tissue with a greater sample mass than AMF hyphae, sporocarps of *Agaricus bisporus* (J. E. LANGE) IMBACH treated with either the enzyme or sodium-hexametaphosphate solution were compared with non-treated controls.

Stable isotope analysis

Hyphal material (soil hyphae $n = 8$, intraradical hyphae: mechanic $n = 8$, enzymatic $n = 4$; $n = 20$ per plant species) was suspended in 200 µL deionized water, transferred into tin capsules (4 × 6 mm) and dried for 24 h at 60 °C. This procedure was repeated until the complete hyphal suspension was dried into the tin capsules. Due to the low weight of hyphae, the 'N blank effect', occurring when the O_2 pulse is supplied in the elemental analyser isotope ratio mass spectrometer (EA-IRMS), can lead to increasingly inaccurate ^{15}N values, while ^{13}C is not affected (Crotty et al. 2013). Therefore, a subset of eight hyphal samples (soil hyphae $n = 4$; intraradical hyphae: mechanic $n = 4$; $n = 2$ per species) was analysed with a Micro Elemental Analyser Isotope Ratio Mass Spectrometer (µEA-IRMS), specialized for samples with a low weight and sample size. The results of these measurements show the combination of $\delta^{15}N$ and $\delta^{13}C$ values of AMF hyphae and corroborate the ^{13}C data of soil hyphae and intraradical hyphae (both mechanic and enzymatic isolation) gained from the EA-IRMS measurement. Hyphal samples with unreliable signal intensity for $\delta^{15}N$ were omitted for this study, resulting in a total of twelve hyphal samples for ^{15}N ($n = 3$ for soil hyphae, $n = 3$ for mechanically isolated intraradical hyphae per plant species).

Plant leaves ($n = 12$ per plant species), roots ($n = 6$ per plant species), soil (HC, $n = 6$ per plant species), fruiting bodies of *Agaricus bisporus* ($n = 24$) and hyphae were analysed for stable isotope natural abundance of $\delta^{13}C$, $\delta^{15}N$ and C- and N- concentrations at the BayCEER Laboratory of Isotope-Biogeochemistry (EA-IRMS; University of Bayreuth, Germany) and the Centre for Stable Isotope Research and Analysis (µEA-IRMS; Georg-August-University, Göttingen, Germany). The isotope abundances are expressed as δ-notation relative to Vienna-PDBelemite (^{13}C standard) or air (^{15}N standard): $\delta^{13}C$ or $\delta^{15}N = (R_{sample}/R_{standard} - 1) \times 1000$ (‰), whereby R is the ratio of the heavy to the respective light isotope.

Statistics

Software RStudio 1.2.5019 (RStudio Team 2019) was used for statistical analysis, and graphics were created with RStudio or SigmaPlot 11.0 (Systat Software, San Jose, USA). Shapiro-Wilk's test for all data supported a non-parametric test procedure. One-tailed Kruskal-Wallis (H) tests followed by pairwise Wilcoxon post hoc test procedures (Z) were applied for differences across hyphal, plant and soil samples as well as across the hyphae isolation methods. P values were adjusted with a Holm-Bonferroni correction. Mann-Whitney U tests were applied to evaluate chemical-induced differences between treated samples and controls. The level of significance was $\alpha = 0.05$.

Results and discussion

Isotopic patterns of AM hyphae relative to associated plants and soil

Our data show for the first time, to our knowledge, stable $\delta^{13}C$ and $\delta^{15}N$ isotope natural abundances of intraradical AM hyphae (Fig. 2a). The isolated AM fungal material was *c*. 6.5‰ enriched relative to leaves and *c*. 4.6‰ relative to roots in ^{13}C and *c*. 4.2‰ enriched relative to leaves and *c*. 4.9‰ relative to roots in ^{15}N (Fig. 2a). The ^{13}C signatures of soil and AM fungal material were clustered together yet showed distinct ^{15}N enrichment with 2.4‰ higher ^{15}N enrichment of the AM hyphae compared with the soil. No significant differences in hyphal $\delta^{13}C$ were discovered among the three isolation approaches either for hyphae from the grass ($H = 2.479$, df = 2, $P = 0.29$) or from the legume ($H = 0.106$, df = 2, $P = 0.95$; Fig. 2b). The same holds true for $\delta^{15}N$ comparing the two groups of soil hyphae isolated by sieving and the mechanically isolated intraradical hyphae (grass $U(3,3) = 5$, $P = 1.000$, legume $U(3,3) = 2$, $P = 0.383$; Fig. 2a). No influence of involved extracting agents was detected (Table S2). Hyphae samples were significantly enriched in $\delta^{13}C$ and $\delta^{15}N$ relative to leaves, roots and soil of *Festuca* ($\delta^{13}C$: $H = 24.296$, df = 3, $P < 0.001$; $\delta^{15}N$: $H = 25.211$, df = 3, $P < 0.001$) and of *Medicago* ($\delta^{13}C$: $H = 22.734$, df = 3, $P < 0.001$; $\delta^{15}N$: $H = 25.203$, df = 3, $P < 0.001$) (Fig. 2a; pairwise comparisons Table S1). The dual isotope approach supports an isotopic separation of hyphae from soil in ^{15}N and hyphae from plant in ^{13}C and ^{15}N.

Higher transpiration rates and lower water use efficiency in the C_3 monocot grass relative to the dicotyledon legume (Rawson et al. 1977; Adams et al. 2016) likely resulted in significantly $\delta^{13}C$ enriched legume leaves relative to grass leaves ($U(12,12) = 135$, $P < 0.001$), while more depleted legume leaf $\delta^{15}N$ values ($U(12,12) = 32$, $P = 0.020$) relative to the grass may indicate a contribution of the N-fixing bacteria within the 78-day growth period, although the soil was sterilized at the beginning. Mycorrhizal fungi transfer mineral nutrients via their hyphae to their plant partners in exchange for carbohydrates originating from photosynthesis (Wipf et al.

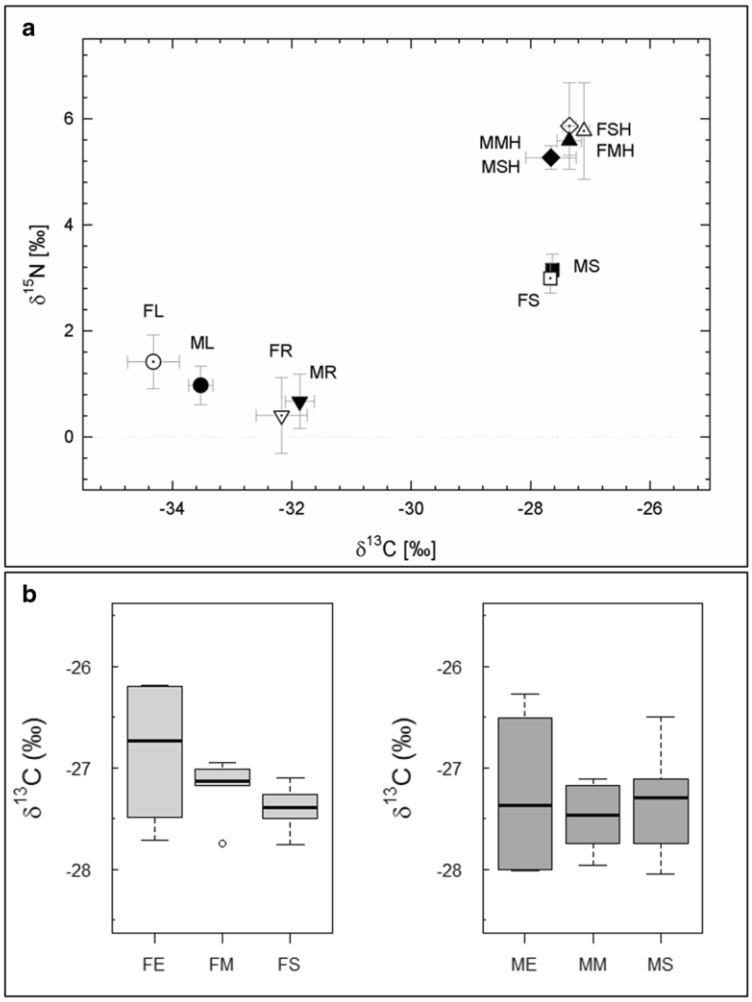

Fig. 2 **a** Scatter plot of $\delta^{13}C$ and $\delta^{15}N$ stable isotope natural abundances of leaves (circles), roots (downwards triangles), soil (squares), soil hyphae (diamonds) and mechanically isolated intraradical hyphae (upwards triangles) from the grass *Festuca ovina* (white symbols) and the legume *Medicago sativa* (black symbols) microcosms. FL *Festuca* leaves, ML *Medicago* leaves, FR *Festuca* roots, MR *Medicago* roots, FS *Festuca* soil, MS *Medicago* soil, FSH *Festuca* soil hyphae, FMH *Festuca* mechanically isolated hyphae, MSH *Medicago* soil hyphae, MMH *Medicago* mechanically isolated hyphae. Error bars indicate standard deviation (SD). **b** Whisker boxplot of $\delta^{13}C$ values of AM fungal hyphae from the grass (left) and the legume (right), respectively, shown for the different isolation methods (soil hyphae; intraradical hyphae: mechanic vs enzymatic). FS *Festuca* soil hyphae, MS *Medicago* soil hyphae, FM *Festuca* mechanically isolated hyphae, MM *Medicago* mechanically isolated hyphae, FE *Festuca* enzymatically isolated hyphae, ME *Medicago* enzymatically isolated hyphae. The black line in the centre of the box indicates the median, box margins represent the 25th and 75th percentiles. The length of the box is the inter quartile range (IQR), whiskers indicate the minimum (25th percentile − 1.5 × IQR) and the maximum (75th percentile + 1.5 × IQR). Outliers are shown as circles

2019). The ^{13}C enrichment of AM hyphae potentially results from the gain of ^{13}C-enriched carbohydrates from the plant (cf. Gleixner et al. 1993). Additionally, AM fungi lack the ability of lipid synthesis. Thus, lipids originated from the plant partner (Luginbuehl et al. 2017; Jiang et al. 2017; Keymer et al. 2017; Rich et al. 2017) likely represent a supplemental carbon source. Lipids were shown to be ^{13}C-depleted relative to bulk tissue by Gleixner et al. (1993). We here detected ^{13}C enrichment of AM soil hyphae and intraradical hyphae of about 6‰ relative to the plant which is consistent with findings on AM soil hyphae by Walder et al. (2012), but also is less pronounced than the relative ^{13}C enrichment of ectomycorrhizal fruiting bodies relative to their associated plants of about 6–10‰ (cf. Trudell et al. 2004; Gebauer et al. 2016; Schiebold et al. 2017; Chen et al. 2019). While ectomycorrhizal fungi mostly rely on plant-derived carbohydrates, the ^{13}C enrichment of AM fungi appears to be counterbalanced by a mixture of two carbon sources, plant-originated carbohydrates and lipids. Walder et al. (2012) claimed contamination by soil particles could not be excluded while the ^{13}C and ^{15}N dual isotope approach utilized here supports an isotopic separation of hyphae relative to soil.

Arbuscular mycorrhizal fungi are assumed to possess limited saprotrophic capability (Nakano et al. 1999; Smith and

Read 2008; Tisserant et al. 2013) which should ultimately result in the utilization of similar inorganic nitrogen sources as the plant partner. Therefore, an insignificant difference in ^{15}N natural abundance between plant and AM hyphae was expected. To the contrary, our data show an ^{15}N enrichment for the AM hyphae relative to plant leaf material by *c.* 4.2‰. Perhaps, the AM fungi also might utilize low molecular weight organic nitrogen sources that possibly were released from bacterial biomass by the steam-sterilizing process. A labile organic nitrogen source might explain the ^{15}N enrichment, despite translocation of ammonium and nitrate to the plants. This is concurrent with earlier analysis by Gebauer and Dietrich (1993) on ectomycorrhizas. Nonetheless, a part of the ^{15}N enrichment is likely still a result of trophic enrichment (DeNiro and Epstein 1981, Peterson and Fry 1987). The gain of nitrogen from organic material (cf. Hodge et al. 2001; Leigh et al. 2009) might be dependent on AMF species and strain.

Furthermore, our findings of ^{13}C and ^{15}N enrichment support studies of mycoheterotrophic plants and their AM fungi, which so far may have been compromised by surrogates for AM fungal isotopic signatures. Mycoheterotrophic plants (MHP) partially or completely cover their carbon demand from a fungal source (Hynson et al. 2013; Merckx 2013). The MHP leaves' ^{15}N patterns were found to be determined by the MHP's root fungi (Schiebold et al. 2017). Hitherto, ^{13}C and frequently ^{15}N enrichments of MHP with AM fungi were associated with fungal identity, different fungal communities and different geographic origin (Merckx et al. 2010; Courty et al. 2011; Giesemann et al. 2020; Gomes et al. 2020). The previous lack of proof of ^{13}C and ^{15}N enrichment of the AM fungus itself was a major point of limitation, which can now be addressed with the methods described here.

Practicability of AM hyphal isotopic patterns

Several studies have shown successful accessing of AM fungal spores and specific fungal compounds, such as PLFA/NLFA 16:1ω5, for stable isotope analyses (Allen and Allen 1990; Nakano et al. 1999; Courty et al. 2011; Walder et al. 2012, 2013; Courty et al. 2015; Suetsugu et al. 2020). Nevertheless, spores and PLFAs/NLFAs biomarkers often show different isotopic signatures than hyphae. Spores' range from a 1.5 to 5.2‰ ^{13}C depletion relative to the root (Allen and Allen 1990; Nakano et al. 1999; Walder et al. 2012) and 1.2 to 4.9‰ ^{13}C enrichment relative to the plant (Courty et al. 2011; Suetsugu et al. 2020). PLFA C16:1ω5 was approx. 2.4‰ more ^{13}C-depleted than roots (Walder et al. 2013; Ven et al. 2020) and NLFA C16:1ω5 was approx. 3.7‰ more ^{13}C-depleted than roots (Ven et al. 2020). In contrast, AM hyphae have previously been shown to be continuously ^{13}C-enriched by around 5‰ (Walder et al. 2012, and this study) relative to plant leaves, a pattern also found for other mycorrhizas (ECM) (e.g. Gebauer et al. 2016; Chen et al. 2019). Thus, when isotopic data on hyphae as the active nutrient pathway are required in future research, the approach presented here could be considered.

Isolation of coenocytic AM hyphae bears the risk of loss of cytoplasm and the inclusion of bacterial biofilms. In our study, the aim was to minimize the risk of isotopic fractionation induced by chemicals, wherefore the vitality of hyphae was neglected. Applying the approach presented in Saito (1995) allows for the gain of living hyphae (due to the presence of several buffers and solutions) with minimized loss of cytoplasm. Eventually, the trade-off between intact, living hyphae or the minimization of chemical-induced isotopic fractionation needs to be evaluated. An impact of bacterial biofilms adhering to hyphal surfaces cannot be excluded completely. Nevertheless, this impact should be present, despite varying bacterial diversity, for soil hyphae and plant roots (Marilley et al. 1998; Roesch et al. 2008), plus potentially for AM fungal spores. In addition, an influence of bacteria might also occur in PLFA analyses, as the frequently applied AM fungi–specific PLFA C16:1ω5 was also found in some Gram-negative bacteria and can be affected by degrading spores (Nichols et al. 1986; Joergensen and Wichern 2008; Ngosong et al. 2012; Paterson et al. 2016). NLFA 16:1ω5 are considered more specific to AM fungi than PLFA 16:1ω5 as they accumulate as a carbon storage compound in biomass (Olsson et al. 2005) and the ratio between NLFA and PLFA 16:1ω5 is higher in AM fungi than in bacteria (Olsson 1999). However, background NLFA 16:1ω5 concentrations of spores and free neutral lipids from non-living biomass with a long residence time also were described for these biomarkers (Paterson et al. 2016). Lately, the absence of a completely AM fungi–specific fatty acid and differences in the fatty acid composition between AM fungal species and genera need to be considered (Olsson 1999). While both AM hyphae and biomarkers can be affected by bacteria, PLFA/NLFA biomarkers for ^{13}C AM isotopic data may be supplemented by ^{15}N isotope natural abundance signatures of the AM hyphae.

When aiming to transfer the approaches presented here for isolation of AM fungal hyphae to field trials, the question of separation from other fungal groups occurs. For soil hyphae, AMF could be separated from other fungal groups under the dissecting microscope via the presence or absence of septa (Smith and Read 2008). Choosing the isolation of intraradical hyphae from roots potentially reduces the diversity of other fungal groups than AM fungi relative to soil (Gao et al. 2019; Mahmoudi et al. 2019) due to plants' selection mechanisms, while potentially increasing the AM fungal diversity (Mahmoudi et al. 2019). To increase chances of high AM fungal colonization, multiple fine-root fragments instead of single long roots should be sampled (cf. Mahmoudi et al. 2019).

Outlook

The constancy of stable isotope ^{13}C and ^{15}N patterns needs to be analysed on a broader scale and along different genera, species and strains of AM fungi. Assuming the existence of relatively defined isotopic variability within AM fungi, the comparison of dual or multi-isotope patterns of different fungal groups may represent a possibility to estimate the contribution of fungal groups to nutrient trading within mycorrhizal networks, especially in field trials. Picking-up the C_3-C_4-Common Mycorrhizal Network approach conducted by Walder et al. (2012), (2013) and Courty et al. (2015), the analysis of intraradical hyphal isotopic patterns complementary to soil hyphae, spores or biomarkers might reveal an interesting perspective. Finally, the possibility of intraradical hyphae extraction might further support research on AM mycoheterotrophic plants and shed light on the insufficiently known function of difficult to access ascomycotan dark septate endophytes or basidiomycotan *Rhizoctonia*-like fungi.

Acknowledgements We thank the Laboratory of Isotope Biogeochemistry at the University of Bayreuth and the Centre for Stable Isotope Research and Analysis at the Georg August University Göttingen for stable isotope analyses. We thank Gerhard Gebauer for input on the results and Adrienne Keller for native speaker language improvement and commenting. Special thanks to the Editor David P. Janos and an anonymous reviewer for their helpful comments, which greatly improved this work.

Authors' contribution Saskia Klink, Philipp Giesemann and Johanna Pausch conceived the experimental design. Experimental set-up was conducted and data analysis was performed by Saskia Klink, Philipp Giesemann and Timo Hubmann. Saskia Klink wrote the first draft of the manuscript. Comments and approval on all previous versions and the final version of the manuscript were given by all authors.

Funding information Open Access funding provided by Projekt DEAL. This work was funded by the German Research Foundation (DFG project No.: PA2377/2-1).

Availability of data and material The single $\delta^{13}C$, $\delta^{15}N$, N-content and C:N ratio values can be obtained from the supplemental material (Table S3).

Compliance with ethical standards

Conflict of interest The authors declare that they have no conflict of interest.

Code availability Not applicable.

References

Adams MA, Turnbull TL, Sprent JI, Buchmann N (2016) Legumes are different: leaf nitrogen, photosynthesis, and water use efficiency. Proc Natl Acad Sci U S A 113:4098–4103

Allen EB, Allen MF (1990) The mediation of competition by mycorrhizae in successional and patchy environments. In: Grace JB (ed) Perspectives on plant competition. Acad. Press, San Diego, pp 367–389

Brundrett M, Addy H, McGonigle T (1994) Extraction and staining of hyphae from soil. In: Brundrett M, Melville L, Peterson L (eds) . Mycologue Publications, Guelph, pp 24–34

Chen J, Heikkinen J, Hobbie EA, Rinne-Garmston KT, Penttilä R, Mäkipää R (2019) Strategies of carbon and nitrogen acquisition by saprotrophic and ectomycorrhizal fungi in Finnish boreal *Picea abies*-dominated forests. Fungal Biol 123:456–464

Courty P-E, Doubková P, Calabrese S, Niemann H, Lehmann MF, Vosátka M, Selosse M-A (2015) Species-dependent partitioning of C and N stable isotopes between arbuscular mycorrhizal fungi and their C_3 and C_4 hosts. Soil Biol Biochem 82:52–61

Courty P-E, Walder F, Boller T, Ineichen K, Wiemken A, Rousteau A, Selosse M-A (2011) Carbon and nitrogen metabolism in mycorrhizal networks and mycoheterotrophic plants of tropical forests: a stable isotope analysis. Plant Physiol 156:952–961

Cranenbrouck S, Voets L, Bivort C, Renard L, Strullu D-G, Declerck S (2005) Methodologies for in vitro cultivation of arbuscular mycorrhizal fungi with root organs. In: Declerck S, Fortin JA, Strullu D-G (eds) In vitro culture of Mycorrhizas. Springer-Verlag Berlin Heidelberg, Berlin, pp 341–375

Crotty FV, Stocki M, Knight JD, Adl SM (2013) Improving accuracy and sensitivity of isotope ratio mass spectrometry for $\delta^{13}C$ and $\delta^{15}N$ values in very low mass samples for ecological studies. Soil Biol Biochem 65:75–77

DeNiro MJ, Epstein S (1981) Influence of diet on the distribution of nitrogen isotopes in animals. Geochim et Cosmochim Acta 45(3): 341–351

Field KJ, Pressel S (2018) Unity in diversity: structural and functional insights into the ancient partnerships between plants and fungi. New Phytol 220:996–1011

Gao C, Montoya L, Xu L, Madera M, Hollingsworth J, Purdom E, Hutmacher RB, Dahlberg JA, Coleman-Derr D, Lemaux PG, Taylor JW (2019) Strong succession in arbuscular mycorrhizal fungal communities. ISME J 13:214–226

Gebauer G, Dietrich P (1993) Nitrogen isotope ratios in different compartments of a mixed stand of spruce, larch and beech trees and of understorey vegetation including fungi. Isot Environ Healt S 29:35–44

Gebauer G, Preiss K, Gebauer AC (2016) Partial mycoheterotrophy is more widespread among orchids than previously assumed. New Phytol 211:11–15

Giesemann P, Rasmussen HN, Liebel HT, Gebauer G (2020) Discreet heterotrophs: green plants that receive fungal carbon through *Paris*-type arbuscular mycorrhiza. New Phytol 226:960–966

Gleixner G, Danier HJ, Werner RA, Schmidt HL (1993) Correlations between the ^{13}C content of primary and secondary plant products in different cell compartments and that in decomposing Basidiomycetes. Plant Physiol 102:1287–1290

Gomes SIF, Merckx VSFT, Kehl J, Gebauer G (2020) Mycoheterotrophic plants living on arbuscular mycorrhizal fungi are generally enriched in ^{13}C, ^{15}N, and ^{2}H isotopes. J Ecol 108: 1250–1261

Hodge A, Campbell CD, Fitter AH (2001) An arbuscular mycorrhizal fungus accelerates decomposition and acquires nitrogen directly from organic material. Nature 413:297–299

Hodge A, Fitter AH (2010) Substantial nitrogen acquisition by arbuscular mycorrhizal fungi from organic material has implications for N cycling. Proc Natl Acad Sci U S A 107:13754–13759

Hynson NA, Madsen TP, Selosse M-A, Adam IKU, Ogura-Tsujita Y, Roy M, Gebauer G (2013) The physiological ecology of mycoheterotrophy. In: Merckx VSFT (ed) Mycoheterotrophy: the biology of plants living on Fungi. Springer, New York, pp 297–342

Jiang Y, Wang W, Xie Q, Liu N, Liu L, Wang D, Zhang X, Yang C, Chen X, Tang D, Wang E (2017) Plants transfer lipids to sustain colonization by mutualistic mycorrhizal and parasitic fungi. Science 356: 1172–1175

Joergensen R, Wichern F (2008) Quantitative assessment of the fungal contribution to microbial tissue in soil. Soil Biol Biochem 40:2977–2991

Keymer A, Pimprikar P, Wewer V, Huber C, Brands M, Bucerius SL, Delaux P-M, Klingl V, von Röpenack-Lahaye E, Wang TL, Eisenreich W, Dörmann P, Parniske M, Gutjahr C (2017) Lipid transfer from plants to arbuscular mycorrhiza fungi. eLife 6:e29107

Leigh J, Hodge A, Fitter AH (2009) Arbuscular mycorrhizal fungi can transfer substantial amounts of nitrogen to their host plant from organic material. New Phytol 181:199–207

Luginbuehl LH, Menard GN, Kurup S, van Erp H, Radhakrishnan GV, Breakspear A, Oldroyd GED, Eastmond PJ (2017) Fatty acids in arbuscular mycorrhizal fungi are synthesized by the host plant. Science 356:1175–1178

Mahmoudi N, Cruz C, Mahdhi M, Mars M, Caeiro MF (2019) Arbuscular mycorrhizal fungi in soil, roots and rhizosphere of Medicago truncatula: diversity and heterogeneity under semi-arid conditions. PeerJ 7:e6401

Marilley L, Vogt G, Blanc M, Aragno M (1998) Bacterial diversity in the bulk soil and rhizosphere fractions of *Lolium perenne* and *Trifolium repens* as revealed by PCR restriction analysis of 16S rDNA. Plant Soil 198:219–224

Merckx V, Stöckel M, Fleischmann A, Bruns TD, Gebauer G (2010) ^{15}N and ^{13}C natural abundance of two mycoheterotrophic and a putative partially mycoheterotrophic species associated with arbuscular mycorrhizal fungi. New Phytol 188:590–596

Merckx VSFT (2013) Mycoheterotrophy: an introduction. In: Merckx VSFT (ed) Mycoheterotrophy: the biology of plants living on Fungi. Springer, New York, pp 1–17

Michelsen A, Quarmby C, Sleep D, Jonasson S (1998) Vascular plant ^{15}N natural abundance in heath and forest tundra ecosystems is closely correlated with presence and type of mycorrhizal fungi in roots. Oecologia 115:406–418

Michelsen A, Schmidt IK, Jonasson S, Quarmby C, Sleep D (1996) Leaf ^{15}N abundance of subarctic plants provides field evidence that ericoid, ectomycorrhizal and non-and arbuscular mycorrhizal species access different sources of soil nitrogen. Oecologia 105:53–63

Nakano A, Takahashi K, Kimura M (1999) The carbon origin of arbuscular mycorrhizal fungi estimated from $\delta^{13}C$ values of individual spores. Mycorrhiza 9:41–47

Ngosong C, Gabriel E, Ruess L (2012) Use of the signature fatty acid 16: 1ω5 as a tool to determine the distribution of arbuscular mycorrhizal fungi in soil. J Lipids 2012:236807

Nichols P, Stulp BK, Jones JG, White DC (1986) Comparison of fatty acid content and DNA homology of the filamentous gliding bacteria *Vitreoscilla*, *Flexibacter*, *Filibacter*. Arch Microbiol 146:1–6

Olsson P (1999) Signature fatty acids provide tools for determination of the distribution and interactions of mycorrhizal fungi in soil. FEMS Microbiol Ecol 29:303–310

Olsson PA, van Aarle IM, Gavito ME, Bengtson P, Bengtsson G (2005) ^{13}C incorporation into signature fatty acids as an assay for carbon allocation in arbuscular mycorrhiza. Appl Environ Microbiol 71: 2592–2599

Paterson E, Sim A, Davidson J, Daniell TJ (2016) Arbuscular mycorrhizal hyphae promote priming of native soil organic matter mineralisation. Plant Soil 408:243–254

Peterson BJ, Fry B (1987) Stable isotopes in ecosystem studies. Annu Rev Ecol Syst 18(1):293–320

Rawson HM, Begg JE, Woodward RG (1977) The effect of atmospheric humidity on photosynthesis, transpiration and water use efficiency of leaves of several plant species. Planta 134:5–10

Rich MK, Nouri E, Courty P-E, Reinhardt D (2017) Diet of arbuscular mycorrhizal fungi: bread and butter? Trends Plant Sci 22:652–660

Roesch LFW, Camargo FAO, Bento FM, Triplett EW (2008) Biodiversity of diazotrophic bacteria within the soil, root and stem of field-grown maize. Plant Soil 302:91–104

RStudio Team (2019) RStudio: integrated development for R. MA, Boston

Saito M (1995) Enzyme activities of the internal hyphae and germinated spores of an arbuscular mycorrhizal fungus, *Gigaspora margarita* Becker & Hall. New Phytol 129:425–431

Schiebold JM-I, Bidartondo MI, Karasch P, Gravendeel B, Gebauer G (2017) You are what you get from your fungi: nitrogen stable isotope patterns in *Epipactis* species. Ann Bot 119:1085–1095

Schulze E-D, Chapin FS, Gebauer G (1994) Nitrogen nutrition and isotope differences among life forms at the northern treeline of Alaska. Oecologia 100:406–412

Smith SE, Read DJ (2008) Mycorrhizal symbiosis, 3rd edn. Academic Press, London

Suetsugu K, Matsubayashi J, Ogawa NO, Murata S, Sato R, Tomimatsu H (2020) Isotopic evidence of arbuscular mycorrhizal cheating in a grassland gentian species. Oecologia 192:929–937

Tisserant E, Malbreil M, Kuo A, Kohler A, Symeonidi A, Balestrini R, Charron P, Duensing N, Frei dit Frey N, Gianinazzi-Pearson V, Gilbert LB, Handa Y, Herr JR, Hijri M, Koul R, Kawaguchi M, Krajinski F, Lammers PJ, Masclaux FG, Murat C, Morin E, Ndikumana S, Pagni M, Petitpierre D, Requena N, Rosikiewicz P, Riley R, Saito K, San Clemente H, Shapiro H, van Tuinen D, Bécard G, Bonfante P, Paszkowski U, Shachar-Hill YY, Tuskan GA, Young JPW, Young PW, Sanders IR, Henrissat B, Rensing SA, Grigoriev IV, Corradi N, Roux C, Martin F (2013) Genome of an arbuscular mycorrhizal fungus provides insight into the oldest plant symbiosis. Proc Natl Acad Sci U S A 110:20117–20122

Trudell SA, Rygiewicz PT, Edmonds RL (2004) Patterns of nitrogen and carbon stable isotope ratios in macrofungi, plants and soils in two old-growth conifer forests. New Phytol 164:317–335

Ven A, Verbruggen E, Verlinden MS, Olsson PA, Wallander H, Vicca S (2020) Mesh bags underestimated arbuscular mycorrhizal abundance but captured fertilization effects in a mesocosm experiment. Plant Soil 446:563–575

Walder F, Niemann H, Lehmann MF, Boller T, Wiemken A, Courty P-E (2013) Tracking the carbon source of arbuscular mycorrhizal fungi colonizing C_3 and C_4 plants using carbon isotope ratios ($\delta^{13}C$). Soil Biol Biochem 58:341–344

Walder F, Niemann H, Natarajan M, Lehmann MF, Boller T, Wiemken A (2012) Mycorrhizal networks: common goods of plants shared under unequal terms of trade. Plant Physiol 159:789–797

Wipf D, Krajinski F, van Tuinen D, Recorbet G, Courty P-E (2019) Trading on the arbuscular mycorrhiza market: from arbuscules to common mycorrhizal networks. New Phytol 223:1127–1142

Supporting Information

Stable C and N isotope natural abundances of intraradical hyphae of arbuscular mycorrhizal fungi

Authors: **Saskia Klink**, Philipp Giesemann, Timo Hubmann, Johanna Pausch

The following Supporting Information is available for this article:

Table S1 All pairwise multiple comparison (Pairwise Wilcoxon *post hoc* test with 'Holm-Bonferroni correction') of hyphae to leaves, roots and soil from either *Festuca ovina* or *Medicago sativa* rhizoboxes in $\delta^{13}C$ and $\delta^{15}N$.

Table S2 Mann-Whitney *U* tests of *Agaricus bisporus* fruiting bodies treated with enzyme solution or sodium-hexametaphosphate relative to a non-treated *Agaricus* control.

Table S3 Single $\delta^{13}C$ values, $\delta^{15}N$ values, N-content [mmol g dwt^{-1}] and C:N ratio of AM hyphae, plant leaves, roots, soil and fruiting bodies of *Agaricus bisporus*.

Table S1 All pairwise multiple comparison (Pairwise Wilcoxon *post hoc* test with 'Holm-Bonferroni correction') of hyphae to leaves, roots and soil from either *Festuca ovina* or *Medicago sativa* rhizoboxes in $\delta^{13}C$ and $\delta^{15}N$. Significant differences are highlighted in bold. Note, since soil hyphae and root hyphae showed similar $\delta^{13}C$ and $\delta^{15}N$ values we combined these for comparison with plant tissues and soil

	Sample (*N*)	$\delta^{13}C$		$\delta^{15}N$	
		Z	*P*	*Z*	*P*
Medicago rhizoboxes	Leaves (*12*) *vs*. hyphae (6)	- 3.3335	0.0051	- 3.3266	0.0053
	Roots (*6*) *vs*. hyphae (6)	- 2.8022	0.0152	- 2.8022	0.0203
	Soil (*6*) *vs*. hyphae (6)	- 0.8807	0.3785	-2.8022	0.0203
	Leaves (*12*) *vs*. roots (*6*)	- 3.3249	0.0053	- 1.0313	0.3024
	Leaves (*12*) *vs*. soil (*6*)	- 3.3249	0.0053	- 3.3266	0.0044
	Roots (*6*) *vs*. soil (*6*)	- 2.8022	0.0175	- 2.8022	0.0101
Festuca rhizoboxes	Leaves (*12*) *vs*. hyphae (6)	- 3.3283	0.0052	- 3.3283	0.0052
	Roots (*6*) *vs*. hyphae (6)	- 2.8022	0.0148	- 2.8022	0.0203
	Soil (*6*) *vs*. hyphae (6)	- 2.8121	0.0148	- 2.8022	0.0203
	Leaves (*12*) *vs*. roots (*6*)	- 3.3249	0.0053	- 2.7658	0.0101
	Leaves (*12*) *vs*. soil (*6*)	- 3.3249	0.0053	- 3.3283	0.0044
	Roots (6) *vs*. soil (6)	- 2.8022	0.0175	- 2.8022	0.0101

Table S2 Mann-Whitney *U* tests of *Agaricus bisporus* fruiting bodies treated with enzyme solution or sodium-hexametaphosphate relative to a non-treated *Agaricus* control. The effect of the chemicals used was statistically evaluated in ^{13}C and ^{15}N. Note that different sporocarps of *Agaricus bisporus* were used (I-IV)

	$\delta^{13}C$		$\delta^{15}N$	
	U	*P*	*U*	*P*
Fruiting Bodies (*N*)				
Control I (*3*) *vs*. enzyme I (*3*)	8	0.190	9	0.081
Control II (*3*) *vs*. enzyme II (*3*)	2	0.383	6	0.663
Control III (*3*) *vs*. enzyme III (*3*)	4	1.000	9	0.081
Control IV (*3*) *vs*. SHMP IV (*3*)	7	0.860	10	0.216

SHMP: sodium-hexametaphosphate

Table S3 Single $\delta^{13}C$ values, $\delta^{15}N$ values, N-content [mmol g dwt^{-1}] and C:N ratio of AM hyphae, plant leaves, roots, soil and fruiting bodies of *Agaricus bisporus*. Hyphae measured at µEA-IRMS are indicated by an asterix (*). Note that different sporocarps were used for *Agaricus bisporus*, but always the same for a control and treatment comparison

Tissue/compartment	$\delta^{13}C$ [‰]	$\delta^{15}N$ [‰]	N-content [mmol g dwt^{-1}]	C:N ratio
Festuca soil hyphae*	-27.31	6.77	2.17	11.72
Festuca soil hyphae*	-27.48	5.19	3.14	10.80
Festuca hyphae. mechanical*	-27.01	5.67	1.85	10.78
Festuca hyphae. mechanical*	-27.18	4.91	4.92	10.24
Medicago soil hyphae*	-28.04	5.37	1.41	14.61
Medicago soil hyphae*	-27.20	5.01	4.80	10.36
Medicago hyphae. mechanical*	-27.45	5.80	3.98	10.56
Medicago hyphae. mechanical*	-27.49	5.27	2.58	10.18
Festuca soil hyphae	-27.21	NA	NA	NA
Festuca soil hyphae	-27.75	NA	NA	NA
Festuca soil hyphae	-27.07	NA	NA	NA
Festuca soil hyphae	-27.26	5.63	2.19	13.49
Festuca hyphae. mechanical	-27.13	NA	NA	NA
Festuca hyphae. mechanical	-27.13	6.73	2.03	9.87
Festuca hyphae. mechanical	-27.63	NA	NA	NA
Festuca hyphae. mechanical	-26.95	NA	NA	NA
Festuca hyphae. enzymatic	-27.71	NA	NA	NA
Festuca hyphae. enzymatic	-27.26	NA	NA	NA
Festuca hyphae. enzymatic	-26.19	NA	NA	NA
Festuca hyphae. enzymatic	-26.21	NA	NA	NA
Medicago soil hyphae	-27.12	NA	NA	NA
Medicago soil hyphae	-26.47	NA	NA	NA
Medicago soil hyphae	-27.84	5.41	2.14	13.01
Medicago soil hyphae	-27.27	NA	NA	NA
Medicago hyphae. mechanical	-27.18	NA	NA	NA
Medicago hyphae. mechanical	-27.13	5.67	2.30	9.92
Medicago hyphae. mechanical	-27.75	NA	NA	NA

Medicago hyphae. mechanical	-27.96	NA	NA	NA
Medicago hyphae. enzymatic	-27.99	NA	NA	NA
Medicago hyphae. enzymatic	-26.28	NA	NA	NA
Medicago hyphae. enzymatic	-28.02	NA	NA	NA
Medicago hyphae. enzymatic	-26.75	NA	NA	NA
Festuca leaves	-33.28	0.24	1.67	17.11
Festuca leaves	-33.72	0.49	1.63	18.84
Festuca leaves	-34.50	1.68	1.84	17.77
Festuca leaves	-34.62	1.65	1.87	17.67
Festuca leaves	-34.58	1.56	1.87	17.49
Festuca leaves	-34.62	1.71	1.87	17.75
Festuca leaves	-34.69	1.81	1.90	17.52
Festuca leaves	-34.42	1.71	1.81	18.44
Festuca leaves	-34.10	1.43	1.74	19.01
Festuca leaves	-34.16	1.50	1.78	18.63
Festuca leaves	-34.50	1.55	1.86	17.80
Festuca leaves	-34.66	1.65	1.90	17.50
Medicago leaves	-33.27	0.94	1.85	18.35
Medicago leaves	-33.27	0.93	1.75	18.36
Medicago leaves	-33.25	0.65	1.78	18.69
Medicago leaves	-33.74	1.25	3.44	9.77
Medicago leaves	-33.70	1.73	3.45	9.75
Medicago leaves	-33.70	1.24	3.44	9.77
Medicago leaves	-33.71	1.13	3.46	9.70
Medicago leaves	-33.52	0.93	3.65	9.36
Medicago leaves	-33.64	0.86	3.66	9.32
Medicago leaves	-33.59	0.77	3.64	9.36
Medicago leaves	-33.69	1.04	3.67	9.31
Medicago leaves	-33.27	0.24	3.21	9.81
Festuca roots	-32.31	1.18	0.89	27.97
Festuca roots	-32.42	-0.04	1.60	17.51

Festuca roots	-32.55	0.88	1.59	18.63
Festuca roots	-32.50	0.96	2.08	14.62
Festuca roots	-31.63	-0.68	1.43	18.94
Festuca roots	-31.64	0.13	2.02	15.38
Medicago roots	-31.79	0.86	2.23	14.18
Medicago roots	-32.08	1.14	1.85	15.47
Medicago roots	-31.96	0.19	1.64	16.68
Medicago roots	-32.16	1.30	1.87	15.08
Medicago roots	-31.69	0.51	2.07	15.02
Medicago roots	-31.53	0.03	1.87	15.21
Festuca soil	-27.71	2.65	0.05	13.55
Festuca soil	-27.79	3.46	0.05	12.63
Festuca soil	-27.58	2.85	0.05	13.09
Festuca soil	-27.71	2.97	0.05	13.64
Festuca soil	-27.58	3.15	0.05	13.03
Festuca soil	-27.65	2.86	0.05	13.30
Medicago soil	-27.73	3.42	0.05	13.36
Medicago soil	-27.61	3.28	0.05	13.56
Medicago soil	-27.68	3.18	0.05	13.36
Medicago soil	-27.70	3.43	0.05	13.14
Medicago soil	-27.54	2.74	0.04	14.14
Medicago soil	-27.56	2.84	0.05	13.80
Agaricus control I	-23.90	17.10	2.89	9.86
Agaricus control I	-23.44	17.90	3.03	9.26
Agaricus control I	-23.17	17.87	3.35	8.60
Agaricus enzyme I	-24.19	14.84	3.73	8.40
Agaricus enzyme I	-23.63	16.31	4.05	7.91
Agaricus enzyme I	-24.42	15.85	4.10	7.86
Agaricus control II	-25.33	5.04	8.26	10.44
Agaricus control II	-23.16	12.34	4.05	7.07
Agaricus control II	-23.19	11.72	4.21	6.89

Agaricus enzyme II	-23.10	10.03	3.45	7.88
Agaricus enzyme II	-23.62	10.04	3.46	9.36
Agaricus enzyme II	-23.08	9.78	3.64	7.61
Agaricus control III	-22.63	11.58	3.60	7.56
Agaricus control III	-22.42	21.83	4.20	6.65
Agaricus control III	-22.71	11.96	3.77	7.10
Agaricus enzyme III	-22.52	9.30	3.19	8.00
Agaricus enzyme III	-22.78	9.41	3.09	8.13
Agaricus enzyme III	-22.32	9.34	3.67	7.40
Agaricus control IV	-21.70	19.52	6.82	4.42
Agaricus control IV	-22.02	18.45	5.90	4.95
Agaricus control IV	-22.62	17.59	5.37	5.48
Agaricus Sodium-Hexametaphosphate	-22.57	11.81	4.12	6.67
Agaricus Sodium-Hexametaphosphate	-22.61	17.57	5.25	5.67
Agaricus Sodium-Hexametaphosphate	-22.47	17.33	5.17	5.79
Agaricus Sodium-Hexametaphosphate	-21.83	18.51	5.59	5.52

Manuscript 2

Stable isotopes reveal that fungal residues contribute more to mineral-associated organic matter pools than plant residues

Saskia Klink[1], Adrienne B. Keller[2a], Andreas J. Wild[1,5], Vera L. Baumert[4,5], Matthias Gube[6], Eva Lehndorff[3], Nele Meyer[3], Carsten W. Mueller[7], Richard P. Phillips[2], Johanna Pausch[1]

Soil Biology and Biochemistry, submitted on 11 October 2021 (ID: SBB19061)

[1]Department of Agroecology, Bayreuth Center of Ecology and Environmental Research (BayCEER), University of Bayreuth, 95440 Bayreuth, Germany

[2]Department of Biology, Indiana University Bloomington, IN 47405, USA

[3]Soil Ecology, Bayreuth Center of Ecology and Environmental Research (BayCEER), University of Bayreuth, 95448 Bayreuth, Germany

[4]Bavarian State Research Center for Agriculture, Institute for Organic Farming, Soil and Resource Management, 85354 Freising, Germany

[5]Chair of Soil Science, School of Life Sciences, Technical University of Munich, 85354 Freising, Germany

[6]Soil Science of Temperate Ecosystems, Büsgen-Institute, Georg-August University Göttingen, 37077 Göttingen, Germany

[7]Department of Geosciences and Natural Resource Management, University of Copenhagen, 1350 Copenhagen K, Denmark

[a]Current address: Department of Ecology, Evolution, and Behavior, University of Minnesota, Saint Paul, 55108, USA

Key words: Amino sugars, Mineral-associated organic matter, MEMS hypothesis, Particulate organic matter, Stable isotopes, Soil organic matter dynamics

Abstract

We still lack crucial knowledge about the contribution of plant *vs*. microbial residues to specific SOM pools, particularly the relative contribution of arbuscular (AM), ectomycorrhizal (ECM), and saprotrophic (SAP) fungi.

We investigated sources of particulate and mineral organic matter (POM and MAOM) around trees with distinct mycorrhizal types, *Liriodendron tulipifera* (AM-association) and *Quercus alba* (ECM-association), in a temperate deciduous forest in Indiana, USA. Combining ^{13}C and ^{15}N natural abundance analyses with measurements of microbial residues using amino sugars, the isotope signatures of large, medium and small-sized POM and MAOM fractions were compared with those of leaves, roots and biomass of mycorrhizal and saprotrophic fungi. A Bayesian inference isotope mixing model calculated sources of C and N to SOM fractions.

While the isotope composition of POM resembled that of plant materials, MAOM was close to fungal values. This was confirmed by mixing model calculations and microbial residue analysis, which additionally and independent from tree partner suggested a high contribution of saprobic fungi to POM and MAOM, as opposed to ECM contributions.

Our results suggest fungal, not plant residues, as the source of the most putatively stable OM pool; thus, altering fungal communities may enhance efforts to increase long-term soil C storage.

1. Introduction

Soil organic matter consists of a multitude of organic compounds forming a continuum of decay, ranging from fresh detritus to highly processed organic matter either in the form of particles or associated with mineral surfaces (Schmidt et al., 2011; Lehmann and Kleber, 2015). Along the path of SOM formation and turnover, entities of different size, complexity and degree of decomposition are established (Angst et al., 2021; Lehmann et al., 2020). Hence, distinct fractions of organic matter can be defined in soil, which differ in their formation, chemical composition, persistence, and function (Golchin et al., 1994; Lavallee et al., 2020). Nevertheless, we lack a foundational understanding of the source and stability of most SOM fractions.

Due to the complex continuum of SOM compartments differing in composition and turnover time, characterizing and understanding SOM dynamics requires separation of SOM into measurable fractions in order to elucidate the fate of certain carbon (C) pools (Poeplau et al., 2018). One approach to elucidate differences between C and nitrogen (N) storage and sequestration in organic matter (OM) particles *vs*. OM associated with mineral surfaces and thus predict SOM dynamics, is the separation into particulate organic matter (POM) and mineral-associated organic matter (MAOM) fractions (Golchin et al., 1994; Lavallee et al., 2020; Angst et al., 2021). Particulate OM is dominated by structural C compounds of plant origin (Baldock and Skjemstad, 2000; Lavallee et al., 2020; Angst et al., 2021) and the major part of the C-rich, complex inputs to POM are relatively vulnerable to microbial decay (Christensen, 2001; Lützow et al., 2007; Cotrufo et al., 2019). In contrast, part of the POM pool can be highly persistent due to occlusion within aggregates and high aromaticity or aliphaticity (Mueller and Koegel-Knabner, 2009). Particulate OM acts itself as a hot spot for the formation of MAOM due to the high microbial activity at the POM-soil-mineral interface (Witzgall et al., 2021). Thus, contrast to POM, which is derived principally from plant inputs, MAOM consists mainly of microbial residues (Kopittke et al., 2018; Kopittke et al., 2020), although plant

biomolecules, e.g., leachates from litter, may contribute (Mikutta et al., 2019; Sokol and Bradford, 2019; Angst et al., 2021).

It has been proposed that the contribution of microbial residues to MAOM is higher in systems with high litter quality and environmental conditions optimal for microbial activity and growth (cf. Microbial Efficiency-Matrix Stabilization (MEMS) framework (Cotrufo et al., 2013)). While numerous studies confirmed the MEMS framework (e.g. Bradford et al., 2013; Craig et al., 2018; Cyle et al., 2016; Rumpel et al., 2015), finding greater MAOM-N in AM-dominated plots with faster decaying litter than in ECM plots (Craig et al., 2018) or highlighting the importance of the microbial use efficiency (Rumpel et al., 2015), other studies challenged the MEMS framework. Castellano et al. (2015) highlighted the consideration of C saturation of the mineral surface and of litter quantity for MAOM formation. Further, as discussed in Evans et al. (2020), priming of microorganisms by high quality litters appears to increase MAOM mineralization (see also Córdova et al., 2018). Finally, Huang et al. (2019) underpinned the importance of lignin-derived C contributing to MAOM in addition to microbial residues. Thus, further research appears necessary to decipher the processes of MAOM formation and the role of microbial inputs in dependence of litter quality.

Despite the small contribution of living microbial biomass to total soil C (Frey, 2019, but see Simpson et al., 2007), fungal necromass is responsible for up to 70% of microbial-derived residues in soil (Joergensen, 2018; Li et al., 2015). Among soil microorganisms, root-associated mycorrhizal fungi make up more than 30% of microbial biomass (Högberg and Högberg, 2002; Frey, 2019). Mycorrhizal fungi use plant-derived C for biomass production and metabolism (e.g. respiration), releasing C to soil from living hyphae (e.g., organic acids and extracellular enzymes) and dead hyphal biomass (Frey, 2019). In this way, mycorrhizal hyphae can contribute directly to the POM and MAOM fractions (Frey, 2019; Godbold et al., 2006). Besides, free-living saprotrophs also produce their own residues and exudates (e.g. Verbruggen

et al., 2017), and form necromass upon death that may be attached to mineral surfaces (Li et al., 2015; Joergensen, 2018; Witzgall et al., 2021). Recently it was shown that via the expansion of their mycelium, fungi can translocate C into deeper soil layers where fungal exudates and residues can bind to minerals (Witzgall et al., 2021). While many factors are known to influence microbially-mediated SOM dynamics (Fan and Liang, 2015; Liang et al., 2019), we still know remarkably little about the contribution from varying microbial sources such as mycorrhizal or saprotrophic (SAP) fungi and bacteria affecting the various SOM fractions' capability of C and N storage.

Tracking the input from different origins to SOM fractions is methodologically challenging owing to the intimacy of the associations between roots and microbes and the dynamic nature of root-microbial and microbe-microbe interactions. Stable isotope natural abundance approaches are a valuable tool to trace the transfer of plant and fungal C and N inputs to SOM fractions, as stable isotopes possess both information about the ongoing process (process information) and the origin of the signature (source information) (Fry, 2008). For example, plants are relatively depleted in ^{13}C compared to most soil fungi (e.g. Högberg et al., 1999) owing to the fractionation that occurs in heterotrophs from enzymatic decomposition of cellulose in wood or litter (Gleixner et al., 1993; Kohzu et al., 1999). The ^{15}N of fungi depends, in large part, on the source of N (Gebauer and Taylor, 1999), and whether N is shared with an associated plant or not (cf. Gebauer and Dietrich, 1993). Thus, along the process of leaf litter decay to form POM and MAOM, a shift from relatively depleted plant-related C and N isotopic ratios to relatively enriched fungal-related C and N isotopic ratios should occur. Although most of the C that mycorrhizal fungi receive is plant-derived, mycorrhizal fungi $\delta^{13}C$ isotopic signatures often are more enriched relative to those of the plant. While previous investigations have uncovered variations in the isotopes of plant and microbial inputs, we still lack understanding of the linkages of these inputs to fast and slow-cycling SOM fractions in forests.

We sought to investigate the sources of POM and MAOM in a temperate deciduous forest in Indiana, USA around two dominant tree species - tulip poplar (*Liriodendron tulipifera* L.) and white oak (*Quercus alba* L.). These species differ in multiple traits and characteristics, such as the type of mycorrhizal fungi they associate with (arbuscular mycorrhizal fungi for tulip poplar; ectomycorrhizal fungi for white oak), their litter quality (tulip > oak; Midgley et al., 2015), and the soil microbial communities they promote (Rosling et al., 2016; Mushinski et al., 2020). In ECM-associated systems we expect ECM fungi as main contributors to SOM, while in AM-associated systems SAP fungi should be the primary contributors due to activation by arbuscular mycorrhizal (AM) fungi and the low biomass of AM fungi (Verbruggen et al., 2017; Cheeke et al., 2021). We tracked the transfer of plant and fungal inputs into various SOM pools by comparing the isotopic signatures of different fungal groups to isotopic signatures of multiple POM and MAOM fractions. Moreover, we used analyses of amino sugars (cell wall components of bacteria and fungi) as an independent parameter from that of isotopes to classify which microbial groups contribute to soil C storage in different SOM fractions (Amelung, 2001). Estimates of the contribution of fungal and bacterial compounds to soil C will aid to describe how microbial products contribute to SOM formation. Combining stable isotope natural abundance analyses and amino sugar analyses, we tested the following predictions:

(i) Plant residues are the predominant source of POM-C and -N, while fungal residues are the dominant source of MAOM-C and -N. This will be represented by a gradual isotopic enrichment in ^{13}C and ^{15}N from POM to MAOM fractions.

(ii) Ectomycorrhizal (ECM) fungi will be the dominant source of C and N to SOM fractions under white oak (ECM-associating trees) while saprotrophic (SAP) fungi contributions will be dominant under tulip poplar (AM-associating trees).

(iii) Amino sugar analyses will show bacteria affecting soil C storage for both POM and MAOM fractions and a shift to higher fungal contribution for MAOM fractions.

2. Materials and methods

2.1 Study site

The study site Moore's Creek is a *c*. 80-year-old temperate deciduous forest in south-central Indiana, USA, which is part of Indiana University's Research and Teaching Preserve (39°05′ N, 86°28′ W, *cf*. Midgley and Phillips, 2016). The region is characterized by a humid continental climate with a mean annual precipitation of *c*. 1200 mm and a mean annual temperature of 11.6 °C. Moore's Creek was unaffected during the southern advance of the last glacial event (the Wisconsin glaciation) and as such, there is steep ridge-ravine topography, and nutrient-poor silty-loam soils derived from sandstone and shale (mesic Typic Dystrochrepts). More detailed information about the study site is given in Phillips et al. (2013), Midgley and Phillips (2019) and Mushinski et al. (2019). Dominant tree species at the site include trees that associate with arbuscular mycorrhizal fungi (*Liriodendron tulipifera* L., *Acer saccharum* MARSHALL, *Sassafras albidum* (NUTT.) and *Prunus serotina* EHRH.) and those associating with ectomycorrhizal (ECM) fungi (*Quercus alba* L., *Fagus grandifolia* EHRH., *Quercus rubra* L., *Quercus velutina* LAM. and *Carya glabra* MILL.). Sampling was conducted in June (peak growing season) and October (late growing season) 2018 around five canopy trees: two individuals of *Q. alba* L. (white oak) and three individuals of *L. tulipifera* L. (tulip poplar). Additionally, two individuals of *F. grandifolia* EHRH. (American beech) and *A. saccharum* MARSHALL (sugar maple) were sampled only for stable isotope analysis (**Supporting material Fig. S1**). To control for topography, only trees growing on the upper third of north-facing ridges were chosen. The distance between each focal tree to a neighboring canopy tree was at least 3 meters.

2.2 Sampling procedure

Mature, healthy, sunlit leaves (6 to 7 per tree species) of each focal tree were collected by shooting twigs (shotgun) or by cutting leaves from freshly broken twigs. Roots (first four root orders) were excavated approximately 0.5 m from each tree trunk at four spots and traced back

to the target tree species to ensure correct tree association. In the lab, roots were washed with water, cleaned from debris with tweezers and sub-divided for stable isotope analysis (4 composite samples per tree species), fungal isolation, and DNA analyses. Arbuscular mycorrhizal (AM) fungi were isolated from roots of AM-associated tulip poplar via a mechanical isolation approach presented in Klink et al. (2020) and pooled to six composite samples to increase sample mass for isotopic analyses. This procedure was chosen over soil isolation to reduce the impact of other soil fungi on isotopic patterns and to increase the abundance of AM fungi. However, the presence of other fungal root endophytes, such as dark septate endophyte (DSE) fungi could not be excluded completely. For ECM-associated white oak roots, root tips with ectomycorrhizal (ECM) fungal sheath were separated and pooled into three composite samples to increase sample amount for isotopic measurements. Under each tulip poplar tree, sporocarps of 6 ECM and 12 SAP fungi (6 on wood, 6 on soil) were collected, and under each white oak tree 6 ECM and 4 SAP fungi (3 on wood, 1 on soil) were collected. The selection of both soil and wood SAPs was done in order to trace the effect of different food sources on SAP fungal isotopic signature for the specific habitat. All samples were collected within a radius of 2 m of each tree trunk and photo-documented. Wood and leaf litter, which are substrates for growing fungi, were collected. Recently fallen leaf litter was sampled from the soil surface in a 2 m radius around the tree trunk. Bulk soil was collected with a PVC soil corer (5 cm diameter) to a depth of 15 cm at four locations around each tree trunk. Bulk soil was sieved to 2 mm, cleaned of root particles and stones, weighed, and divided into one sub-sample for bulk analysis and one sub-sample for soil fractionation. For transportation and until further processing in the lab, leaf samples were stored in paper bags, and root, fungi, and soil samples were put in zip-lock bags on ice.

2.3 Soil fractionation

The bulk soils were subjected to a combined particle size and density fractionation in order to quantify the contribution of POM *vs*. MAOM to the overall C and N storage as well as the

fractions' elemental and isotopic composition (cf. Mueller et al., 2014). Sub-samples (30 g) of bulk soil from white oak and tulip poplar soils were separated into multiple POM and MAOM fractions using a modified particle size and density fractionation method (**Supporting material Fig. S2**; Amelung and Zech (1999) and Mueller et al. (2014)). Bulk soil was suspended with deionized water (1:5, m:v) and capillary saturated for one hour. Next, ultrasonic dispersion (SonoplusHD2200, Bandelin, Berlin, Germany) with an energy input of 440 J ml^{-1} (Amelung and Zech, 1999, probe tip at 15 mm) was applied to ensure strong dispersion of soil aggregates while organic matter structure was retained (Schmidt et al., 1999). Sonicated samples were subsequently separated by wet sieving using sieves of 63 µm and 20 µm mesh sizes. This resulted in size fractions of > 63 µm, > 20 µm and < 20 µm. To yield clean POM and MAOM fractions, these particle size fractions were further separated based on their density using sodium polyungstrate (SPT; 1.8 g cm^3). This allowed to recover POM floating on the SPT solution free from mineral particles, and MAOM sank down as heavy sediment free of POM. The resulting six fractions (> 63 µm (MAOM), > 20 µm (MAOM), < 20 µm (MAOM), > 63 µm (POM), > 20 µm (POM), < 20 µm (POM)) were cleaned from residues of SPT by rinsing them with deionized water and repeated centrifugation (> 63 µm and > 20 µm MAOM) or by pressure filtration (< 20 µm fractions) with deionized water until an electric conductivity below 5 µS cm^{-1} was reached in the percolated water. Samples were subsequently freeze-dried, finely ground using a ball mill, and stored in desiccators until further processing. Due to the low C- and N-content of the fraction > 20 µm (MAOM), no reliable stable isotope measurements could be conducted for this fraction. The average recovery of the soil fractionation process was 97.8% ± 0.5. In total, the soil fractionation resulted in n = 12 for tulip poplar and n = 8 for white oak for each of the five analyzed soil fractions. Hereafter, these fractions will be referred to as large MAOM or large POM (> 63 µm), medium POM (> 20 µm) and small MAOM or POM (< 20 µm).

Particle size fractionation is ecologically relevant given that the larger sand-sized fractions

typically consist mostly of carbohydrate-rich POM rich, whereas POM and increasing amounts of MAOM (the smaller the fraction the higher the amount of mineral-associated OM) in the smaller silt or clay-sized fractions are more dominated by aliphatic and/or aromatic compounds (Wagai et al., 2009; Angst et al., 2017). Additionally, the formation of organo-mineral associations, mostly in fine sized mineral fractions, supports the stabilization of otherwise bioavailable carbohydrates and microbial residues (Schöning et al., 2005; Kopittke et al., 2020).

2.4 Stable isotope analyses

Plant leaves, roots, and fungal sporocarps were washed with deionized water, and roots and sporocarps were further cleaned of debris using tweezers. All samples were dried to constant weight (60 °C) for 48 h. Afterwards, samples were ground to fine powder in a ball mill (MM2, RETSCH, Haan, Germany) and stored in desiccators filled with silica gel. Due to their small size, mycorrhizal root tips of white oak were weighed into tin capsules without being ground.

For stable isotope analyses, ground samples were weighed into tin or silver capsules (for AM hyphae). An elemental analyzer isotope ratio mass spectrometer (EA-IRMS; Elemental Analyzer 1108, CE Instruments, Milan, Italy; ConFlo III interface, Thermo Fisher Scientific, Bremen, Germany; IRMS Delta S, Finnigan MAT, Bremen, Germany) was used to determine the ratios of $^{13}C/^{12}C$, $^{15}N/^{14}N$ and the C- and N-content of the samples. For AM hyphae, a µEA-IRMS (µElemental Analyzer, Eurovector, Pavia, Italy; ConFlo IV interface, Thermo Fisher Scientific, Bremen, Germany; IRMS Delta 5 plus, Thermo Fisher Scientific, Bremen, Germany) specialized for small samples was used.

The stable isotope natural abundances are expressed as δ-values relative to international standards. Delta-values were calculated according to equation 1, whereby R describes the ratio of the heavy to the light isotope.

$$\delta^{13}C \text{ or } \delta^{15}N = (R_{sample}/R_{standard} - 1) \times 1000\ (‰) \qquad \text{(Equation 1)}$$

Vienna-Pee Dee Belemnite (V-PDB; $R_{standard}$ = 0.0111802) was the standard material for C and air was the standard for N ($R_{standard}$ = 0.0036765). Calculation of C- and N- concentrations was done by calibrating with acetanilide ($C_6H_5NH(COCH_3)$).

2.5 Fungal identification

Fungal sporocarps were identified via macroscopic and microscopic features. Photographs of the sampled sporocarps are available on iNaturalist project 'Fungi Moores Creek 2018'. Genera of ECM fungi comprised *Russula, Boletus, Hygrophorus, Laccaria, Cortinarius, Lactarius, Cantharellus, Inocybe* and *Tricholoma,* SAP fungi belonged to the genera *Laetiporus, Hygrocybe, Agaricus, Marasmius, Gymnopus, Lycoperdon, Rhodocollybia, Mycena, Stereum, Grifola, Lenzites, Singerocybe, Rhizomarasmius, Ramaria, Fuscoporia, Gymnopilus, Macrolepiota, Merulius, Ischnoderma, Psathyrella, Bisporella* and *Hymenochaete*. These identifications are broadly in line with soil DNA sequencing results by Eagar et al. (2021), who found that ECM soils were dominated in decreasing order of relative abundance by the families Russulaceae > Tricholomataceae and Amanitaceae > Hydnangiaceae (*Laccaria* genus), Clavulinaceae and Cortinariaceae. AM soils were dominated by Russulaceae > Mortierellaceae > Hygrophoraceae. Thus, the collected sporocarps captures most of the dominant fungal taxa at the site (except for Amanitaceae, Clavulinaceae).

DNA sequencing and analyses were performed at Leiden University, Netherlands for fungi in roots of tulip poplar and white oak. Tulip poplar roots hosted Glomeraceae, e.g. the genera *Rhizophagus* and *Archaeospora*, but also DSE and ECM fungi. For description of DNA handling refer to **Supporting material Methods S1**.

2.6 Amino sugar analysis

Amino sugar analyses were conducted using sub-samples of small MAOM and large POM to evaluate portions of microbial and plant residues, respectively. Amino sugars are correlated to microbial residues (Parsons, 1981) and used to calculate the contribution of bacterial- and fungal-derived C. Analysis of individual amino sugars glucosamine (GlcN), galactosamine

(GalN), mannosamine (ManN), and muramic acid (MurN) was conducted according to Zhang and Amelung (1996). Specifically, Glucosamine is often considered as an indicator of fungal residues, whereas muramic acid is considered as an indicator of bacterial residues (Joergensen, 2018).

In brief, an amount of soil corresponding to 0.3 mg N was extracted by hydrolysis in 6 M HCl for 8 h at 105 °C after adding myo-inositol as internal standard. The hydrolysate was filtered and dried. The residue was dissolved with water, neutralized by adjusting the pH to 6.7 (+/- 0.1) using KOH, and centrifuged. The supernatant was freeze-dried, dissolved with methanol, centrifuged, dried, dissolved with H_2O, and freeze-dried. Derivatization of amino sugars to aldononitrile acetates was conducted according to Guerrant and Moss (1984). Afterwards, a second internal standard (ß-endosulfan) was added and samples were dried and dissolved in ethyl acetate–hexane (1:1, v/v).

The amino sugar derivatives were analyzed on a gas chromatograph (GC 2000, Shimadzu, Japan) equipped with an OPTIMA® column (30 m×0.32 mm ID with 0.25 µm film thickness, Macherey-Nagel, Germany) using a flame ionization detector according to Zhang and Amelung (1996). Amino sugars were quantified using myo-inositol as first internal standard (for recovery calculation) and ß-endosulfan as second internal standard (for quantification). Amino sugar identification was done using external standards (GlcN, GluN, ManN, and MurN). Bacterial C was calculated by multiplying MurN by a conversion factor of 45 (Appuhn and Joergensen, 2006). Fungal C was calculated according to equation 2 and in line with Appuhn and Joergensen (2006) and Faust et al. (2017), where 179.17 is the molecular weight of GlcN, 253.23 is the molecular weight of MurN, and 9 is a conversion factor from fungal GlcN to fungal residue C.

$$\mu g \text{ fungal C } g^{-1} \text{ soil} = (((\mu g \text{ GlcN } g^{-1} \text{ soil} / 179.17) - (2 \times \mu g \text{ MurN } g^{-1} \text{ soil} / 253.23)) \times 179.17) \times 9 \quad \text{(Equation 2)}$$

2.7 Data analysis

Software R version 3.6.1 (2019) and SigmaPlot version 11.0 (2008) were used for statistical analyses and figures. Shapiro Wilk's test indicated that the majority of the data set was not normally distributed and therefore a conservative statistical analysis using non-parametric tests was chosen. Kruskal-Wallis rank sum tests (χ^2) were performed to compare plant tissues, soil compartments, and fungi in $\delta^{13}C$ and $\delta^{15}N$ stable isotope natural abundances for each of the two tree species. The same procedure was performed for C-, N-content and C:N ratio data. Pairwise *post hoc* tests where then performed for the afore mentioned groups using Dunn's method for unequal sample sizes and the Tukey method when equal sample sizes were given. The Holm-Bonferroni correction was applied to adjust *P* values. For comparisons between tulip poplar and white oak for each aforementioned group, Mann-Whitney *U* tests were applied. For amino sugar analyses parametric *t*-tests were performed to compare tree species differences in amino sugar content, fungal C and fungal to bacterial C ratio (F:B) of large POM and small MAOM fractions. Statistical significance between groups (pairwise comparison) was tested for groups with $n = 3$ or higher. A level of significance of $\alpha = 0.05$ was set.

A Bayesian Inference isotopic mixing model (R package 'SIAR', version 4.2; Parnell et al., 2010; Parnell and Jackson, 2013) was applied to partition plant and fungal inputs into POM and MAOM fractions. This mixing model allows for probability estimates of input proportions, while accounting for variability and uncertainty in parameters (Parnell et al., 2010). In addition to greater statistical power, the Bayesian Inference isotopic mixing model allows the inclusion of discrimination factors, prior information, and many sources of variability (Parnell et al., 2010; Bond and Diamond, 2011). The model was informed with C and N isotopic data and concentrations of the sources leaves and fungal groups (AM, ECM, SAP) and of the POM and MAOM fractions. The model was not informed with fractionation factors for our dataset, as the variety of fractionation processes present could not be deciphered or are unknown. We are aware that this affects the precision of the model (cf. Parnell et al., 2010) but chose to avoid the

inclusion of a large error due to unknown or indeterminate fractionation factors. For both tulip poplar and white oak datasets, 500,000 iterations and a burnin with initial discard of 50,000 were used, resulting in a 30,000 posterior draw output. After verification of normal distribution of posterior draw output data, we applied the Student's *t*-test to test for significant differences between the single input sources to SOM fractions. We are aware that the proportional contributions of the fungal groups identified by the Bayesian inference mixing model underly certain restrictions. Other contributors to MAOM fractions such as bacteria, viruses or dissolved organic matter (DOM) were neglected for this model due to challenges in gaining their stable isotope signatures under field conditions. Therefore, the relative proportions of these groups contributing to MAOM fractions need to be subtracted from the proportions found for leaves and fungi in our study.

2.8 Accession numbers

Raw sequences have been deposited in the European Nucleotide Archive under the accession number PRJNA678944.

3. Results

3.1 Contribution of individual SOM fractions to total soil organic C

From the soil subsample used for particle size density fractionation ~ 3.33% organic C was recovered for both tulip poplar and white oak soils (**Table 1**). Distribution of C and N in SOM fractions was similar between tulip poplar and white oak, except for a higher C content in the small MAOM of tulip poplar compared to the small MAOM fraction of white oak (**Table 1**).

3.2 Stable isotope natural abundances

Plant tissues were significantly depleted relative to fungal biomass in their ^{13}C and ^{15}N isotopes, and patterns were similar for tulip poplar and white oak (**Fig. 1**). Overall, saprotrophic fungi were the most ^{13}C enriched and mycorrhizal fungi were the most ^{15}N enriched. Further, a progressive enrichment in ^{13}C and ^{15}N occurred from POM to MAOM fractions and with

decreasing particle size (i.e., the most ^{13}C and ^{15}N enriched fractions were the small MAOM fractions).

Significant differences between plant material, mycorrhizal fungi, SAP fungi and bulk soil were reported for white oak plots for both ^{13}C (χ^2 = 24.56, df = 3, P = 0) and ^{15}N (χ^2 = 22.21, df = 3, P = < 0.001). The same holds true for tulip poplar plots ($\delta^{13}C$: χ^2 = 32.33, df = 3, P < 0.001; $\delta^{15}N$: χ^2 = 30.80, df = 3, P = < 0.001). White oak plant material was significantly ^{13}C depleted relative to SAP fungi (Z = –4.156, P = 0.001) and soil (Z = –2.89, P = 0.007), and more ^{13}C (Z = 3.150, P = 0.004) and ^{15}N (Z = 4.314, P < 0.001) depleted than mycorrhizal fungi. Isotopic signatures of leaf litter were –29.3‰ in $\delta^{13}C$ and –4.3‰ in $\delta^{15}N$ for tulip poplar and –29.1‰ in $\delta^{13}C$ and –4.8‰ in $\delta^{15}N$ for white oak. Tulip poplar plant material was significantly ^{13}C depleted relative to SAP fungi (Z = –5.641, P < 0.001) and more ^{15}N depleted than mycorrhizal fungi (Z = 5.458, P < 0.001). Mycorrhizal fungi at tulip poplar plots were more ^{13}C depleted (Z = –3.402, P = 0.002) and more ^{15}N enriched relative to SAP fungi (Z = 3.511, P = 0.001). For SOM fractions, POM was more ^{13}C and ^{15}N depleted than MAOM for both white oak ($\delta^{13}C$: U(16, 24) = 384, P < 0.001; $\delta^{15}N$: U(16, 24) = 348, P < 0.001) and tulip poplar plots ($\delta^{13}C$: U(24, 36) = 822.5, P < 0.001; $\delta^{15}N$: U(24, 36) = 775.5, P < 0.001).

When comparing tulip poplar and white oak no significant differences were reported for plant material, mycorrhizal fungi, SAP fungi or bulk soil for either $\delta^{13}C$ or $\delta^{15}N$. However, MAOM fractions of white oak plots were significantly more ^{13}C enriched than those of tulip poplar plots (U(16, 24) = 296.5, P = 0.004). Regarding C:N ratios, the leaf litter, wood, and roots had the highest values, while fungal biomass had the lowest values (**Supporting material Table S1, S2**). Notably, the C:N ratio of the MAOM fractions (mean white oak: 14.03, mean tulip poplar: 12.70) were similar to those of the mycorrhizal fungi (mean white oak: 10.57, mean tulip poplar: 10.98; **Supporting material Table S1**).

3.3 Plant and fungal contributions to POM and MAOM fractions

Overall, our Bayesian Inference mixing model indicated that the POM fractions were dominated by plant inputs and the MAOM fractions were dominated by fungal inputs, with few differences between tulip *vs*. oak soils (**Fig. 2, Supporting material Figures S3, S4**). For both tulip poplar and white oak the mixing model calculated a predominantly plant-derived contribution to small, medium, and large POM (tulip poplar leaves: 7 – 50%, tulip poplar roots: 18 – 54%; white oak leaves: 24 – 52%, white oak roots:29 – 62%). Free-living SAP fungal inputs contributed to POM with a probability of about 4 – 53%, while the probability of mycorrhizal fungi contribution was lower (ECM: 1 – 12%; AM: 1 – 4%). With decreasing particle size of POM, fungal contribution slightly increased to a maximum of 53% for SAP and 12% for ECM. For MAOM fractions, fungal inputs (2 – 63%) dominated over plant inputs (1 – 39%) for both tulip poplar and white oak soils. Again, with decreasing particle size of MAOM the contribution of fungi increased, demonstrating a larger contribution of ECM fungi (22 – 43%) together with SAP fungi (23 – 42%) to the small MAOM fraction. The contribution of AM fungi was only relevant for the small MAOM fraction (5 – 11%).

Fungal-derived C contributed 42.7% ± 6 to the C in MAOM and 28.9% ± 3 in POM fractions and was generally independent from tree species (**Supporting material Fig. S5**, except for significantly less fungal C in MAOM under white oak (t = 6.422, df = 4, P = 0.003). Hence, the portion of fungal-derived C was almost doubled in MAOM as compared to POM fractions. In contrast, bacterial-derived C contributed 12.1% ± 2 to MAOM-C and 2.1% ± 1 to POM-C fractions.

Total amino sugars, fungal residue correlated glucosamine and bacterial residue related muramic acid indicated that both the POM and MAOM fractions were comprised of more fungal relative to bacterial residues (U(8,8) = 36, P < 0.001; **Fig. 3**, **Supporting material Fig. S5**). The portion of fungal C was highest for POM under white oak (**Fig. 3**, t = –3.46, df = 6,

P = 0.014). However, the portions of fungal C in total C was elevated in MAOM fractions by about 40% (**Fig. 3**) due to the low total C contents in MAOM (**Supporting material Table S1**).

4 Discussion

Our study combined stable isotope analyses in a Bayesian Inference mixing model with amino sugar analyses to determine the contribution of plant and microbial C and N to various SOM fractions. While we found that plant-related inputs dominated POM fractions, a shift to fungal-related inputs occurred for MAOM fractions, with SAP fungi dominating over ECM fungi regardless of dominant tree. Of the microbial residues, fungal C predominantly contributes to POM fractions, whereas fungal and bacterial C were both important contributors to MAOM fractions. These differences in microbial contributions imply different microbial groups affecting C and N storage in POM *vs*. MAOM fractions.

4.1 Stable isotope patterns

In general, the $\delta^{13}C$, $\delta^{15}N$ isotopic composition of the MAOM fractions shifted towards the isotopic values of fungi, particularly ECM fungi in our study. We argue that this results from the predominant contribution of fungal biomass (necromass) to these fractions. The $\delta^{13}C$ and $\delta^{15}N$ isotope signature of fungi is typically a function of their C and N sources, metabolic (including degradative capabilities) and fractionation processes (e.g. Gleixner et al., 1993; Taylor et al., 1997; Kohzu et al., 1999; Hobbie et al., 2012), leading to an enrichment relative to plant tissues.

Historically, it was believed that decomposition occurred via preferential decay of easily accessible compounds depleted in ^{13}C (discussed in Ehleringer et al., 2000; Menichetti et al., 2015), leaving behind ^{13}C enriched compounds and potentially interfering with the use of isotopic mixing models to determine the source of SOM. For instance, Menichetti et al. (2015) described a ^{13}C enrichment of ~ 2‰ of bulk soil over the duration of SOM decay at long-term bare fallow sites with arrested C inputs, aligning with the ^{13}C enrichment from POM to MAOM fractions in our study. Preferential decay of depleted C compounds was considered to explain

the increase in ^{13}C in older SOM compartments over time, also leading to an increase in ^{13}C of SOM with soil depth (Nadelhoffer and Fry, 1988; Kohl et al., 2015). Yet, this assumption is not entirely consistent with the observed ^{13}C-depletion of some plant residues in soil with longer residence times. Lignin, for instance, is ^{13}C depleted, whereas rapidly utilized primary sugars are ^{13}C enriched (Gleixner et al., 1993). Thus, lignin accumulation in deeper soil layers should favor a ^{13}C depletion rather than an ^{13}C enrichment (Schleuss *et al*., *unpublished*, person. communication). However, selective preservation of ^{13}C-depleted litter components *per se* has long been questioned in the literature (Marschner et al., 2008; Nadelhoffer and Fry, 1988). Rather, it has been argued that ^{13}C enrichment in older parts of the soil, e.g., along the depth profile, is due to a higher contribution of microbial residues. As a result of carboxylation reactions, microbes are enriched in ^{13}C relative to their food source (Ehleringer et al., 2000). This is also consistent with a study by Kohl et al. (2015) showing that ^{13}C enrichment along a depth profile is attributable to a shift in fungal and bacterial biomass proportions, rather than ^{13}C-enrichment caused by preferential decomposition of ^{12}C. Therefore, we argue that an accumulation of ^{13}C enriched microbial residues is the most reliable explanation for the similarity of our MAOM fractions and fungal biomass, allowing for the application and interpretation of the endmember mixing model.

Plant-related and fungal-related C and N isotopic signatures embed POM and MAOM fractions' isotopic signatures, indicating a shift in isotopic enrichment from plant to microbial tissue inputs to SOM fractions and suggesting a preferential preservation of ^{13}C enriched microbial biomass deposits in a temperate deciduous forest. The high contribution of fungal inputs particularly to MAOM in our study conforms with mechanistic microbial model estimates of the contribution of microbial-derived C to SOM ranging from 47% to 80% depending on environment-specific factors such as litter input rate, biomass and necromass turnover or fungal to bacterial ratios (Fan and Liang, 2015; Liang et al., 2019). However, other studies showed a contribution of microbial C to stable SOM smaller than 50%, while plant-related inputs were

more important (Angst et al., 2021). While also our MAOM fractions contained plant-related soil C, the dominance of microbially-related soil C with ~ 60% was evident.

4.2 Amino sugar patterns

Our results provide insights into the fate of plant- and microbial-derived OM in POM and MAOM fractions. The high contribution of fungal residues to POM fractions and the contribution of both fungal and bacterial residues to MAOM fractions as based on amino sugar analyses demonstrate the dominant role of microbes for soil C and N stabilization in mineral associations. These estimates fit with results by Vidal et al. (2021) demonstrating that hyphae of saprotrophic fungi transfer C and N from needle litter to surrounding bulk soil where fungal residues accumulate at minerals and form MAOM. Thus, the presence and processive activity of fungi in plant-dominated POM fractions represents a necessary prerequisite for the establishment of MAOM, but also acts as a transfer mechanism of C and N from POM and MAOM fractions (cf. Vidal et al., 2021).

While we were not able to include bacteria in isotopic analyses and, hence, to our mixing model, their isotopic signatures likely would have shown an even stronger ^{13}C enrichment relative to SAP fungi as reported by Kohl et al. (2015) from PLFA analyses. Hence, we would expect a smaller contribution of bacterial residues to MAOM fractions compared to fungal residues as also indicated by the amino sugar data. Future analysis of the C and N isotopic signature of amino sugars may aid to elucidate the influence of bacterial and fungal residues on SOM fractions more closely. This might be combined with compound-specific analysis to trace the fate of different compounds from various sources to POM and MAOM fractions.

4.3 Role of mycorrhizal association for SOM

Despite an expected difference between ECM (oak) and AM (tulip poplar) systems in nutrient cycling and litter quality (e.g. Phillips et al., 2013; Midgley et al., 2015), we found few notable isotopic differences between fungal guilds and no tree species specific differences between tulip

poplar and white oak soils. We expected ECM fungi to be the dominant contributor to MAOM for white oak and SAP fungi to be the dominant contributor to MAOM for tulip poplar. In contrast, SAP fungi were the dominant contributor to MAOM fractions for both tree species. Our analysis showed that in mixed forests the co-existence and mixing of mycorrhizal types across the soil landscape is important for soil C storage patterns. In particular, the extensive growth of mycelia (e.g. Anderson and Cairney, 2007 and literature therein) can span large soil areas and contribute to soil C and N cycling patterns. The negligible AM fungi contribution to soil fractions' C and N likely results from their low biomass production (cf. Cheeke et al., 2021), but components other than hyphae, for example, exudates such as glomalin, hydrophobins, chaplins or SC15 (Rillig, 2004; Etcheverría et al., 2009; Rillig et al., 2007) may contribute more substantially to stable SOM.

Differences between ECM- and AM-associated systems are frequently driven by the C utilization and N acquisition strategies of associated fungi (Phillips et al., 2013). A study by Keller et al. (2020) identified roots inputs as the predominant source of MAOM, with greater root C inputs in AM compared to ECM soils. This mycorrhizal type difference could result from higher exudation and faster turnover of AM root and fungal biomass (Keller et al., 2020) causing a stimulation of SAP fungal growth (Verbruggen et al., 2017). Recent literature describes the activation and fueling of saprotrophic organisms with C by AM fungi in order to access nutrients released by enhanced SOM decomposition (Verbruggen et al., 2017; Kaiser et al., 2015). This may explain the high contribution of SAP fungal residues to the SOM fractions in the AM-associated tulip poplar system. Studies from Beidler et al. (2020) and Eagar et al. (2021) conducted in the same forest as this study further supports the expectation of AM systems being driven by saprotrophic organisms, as the authors described more saprotrophic fungi and molds in soils under AM vegetation compared to ECM vegetation. Similar findings were reported by Bahram et al. (2020) for topsoil microbiomes of sites in the Baltic region.

Overall, the interaction between mycorrhizal and saprotrophic fungi appears relevant for the C and N inputs contributing to MAOM fractions.

While for AM-associated trees the facilitation of saprotrophic organisms to mine for nutrients explains the dominance of SAP fungi, for ECM-associated trees both ECM and SAP fungi are actively contributing to SOM formation.

Conclusion

Our study provides clear evidence for the high contribution of fungal biomass for the build-up of MAOM. This clearly highlights the importance of both, mycorrhizal and saprotrophic fungi, for the formation of persistent SOM. Thus, our results underpin the need to consider fungal contributions to SOM for predictions of soil C and N storage and release.

Acknowledgements

We want to thank IU RTP and preserve manager Michael Chitwood. Special thanks to Elizabeth Huenupi-Pena for assistance with organizing field and lab equipment and shipping and to Ilse Thaufelder for helping with sampling and sample preparation. We thank Steven Russell and Ronald Kerner for their help with fungal sporocarp identification. Thanks to Sofia Gomes for DNA analyses of fungi in tree roots. Many thanks to the BayCEER Laboratory of Isotope Biogeochemistry (University of Bayreuth, Germany) and the Centre for Stable Isotope Research and Analysis (Georg-August-University Göttingen, Germany) for stable isotope analyses. This work was funded by the German Research Foundation (DFG) under project PA 2377/2-1/GU 1309/5-1 “Towards a predictive understanding on how mycorrhizal types influence the decomposition of soil organic matter”. Part of the lab work and chemical analyzes were funded by the DFG project “Rhizosphere as driver of subsoil organic matter distribution and composition” (MU3021/4-2) in the frame of the research unit “The Forgotten Part of Carbon Cycling: Soil Organic Matter Storage and Turnover in Subsoils (SUBSOM)” (FOR1806).

Author contributions

SK, RPP and JP developed the research design. SK and AK conducted the field survey and performed the laboratory analyses accompanied by AJW, VLB and NM. SK and NM analyzed the results. SK wrote the first draft of the manuscript. All coauthors contributed to the manuscript.

Data statement

The raw data are available in the Supporting material (**Supporting material Table S3**).

References

Amelung, W., 2001. Methods using amino sugars as markers for microbial residues in soil. Assessment methods for soil carbon, 233–270.

Amelung, W., Zech, W., 1999. Minimisation of organic matter disruption during particle-size fractionation of grassland epipedons. Geoderma 92, 73–85.

Anderson, I.C., Cairney, J.W.G., 2007. Ectomycorrhizal fungi: exploring the mycelial frontier. FEMS microbiology reviews 31, 388–406.

Angst, G., Mueller, K.E., Kögel-Knabner, I., Freeman, K.H., Mueller, C.W., 2017. Aggregation controls the stability of lignin and lipids in clay-sized particulate and mineral associated organic matter. Biogeochemistry 132, 307–324.

Angst, G., Mueller, K.E., Nierop, K.G.J., Simpson, M.J., 2021. Plant- or microbial-derived? A review on the molecular composition of stabilized soil organic matter. Soil Biology and Biochemistry 156, 108189.

Appuhn, A., Joergensen, R.G., 2006. Microbial colonisation of roots as a function of plant species. Soil Biology and Biochemistry 38, 1040–1051.

Bahram, M., Netherway, T., Hildebrand, F., Pritsch, K., Drenkhan, R., Loit, K., Anslan, S., Bork, P., Tedersoo, L., 2020. Plant nutrient-acquisition strategies drive topsoil microbiome structure and function. New Phytologist 227, 1189–1199.

Baldock, J.A., Skjemstad, J.O., 2000. Role of the soil matrix and minerals in protecting natural organic materials against biological attack. Organic Geochemistry 31, 697–710.

Beidler, K.V., Phillips, R.P., Andrews, E., Maillard, F., Mushinski, R.M., Kennedy, P.G., 2020. Substrate quality drives fungal necromass decay and decomposer community structure under contrasting vegetation types. Journal of Ecology 108, 1845–1859.

Bond, A.L., Diamond, A.W., 2011. Recent Bayesian stable-isotope mixing models are highly sensitive to variation in discrimination factors. Ecological applications : a publication of the Ecological Society of America 21, 1017–1023.

Bradford, M.A., Keiser, A.D., Davies, C.A., Mersmann, C.A., Strickland, M.S., 2013. Empirical evidence that soil carbon formation from plant inputs is positively related to microbial growth. Biogeochemistry 113, 271–281.

Castellano, M.J., Mueller, K.E., Olk, D.C., Sawyer, J.E., Six, J., 2015. Integrating plant litter quality, soil organic matter stabilization, and the carbon saturation concept. Global change biology 21, 3200–3209.

Cheeke, T.E., Phillips, R.P., Kuhn, A., Rosling, A., Fransson, P., 2021. Variation in hyphal production rather than turnover regulates standing fungal biomass in temperate hardwood forests. Ecology 102, e03260.

Christensen, B.T., 2001. Physical fractionation of soil and structural and functional complexity in organic matter turnover. European Journal of Soil Science 52, 345–353.

Córdova, S.C., Olk, D.C., Dietzel, R.N., Mueller, K.E., Archontouilis, S.V., Castellano, M.J., 2018. Plant litter quality affects the accumulation rate, composition, and stability of mineral-associated soil organic matter. Soil Biology and Biochemistry 125, 115–124.

Cotrufo, M.F., Ranalli, M.G., Haddix, M.L., Six, J., Lugato, E., 2019. Soil carbon storage informed by particulate and mineral-associated organic matter. Nature Geoscience 12, 989–994.

Cotrufo, M.F., Wallenstein, M.D., Boot, C.M., Denef, K., Paul, E., 2013. The Microbial Efficiency-Matrix Stabilization (MEMS) framework integrates plant litter decomposition with soil organic matter stabilization: do labile plant inputs form stable soil organic matter? Global change biology 19, 988–995.

Craig, M.E., Turner, B.L., Liang, C., Clay, K., Johnson, D.J., Phillips, R.P., 2018. Tree mycorrhizal type predicts within-site variability in the storage and distribution of soil organic matter. Global change biology 24, 3317–3330.

Cyle, K.T., Hill, N., Young, K., Jenkins, T., Hancock, D., Schroeder, P.A., Thompson, A., 2016. Substrate quality influences organic matter accumulation in the soil silt and clay fraction. Soil Biology and Biochemistry 103, 138–148.

Eagar, A.C., Mushinski, R.M., Horning, A.L., Smemo, K.A., Phillips, R.P., Blackwood, C.B., 2021. Arbuscular mycorrhizal tree communities have greater soil fungal diversity and relative abundances of saprotrophs and pathogens compared to ectomycorrhizal tree communities. Applied and environmental microbiology, AEM0178221.

Ehleringer, J.R., Buchmann, N., Flanagan, L.B., 2000. Carbon Isotope Ratios In Belowground Carbon Cycle Processes. Ecological applications : a publication of the Ecological Society of America 10, 412–422.

Etcheverría, P., Huygens, D., Godoy, R., Borie, F., Boeckx, P., 2009. Arbuscular mycorrhizal fungi contribute to 13C and 15N enrichment of soil organic matter in forest soils. Soil Biology and Biochemistry 41, 858–861.

Evans, L.R., Pierson, D., Lajtha, K., 2020. Dissolved organic carbon production and flux under long-term litter manipulations in a Pacific Northwest old-growth forest. Biogeochemistry 149, 75–86.

Fan, Z., Liang, C., 2015. Significance of microbial asynchronous anabolism to soil carbon dynamics driven by litter inputs. Scientific reports 5, 9575.

Faust, S., Heinze, S., Ngosong, C., Sradnick, A., Oltmanns, M., Raupp, J., Geisseler, D., Joergensen, R.G., 2017. Effect of biodynamic soil amendments on microbial communities in comparison with inorganic fertilization. Applied Soil Ecology 114, 82–89.

Frey, S.D., 2019. Mycorrhizal Fungi as Mediators of Soil Organic Matter Dynamics. Annual Review of Ecology, Evolution, and Systematics 50, 237–259.

Fry, B., 2008. Stable Isotope Ecology. Springer, New York.

Gebauer, G., Dietrich, P., 1993. Nitrogen Isotope Ratios in Different Compartments of a Mixed Stand of Spruce, Larch and Beech Trees and of Understorey Vegetation Including Fungi. Isotopenpraxis Isotopes in Environmental and Health Studies 29, 35–44.

Gebauer, G., Taylor, A.F.S., 1999. 15N natural abundance in fruit bodies of different functional groups of fungi in relation to substrate utilization. New Phytologist 142, 93–101.

Gleixner, G., Danier, H.J., Werner, R.A., Schmidt, H.L., 1993. Correlations between the 13C Content of Primary and Secondary Plant Products in Different Cell Compartments and That in Decomposing Basidiomycetes. Plant physiology 102, 1287–1290.

Godbold, D.L., Hoosbeek, M.R., Lukac, M., Cotrufo, M.F., Janssens, I.A., Ceulemans, R., Polle, A., Velthorst, E.J., Scarascia-Mugnozza, G., Angelis, P. de, Miglietta, F., Peressotti, A., 2006. Mycorrhizal Hyphal Turnover as a Dominant Process for Carbon Input into Soil Organic Matter. Plant and Soil 281, 15–24.

Golchin, A., Oades, J.M., Skjemstad, J.O., Clarke, P., 1994. Soil structure and carbon cycling. Soil Research 32, 1043.

Guerrant, G.O., Moss, C.W., 1984. Determination of monosaccharides as aldononitrile, O-methyloxime, alditol, and cyclitol acetate derivatives by gas chromatography. Analytical Chemistry 56, 633–638.

Hobbie, E.A., Sánchez, F.S., Rygiewicz, P.T., 2012. Controls of isotopic patterns in saprotrophic and ectomycorrhizal fungi. Soil Biology and Biochemistry 48, 60–68.

Högberg, M.N., Högberg, P., 2002. Extramatrical ectomycorrhizal mycelium contributes one-third of microbial biomass and produces, together with associated roots, half the dissolved organic carbon in a forest soil. New Phytologist 154, 791–795.

Högberg, P., Plamboeck, A.H., Taylor, A.F., Fransson, P.M., 1999. Natural (13)C abundance reveals trophic status of fungi and host-origin of carbon in mycorrhizal fungi in mixed forests. Proceedings of the National Academy of Sciences of the United States of America 96, 8534–8539.

Huang, W., Hammel, K.E., Hao, J., Thompson, A., Timokhin, V.I., Hall, S.J., 2019. Enrichment of Lignin-Derived Carbon in Mineral-Associated Soil Organic Matter. Environmental science & technology 53, 7522–7531.

Joergensen, R.G., 2018. Amino sugars as specific indices for fungal and bacterial residues in soil. Biology and Fertility of Soils 54, 559–568.

Kaiser, C., Kilburn, M.R., Clode, P.L., Fuchslueger, L., Koranda, M., Cliff, J.B., Solaiman, Z.M., Murphy, D.V., 2015. Exploring the transfer of recent plant photosynthates to soil microbes: mycorrhizal pathway vs direct root exudation. The New phytologist 205, 1537–1551.

Keller, A.B., Brzostek, E.R., Craig, M.E., Fisher, J.B., Phillips, R.P., 2020. Root-derived inputs are major contributors to soil carbon in temperate forests, but vary by mycorrhizal type. Ecology letters 24, 626–635.

Klink, S., Giesemann, P., Hubmann, T., Pausch, J., 2020. Stable C and N isotope natural abundances of intraradical hyphae of arbuscular mycorrhizal fungi. Mycorrhiza 30, 773–780.

Kohl, L., Laganière, J., Edwards, K.A., Billings, S.A., Morrill, P.L., van Biesen, G., Ziegler, S.E., 2015. Distinct fungal and bacterial δ13C signatures as potential drivers of increasing δ13C of soil organic matter with depth. Biogeochemistry 124, 13–26.

Kohzu, A., Yoshioka, T., Ando, T., Takahashi, M., Koba, K., Wada, E., 1999. Natural 13 C and 15 N abundance of field-collected fungi and their ecological implications. New Phytologist 144, 323–330.

Kopittke, P.M., Dalal, R.C., Hoeschen, C., Li, C., Menzies, N.W., Mueller, C.W., 2020. Soil organic matter is stabilized by organo-mineral associations through two key processes: The role of the carbon to nitrogen ratio. Geoderma 357, 113974.

Kopittke, P.M., Hernandez-Soriano, M.C., Dalal, R.C., Finn, D., Menzies, N.W., Hoeschen, C., Mueller, C.W., 2018. Nitrogen-rich microbial products provide new organo-mineral associations for the stabilization of soil organic matter. Global change biology 24, 1762–1770.

Lavallee, J.M., Soong, J.L., Cotrufo, M.F., 2020. Conceptualizing soil organic matter into particulate and mineral-associated forms to address global change in the 21st century. Global change biology 26, 261–273.

Lehmann, J., Hansel, C.M., Kaiser, C., Kleber, M., Maher, K., Manzoni, S., Nunan, N., Reichstein, M., Schimel, J.P., Torn, M.S., Wieder, W.R., Kögel-Knabner, I., 2020. Persistence of soil organic carbon caused by functional complexity. Nature Geoscience 13, 529–534.

Lehmann, J., Kleber, M., 2015. The contentious nature of soil organic matter. Nature 528, 60–68.

Li, N., Xu, Y.-Z., Han, X.-Z., He, H.-B., Zhang, X.-d., Zhang, B., 2015. Fungi contribute more than bacteria to soil organic matter through necromass accumulation under different

agricultural practices during the early pedogenesis of a Mollisol. European Journal of Soil Biology 67, 51–58.

Liang, C., Amelung, W., Lehmann, J., Kästner, M., 2019. Quantitative assessment of microbial necromass contribution to soil organic matter. Global change biology 25, 3578–3590.

Lützow, M. von, Kögel-Knabner, I., Ekschmitt, K., Flessa, H., Guggenberger, G., Matzner, E., Marschner, B., 2007. SOM fractionation methods: Relevance to functional pools and to stabilization mechanisms. Soil Biology and Biochemistry 39, 2183–2207.

Marschner, B., Brodowski, S., Dreves, A., Gleixner, G., Gude, A., Grootes, P.M., Hamer, U., Heim, A., Jandl, G., Ji, R., Kaiser, K., Kalbitz, K., Kramer, C., Leinweber, P., Rethemeyer, J., Schäffer, A., Schmidt, M.W.I., Schwark, L., Wiesenberg, G.L.B., 2008. How relevant is recalcitrance for the stabilization of organic matter in soils? Journal of Plant Nutrition and Soil Science 171, 91–110.

Menichetti, L., Houot, S., van Oort, F., Kätterer, T., Christensen, B.T., Chenu, C., Barré, P., Vasilyeva, N.A., Ekblad, A., 2015. Increase in soil stable carbon isotope ratio relates to loss of organic carbon: results from five long-term bare fallow experiments. Oecologia 177, 811–821.

Midgley, M.G., Brzostek, E., Phillips, R.P., 2015. Decay rates of leaf litters from arbuscular mycorrhizal trees are more sensitive to soil effects than litters from ectomycorrhizal trees. Journal of Ecology 103, 1454–1463.

Midgley, M.G., Phillips, R.P., 2016. Resource stoichiometry and the biogeochemical consequences of nitrogen deposition in a mixed deciduous forest. Ecology 97, 3369–3378.

Midgley, M.G., Phillips, R.P., 2019. Spatio-temporal heterogeneity in extracellular enzyme activities tracks variation in saprotrophic fungal biomass in a temperate hardwood forest. Soil Biology and Biochemistry 138, 107600.

Mikutta, R., Turner, S., Schippers, A., Gentsch, N., Meyer-Stüve, S., Condron, L.M., Peltzer, D.A., Richardson, S.J., Eger, A., Hempel, G., Kaiser, K., Klotzbücher, T., Guggenberger, G., 2019. Microbial and abiotic controls on mineral-associated organic matter in soil profiles along an ecosystem gradient. Scientific reports 9, 10294.

Mueller, C.W., Gutsch, M., Kothieringer, K., Leifeld, J., Rethemeyer, J., Brueggemann, N., Kögel-Knabner, I., 2014. Bioavailability and isotopic composition of CO2 released from incubated soil organic matter fractions. Soil Biology and Biochemistry 69, 168–178.

Mueller, C.W., Koegel-Knabner, I., 2009. Soil organic carbon stocks, distribution, and composition affected by historic land use changes on adjacent sites. Biology and Fertility of Soils 45, 347–359.

Mushinski, R.M., Payne, Z.C., Raff, J.D., Craig, M.E., Pusede, S.E., Rusch, D.B., White, J.R., Phillips, R.P., 2020. Nitrogen cycling microbiomes are structured by plant mycorrhizal associations with consequences for nitrogen oxide fluxes in forests. Global change biology.

Mushinski, R.M., Phillips, R.P., Payne, Z.C., Abney, R.B., Jo, I., Fei, S., Pusede, S.E., White, J.R., Rusch, D.B., Raff, J.D., 2019. Microbial mechanisms and ecosystem flux estimation for aerobic NOy emissions from deciduous forest soils. Proceedings of the National Academy of Sciences of the United States of America 116, 2138–2145.

Nadelhoffer, K.J., Fry, B., 1988. Controls on Natural Nitrogen-15 and Carbon-13 Abundances in Forest Soil Organic Matter. Soil Science Society of America Journal 52, 1633–1640.

Parnell, A., Jackson, A., 2013. siar: Stable Isotope Analysis in R.

Parnell, A.C., Inger, R., Bearhop, S., Jackson, A.L., 2010. Source partitioning using stable isotopes: coping with too much variation. PloS one 5, e9672.

Parsons, J.W., 1981. Chemistry and distribution of amino sugars in soils and soil organisms. Soil biochemistry, 5, 197–227.

Phillips, R.P., Brzostek, E., Midgley, M.G., 2013. The mycorrhizal-associated nutrient economy: a new framework for predicting carbon-nutrient couplings in temperate forests. New Phytologist 199, 41–51.

Poeplau, C., Don, A., Six, J., Kaiser, M., Benbi, D., Chenu, C., Cotrufo, M.F., Derrien, D., Gioacchini, P., Grand, S., Gregorich, E., Griepentrog, M., Gunina, A., Haddix, M., Kuzyakov, Y., Kühnel, A., Macdonald, L.M., Soong, J., Trigalet, S., Vermeire, M.-L., Rovira, P., van Wesemael, B., Wiesmeier, M., Yeasmin, S., Yevdokimov, I., Nieder, R., 2018. Isolating organic carbon fractions with varying turnover rates in temperate agricultural soils – A comprehensive method comparison. Soil Biology and Biochemistry 125, 10–26.

Rillig, M.C., 2004. Arbuscular mycorrhizae, glomalin, and soil aggregation. Canadian Journal of Soil Science 84, 355–363.

Rillig, M.C., Caldwell, B.A., Wösten, H.A.B., Sollins, P., 2007. Role of proteins in soil carbon and nitrogen storage: controls on persistence. Biogeochemistry 85, 25–44.

Rosling, A., Midgley, M.G., Cheeke, T., Urbina, H., Fransson, P., Phillips, R.P., 2016. Phosphorus cycling in deciduous forest soil differs between stands dominated by ecto- and arbuscular mycorrhizal trees. New Phytologist 209, 1184–1195.

Rumpel, C., Baumann, K., Remusat, L., Dignac, M.-F., Barré, P., Deldicque, D., Glasser, G., Lieberwirth, I., Chabbi, A., 2015. Nanoscale evidence of contrasted processes for root-derived organic matter stabilization by mineral interactions depending on soil depth. Soil Biology and Biochemistry 85, 82–88.

Schmidt, M.W.I., Rumpel, C., Kögel-Knabner, I., 1999. Evaluation of an ultrasonic dispersion procedure to isolate primary organomineral complexes from soils. European Journal of Soil Science 50, 87–94.

Schmidt, M.W.I., Torn, M.S., Abiven, S., Dittmar, T., Guggenberger, G., Janssens, I.A., Kleber, M., Kögel-Knabner, I., Lehmann, J., Manning, D.A.C., Nannipieri, P., Rasse, D.P., Weiner, S., Trumbore, S.E., 2011. Persistence of soil organic matter as an ecosystem property. Nature 478, 49–56.

Schöning, I., Morgenroth, G., Kögel-Knabner, I., 2005. O/N-alkyl and alkyl C are stabilised in fine particle size fractions of forest soils. Biogeochemistry 73, 475–497.

SigmaPlot version 11.0, 2008. Systat Software, San Jose, USA.

Simpson, A.J., Simpson, M.J., Smith, E., Kelleher, B.P., 2007. Microbially derived inputs to soil organic matter: are current estimates too low? Environmental science & technology 41, 8070–8076.

Software R version 3.6.1, 2019. R: A language and environment for statistical computing. R Development Core Team, Vienna, Austria.

Sokol, N.W., Bradford, M.A., 2019. Microbial formation of stable soil carbon is more efficient from belowground than aboveground input. Nature Geoscience 12, 46–53.

Taylor, A.F.S., Högbom, L., Högberg, M., Lyon, A.J.E., Näsholm, T., Högberg, P., 1997. Natural 15 N abundance in fruit bodies of ectomycorrhizal fungi from boreal forests. New Phytologist 136, 713–720.

Verbruggen, E., Pena, R., Fernandez, C.W., Soong, J.L., 2017. Mycorrhizal Interactions With Saprotrophs and Impact on Soil Carbon Storage, in: Johnson, N. (Ed.), Mycorrhizal Mediation of Soil. Elsevier, [Place of publication not identified], pp. 441–460.

Vidal, A., Klöffel, T., Guigue, J., Angst, G., Steffens, M., Hoeschen, C., Mueller, C.W., 2021. Visualizing the transfer of organic matter from decaying plant residues to soil mineral surfaces controlled by microorganisms. Soil Biology and Biochemistry 160, 108347.

Wagai, R., Mayer, L.M., Kitayama, K., 2009. Nature of the “occluded” low-density fraction in soil organic matter studies: A critical review. Soil Science and Plant Nutrition 55, 13–25.

Witzgall, K., Vidal, A., Schubert, D.I., Höschen, C., Schweizer, S.A., Buegger, F., Pouteau, V., Chenu, C., Mueller, C.W., 2021. Particulate organic matter as a functional soil component for persistent soil organic carbon. Nature communications 12, 4115.

Zhang, X., Amelung, W., 1996. Gas chromatographic determination of muramic acid, glucosamine, mannosamine, and galactosamine in soils. Soil Biology and Biochemistry 28, 1201–1206.

List of figures and tables

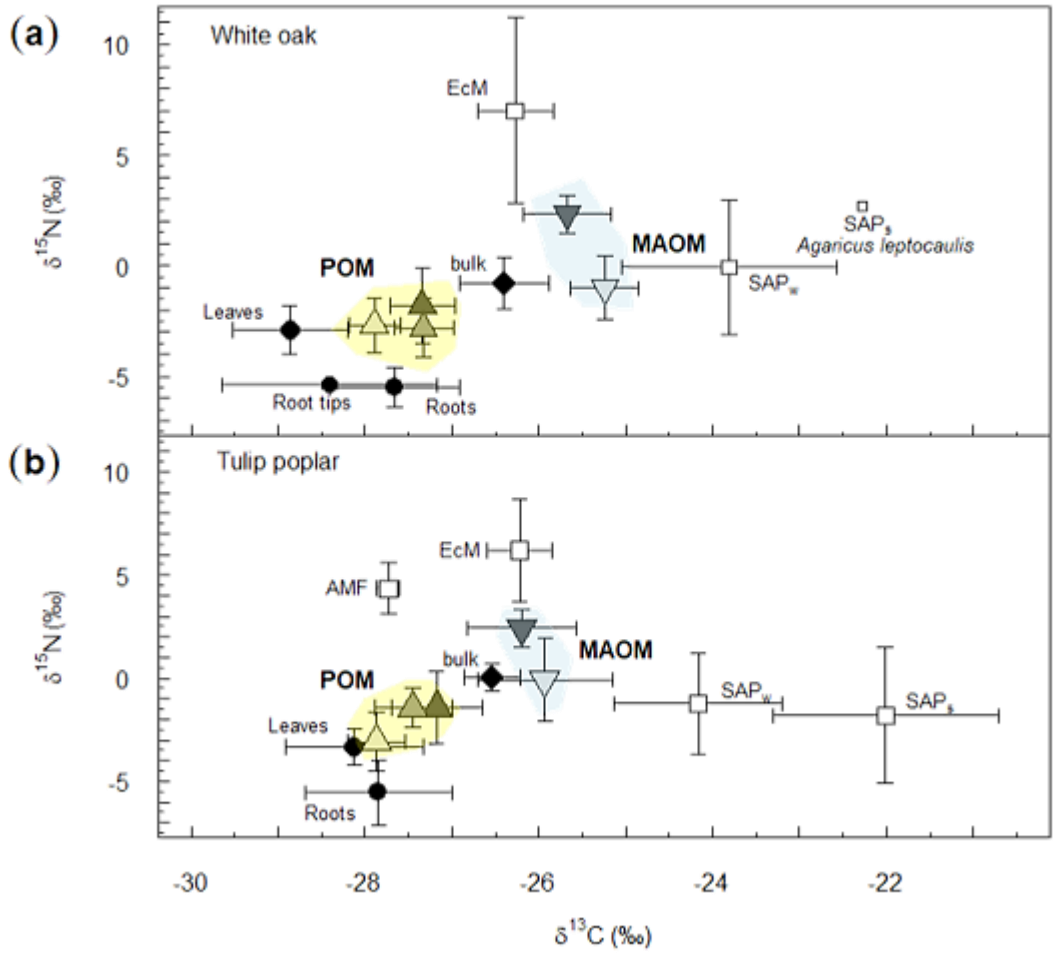

Fig 1 Dual-isotope scatter plot of $\delta^{13}C$ and $\delta^{15}N$ mean values with standard deviation (SD) of (a) white oak and (b) tulip poplar. Circles represent plant tissues (leaf litter, roots, root tips or leaves), upwards triangles represent POM fractions (yellow background), downwards triangles MAOM fractions (blue background). Grey scales: light grey for large fractions (> 63 µm particle size), medium grey for medium fractions (> 20 µm particle size) and dark grey for small fractions (< 20 µm particle size). Bulk soil is represented by a black diamond. Fungal biomass is indicated by white squares. AMF = arbuscular mycorrhizal fungi, ECM = ectomycorrhizal fungi, SAP_w = saprotrophic fungi on wood, SAP_s = saprotrophic fungi on soil. POM = particulate organic matter, MAOM = mineral-associated organic matter.

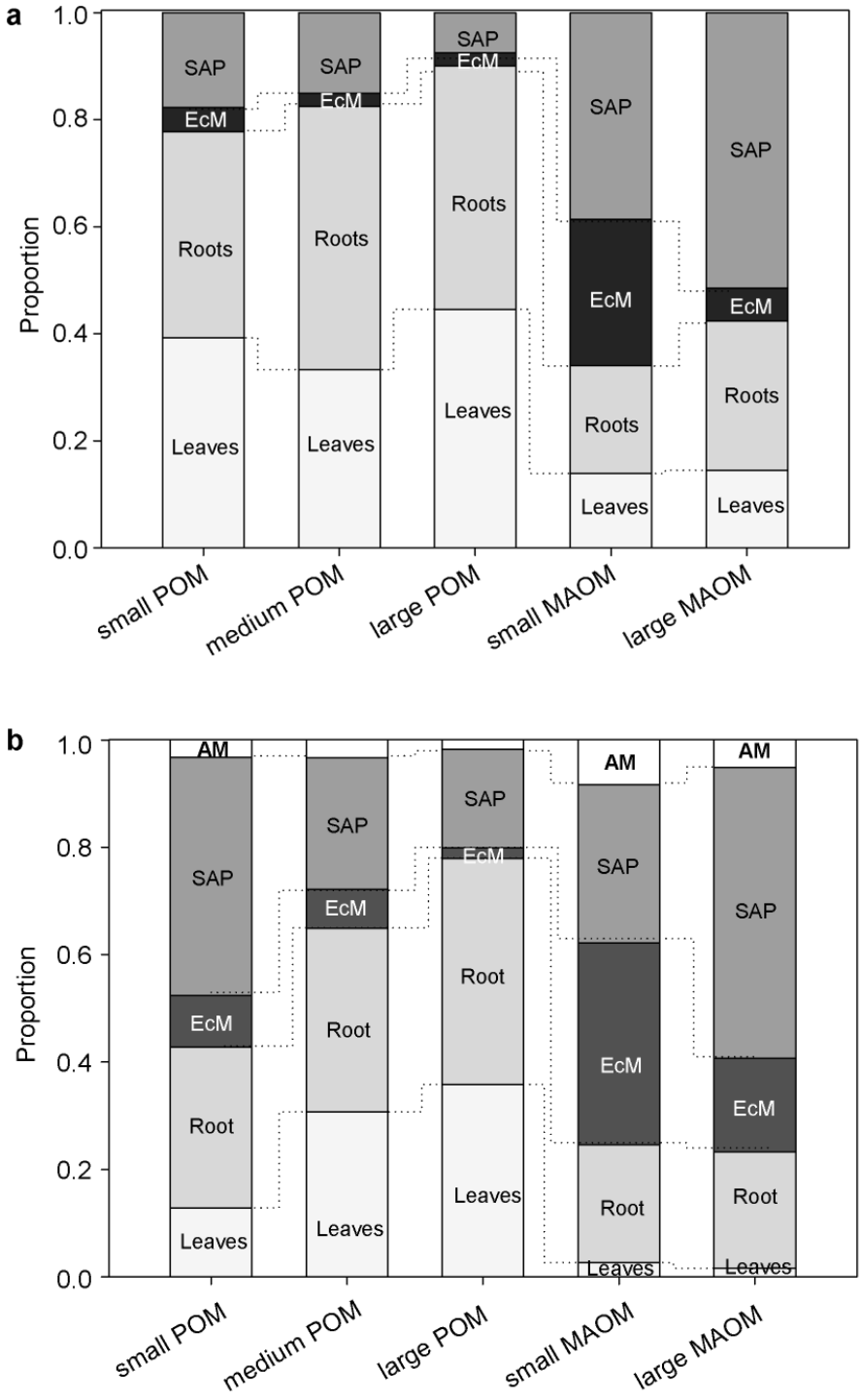

Fig. 2 Stacked bar plot of input contributions to various POM and MAOM fractions under white oak (a) and tulip poplar (b). Inputs were separated into leaves (light grey), roots (grey) ectomycorrhizal fungi (ECM, dark grey), saprotrophic fungi (SAP, medium grey) and arbuscular mycorrhizal fungi (AM, white).

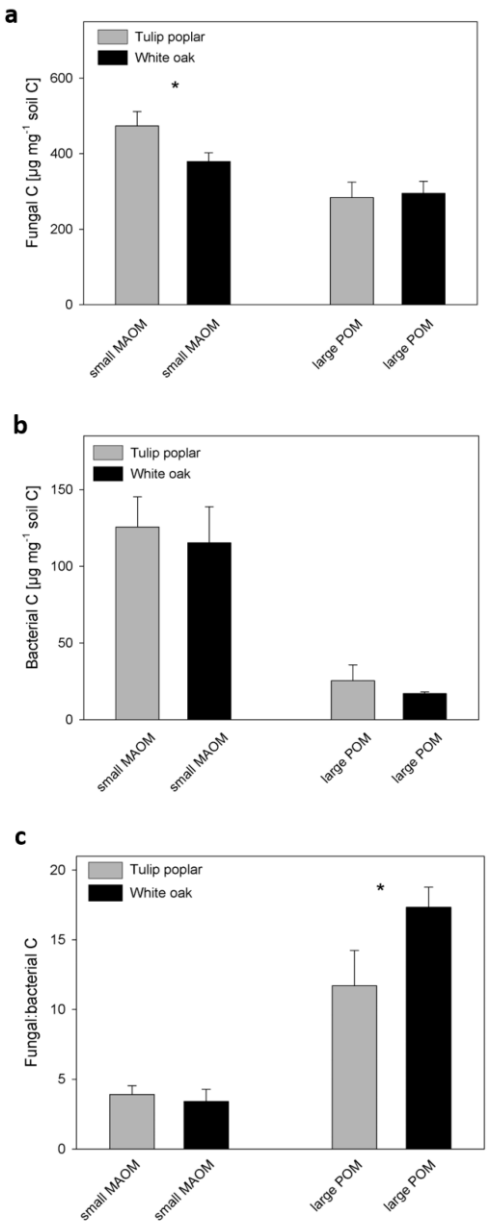

Fig. 3 Bar plots (with SD) of amounts of fungal and bacterial residue C and fungal to bacterial residue C ratio in small (< 20µm) MAOM and large (> 63µm) POM fractions based on amino sugar data. (a) Fungal C in µg per mg soil C for small MAOM and large POM fractions of tulip poplar and white oak. (b) Bacterial C in µg per mg soil for small MAOM and large POM fractions of tulip poplar and white oak. (c) Ratio of fungal to bacterial C in the small MAOM and large POM fractions of tulip poplar and white oak. Significant differences ($P < 0.05$) between tree species are indicated by an asterisk (*).

Table 1 C and N distribution (%) of SOM fractions of tulip poplar and white oak in relation to the bulk soil. Significant differences of C and N contents and C:N ratios of POM and MAOM fractions within tree species are indicated with superscripted small letters. Significant differences between SOM fractions of tulip poplar and white oak are indicated by superscripted capital letters.

	tulip poplar (AM)			white oak (ECM)		
	C [% of bulk soil C]	N [% of bulk soil N]	C/N	C [% of bulk soil C]	N [% of bulk soil N]	C/N
Small POM	$8.0^{b} \pm 5$	$5.1^{b} \pm 4$	$24.5^{b} \pm 4$	$9.8^{a,b} \pm 13$	$5.3^{b,c} \pm 2$	$29.5^{b} \pm 10$
Medium POM	$9.4^{b} \pm 10$	$5.7^{b} \pm 6.7$	$25.2^{b} \pm 4$	$10.5^{a,b} \pm 6$	$5.6^{b,c} \pm 3$	$28.9^{b,a} \pm 9$
Large POM	$17.4^{b} \pm 19$	$8.9^{b} \pm 12$	$34.1^{b} \pm 8$	$17.4^{b,c} \pm 14$	$8.8^{c} \pm 6$	$29.5^{b} \pm 6$
Small MAOM	$61.0^{cA} \pm 29$	$73.0^{cA} \pm 30$	$12.0^{a} \pm 3$	$36.3^{cB} \pm 17$	$42.4^{cB} \pm 12$	$12.4^{c} \pm 3$
Medium MAOM	NA	NA	NA	NA	NA	NA
Large MAOM	$0.4^{a} \pm 0$	$0.5^{aC} \pm 3$	$13.4^{a} \pm 4$	$0.2^{a} \pm 5$	$0.2^{a,cD} \pm 0$	$15.6^{a,c} \pm 2$
Sum POM	~ 34.8%	~ 19.7%		~ 37.6%	~ 19.7%	
Sum MAOM	~ 61.4%	~ 73.5%		~ 36.5%	~ 42.6%	

MAOM, mineral associated organic matter; POM, particulate soil organic matter. NA, not available

Supporting Information

Stable isotopes reveal that fungal residues contribute more to mineral-associated organic matter pools than plant residues

Authors: Saskia Klink, Adrienne B. Keller, Andreas J. Wild, Vera L. Baumert, Matthias Gube, Eva Lehndorff, Nele Meyer, Carsten W. Mueller, Richard P. Phillips, Johanna Pausch

The following Supporting Information is available for this article:

Methods S1: DNA extraction and sequencing

Fig. S1 Dual isotope scatter plot of ^{13}C and ^{15}N mean values with standard deviation (SD) of (a) sugar maple (*Acer saccharum*) and (b) American beech (*Fagus grandifolia*).

Fig. S2 Schematic illustration of the soil fractionation process to gain POM and MAOM fractions of different size classes.

Fig. S3 Conversion of Bayesian Inference isotope mixing model to boxplots for tulip poplar.

Fig. S4 Conversion of Bayesian Inference isotope mixing model to boxplots for white oak.

Fig. S5 Amino sugar content (µm) per mg soil carbon for the large POM fraction (a) and the small MAOM fraction (b).

Table S1 C- and N-content [mg g^{-1}] and C/N ratio of plant tissues, bulk soil and fungal guilds of tulip poplar and white oak plots with standard deviation (SD).

Table S2 C- and N-content [mg g^{-1}] and C/N ratio of plant tissues, bulk soil and fungal guilds of sugar maple and American beech plots with standard deviation (SD).

Table S3 Raw data of stable isotope ^{13}C and ^{15}N values, N- and C- content, C/N ratio of plant tissues, fungal biomass, soil and SOM fractions (where available) of *Liriodendron tulipifera*, *Quercus alba*, *Acer saccharum* and *Fagus grandifolia*. [provided as an Excel Sheet].

Methods S1: DNA extraction and sequencing

DNA was extracted with the NucleoMag Plant Kit (Macherey-Nagel Gmbh & Co., Duren, Germany). We amplified fungal DNA using the fITS7/ITS4 primers (White et al., 1990; Ihrmark et al., 2012) containing an Illumina adaptor overhang. PCR products were purified using 0.9 × NucleoMag NGS Clean-Up and Size Selectbeads (Macherey-Nagel, Düren, Germany) according to the manufacturer's instructions, and the Illumina Nextera XT adaptors were added to the amplicons. The concentration of these individual indexed amplicons was measured with the QIAxcel using the DNA Screening Kit (Qiagen, Venlo) and was normalized and pooled equimolar in individual libraries. The two pools had a final clean up with 0.9 × NucleoMag NGS Clean-Up and Size Selectbeads (Macherey-Nagel, Düren, Germany). The quality and quantity of these two pools were checked on the Bioanalyzer using a high sensitivity chip (Agilent). Sequencing was done in with Illumina MiSeq platform using the paired-end 300 bp kit (BaseClear, Netherlands).

Raw reads were paired with a minimum overlap of 30 nucleotides and primers were removed. Subsequently, sequences with expected error > 0.1 were discarded and sequences were denoised using the UNOISE3 algorithm (Nearing et al., 2018) to create zero radius operational taxonomic units (Z OTUs), including chimera removal. Taxonomic assignments were made using the Blast algorithm against the curated UNITE+INSD fungal ITS database (version released on 02.02.2019) and correspond to the highest hit. Functional groups were assigned based on FUNGuild (Nguyen *et al.*, 2016).

References

- Ihrmark, K., Bödeker, I. T. M., Cruz-Martinez, K., Friberg, H., Kubartova, A., Schenck, J., et al. (2012). New primers to amplify the fungal ITS2 region - evaluation by 454-sequencing of artificial and natural communities. FEMS Microbiol. Ecol. 82, 666–677. doi: 10.1111/j.1574-6941.2012.01437.x
- Nearing, J. T., Douglas, G. M., Comeau, A. M., and Langille, M. G. I. (2018). Denoising the Denoisers: an independent evaluation of microbiome sequence error-correction approaches. PeerJ 6:e5364. doi: 10.7717/peerj. 5364
- Nguyen NH, Song Z, Bates ST, Branco S, Tedersoo L, Menke J, Schilling JS, Kennedy PG. 2016. FUNGuild: An open annotation tool for parsing fungal community datasets by ecological guild. *Fungal Ecology* 20.
- White, T. J., Bruns, T., Lee, S., and Taylor, J. (1990). "Amplification and direct sequencing offungal ribosomal RNA genes for phylogenetics," in PCR Protocols: A Guide to Methods and Applications, eds M. A. Innis, D. H. Gelfand, J. J. Sninsky, and T. J. White (San Diego: Academic Press), 315–322. doi: 10.1016/ b978-0-12-372180-8.50042-1

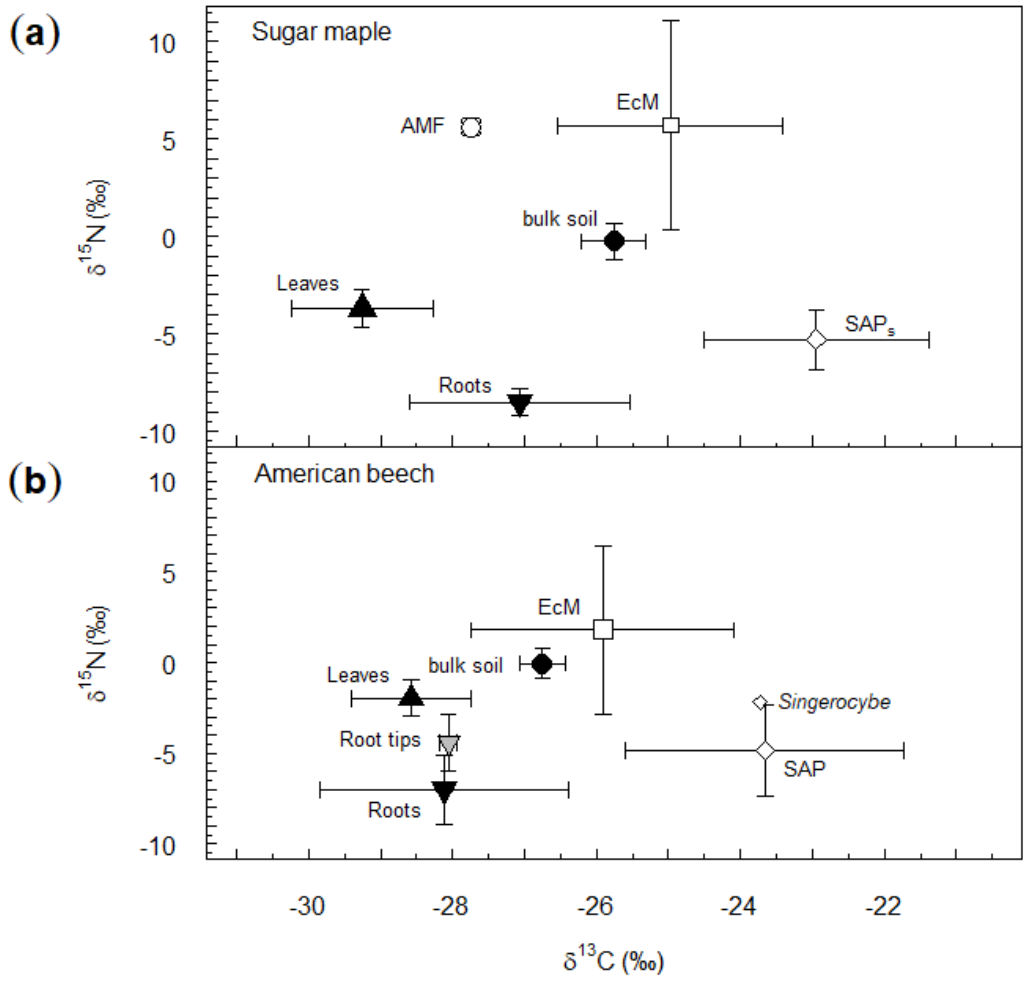

Fig. S1: Dual isotope scatter plot of $\delta^{13}C$ and $\delta^{15}N$ mean values with standard deviation (SD) of (a) sugar maple (Acer saccharum) and (b) American beech (Fagus grandifolia). Black upwards triangles represent leaves, black downwards triangles root tissue. Root tips are given with grey downwards triangles. Bulk soil is represented by black circles, white symbols represent fungi (circles for AMF, square for ECM, diamond for SAP). AMF = arbuscular mycorrhizal fungi, ECM = ectomycorrhizal fungi, SAP = saprotrophic fungi.

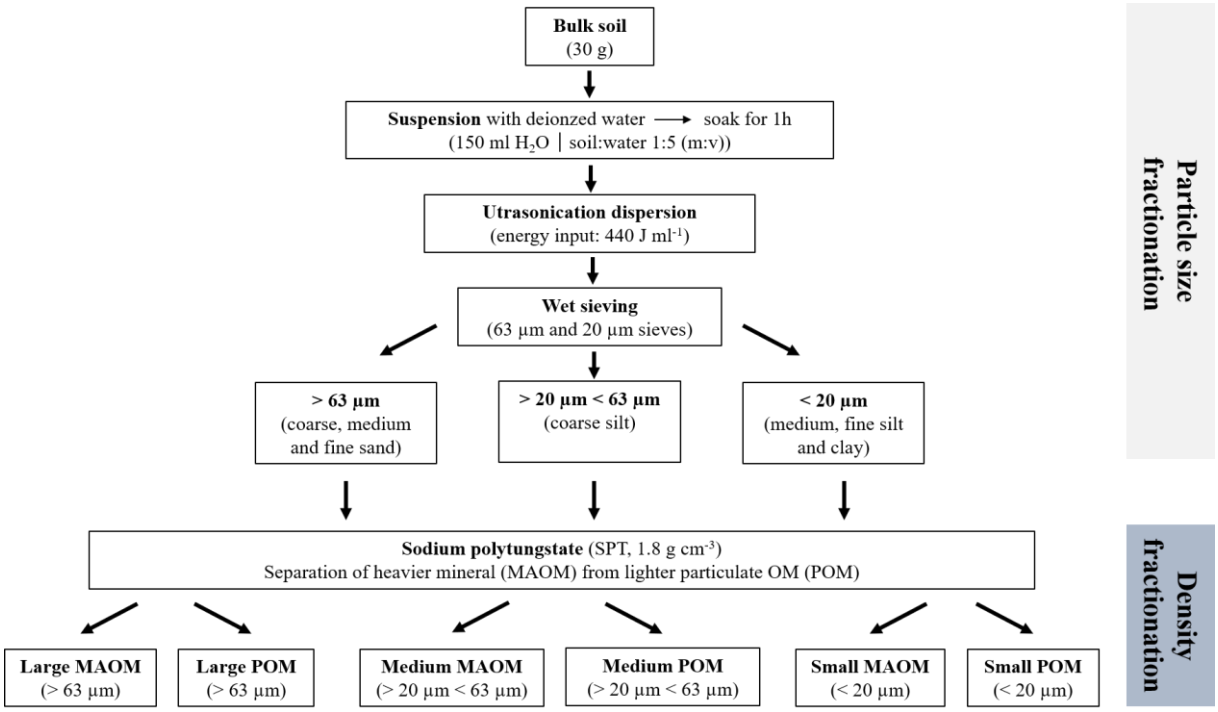

Fig. S2: Schematic illustration of the soil fractionation process to gain POM and MAOM fractions of different size classes. A particle size fractionation was conducted on bulk soil, followed by a density fractionation by sodium polytungstate (SPT). POM = particulate organic matter, MAOM = mineral-associated organic matter, OM = organic matter.

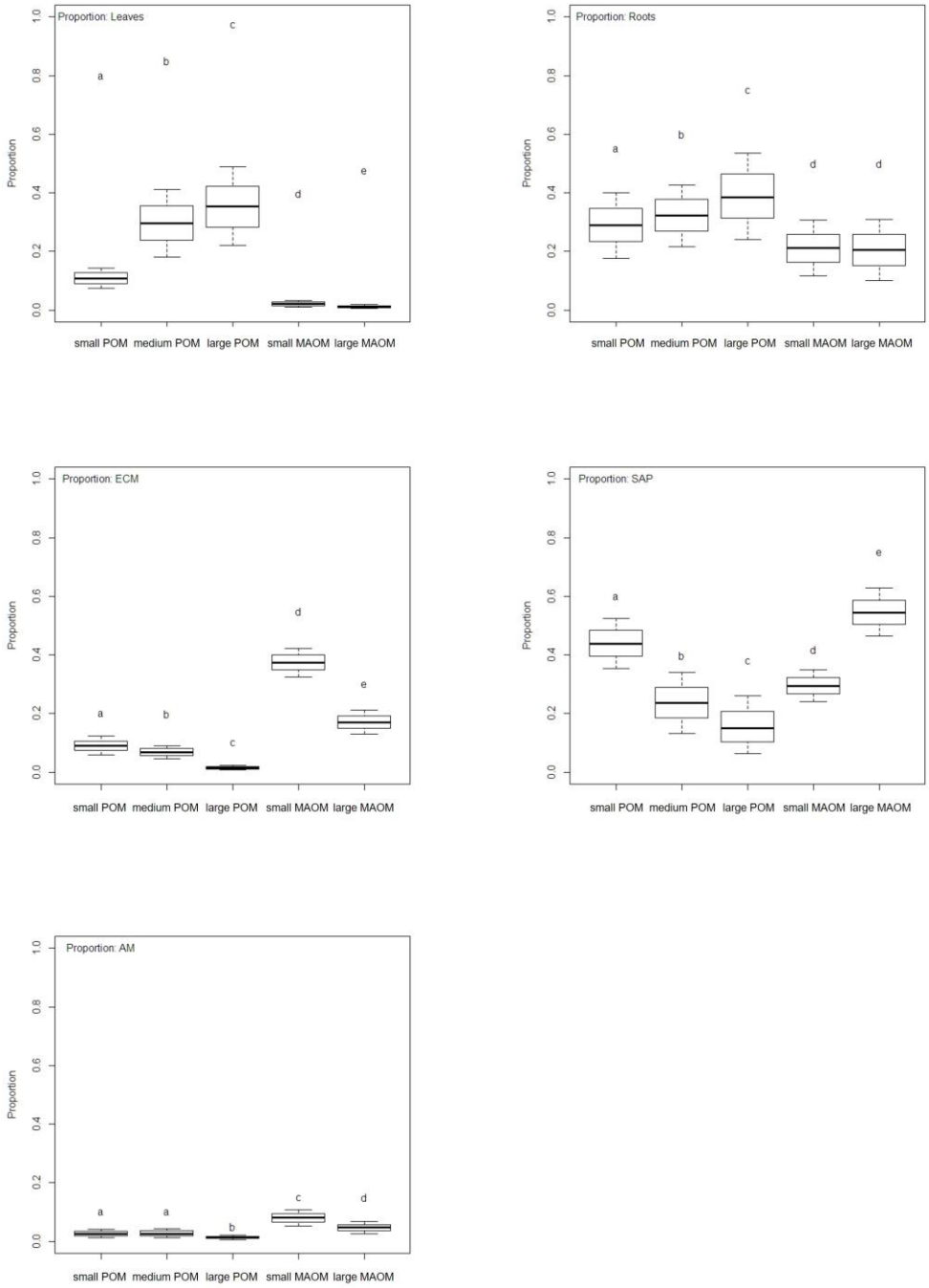

Fig. S3: Conversion of Bayesian Inference isotope mixing model to boxplots for tulip poplar. The box length is the interquartile range (IQR), the 25th and 75th percentile are indicated by the margins of the box. Whiskers give the minimum (25th percentile – 1.5 x IQR) or maximum (75th percentile + 1.5 x IQR); the median is given by the black line in the middle of the box. Extreme outliers were excluded. The model was informed with ^{13}C and ^{15}N isotopic signatures and C and N concentrations of tree leaves, tree roots, mycorrhizal fungi (AM fungi, ECM fungi) and SAP fungi as input sources. The POM and MAOM fractions of different size classes (small, medium, large) were set as input pools. The medium sized MAOM fraction could not be included into the analysis due to C and N concentrations below detection level. Significant differences between the fractions are indicated by unequal letters. The median is given by the black line in the centre of the box. POM = particulate organic matter, MAOM = mineral-associated organic matter, AM = arbuscular mycorrhizal, ECM = ectomycorrhizal, SAP = free-living saprotrophic fungi,

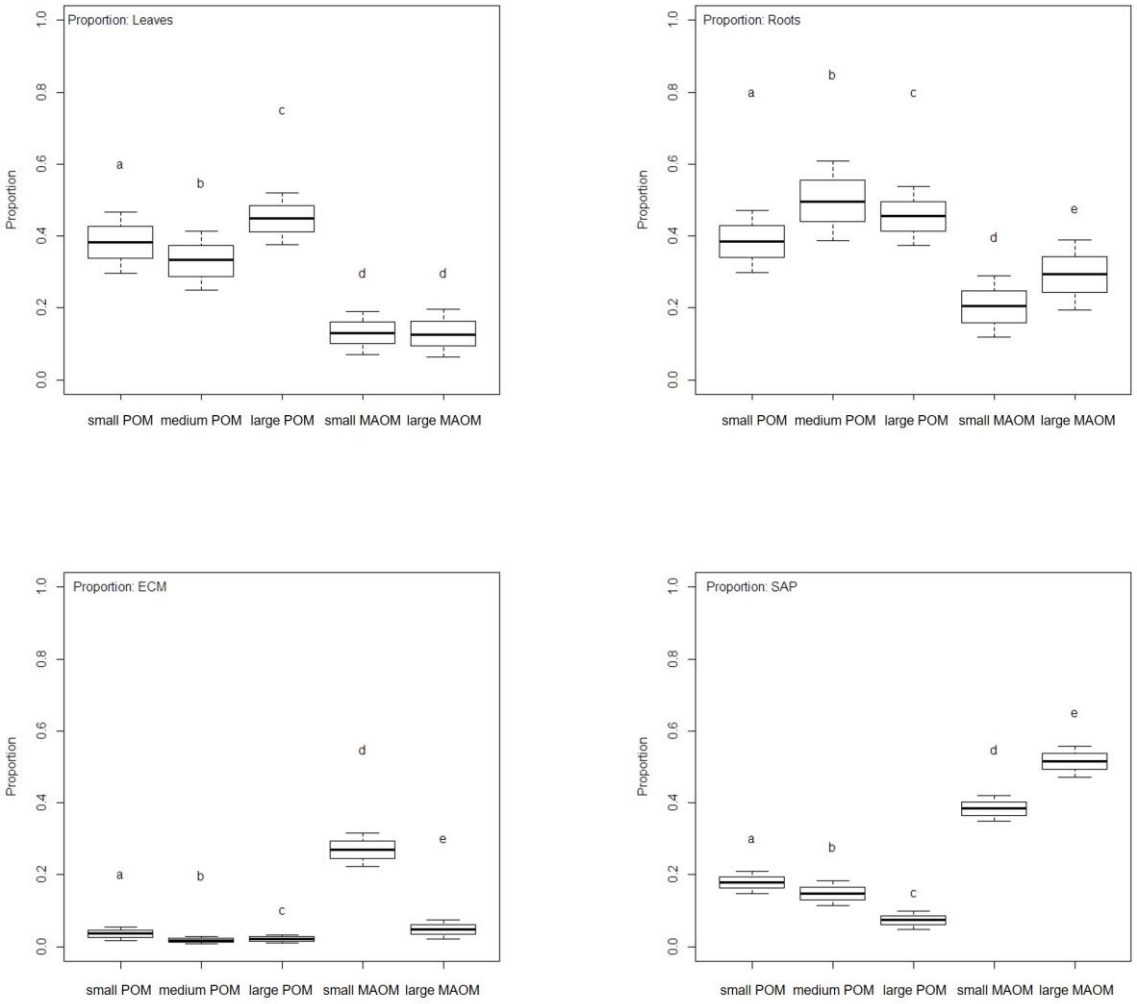

Fig.S4: Conversion of Bayesian Inference isotope mixing model to boxplots for white oak. The box length is the interquartile range (IQR), the 25th and 75th percentile are indicated by the margins of the box. Whiskers give the minimum (25th percentile – 1.5 x IQR) or maximum (75th percentile + 1.5 x IQR); the median is given by the black line in the middle of the box. Extreme outliers were excluded. The model was informed with ^{13}C and ^{15}N isotopic signatures and C and N concentrations of tree leaves, tree roots, mycorrhizal fungi (AM fungi, ECM fungi) and SAP fungi as input sources. The POM and MAOM fractions of different size classes (small, medium, large) were set as input pools. The medium sized MAOM fraction could not be included into the analysis due to C and N concentrations below detection level. Significant differences between the fractions are indicated by unequal letters. The median is given by the black line in the centre of the box. POM = particulate organic matter, MAOM = mineral-associated organic matter, AM = arbuscular mycorrhizal, ECM = ectomycorrhizal, SAP = free-living saprotrophic fungi.

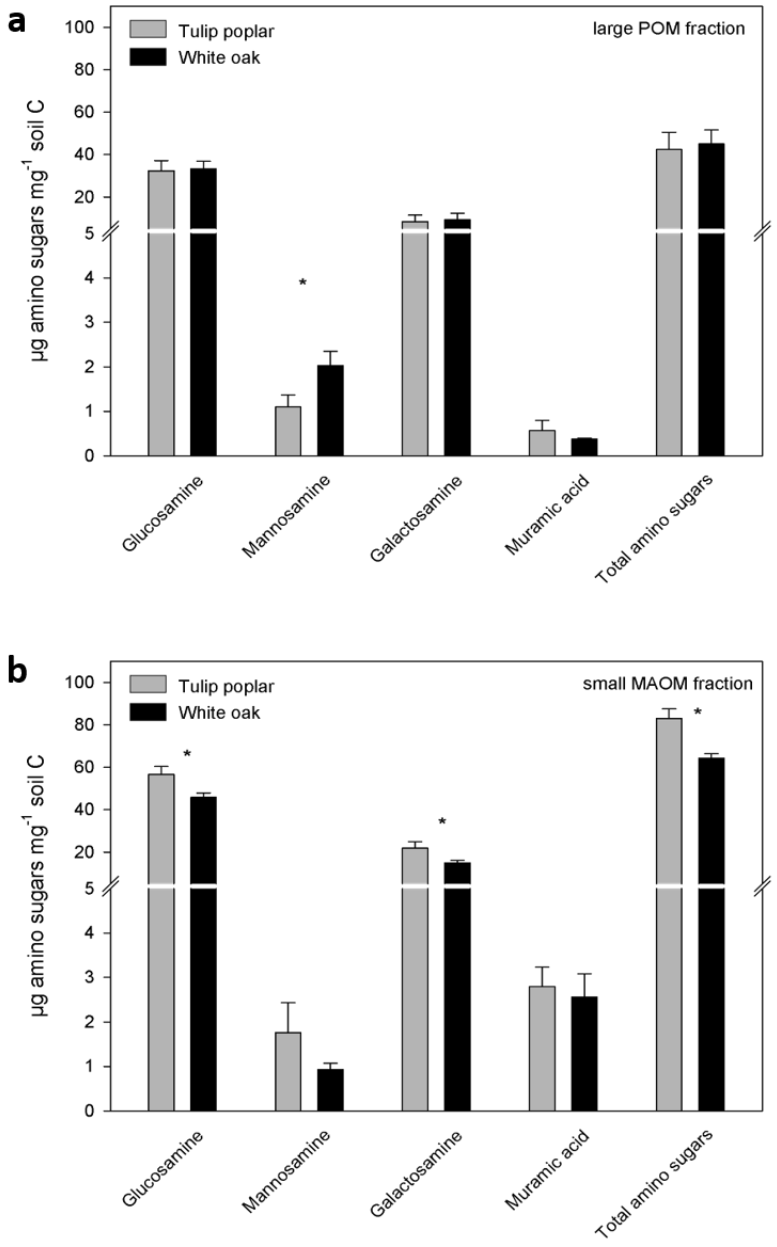

Fig. S5: Amino sugar content (µm) per mg soil carbon for the large POM fraction (a) and the small MAOM fraction (b). In the large POM (A), the content of mannosamine was significantly higher under white oak ($t = -3.851$, $df = 4$, $P = 0.018$) relative to tulip poplar. Within the small MAOM (b) contents of glucosamine ($t = 4.302$, $df = 4$, $P = 0.013$), galactosamine ($t = 3.558$, $df = 4$, $P = 0.024$) and total amino sugars ($t = 6.422$, $df = 4$, $P = 0.018$) were significantly higher under tulip poplar than under white oak. The mannosamine content was not significantly different according to t-test ($t = 2.104$, $df = 4$, $P = 0.103$).

Table S1: C- and N-content [mg g^{-1}] and C/N ratio of plant tissues, bulk soil and fungal guilds of tulip poplar and white oak plots with standard deviation (SD).

	tulip poplar (AM)			white oak (ECM)		
Sample	C [mg g^{-1}]	N [mg g^{-1}]	C/N	C [mg g^{-1}]	N [mg g^{-1}]	C/N
Leaves	489.7 ± 5	24.1 ± 4	20.7 ± 4	481.3 ± 7	20.7 ± 1	23.4 ± 1
Plant litter	441.3	14.0	31.9	467.3	14.2	33.3
Wood substrate	459.4 ± 46	14.2 ± 4	35.2 ± 13	NA	NA	NA
Roots	446.5 ± 28	12.0 ± 4	41.6 ± 20	378.6 ± 22	9.2 ± 3	44.1 ± 13
Root tips	NA	NA	NA	399.5 ± 29	13.7 ± 0	29.2 ± 2
AMF	181.7 ± 111	14.9 ± 8	12.1 ± 1	NA	NA	NA
ECM	434.9 ± 17	45.2 ± 10	10.0 ± 2	448.6 ± 14	42.8 ± 4	10.6 ± 1
SAP_s	426.3 ± 7	68.7 ± 29	7.6 ± 5	413.3	113.9	3.6
SAP_w	437.0 ± 10	34.4 ± 25	17.9 ± 10	468.6 ± 33	19.2 ± 8	27.2 ± 11
Bulk soil	35.8 ± 10	2.5 ± 1	14.8 ± 2	28.5 ± 10	1.9 ± 1	15.8 ± 5

AMF, arbuscular mycorrhizal fungi; ECM, ectomycorrhizal fungi; SAP_s, saprotrophic fungi on soil; SAP_w, saprotrophic fungi on wood

Table S2: C- and N-content [mg g^{-1}] and C/N ratio of plant tissues, bulk soil and fungal guilds of sugar maple and American beech plots with standard deviation (SD).

	sugar maple (AM)			american beech (ECM)		
Sample	C [mg g^{-1}]	N [mg g^{-1}]	C/N	C [mg g^{-1}]	N [mg g^{-1}]	C/N
Leaves	469.8 ± 8	18.4 ± 3	25.9 ± 4	477.4 ± 14	22.36 ± 3	21.5 ± 2
Wood substrate	473.9	10.1	46.8	NA	NA	NA
Roots	461.3 ± 17	9.0 ± 2	53.1 ± 13	466.6 ± 17	10.6 ± 4	48.3 ± 17
Root tips	NA	NA	NA	420.8 ± 14	15.1 ± 2	28.4 ± 5
AMF	134.2 ± 22	11.5 ± 8	11.7 ± 1	NA	NA	NA
ECM	389.6 ± 79	49.1 ± 23	8.9 ± 3	416.6 ± 32	42.1 ± 11	10.4 ± 2
SAP_s	441.9 ± 10	19.1 ± 2	23.3 ± 3	441.1 ± 36	32.5 ± 5	13.6 ± 1
Bulk soil	25.5 ± 13	1.9 ± 1	13.7 ± 3	42.4 ± 17	2.4 ± 1	17.7 ± 1

AMF, arbuscular mycorrhizal fungi; ECM, ectomycorrhizal fungi; SAP_s, saprotrophic fungi on soil

Table S3 Raw data of stable isotope ^{13}C and ^{15}N values, N- and C- content, C/N ratio of plant tissues, fungal biomass, soil and SOM fractions (where available) of *Liriodendron tulipifera*, *Quercus alba*, *Acer saccharum* and *Fagus grandifolia*.

Saskia Klink, Adrienne B. Keller, Andreas J. Wild, Vera L. Baumert, Matthias Gube, Eva Lehndorff, Nele Meyer, Carsten W. Mueller, Richard P. Phillips, Johanna Pausch. Stable isotopes reveal that fungal residues contribute more to mineral-associated organic matter pools than plant residues. Submitted to Soil Biology and Biogeochemistry

Liriodendron tulipifera & *Quercus alba*

	ID	Fraction	Comments	Info	Total N [mmol g_{dw}^{-1}]	Total N mg/g	$\delta^{15}N$ [‰]	Total C [mmol g_{dw}^{-1}]	Total C mg/g	$\delta^{13}C$ [‰]	C/N
Soil fractions											
	12.10.-2-C3-1 (T-1)	< 20 µm (MAOM)	*Liriodendron tulipifera* 1	soil fractions	0.37	5.19	2.89	5.44	65.36	-26.94	12.58
	12.10.-2-C3-2 (T-2)	< 20 µm (MAOM)	*Liriodendron tulipifera* 1	soil fractions	0.17	2.38	3.72	2.19	26.28	-26.09	11.05
	12.10.-2-C3-3 (T-3)	< 20 µm (MAOM)	*Liriodendron tulipifera* 1	soil fractions	0.28	3.89	3.39	3.96	47.59	-26.49	12.23
	12.10.-2-C3-4 (T-4)	< 20 µm (MAOM)	*Liriodendron tulipifera* 1	soil fractions	0.16	2.28	3.03	2.15	25.80	-25.91	11.33
	17.10.-20-C3-1 (T-5)	< 20 µm (MAOM)	*Liriodendron tulipifera* 2	soil fractions	0.24	3.42	2.49	3.87	46.48	-26.87	13.58
	17.10.-20-C3-2 (T-6)	< 20 µm (MAOM)	*Liriodendron tulipifera* 2	soil fractions	0.24	3.40	2.34	2.92	35.09	-25.56	10.33
	17.10.-20-C3-3 (T-7)	< 20 µm (MAOM)	*Liriodendron tulipifera* 2	soil fractions	0.31	4.29	1.15	2.92	35.06	-27.17	8.18
	17.10.-20-C3-4 (T-8)	< 20 µm (MAOM)	*Liriodendron tulipifera* 2	soil fractions	0.16	2.21	2.15	1.81	21.77	-26.01	9.83
	29.10.-8-C3-1 (T-9)	< 20 µm (MAOM)	*Liriodendron tulipifera* 3	soil fractions	0.17	2.43	2.74	2.22	26.68	-25.82	10.98

29.10.-8-C3-2 (T-10)	< 20 µm (MAOM)	*Liriodendron tulipifera* 3	soil fractions	0.25	3.46	3.05	5.54	66.55	-26.66	19.22
29.10.-8-C3-3 (T-11)	< 20 µm (MAOM)	*Liriodendron tulipifera* 3	soil fractions	0.05	0.73	0.44	0.73	8.74	-25.12	12.04
29.10.-8-C3-4 (T-12)	< 20 µm (MAOM)	*Liriodendron tulipifera* 3	soil fractions	0.14	2.02	1.79	2.18	26.15	-25.71	12.92
12.10.-2-C3-1 (T-1)	< 20 µm (POM)	*Liriodendron tulipifera* 1	soil fractions	1.43	20.06	1.72	29.40	353.11	-27.58	17.59
12.10.-2-C3-2 (T-2)	< 20 µm (POM)	*Liriodendron tulipifera* 1	soil fractions	1.05	14.69	-1.31	30.67	368.31	-27.03	25.06
12.10.-2-C3-3 (T-3)	< 20 µm (POM)	*Liriodendron tulipifera* 1	soil fractions	1.23	17.24	0.79	33.11	397.66	-28.08	23.04
12.10.-2-C3-4 (T-4)	< 20 µm (POM)	*Liriodendron tulipifera* 1	soil fractions	1.02	14.32	-2.92	32.09	385.37	-27.14	26.89
17.10.-20-C3-1 (T-5)	< 20 µm (POM)	*Liriodendron tulipifera* 2	soil fractions	1.14	15.99	-0.50	32.42	389.34	-27.68	24.32
17.10.-20-C3-2 (T-6)	< 20 µm (POM)	*Liriodendron tulipifera* 2	soil fractions	1.19	16.60	-3.14	29.49	354.24	-26.23	21.33
17.10.-20-C3-3 (T-7)	< 20 µm (POM)	*Liriodendron tulipifera* 2	soil fractions	1.10	15.46	-0.66	30.08	361.32	-26.83	23.35
17.10.-20-C3-4 (T-8)	< 20 µm (POM)	*Liriodendron tulipifera* 2	soil fractions	1.21	16.95	-1.63	26.65	320.03	-27.32	18.86
29.10.-8-C3-1 (T-9)	< 20 µm (POM)	*Liriodendron tulipifera* 3	soil fractions	0.98	13.67	-0.60	29.33	352.25	-26.72	25.75
29.10.-8-C3-2 (T-10)	< 20 µm (POM)	*Liriodendron tulipifera* 3	soil fractions	1.35	18.87	-1.35	37.32	448.25	-27.76	23.74
29.10.-8-C3-3 (T-11)	< 20 µm (POM)	*Liriodendron tulipifera* 3	soil fractions	0.88	12.33	-4.20	32.61	391.65	-26.94	31.73
29.10.-8-C3-4 (T-12)	< 20 µm (POM)	*Liriodendron tulipifera* 3	soil fractions	0.91	12.68	-3.15	33.88	406.88	-26.82	32.07

12.10.-2-C3-1 (T-1)	> 20 µm (POM)	*Liriodendron tulipifera* 1	soil fractions	1.45	20.31	-1.75	37.94	455.72	-27.64	22.41
12.10.-2-C3-2 (T-2)	> 20 µm (POM)	*Liriodendron tulipifera* 1	soil fractions	1.24	17.37	-0.81	38.36	460.68	-27.89	26.50
12.10.-2-C3-3 (T-3)	> 20 µm (POM)	*Liriodendron tulipifera* 1	soil fractions	1.24	17.43	-0.88	36.82	442.29	-28.22	25.36
12.10.-2-C3-4 (T-4)	> 20 µm (POM)	*Liriodendron tulipifera* 1	soil fractions	1.28	17.86	-2.37	36.57	439.20	-27.72	24.57
17.10.-20-C3-1 (T-5)	> 20 µm (POM)	*Liriodendron tulipifera* 2	soil fractions	1.21	17.01	-2.91	36.77	441.66	-27.30	25.94
17.10.-20-C3-2 (T-6)	> 20 µm (POM)	*Liriodendron tulipifera* 2	soil fractions	1.46	20.37	-1.90	36.88	442.99	-26.84	21.73
17.10.-20-C3-3 (T-7)	> 20 µm (POM)	*Liriodendron tulipifera* 2	soil fractions	1.58	22.07	-0.67	34.95	419.78	-26.79	19.00
17.10.-20-C3-4 (T-8)	> 20 µm (POM)	*Liriodendron tulipifera* 2	soil fractions	1.44	20.13	-1.23	38.50	462.43	-27.90	22.95
29.10.-8-C3-1 (T-9)	> 20 µm (POM)	*Liriodendron tulipifera* 3	soil fractions	1.03	14.38	0.24	30.93	371.45	-27.08	25.82
29.10.-8-C3-2 (T-10)	> 20 µm (POM)	*Liriodendron tulipifera* 3	soil fractions	1.25	17.47	-0.46	33.88	406.89	-27.58	23.27
29.10.-8-C3-3 (T-11)	> 20 µm (POM)	*Liriodendron tulipifera* 3	soil fractions	1.00	14.05	-1.81	34.32	412.15	-27.25	29.31
29.10.-8-C3-4 (T-12)	> 20 µm (POM)	*Liriodendron tulipifera* 3	soil fractions	0.79	11.08	-2.71	33.34	400.43	-27.14	36.11
12.10.-2-C3-1 (T-1)	> 63 µm (MAOM)	*Liriodendron tulipifera* 1	soil fractions	0.05	0.67	1.29	0.74	8.84	-26.58	13.14
12.10.-2-C3-2 (T-2)	> 63 µm (MAOM)	*Liriodendron tulipifera* 1	soil fractions	0.02	0.25	-0.82	0.29	3.45	-25.07	13.88
12.10.-2-C3-3 (T-3)	> 63 µm (MAOM)	*Liriodendron tulipifera* 1	soil fractions	0.04	0.51	1.53	0.53	6.36	-25.99	12.39

12.10.-2-C3-4 (T-4)	> 63 µm (MAOM)	*Liriodendron tulipifera* 1	soil fractions	0.04	0.62	1.00	1.06	12.76	-26.95	20.58
17.10.-20-C3-1 (T-5)	> 63 µm (MAOM)	*Liriodendron tulipifera* 2	soil fractions	0.03	0.43	1.01	0.28	3.39	-24.39	7.93
17.10.-20-C3-2 (T-6)	> 63 µm (MAOM)	*Liriodendron tulipifera* 2	soil fractions	0.05	0.66	1.28	0.56	6.74	-25.08	10.15
17.10.-20-C3-3 (T-7)	> 63 µm (MAOM)	*Liriodendron tulipifera* 2	soil fractions	0.06	0.86	0.69	1.29	15.49	-26.86	18.03
17.10.-20-C3-4 (T-8)	> 63 µm (MAOM)	*Liriodendron tulipifera* 2	soil fractions	0.04	0.58	0.80	0.56	6.72	-25.74	11.50
29.10.-8-C3-1 (T-9)	> 63 µm (MAOM)	*Liriodendron tulipifera* 3	soil fractions	0.04	0.57	-0.18	0.75	9.03	-26.34	15.84
29.10.-8-C3-2 (T-10)	> 63 µm (MAOM)	*Liriodendron tulipifera* 3	soil fractions	0.05	0.65	0.71	0.29	3.50	-26.47	5.34
29.10.-8-C3-3 (T-11)	> 63 µm (MAOM)	*Liriodendron tulipifera* 3	soil fractions	0.02	0.29	-3.15	0.29	3.51	-25.86	12.08
29.10.-8-C3-4 (T-12)	> 63 µm (MAOM)	*Liriodendron tulipifera* 3	soil fractions	0.01	0.20	-4.97	0.33	3.91	-25.82	19.67
12.10.-2-C3-1 (T-1)	> 63 µm (POM)	*Liriodendron tulipifera* 1	soil fractions	1.37	19.25	-1.69	37.23	447.21	-28.39	23.21
12.10.-2-C3-2 (T-2)	> 63 µm (POM)	*Liriodendron tulipifera* 1	soil fractions	0.93	13.02	-4.01	39.93	479.57	-28.22	36.80
12.10.-2-C3-3 (T-3)	> 63 µm (POM)	*Liriodendron tulipifera* 1	soil fractions	1.02	14.33	-3.08	37.26	447.55	-28.09	31.19
12.10.-2-C3-4 (T-4)	> 63 µm (POM)	*Liriodendron tulipifera* 1	soil fractions	1.01	14.11	-3.42	37.89	455.05	-27.95	32.23
17.10.-20-C3-1 (T-5)	> 63 µm (POM)	*Liriodendron tulipifera* 2	soil fractions	0.95	13.26	-4.20	39.83	478.40	-27.49	36.04
17.10.-20-C3-2 (T-6)	> 63 µm (POM)	*Liriodendron tulipifera* 2	soil fractions	1.31	18.37	-1.64	36.06	433.11	-27.69	23.56

17.10.-20-C3-3 (T-7)	> 63 µm (POM)	*Liriodendron tulipifera* 2	soil fractions	1.10	15.37	-0.89	34.05	409.02	-27.42	26.58
17.10.-20-C3-4 (T-8)	> 63 µm (POM)	*Liriodendron tulipifera* 2	soil fractions	1.05	14.64	-2.83	37.50	450.36	-27.95	30.73
29.10.-8-C3-1 (T-9)	> 63 µm (POM)	*Liriodendron tulipifera* 3	soil fractions	0.78	10.93	-3.98	38.06	457.13	-27.49	41.77
29.10.-8-C3-2 (T-10)	> 63 µm (POM)	*Liriodendron tulipifera* 3	soil fractions	1.23	17.29	-1.80	46.20	554.92	-28.29	32.07
29.10.-8-C3-3 (T-11)	> 63 µm (POM)	*Liriodendron tulipifera* 3	soil fractions	0.80	11.25	-5.98	40.58	487.44	-27.69	43.30
29.10.-8-C3-4 (T-12)	> 63 µm (POM)	*Liriodendron tulipifera* 3	soil fractions	0.07	1.03	-3.38	4.41	53.01	-27.81	51.65
11.10.-4-C3-1 (E-1)	< 20 µm (MAOM)	*Quercus alba* 1	soil fractions	0.18	2.56	1.55	3.18	38.24	-26.47	14.91
11.10.-4-C3-2 (E-2)	< 20 µm (MAOM)	*Quercus alba* 1	soil fractions	0.08	1.07	1.67	1.46	17.48	-25.83	16.35
11.10.-4-C3-3 (E-3)	< 20 µm (MAOM)	*Quercus alba* 1	soil fractions	0.11	1.54	1.64	2.18	26.15	-26.17	16.98
11.10.-4-C3-4 (E-4)	< 20 µm (MAOM)	*Quercus alba* 1	soil fractions	0.12	1.64	3.60	1.46	17.54	-25.76	10.71
22.10.-22-C3-1 (E-5)	< 20 µm (MAOM)	*Quercus alba* 2	soil fractions	0.15	2.07	3.10	1.79	21.50	-25.30	10.36
22.10.-22-C3-2 (E-6)	< 20 µm (MAOM)	*Quercus alba* 2	soil fractions	0.08	1.16	1.45	0.91	10.92	-24.86	9.37
22.10.-22-C3-3 (E-7)	< 20 µm (MAOM)	*Quercus alba* 2	soil fractions	0.13	1.79	2.34	1.49	17.91	-25.60	10.01
22.10.-22-C3-4 (E-8)	< 20 µm (MAOM)	*Quercus alba* 2	soil fractions	0.17	2.44	3.17	2.18	26.19	-25.39	10.74

11.10.-4-C3-1 (E-1)	< 20 µm (POM)	*Quercus alba* 1	soil fractions	1.06	14.89	0.01	29.68	356.43	-27.71	23.92
11.10.-4-C3-2 (E-2)	< 20 µm (POM)	*Quercus alba* 1	soil fractions	0.60	8.46	-2.47	34.72	417.01	-27.83	49.23
11.10.-4-C3-3 (E-3)	< 20 µm (POM)	*Quercus alba* 1	soil fractions	0.68	9.49	-3.53	33.33	400.33	-27.28	42.16
11.10.-4-C3-4 (E-4)	< 20 µm (POM)	*Quercus alba* 1	soil fractions	0.95	13.30	-2.37	30.21	362.85	-27.72	27.25
22.10.-22-C3-1 (E-5)	< 20 µm (POM)	*Quercus alba* 2	soil fractions	1.16	16.30	-1.88	31.80	381.92	-26.93	23.41
22.10.-22-C3-2 (E-6)	< 20 µm (POM)	*Quercus alba* 2	soil fractions	1.08	15.19	-2.43	28.79	345.81	-26.89	22.75
22.10.-22-C3-3 (E-7)	< 20 µm (POM)	*Quercus alba* 2	soil fractions	1.08	15.06	-3.21	27.65	332.15	-27.17	22.03
22.10.-22-C3-4 (E-8)	< 20 µm (POM)	*Quercus alba* 2	soil fractions	0.99	13.88	1.43	29.49	354.19	-27.18	25.49
11.10.-4-C3-1 (E-1)	> 20 µm (POM)	*Quercus alba* 1	soil fractions	1.08	15.17	-3.89	38.38	460.99	-27.47	30.37
11.10.-4-C3-2 (E-2)	> 20 µm (POM)	*Quercus alba* 1	soil fractions	0.79	11.08	-3.82	41.72	501.06	-27.75	45.20
11.10.-4-C3-3 (E-3)	> 20 µm (POM)	*Quercus alba* 1	soil fractions	0.86	12.04	-5.31	40.76	489.61	-27.10	40.63
11.10.-4-C3-4 (E-4)	> 20 µm (POM)	*Quercus alba* 1	soil fractions	1.30	18.26	-1.89	37.03	444.75	-27.71	24.33
22.10.-22-C3-1 (E-5)	> 20 µm (POM)	*Quercus alba* 2	soil fractions	1.50	20.98	-2.03	39.00	468.47	-26.81	22.31
22.10.-22-C3-2 (E-6)	> 20 µm (POM)	*Quercus alba* 2	soil fractions	1.46	20.39	-1.86	38.72	465.03	-27.26	22.79
22.10.-22-C3-3 (E-7)	> 20 µm (POM)	*Quercus alba* 2	soil fractions	1.39	19.47	-1.90	37.49	450.23	-27.50	23.11

22.10.-22-C3-4 (E-8)	> 20 µm (POM)	*Quercus alba* 2	soil fractions	1.36	19.03	-1.79	35.57	427.22	-27.01	22.43
11.10.-4-C3-1 (E-1)	> 63 µm (MAOM)	*Quercus alba* 1	soil fractions	0.03	0.45	-3.92	0.70	8.41	-25.70	18.50
11.10.-4-C3-2 (E-2)	> 63 µm (MAOM)	*Quercus alba* 1	soil fractions	0.02	0.27	-0.36	0.38	4.55	-24.78	16.66
11.10.-4-C3-3 (E-3)	> 63 µm (MAOM)	*Quercus alba* 1	soil fractions	0.02	0.35	0.85	0.50	6.03	-25.30	17.33
11.10.-4-C3-4 (E-4)	> 63 µm (MAOM)	*Quercus alba* 1	soil fractions	0.02	0.29	-1.67	0.44	5.32	-25.07	18.45
22.10.-22-C3-1 (E-5)	> 63 µm (MAOM)	*Quercus alba* 2	soil fractions	0.04	0.53	-0.14	0.53	6.39	-24.94	12.01
22.10.-22-C3-2 (E-6)	> 63 µm (MAOM)	*Quercus alba* 2	soil fractions	0.02	0.34	-1.53	0.42	5.04	-25.00	14.79
22.10.-22-C3-3 (E-7)	> 63 µm (MAOM)	*Quercus alba* 2	soil fractions	0.04	0.55	-1.07	0.63	7.56	-25.91	13.73
22.10.-22-C3-4 (E-8)	> 63 µm (MAOM)	*Quercus alba* 2	soil fractions	0.04	0.59	-0.35	0.66	7.98	-25.24	13.58
11.10.-4-C3-1 (E-1)	> 63 µm (POM)	*Quercus alba* 1	soil fractions	1.14	15.92	-4.09	40.16	482.38	-28.15	30.27
11.10.-4-C3-2 (E-2)	> 63 µm (POM)	*Quercus alba* 1	soil fractions	0.78	10.88	-4.65	39.55	475.07	-28.04	43.64
11.10.-4-C3-3 (E-3)	> 63 µm (POM)	*Quercus alba* 1	soil fractions	1.13	15.78	-1.72	40.24	483.29	-27.92	30.61
11.10.-4-C3-4 (E-4)	> 63 µm (POM)	*Quercus alba* 1	soil fractions	1.24	17.41	-2.87	37.23	447.21	-28.07	25.66
22.10.-22-C3-1 (E-5)	> 63 µm (POM)	*Quercus alba* 2	soil fractions	1.24	17.34	-2.95	39.11	469.71	-27.49	27.06
22.10.-22-C3-2 (E-6)	> 63 µm (POM)	*Quercus alba* 2	soil fractions	1.19	16.69	-1.08	37.87	454.82	-28.03	27.22

	22.10.-22-C3-3 (E-7)	> 63 µm (POM)	*Quercus alba* 2	soil fractions	1.30	18.17	-1.87	38.63	463.97	-28.08	25.52
	22.10.-22-C3-4 (E-8)	> 63 µm (POM)	*Quercus alba* 2	soil fractions	1.28	17.97	-2.47	38.67	464.43	-27.37	25.82
Roots											
	Quercus alba			roots	0.77	10.75	-5.81	29.14	349.99	-26.89	32.54
	Quercus alba			roots	0.47	6.58	-4.47	30.97	371.97	-27.51	56.51
	Quercus alba			roots	0.52	7.27	-6.51	32.85	394.55	-27.56	54.25
	Quercus alba			roots	0.86	12.02	-4.89	33.12	397.82	-28.95	33.08
	Liriodendron tulipifera			roots	1.00	13.97	-4.67	35.37	424.79	-28.92	30.39
	Liriodendron tulipifera			roots	0.87	12.18	-4.47	35.19	422.69	-27.87	34.67
	Liriodendron tulipifera			roots	0.48	6.78	-7.87	39.90	479.21	-27.72	70.66
	Liriodendron tulipifera			roots	1.07	14.93	-5.17	38.22	459.10	-26.86	30.72
Root tips (mycorrhizal)											
	Quercus alba			root tips	0.97	13.58	-5.39	36.00	432.41	-27.06	31.82
	Quercus alba			root tips	0.99	13.87	-5.55	32.23	387.07	-28.68	27.88
	Quercus alba			root tips	0.97	13.63	-5.24	31.56	379.11	-29.48	27.79
Fungi											
	Quercus alba	*Cortinarius* sp.	MC-2018-10	ECM fungi	3.20	44.74	8.29	36.13	433.92	-26.90	9.69
	Quercus alba	*Lactarius quietus*	MC-2018-11	ECM fungi	2.76	38.60	5.78	39.57	475.30	-25.56	12.30

Quercus alba	*Tricholoma subresplendens*	MC-2018-38	ECM fungi	3.03	42.41	10.33	36.90	443.17	-26.28	10.44
Quercus alba	*Russula rubriceps*	MC-2018-6	ECM fungi	2.73	38.26	-0.96	37.28	447.80	-26.29	11.69
Quercus alba	*Hygrophorus russula*	MC-2018-7	ECM fungi	3.31	46.36	8.97	37.52	450.61	-26.10	9.71
Quercus alba	*Laccaria laccata*	MC-2018-9	ECM fungi	3.30	46.19	9.56	36.90	443.18	-26.48	9.59
Quercus alba	*Agaricus leptocaulis*	MC-2018-8	SAP soil	8.14	113.94	2.70	34.44	413.69	-22.28	3.63
Quercus alba	*Fuscoporia gilva*	MC-2018-39	SAP wood	1.40	19.63	-3.57	39.89	479.14	-25.24	24.39
Quercus alba	*Laetiporus sulphureus*	MC-2018-40	SAP wood	0.79	11.12	2.07	35.98	432.17	-23.15	38.81
Quercus alba	*Gymnopilus liquiritiae*	MC-2018-41	SAP wood	1.92	26.91	1.29	41.26	495.60	-23.04	18.40
Liriodendron tulipifera	*Cortinarius* sp.	MC-2018-13	ECM	2.44	34.10	8.49	35.79	429.92	-26.63	12.59
Liriodendron tulipifera	*Cantharellus lateritius*	MC-2018-15	ECM	2.52	35.23	5.41	36.66	440.32	-26.25	12.49
Liriodendron tulipifera	*Cortinarius* sp.	MC-2018-18	ECM	3.49	48.90	5.41	36.43	437.58	-26.38	8.94
Liriodendron tulipifera	*Cortinarius* sp.	MC-2018-21	ECM	3.58	50.10	8.25	36.41	437.29	-26.24	8.72
Liriodendron tulipifera	*Inocybe* sp.	MC-2018-26	ECM	3.11	43.50	1.88	33.96	407.87	-26.31	9.37
Liriodendron tulipifera	*Amanita suballiacea*	MC-2018-32	ECM	4.25	59.56	7.71	38.19	458.67	-25.51	7.69
Liriodendron tulipifera	Glomeraceae		AM fungi	2.28	31.88	1.90	33.89	407.00	-27.94	12.74

Liriodendron tulipifera	Glomeraceae		AM fungi	0.82	11.49	4.78	10.54	126.60	-27.63	10.97
Liriodendron tulipifera	Glomeraceae		AM fungi	0.94	13.09	4.83	13.01	156.20	-27.63	11.89
Liriodendron tulipifera	Glomeraceae		AM fungi	0.721	10.09	4.40	10.30	123.70	-27.66	12.27
Liriodendron tulipifera	Glomeraceae		AM fungi	0.76	10.58	5.28	10.28	123.50	-27.67	11.63
Liriodendron tulipifera	Glomeraceae		AM fungi	0.88	12.29	4.89	12.76	153.30	-27.86	12.48
Liriodendron tulipifera	*Marasmius strictipes*	MC-2018-12	SAP soil	6.71	93.99	-0.77	36.19	434.65	-23.39	4.62
Liriodendron tulipifera	*Gymnopus dryophilus*	MC-2018-14	SAP soil	4.34	60.79	0.77	35.39	425.11	-24.40	7.00
Liriodendron tulipifera	*Lycoperdon* sp.	MC-2018-16	SAP soil	6.79	95.11	-1.17	35.24	423.23	-23.74	4.45
Liriodendron tulipifera	*Rhodocollybia butyracea*	MC-2018-19	SAP soil	6.35	88.94	1.97	35.92	431.40	-23.01	4.85
Liriodendron tulipifera	*Rhodocollybia butyracea*	MC-2018-20	SAP soil	1.68	23.53	-4.12	35.69	428.67	-24.81	18.20
Liriodendron tulipifera	*Psathyrella* sp.	MC-2018-49	SAP soil	3.58	50.14	-4.02	34.53	414.70	-25.63	8.27
Liriodendron tulipifera	*Stereum* sp.	MC-2018-25	SAP wood	1.23	17.17	-2.82	36.16	434.28	-20.93	25.27
Liriodendron tulipifera	*Grifola frondosa*	MC-2018-30	SAP wood	2.98	41.75	1.19	36.80	441.98	-22.34	10.58
Liriodendron tulipifera	*Trametes betulina*	MC-2018-31	SAP wood	0.91	12.70	-6.04	35.47	425.99	-22.16	33.51
Liriodendron tulipifera	*Merulius tremellosus*	MC-2018-44	SAP wood	1.68	23.47	-1.34	36.79	441.84	-23.57	18.81
Liriodendron tulipifera	*Ischnoderma resinosum*	MC-2018-45	SAP wood	5.78	80.98	2.57	37.65	452.21	-20.08	5.58

	Liriodendron tulipifera	*Bisporella citrina*	MC-2018-50	SAP wood	2.18	30.52	-4.45	35.46	425.94	-22.98	13.95
Substrate											
	Liriodendron tulipifera		MC-2018-50	fungi substrate	0.77	10.85	-7.09	40.71	488.96	-26.54	45.03
	Liriodendron tulipifera		MC-2018-45 wood	fungi substrate	1.14	16.00	-4.11	32.66	392.29	-27.93	24.50
	Liriodendron tulipifera		MC-2018-30 wood	fungi substrate	0.73	10.28	-7.76	40.42	485.53	-26.42	47.18
	Liriodendron tulipifera		MC-2018-25 wood	fungi substrate	1.40	19.63	-4.06	39.32	472.30	-26.73	24.03
						14.19					
Leaves											
	Quercus alba			leaves	1.47	20.59	-3.29	39.89	479.16	-28.56	23.24
	Quercus alba			leaves	1.37	19.19	-4.72	40.01	480.55	-28.45	25.02
	Quercus alba			leaves	1.60	22.41	-2.01	40.35	484.63	-29.42	21.57
	Quercus alba			leaves	1.52	21.30	-3.11	40.77	489.66	-29.19	23.05
	Quercus alba			leaves	1.40	19.61	-3.47	39.69	476.74	-29.68	24.23
	Quercus alba			leaves	1.56	21.85	-1.62	40.67	488.43	-29.04	22.38
	Quercus alba			leaves	1.43	20.03	-2.12	40.14	482.08	-27.74	24.03
	Liriodendron tulipifera			leaves	1.31	18.35	-4.38	40.45	485.79	-27.88	26.51
	Liriodendron tulipifera			leaves	1.47	20.59	-2.54	39.71	476.99	-28.56	23.09
	Liriodendron tulipifera			leaves	2.00	28.01	-2.78	41.09	493.57	-28.73	17.60
	Liriodendron tulipifera			leaves	1.94	27.17	-4.46	39.82	478.21	-28.87	17.61
	Liriodendron tulipifera			leaves	1.74	24.37	-2.90	41.25	495.46	-27.98	20.37

	Liriodendron tulipifera		leaves	1.87	26.19	-2.88	41.59	499.53	-26.73	19.05
Leaf litter										
	Quercus alba	Litter		0.93	13.05	-5.11	40.68	488.58	-29.11	37.40
	Quercus alba	Litter		1.09	15.28	-4.45	37.20	446.82	-29.15	29.21
	Liriodendron tulipifera	Litter		1.08	15.16	-4.14	34.69	416.70	-29.44	27.46
	Liriodendron tulipifera	Litter		0.92	12.86	-4.36	38.86	466.68	-29.07	36.26
Bulk soil										
	Quercus alba	bulk soil		0.17	2.38	-0.45	4.16	49.99	-27.17	21.02
	Quercus alba	bulk soil		0.08	1.11	0.66	1.94	23.24	-26.62	20.83
	Quercus alba	bulk soil		0.08	1.15	-1.23	1.83	21.97	-26.45	19.12
	Quercus alba	bulk soil		0.14	1.94	-1.83	1.65	19.87	-25.66	10.21
	Quercus alba	bulk soil		0.17	2.36	-2.19	2.27	27.31	-26.44	11.57
	Quercus alba	bulk soil		0.17	2.36	0.36	2.40	28.81	-26.05	12.19
	Liriodendron tulipifera	bulk soil		0.12	1.66	0.47	2.18	26.19	-26.38	15.79
	Liriodendron tulipifera	bulk soil		0.14	1.96	0.34	2.95	35.41	-26.95	18.06
	Liriodendron tulipifera	bulk soil		0.12	1.68	0.64	2.23	26.78	-26.53	15.97
	Liriodendron tulipifera	bulk soil		0.18	2.51	-1.05	2.33	27.98	-26.27	11.15
	Liriodendron tulipifera	bulk soil		0.26	3.70	-0.44	3.80	45.67	-26.18	12.33

Liriodendron tulipifera		bulk soil		0.24	3.42	0.39	4.43	53.16	-26.91	15.54
Acer saccharum* & *Fagus grandifolia										
Fungi										
Acer saccharum	*Cortinarius* sp.	MC-2018-51	ECM fungi	5.17	72.43	0.02	33.04	396.79	-23.16	5.47
Acer saccharum	*Cortinarius* sp.	MC-2018-52	ECM fungi	1.87	26.23	6.38	25.56	307.05	-25.86	11.70
Acer saccharum	*Tricholoma subresplendens*	MC-2018-47	ECM fungi	3.47	48.64	10.71	38.72	465.02	-25.87	9.55
Acer saccharum	*Hymenochaete* sp.	MC-2018-54	SAPs	1.50	20.94	-5.14	36.90	443.20	-23.53	21.14
Acer saccharum	*Stereum* sp.	MC-2018-28	SAPs	1.37	19.23	-3.83	35.92	431.41	-24.14	22.41
Acer saccharum	*Stereum* sp.	MC-2018-29	SAPs	1.22	17.12	-6.88	37.55	451.04	-21.17	26.32
Acer saccharum	Glomeraceae		AM fungi	0.74	10.40	6.26	9.63	115.700	-27.65	11.07
Acer saccharum	Glomeraceae		AM fungi	0.77	10.74	5.91	10.17	122.100	-27.90	11.35
Acer saccharum	Glomeraceae		AM fungi	0.89	12.46	4.92	14.40	173.000	-27.59	13.87
Acer saccharum	Glomeraceae		AM fungi	0.77	10.84	5.66	9.81	117.800	-27.72	10.85
Acer saccharum	Glomeraceae		AM fungi	0.87	12.22	5.43	10.69	128.400	-27.64	10.50
Acer saccharum	Glomeraceae		AM fungi	0.86	12.04	5.57	12.31	147.900	-27.89	12.28

Fagus grandifolia	*Amanita lavendula*	MC-2018-48	ECM fungi	2.86	40.01	2.68	31.91	383.28	-26.87	9.57
Fagus grandifolia	*Inocybe* sp.	MC-2018-35	ECM fungi	3.48	48.77	-3.29	36.19	434.67	-27.22	8.90
Fagus grandifolia	*Laccaria laccata*	MC-2018-23	ECM fungi	2.62	36.73	-2.98	29.71	356.81	-26.30	9.71
Fagus grandifolia	*Ramaria* sp.	MC-2018-36	ECM fungi	3.47	48.61	9.70	37.59	451.48	-25.44	9.28
Fagus grandifolia	*Russula rubriceps*	MC-2018-22	ECM fungi	2.21	30.93	-1.44	36.53	438.72	-26.47	14.17
Fagus grandifolia	*Russula* sp.	MC-2018-37	ECM fungi	2.38	33.38	2.63	35.44	425.69	-26.86	12.74
Fagus grandifolia	*Tricholoma sejunctum*	MC-2018-43	ECM fungi	2.44	34.11	6.86	33.74	405.23	-26.53	11.87
Fagus grandifolia	*Tricholoma susplendens*	MC-2018-42	ECM fungi	4.61	64.58	0.26	36.39	437.08	-21.58	6.76
Fagus grandifolia	*Singerocybe adirondackensis*	MC-2018-33	fungi	4.38	61.34	-2.19	35.69	428.70	-23.73	6.98
Fagus grandifolia	*Mycena galericulata*	MC-2018-24	SAP	2.58	36.14	-3.08	38.85	466.60	-22.30	12.90
Fagus grandifolia	*Rhizomarasmius pyrrhocephalus*	MC-2018-34	SAP	2.06	28.86	-6.60	34.61	415.65	-25.03	14.39
Roots										
Acer saccharum			roots	0.63	8.79	-8.41	38.75	465.41	-25.54	52.90
Acer saccharum			roots	0.49	6.85	-9.28	39.71	476.89	-26.85	69.53
Acer saccharum			roots	0.83	11.66	-8.72	36.42	437.44	-29.18	37.47

	Acer saccharum	roots	0.63	8.87	-7.63	38.76	465.50	-26.68	52.45
	Fagus grandifolia	roots	0.56	7.82	-6.31	38.13	457.95	-28.37	58.48
	Fagus grandifolia	roots	0.87	12.23	-9.43	39.12	469.85	-30.44	38.40
	Fagus grandifolia	roots	1.08	15.06	-4.84	37.45	449.83	-27.17	29.85
	Fagus grandifolia	roots	0.53	7.36	-7.42	40.71	488.90	-26.49	66.38
Root tips (mycorrhizal)									
	Fagus grandifolia	root tips	0.98	13.70	-3.80	36.32	436.25	-28.20	31.82
	Fagus grandifolia	root tips	1.27	17.83	-3.24	34.62	415.75	-28.02	23.30
	Fagus grandifolia	root tips	0.97	13.65	-6.21	34.18	410.51	-27.96	30.05
leaves									
	Fagus grandifolia	leaves	1.69	23.63	-3.11	40.84	490.54	-28.45	20.74
	Fagus grandifolia	leaves	1.51	21.07	-1.62	38.16	458.38	-29.03	21.73
	Fagus grandifolia	leaves	1.83	25.61	-2.38	40.57	487.22	-29.35	19.01
	Fagus grandifolia	leaves	1.85	25.86	-0.76	41.35	496.61	-27.45	19.18
	Acer saccharum	leaves	1.19	16.64	-4.04	39.14	470.10	-29.16	28.22

	Acer saccharum		leaves	1.25	17.52	-4.41	38.16	458.29	-30.31	26.13
	Acer saccharum		leaves	1.20	16.78	-4.31	39.24	471.33	-30.48	28.07
	Acer saccharum		leaves	1.66	23.30	-1.61	38.61	463.75	-29.07	19.89
	Acer saccharum		leaves	1.31	18.39	-3.55	38.77	465.66	-29.55	25.30
	Acer saccharum		leaves	1.12	15.70	-4.49	40.09	481.55	-28.65	30.64
	Acer saccharum		leaves	1.46	20.46	-3.42	39.81	478.20	-27.61	23.35
substrate	*Acer saccharum*	MC-2018-29 wood	wood	0.72	10.13	-6.52	39.45	473.87	-26.94	46.76
soil	*Acer saccharum*	bulk soil		0.07	0.95	-1.66	1.03	12.33	-25.08	12.97
	Acer saccharum	bulk soil		0.09	1.23	0.35	1.47	17.68	-25.75	14.34
	Acer saccharum	bulk soil		0.16	2.22	0.94	3.28	39.44	-26.20	17.71
	Acer saccharum	bulk soil		0.10	1.46	-0.79	1.89	22.76	-25.91	15.57
	Acer saccharum	bulk soil		0.26	3.57	-0.27	3.60	43.20	-26.18	12.08
	Acer saccharum	bulk soil		0.13	1.87	-0.07	1.46	17.54	-25.42	9.40

Fagus grandifolia	bulk soil	0.31	4.29	1.19	5.76	69.24	-26.76	16.14
Fagus grandifolia	bulk soil	0.13	1.76	0.12	2.75	33.08	-26.71	18.83
Fagus grandifolia	bulk soil	0.21	2.94	0.15	4.52	54.25	-27.15	18.45
Fagus grandifolia	bulk soil	0.19	2.63	-0.26	3.87	46.45	-27.07	17.66
Fagus grandifolia	bulk soil	0.09	1.32	-1.33	1.99	23.85	-26.29	18.11
Fagus grandifolia	bulk soil	0.11	1.60	-0.16	2.30	27.61	-26.52	17.21

Manuscript 3

Nitrogen fluxes between *Pinus sylvestris* and ectomycorrhizal fungi with different decomposition abilities – an *in vitro* stable isotope approach

Cara I. Meyer[1], **Saskia Klink[1]**, Johanna Pausch[1], Matthias Gube[2]

In preparation

[1]Department of Agroecology, Bayreuth Center of Ecology and Environmental Research (BayCEER), University of Bayreuth, 95440 Bayreuth, Germany

[2]Soil Science of Temperate Ecosystems, Büsgen Institute, Georg-August University Göttingen, 37077 Göttingen, Germany

Key words: Degradative capabilities, nitrogen sources, ectomycorrhiza, stable isotopes

Abstract

Ectomycorrhizal (ECM) fungi are key mediators of soil nitrogen (N) cycling and plant uptake. In particular, they have been shown to enhance plant uptake from inorganic, amino-acid, and even complex organic N sources. However, ECM fungi have arisen from multiple independent evolutionary lineages and have retained different abilities to break down soil organic matter (SOM). This study sought to investigate whether ECM fungi from different evolutionary lineages with different capabilities to break down SOM would access different N forms in soil and confer a different benefit to their plant partners. To answer this question, a microcosm study was set up with *Pinus sylvestris* L. seedlings and four different species of ECM fungi with differing functional morphology, namely *Paxillus involutus* (BATSCH) FR. and *Pisolithus arhizus* (SCOP.) RAUSCHERT (Boletales) as well as *Laccaria* laccata (SCOP.) COOKE and *Laccaria bicolor* (MAIRE) P.D. ORTON (Agaricales). We hypothesized that *P. involutus* and *P. arhizus*, with their greater access to organic N forms, would be more enriched in ^{15}N than *L. bicolor* and *L. laccata* and would confer a growth advantage to their associated plants. Natural abundances of stable N isotopes were used to investigate the capacity of the four fungal species to acquire N from SOM pools. *P. involutus* and *P. arhizus* were found to be more ^{15}N-enriched relative to plant tissue. This effect was not observed in *L. laccata* and *L. bicolor*. These results suggest that certain ECM species have greater access to organic N pools in SOM than others and that symbiosis with a plant and/or N availability play a role in the extent to which ECM fungi utilize these organic N pools.

1 Introduction

Although soil represents the largest reservoir of terrestrial nitrogen (N), most of this N is stored in organic forms (Post et al., 1985) which are less easily accessed by plants (Jones et al., 2005). These organic N forms are usually broken down by soil microorganisms before they can be assimilated into plant tissues (Hodge et al., 2000). Inorganic N forms in soil are rapidly consumed by plants and soil microorganisms and are consequently short-lived and relatively rare in the soil (Attiwill & Adams, 1993). Thus, primary production in many terrestrial ecosystems is limited by N availability (Du et al., 2020; Elser et al., 2007; LeBauer & Treseder, 2008). Plant traits such as root morphology and root lifespan are responsive to N availability in soil (Adams et al., 2013; Li et al., 2015; Wang et al., 2018). Another important trait for plant N acquisition is mycorrhizal association (Averill et al., 2019; Phillips et al., 2013).

Mycorrhizal associations are ubiquitous on land, with over 80% of terrestrial plant species and 92% of terrestrial plant families forming symbiotic relationships with mycorrhizal fungi (Wang & Qiu, 2006). In exchange for photosynthetically derived carbohydrates from the plant partner, mycorrhizal fungi provide growth-limiting nutrients such as N to the plant, satisfying up to 80% of the plant's N requirements (Grelet et al., 2009; Hobbie & Hobbie, 2008; Zijlstra et al., 2005). Association with mycorrhizal fungi can increase a plant's access to N through several mechanisms. The fungal hyphae that branch out from the root with which they are associated can effectively increase the volume of soil mined for nutrients by the plant-fungus partnership (Smith & Read, 2010). Fungal hyphae also have a smaller diameter than plant roots and can access smaller soil pores (Ritz & Young, 2004; Schack-Kirchner et al., 2000). Additionally, certain types of mycorrhizal fungi are thought to have greater abilities to break down organic forms of N in the soil and thus provide a growth advantage to their plant partners in N-limited environments (Lindahl & Tunlid, 2015; Phillips et al., 2013) and by providing N in more easily-assimilated organic forms (Allen et al., 2003).

There are four main types of mycorrhizal fungi: arbuscular mycorrhizae, ericoid mycorrhizae, orchid mycorrhizae, and ectomycorrhizae (ECM) (Smith & Read, 2010). ECM fungi form symbioses with ecologically and economically important plant families, such as Betulaceae, Dipterocarpaceae, Fagaceae, Myrtaceae, Pinaceae, and Salicaceae (Smith & Read, 2010). Additionally, the mycelia of ECM fungi can represent up to 80% of fungal biomass and 30% of microbial biomass in forest soils (Högberg & Högberg, 2002; Wallander, 2006).

ECM fungi evolved dozens of times from separate saprotrophic lineages (Lal, 2004), retained different genes associated with saprotrophic function (Averill et al., 2014; Phillips et al., 2013),

express these genes to different extent (Kohler et al., 2015; Pellitier & Zak, 2018), and have varying abilities to break down SOM (Lindahl & Tunlid, 2015; Phillips et al., 2013). One way of categorizing the functional diversity of ECM fungi is by exploration type, characterized by the hydrophobicity, distance traveled, and branching pattern of extramatrical mycelia (Allen et al., 2003). Although this classification is morphological, it is thought to correspond to a difference in saprotrophic capabilities. Hydrophilic, short and medium distance exploration types are thought to have lower proteolytic capabilities and use more labile C and N sources than hydrophobic, long distance exploration types that use older, more recalcitrant C and N sources in the soil (Orwin et al., 2011).

The four species of ECM fungi in this study represent three evolutionary lineages. *Laccaria bicolor* and *Laccaria laccata* belong to the order Agaricales and probably evolved from litter-decaying saprotrophs (Averill et al., 2014). *Laccaria spp.* appear to have lost most genes encoding enzymes that break down cellulose and lignin (Lal, 2004). *L. bicolor* and *L. laccata* both have hydrophilic, medium-distance, fringe exploration types (Averill et al., 2014; Phillips et al., 2013) and are thought to have limited ability to access organic N forms in the soil (Kohler et al., 2015; Pellitier & Zak, 2018). *Paxillus involutus* and *Pisolithus arhizus* (also known as *Pisolithus tinctorius)* are from the order Boletales, but probably evolved ECM lifestyles independently of each other (Lindahl & Tunlid, 2015; Phillips et al., 2013). Both are hydrophobic, long-distance exploration types with greater proteolytic capabilities (Allen et al., 2003). *Pisolithus involutus* appears to use an oxidative Fenton reaction similar to brown-rot saprotrophic fungi to mobilize N from plant litter (Orwin et al., 2011) when glucose is available (Averill et al., 2014) and also appears to be able to use hydrolytic proteases and chitinases to mobilize organic N and C from fungal necromass (Hibbett et al., 2000). *Paxillus arhizus* also seems to be able to hydrolyze simple organic N compounds and transfer these to its plant partner (Kohler et al., 2015) but this effect could also be due to increased surface area for nutrient absorption of the hydrophobic, long-distance exploration type (Shah et al., 2016; Talbot et al., 2015). Although *P. arhizus* does seem to secrete extracellular proteases under some conditions, this effect seems to differ between different isolates of this species (Pellitier & Zak, 2018). Clearly, there is a great deal of diversity between ECM species and even within ECM species. Moreover, despite evidence from omics studies that different ECM lineages have varying potential capabilities to acquire organic N forms from SOM, it remains difficult to directly assess their *in vivo* capacity to do so. One potential tool to explore this question is stable isotope analysis.

Stable isotope analysis is frequently used in ecological research to investigate the sources and fluxes of various elements in ecosystems (Fry, 2006). The ratio of stable N isotopes ^{15}N:^{14}N is expressed relative to a standard as $\delta^{15}N$. The $\delta^{15}N$ of fungal tissue depends in part on the N source utilized by those fungi, with the $\delta^{15}N$ generally increasing with soil depth (Agerer, 2001; Lilleskov et al., 2011) and being higher for organic N than inorganic N (Chen et al., 2019; Hobbie et al., 2012). The ECM exploration type also affects fungal $\delta^{15}N$, with hydrophobic exploration types tending to be more enriched than hydrophilic exploration types (Kohler et al., 2015).

This study aims to evaluate whether natural abundance of N isotopes is a suitable tool to investigate the differences between ECM species in their ability to utilize N from SOM. To achieve this, the four species were grown in a microcosm with *Pinus sylvestris* seedlings and the $\delta^{15}N$ values of shoots, roots, soil and the fungus were analyzed. We hypothesized that *P. involutus* and *P. arhizus,* with their greater access to organic N forms, would be more enriched in ^{15}N than *L. bicolor* and *L. laccata.*

2 Materials and Methods

2.1 Experimental Setup

2.1.1 Fungal Cultures

Fungal cultures of *Laccaria laccata* (strain number MUCL 28894) and *Laccaria bicolor* (strain number MUCL 28895) were obtained from the Belgian Coordinated Collections of Microorganisms (BCCM). *Pisolithus arhizus* (strain DSM 3245) was obtained from the German Collection of Microorganisms and Cell Cultures (DSMZ). *Paxillus involutus* (strain MG091013_12) was obtained from the lab of Matthias Gube at the University of Göttingen and is also deposited at Jena Microbial Resource Collection (JMRC) under the access number FSU9994. All fungal cultures were subsequently maintained on Modified Melin Nokrans (MMN; Supplementary material Methods S1) agar media (Martin & Selosse, 2008).

2.1.2 Seeds

Pinus sylvestris L. seeds were obtained from the Bavarian Office of Forestry and Plant Breeding. Seeds were soaked in deionized water for 24 h in a beaker on a shaker plate at 90 rpm. The seeds were then drained and soaked in 30% H_2O_2 for 1.5 h in a beaker on a shaker plate at 90 rpm. The seeds were rinsed 3 times with sterilized, deionized water and then rinsed with a sterile 10 mg/mL^{-1} ampicillin solution in a laminar flow hood. In order to detect any contamination, the seeds were germinated on petri dishes with MMN agar with the addition of 10 g/L^{-1} glucose and half the normal amount of ammonium phosphate. They were then left to

germinate for approximately 2 weeks until radicle extended into agar and seedling was approximately 2 cm tall.

2.1.3 Soil

The soil was sampled from a grassland site belonging to the teaching facility, "Landwirtschaftliche Lehranstalten" in Bayreuth, Germany (49° 55′ 46.2″ N, 11° 33′ 2.376″ E). Soil was sampled to a depth of approximately 10 cm on April 1st, 2019. The soil was mixed and sieved through a 2mm sieve. The soil was classified as loamy silt with 67% sand, 11% silt, and 22% clay, and a pH of 5.9 ($CaCl_2$). Total soil organic C and total N contents were 0.95% and 0.08%, respectively. The soil was then placed in an autoclave bag and autoclaved (121°C, 2 bar, 20 min; Systec DE-45 autoclave) every other day for a week and then every week for a month, a total of 7 times.

2.1.4 Microcosms

A 10 mm diameter hole was cut into the lid of a 11cm diameter glass petri dish approximately 5mm from the edge. A 20 mm diameter glass tube of 15 cm height was affixed to the lid of the petri dish around this hole with high temperature silicone sealant (Fischer, Lot #859104). A cellulose stopper (PFF GmbH Kegelstopfen 120) was placed in the top of the glass tube to allow for gas exchange but maintain axenic conditions. A mesh barrier with pore size of 30 µm (SEFAR NITEX 03-30/18) was glued with the same high temperature silicone sealant bisecting the bottom of the petri dish, so that plant roots could not grow through the barrier, while fungal hyphae could. The entire setup was then placed in an autoclave bag and autoclaved (121°C, 2 bar, 20 min). In a laminar flow hood (Safe 2020, Thermo Fisher, Germany), 20 g of the autoclaved soil was weighed into the bottom of the petri dish on one side of the mesh barrier. The microcosm was then placed in an autoclave bag and autoclaved again. MMN agar with 10 g/L^{-1} glucose and half the ammonium phosphate was prepared and poured into both halves of the petri dish bottom. The agar was allowed to cool overnight. The following treatments were then prepared: (i) soil and agar only treatment, for which Petri dishes were covered with a regular lid, sealed with parafilm and wrapped in aluminum foil. (ii) fungus only treatment, for which an ~ 5mm square of agar with fungal culture was transferred to the agar side of the bi-compartmented dish approx. 1 cm from the mesh barrier. The Petri dish was covered with a regular lid, sealed with parafilm and wrapped in aluminum foil. (iii) plant only treatment, for which a small square containing the seedling was cut out of the seed germination plate and inserted into a corresponding square hole that was previously cut out of the agar side of the microcosm. The seedling was placed on the agar side where a line drawn straight from the plant

to the middle of the mesh barrier would intersect the mesh barrier perpendicularly. The shoot of the seedling was then carefully pushed through the hole in the lid of the microcosm and into the affixed tube. The microcosm was sealed with parafilm and the bottom wrapped in aluminum foil to exclude light from the roots, while exposing tube and shoot to light. (iv) fungus and plant treatment, for which the microcosms were prepared similar to the plant only treatment, but with the fungus added as in the fungus only treatment. The microcosms were sealed and wrapped in aluminum foil as described above. For each of the four fungal species, five replicates of the fungus and plant treatment (iv) were set up. The fungus only treatment (ii) comprised six replicates, the plant only treatment (iii) three and the soil and agar only treatments ten replicates. All microcosms were placed in a fully controlled growth chamber (ThermoTEC, Rochlitz, Germany). The growth chamber had 14-hour day and 10-hour night cycles with ambient temperatures of approximately 20 °C during daytime and 18 °C at night. CO_2 concentration was approximately 400 ppm. Humidity was maintained at about 60%. The microcosms were allowed to grow for approximately 12 weeks and randomly distributed every two days to ensure equal light exposure and growth conditions.

2.2 Harvest

For soil and agar only treatments, a quarter of the soil/agar was removed from the plate with scalpels and tweezers and dried in a glass vial at 60 °C for 72 h. The soil was then ground to fine powder on a tube roller with a metal plug inside of the vial. Soil/agar from all treatments was handled in a similar manner. For fungus only treatments, the fungal tissue was carefully peeled off of the soil/agar with tweezers, dried in a glass vial at 60 °C for 72 h and then either ground to fine powder on the tube roller or, for small samples, with a mortar and pestle. In plant only treatments, the plants were carefully removed from the tube and separated into needles and roots. Roots were scanned using a root scanner (described below), afterwards roots and needles were placed in separate paper bags and dried to constant weight at 60 °C for 72 h. Needles were ground to fine powder using a ball mill (MM2000, Retsch, Haan, Germany), roots were directly weight into tin capsules without grinding due to small sample amount. In the plant and fungus treatments, harvest of fungi was performed similarly as for the fungus only treatment and plants were harvested similarly as for the plant only treatment.

2.2.1 Biomass and root length data collection

After oven drying dry weight of shoots and roots was measured, as described above. To cool down, samples were put in a desiccator with silica gel. Dry weight was measured with an electric micro balance (FZ-5000i, Sartorius, Göttingen, Germany). The roots removed from the

soil were scanned in a water bath (EPSON Perfection V800) and analyzed using WinRHIZO (Regular STD4800, Regent Instruments, Canada) to determine total root length of entire sample and root lengths per root diameter class (set at 10 different classes from < 0 mm to > 1.8 mm; Supplementary material Figure S 2, S 3).

2.2.2 Preparation of samples for isotope analysis

Milled samples were stored in desiccators filled with silica gel until stable isotope measurements were carried out. For isotope measurement, samples were weighed into tin capsules. At the Centre for stable isotope Research and Analysis (Georg-August University of Göttingen) stable isotope ratios (^{15}N:^{14}N, ^{13}C:^{12}C) as well as C and N concentrations were determined with an EA-IRMS (Elemental Analyzer-Isotope Ratio Mass Spectrometer). Acetanilide was used to calibrate the C and N concentrations. The standard for C is Vienna Pee Dee Belemite (V-PDB) and for N is air. Isotopic values were annotated as delta-value (δ), which is defined as $\delta^{13}C$ or $\delta^{15}N = (R_{sample}/R_{standard} -1) \times 1000$ [‰]. R describes the ratio of the heavy to the light isotope of the sample or the respective standard.

2.3 Data analysis and statistics

The following calculations were performed over individual samples, not over data collectively:

$$C{:}N \text{ ratio} = \%C_{sample} / \%N_{sample} \quad \text{Eq. 1}$$

$$N \text{ content [mg]} = \text{dry weight}_{sample} \text{ [g]} * (\%N_{sample} / 100) * 1000 \quad \text{Eq. 2}$$

$$\text{Enrichment factor } \varepsilon^{15}N = \delta^{15}N_{fungus} - \delta^{15}N_{leaf} \text{ (Preiss \& Gebauer, 2008)} \quad \text{Eq. 3}$$

Data were analyzed with a histogram and then a Shapiro-Wilk test ($P > 0.05$) to determine whether they were normally distributed. Variance homogeneity was assessed via Levene's test ($P > 0.05$). If these conditions were met, the data were analyzed with a one-way analysis of variance (ANOVA) and a post-hoc Tukey's HSD (Honest Significant Difference) test. If non-normal distribution occurred and/or the variance was not equal across groups, a Kruskal-Wallis test and post-hoc Dunn's test with Benjamini-Hochberg adjustment for multiple comparisons were used. To compare data between the fungus only treatment and the plant and fungus treatment of the same species the Mann-Whitney *U* test was used.

The entire statistical analyses were conducted with R version 3.6.3 (R Core Team, 2020) in RStudio version 1.3.959 (RStudio Team, 2020). Data were reshaped and aggregated using the "reshape2" package (Wickham, 2007) and "dplyr" package (Wickham et al., 2016).

The package ggplot2 was used to create figures (Wickham, 2009). The compact letter displays for statistical significance were produced using the "multcomp" package (Hothorn et al., 2008). The level of significance was set as $\alpha = 0.05$.

3 Results

3.1 Plant Tissues

3.1.1 Plant Biomass

There was a significant effect of associated fungal species on shoot biomass (Figure 1a), $F(4,18) = 8.32$, $P = 0.00055$. Plants associated with *L. laccata*, *P. arhizus*, and *P. involutus* had significantly higher shoot biomass and root biomass (Figure 1b; total biomass see Supplementary materials Figure S 1) than the plant only treatment ($P > 0.05$). The associated fungal species also had a significant effect on the root-to-shoot ratio of *P. sylvestris* (Figure 2), $F(4,18) = 7.68$, $P = 0.00086$. The plants associated with *P. arhizus* and *P. involutus* had a significantly higher root-to-shoot ratio than the plant only treatment.

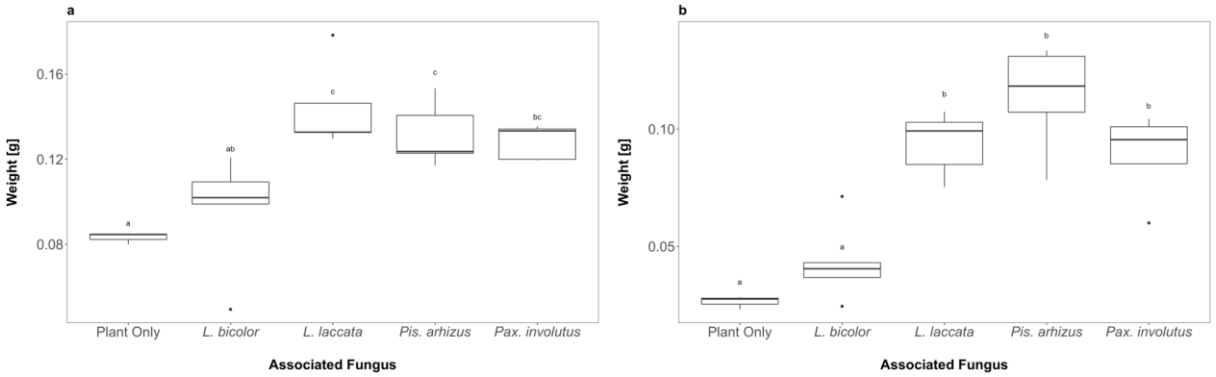

Figure 1: Biomass of (a) shoots by associated fungal species and (b) roots by associated fungal species. Statistical difference ($P < 0.05$) between treatments indicated with small letters above boxplots. The length of the box of the boxplots represents the interquartile range (IQR) with the lower margin being the 25th and the upper margin the 75th percentile. The black line in the centre of the box indicates the median, whiskers indicate the minimum (25th percentile – 1.5 x IQR) or the maximum (75th percentile + 1.5 x IQR). Outliers are given by small dots above or below the boxes.

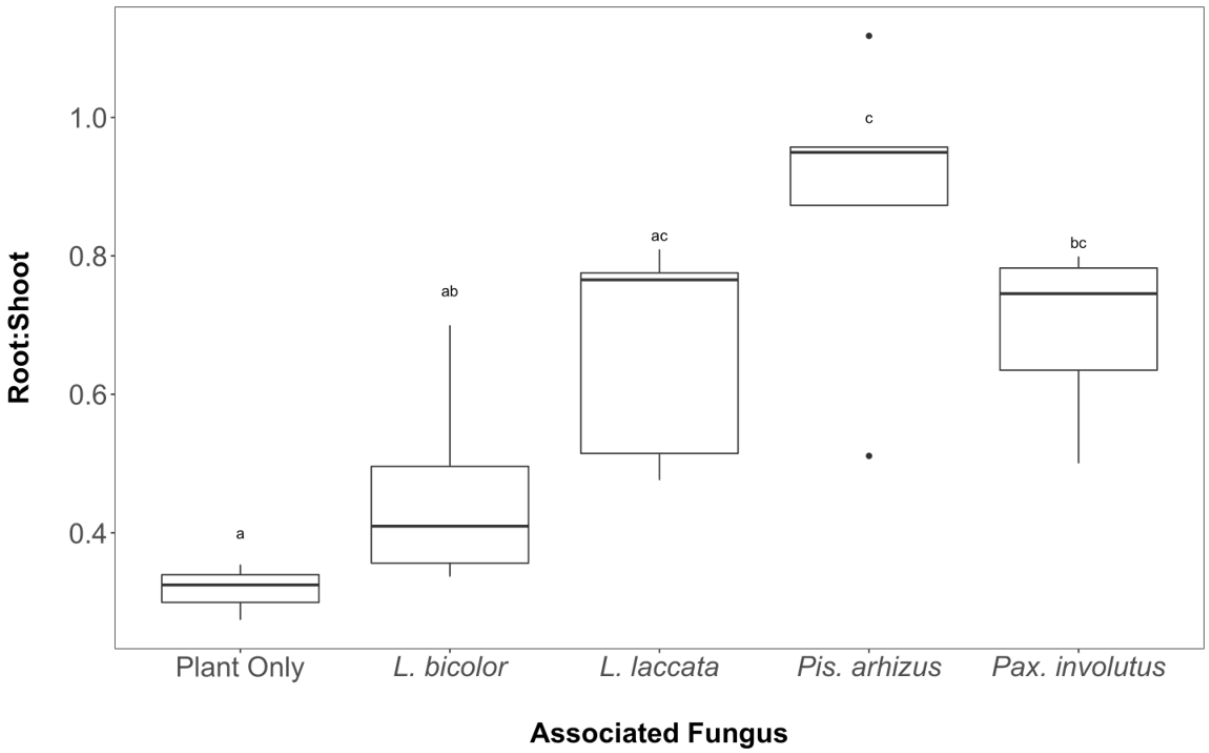

Figure 2: Root-to-shoot ratio by associated fungal species. Statistical difference (P < 0.05) between treatments indicated with small letters above boxplots. The length of the box of the boxplots represents the interquartile range (IQR) with the lower margin being the 25th and the upper margin the 75th percentile. The black line in the centre of the box indicates the median, whiskers indicate the minimum (25th percentile – 1.5 x IQR) or the maximum (75th percentile + 1.5 x IQR). Outliers are given by small dots above or below the boxes.

3.1.2 Plant C and N

Table 1 shows the C and N concentration, N content, and C:N ratio of the roots and shoots of the different treatment groups. For all the above parameters except the shoot C concentration, the associated fungal partner had a significant effect, with *L. laccata* and *P. arhizus* always differing significantly from the plant only treatment and *L. bicolor* never differing significantly from the plant only treatment. *P. involutus* differed significantly from the plant only treatment for the root C concentration, root N content, and root and shoot C:N ratio.

The C concentration of the shoots did not differ significantly between any of the treatments, while for the roots, there was a significant difference between treatments ($F_{4,18}$ = 6.37, P = 0.0023) with that of the plants associated with *L. laccata* (p_{adj} = 0.0019), *P. arhizus* (P_{adj} = 0.011), and *P. involutus* (P_{adj} = 0.037) being significantly higher than the plant only treatment.

The associated fungal species had a significant effect on N concentration of the shoots (χ^2 = 17.452, df = 4, P = 0.001579) and of the roots (χ^2 = 16.443, df = 4, P = 0.002478). Plants associated with *L. laccata* and *P. arhizus* had a significantly lower shoot N concentration

(P = 0.0082 and P = 0.0061, respectively) and root N concentration (P = 0.013 and P = 0.0071, respectively) than the plant only treatment. There were no significant differences in N content between the different treatments in shoots or roots.

The difference in C:N ratio between the different treatments for both shoots ($F_{4,18}$ = 16.43, P = 7.91e^{-06}) and roots ($F_{4,18}$ = 14.22, P = 2.1e^{-05}) was highly significant. Both the shoot and root C:N was higher in plants associated with *L. laccata* (shoot P_{adj} = 0.000056 and root P_{adj} = 0.00068), *P. arhizus* (shoot P_{adj} = 0.00013 and root P_{adj} = 0.00011), and *P. involutus* (shoot P_{adj} = 0.036 and root P_{adj} = 0.012) than in the plant only treatment.

Table 1: Mean values (± standard error, SE) of C-concentration, N-concentration, N-content (N-concentration of sample multiplied by dry weight of sample), and C:N ratio of shoots and roots of different treatments. Statistical difference between groups in columns is indicated by the letters in the following column.

Treatment	% C		% N		N Content [mg]		C:N	
	Shoot	Root	Shoot	Root	Shoot	Root	Shoot	Root
Plant only	48.85 ± 0.89	46.05 ± 0.57 ^{a}	3.48 ± 0.45 ^{a}	2.43 ± 0.38 ^{a}	0.29 ± 0.04	0.06 ± 0.01	14.53 ± 1.90 ^{a}	19.89 ± 3.07 ^{a}
L. bicolor	48.51 ± 0.71	47.21 ± 0.30 ^{ab}	2.63 ± 0.47 ^{a}	1.98 ± 0.20 ^{a}	0.23 ± 0.01	0.08 ± 0.01	20.35 ± 2.77 ^{ab}	24.84 ± 2.43 ^{ab}
L. laccata	49.24 ± 0.35	48.73 ± 0.49 ^{b}	1.29 ± 0.06 ^{b}	1.18 ± 0.08 ^{b}	0.19 ± 0.01	0.11 ± 0.01	38.69 ± 2.15 ^{c}	42.06 ± 3.00 ^{c}
P. arhizus	48.89 ± 0.08	48.26 ± 0.22 ^{b}	1.34 ± 0.09 ^{b}	1.07 ± 0.06 ^{b}	0.18 ± 0.02	0.12 ± 0.01	37.15 ± 2.18 ^{c}	45.83 ± 2.79 ^{c}
P. involutus	49.07 ± 0.37	47.92 ± 0.32 ^{b}	1.90 ± 0.17 ^{ab}	1.35 ± 0.09 ^{ab}	0.24 ± 0.02	0.12 ± 0.01	26.80 ± 2.62 ^{b}	36.15 ± 2.62 ^{bc}

3.1.3 Plant Isotope Data

In δ^{15}N, no significant differenced between the different treatments for either the shoots (Figure 3a) or the roots (Figure 3b) of the plant tissues were discovered. Although the roots of the plants associated with fungi appear to be more enriched in ^{15}N than the plant only treatment, this difference was not statistically significant. Note that the root data areinfluenced by fungal tissue, which are physically difficult to separate entirely from the roots before isotopic analysis.

Figure 3: $\delta^{15}N$ of (a) leaves and (b) roots by associated fungal species. The length of the box of the boxplots represents the interquartile range (IQR) with the lower margin being the 25th and the upper margin the 75th percentile. The black line in the centre of the box indicates the median, whiskers indicate the minimum (25th percentile – 1.5 x IQR) or the maximum (75th percentile + 1.5 x IQR). Outliers are given by small dots above or below the boxes.

3.2 Fungal Tissues

3.2.1 Fungal C and N

Table 2 shows the mean values of C and N concentration, and C:N ratio of the fungal tissue in the fungus only and fungus with plant treatments. For each fungal species and each parameter, the fungus only treatment was compared to the fungus with plant treatment with a Mann-Whitney *U* Test. The N concentration of *P. involutus* was significantly lower in the presence of a plant (W = 30, *P* = 0.0043) than in the fungus only treatment and the C:N ratios of *L. bicolor* and *P. involutus* were significantly higher in the presence of a plant than in the fungus only treatments (W = 0, *P* = 0.0043 for both).

Table 2: Mean values (± standard error SE) of C concentration, N concentration, and C:N ratio in fungal tissues of different species in fungus only or fungus and plant treatment. Significant difference between fungus only and fungus with plant is indicated with an asterisk.

Fungal Species	% C		% N		C:N	
	Fungus Only	With Plant	Fungus Only	With Plant	Fungus Only	With Plant
L. bicolor	34.57 ± 4.95	42.91 ± 1.40	2.34 ± 0.41	1.74 ± 0.13	15.19 ± 0.92	25.20 ± 2.06 *
L. laccata	40.88 ± 2.73	37.54 ± 7.38	2.47 ± 0.51	2.32 ± 0.48	19.15 ± 3.08	16.27 ± 1.09
P. arhizus	42.15 ± 2.73	45.94 ± 0.58	3.3 ± 0.25	3.43 ± 0.04	12.83 ± 0.24	13.41 ± 0.24
P. involutus	42.19 ± 2.07	45.86 ± 1.83	3.11 ± 0.28	2.26 ± 0.10 *	13.97 ± 1.16	20.34 ± 0.47 *

3.2.2 Fungal Isotopes

The $\delta^{15}N$ differed significantly between the fungal species (Figure 4) in the fungus only treatment (χ^2 = 18.053, df = 3, *P* = 0.00043) with *L. laccata* (*P* = 0.014), *P. arhizus* (*P* = 0.0086), and *P. involutus* (*P* = 0.0093) significantly more enriched in ^{15}N than *L. bicolor*. Additionally, the fungal tissue was significantly more ^{15}N-enriched in the plant and fungus treatment than the fungus only treatment for *P. arhizus* (W = 0, *P* = 0.0095) and *P. involutus* (W = 0, *P* = 0.0043).

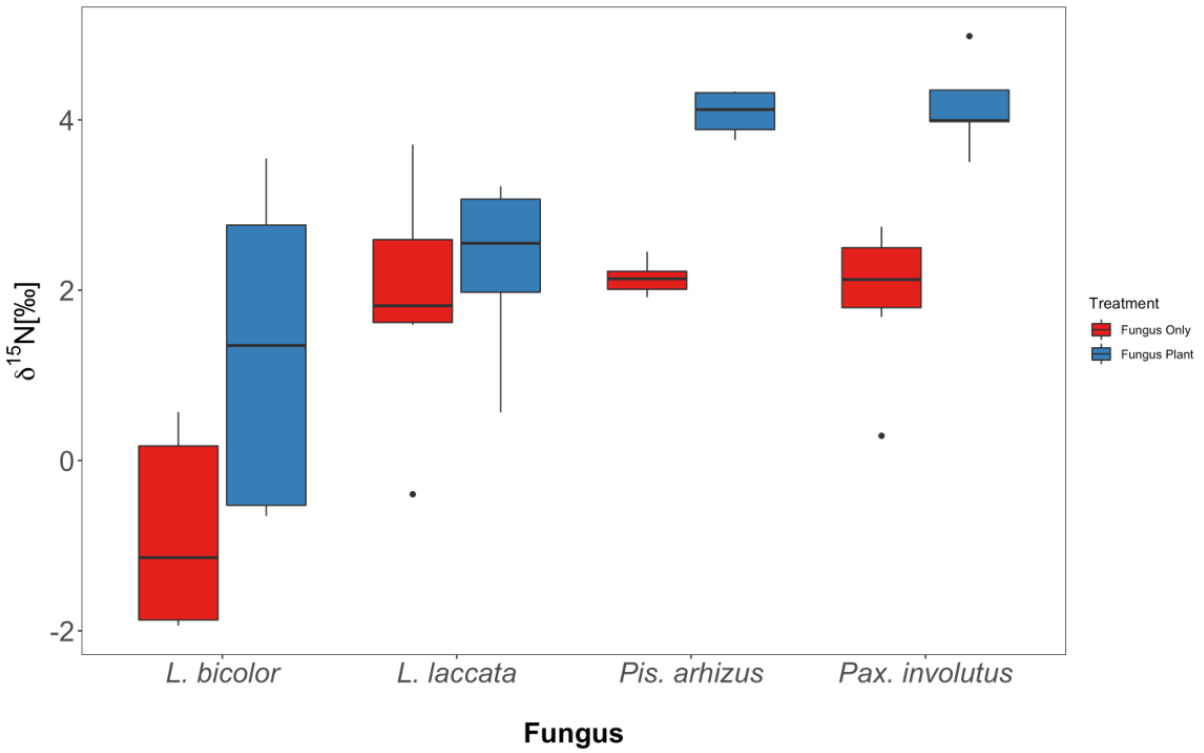

Figure 4: $\delta^{15}N$ of fungal tissues by species in fungus only and fungus with plant treatments. The length of the box of the boxplots represents the interquartile range (IQR) with the lower margin being the 25th and the upper margin the 75th percentile. The black line in the centre of the box indicates the median, whiskers indicate the minimum (25th percentile – 1.5 x IQR) or the maximum (75th percentile + 1.5 x IQR). Outliers are given by small dots above or below the boxes.

Figure 5 shows the $\varepsilon^{15}N$enrichment factor of the fungi relative to their associated plant leaves in the fungus and plant treatment. *P. arhizus* and *P. involutus* appear to be more $\varepsilon^{15}N$-enriched relative to their associated plant leaves than *L. bicolor* and *L. laccata*, but this difference was not statistically significant.

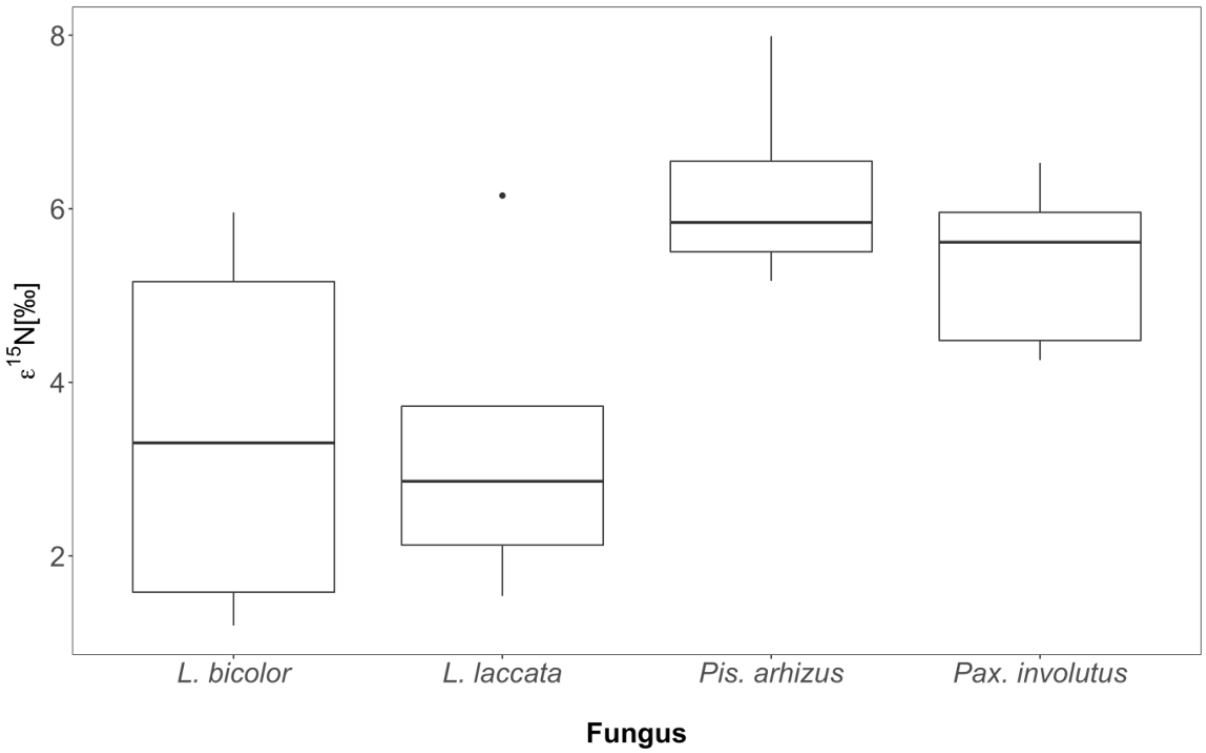

Figure 5: $\varepsilon^{15}N$ enrichment of fungus relative to plant for fungus and plant treatments. The length of the box of the boxplots represents the interquartile range (IQR) with the lower margin being the 25th and the upper margin the 75th percentile. The black line in the centre of the box indicates the median, whiskers indicate the minimum (25th percentile – 1.5 x IQR) or the maximum (75th percentile + 1.5 x IQR). Outliers are given by small dots above or below the boxes.

4 Discussion

The mycorrhizal growth response of plants when inoculated with mycorrhizal fungi is varied in the literature (Agerer, 2001). In this study, the plant biomass production differed depending on the fungal partner. Generally, the associated fungal species had a significant effect on both root and shoot biomass (Fig.1). It was further assumed that the plants associated with *P. arhizus* and *P. involutus* would produce more biomass than the plants associated with *Laccaria* species, which are thought to have less ability to access organic N forms in the soil (Gebauer & Taylor, 1999; Hobbie & Hobbie, 2006; Smith & Read, 2010). The fact that plants associated with *L. laccata*, *P. arhizus*, and *P. involutus* produced significantly more root and shoot biomass than the plant only treatment suggests that these fungal species conferred a significant growth benefit to their plant partners, while *L. bicolor* did not. Furthermore, the fact that there was no significant difference in the root or shoot biomass of the plants associated with those three species but that there was between plants associated with *L. laccata* and *L. bicolor* suggests that, although they belong to the same genus, *L. laccata* and *L. bicolor* may have different enzyme repertoires. Still, an influence of the CO_2 concentration in the microcosm on plant growth cannot be completely excluded. Although the microcosms were not sealed, fungal and

root respiration may also have been influenced by the fungal species, leading to differences in CO_2 concentration in the microcosms.

A CO_2 fertilization effect has been observed in other studies (Kohler et al., 2015), has been shown to increase root biomass (Agerer, 2001), and can differ significantly based on associated mycorrhizal species (Rineau et al., 2012).

Although the associated fungal species did have a significant effect on foliar N concentration, the N content which takes biomass into account did not differ significantly between treatments. One possible explanation for this is a dilution effect. Since N was limited in this microcosm experiment, as plant biomass increased the limited N required by both plant and fungus may have become more diluted in the tissues of both. Therefore, any N transferred from fungus to plant could have been masked by this effect. The shift toward finer roots in plants associated with *L. laccata, P. arhizus,* and *P. involutus* (Supplementary material Fig. A3) may support this N limitation explanation, since the inverse relationship between N availability and fine root production is well-established in the literature (Rineau et al., 2013). However, this difference in fine root production could also be due to differences between the associated mycorrhizal species. Additionally, some studies have shown that in N-limited conditions, ECM fungi tend not to transfer as much N to their plant partners (Akroume et al., 2019).

ECM colonization can increase a plant's access to N relative to non-mycorrhizal plants. Some studies have suggested that there is a depletion in foliar ^{15}N in ECM-associated plants, due to fractionation during transfer of N from fungus to plant (Abuzinadah & Read, 1986; Koide & Kabir, 2001) leaving the fungus enriched in ^{15}N. However, in this study, the $\delta^{15}N$ of shoots did not differ significantly between the seedlings inoculated with ECM fungi and the plant only treatment suggesting that a fractionation during the transfer of N from fungus and plant can be neglected. A trend towards more ^{15}N-enriched shoots even occurred for *L. laccata* and *P. involutus*. The roots of the inoculated seedings were even enriched in ^{15}N compared to the plant without fungi. However, this likely indicates a large contribution of fungal mycelium to our root sample.

When compared with the corresponding fungus only treatment for that species, the fungus and plant treatment of *P. involutus* had a significantly lower N concentration and higher C:N. This was also the case for the C:N of *L. bicolor*. This likely indicates that those species were transferring more nitrogen to or receiving more C from their plant partner. However, because fungal biomass could not be measured in this study and thus N content could not be calculated, this could also be due to the nitrogen dilution effect discussed above.

It has generally been observed that ECM fungi are significantly more enriched than their substrate, their plant hosts, and saprotrophic fungi (Hobbie & Högberg, 2012). The accessibility of different N sources (i.e., mineral N and organically bound N) may largely control the $\delta^{15}N$ value of the fungus. Different N sources in soil vary widely in their isotopic composition, with $\delta^{15}N$ generally increasing with soil depth (Hobbie & Ouimette, 2009a) and being higher for organic N than for inorganic N (Takebayashi et al., 2010). Given that ECM fungi often become dominant with increasing soil depth (Clemmensen et al., 2013) and due to their access to organic N forms, they are generally more enriched in ^{15}N compared to free-living saprotrophic fungi (Gebauer & Taylor, 1999; Henn & Chapela, 2001).

It was hypothesized that the ECM species with greater ability to use organic N sources, i.e. *P. arhizus* and *P. involutus*, would be more enriched in ^{15}N than the *Laccaria* species that are thought to rely more on inorganic N sources. When comparing the fungus only treatment of the four species, *L. laccata, P. arhizus,* and *P. involutus* were all more enriched than *L. bicolor* and were not significantly different from each other. Furthermore, *P. arhizus* and *P. involutus* were more enriched in the plant and fungus treatment than in the fungus only treatment for the same species, while there was no significant difference between these treatments for the *Laccaria* species. Another possible explanation is that as the system became more N-limited, *P. arhizus* and *P. involutus* use more organic N sources from the soil and become consequently more enriched in ^{15}N. Since *L. bicolor* and *L. laccata* appear to have less ability to use organic N forms (Cairney & Chambers, 1997) and are also hydrophilic, shorter distance exploration types (Hobbie & Ouimette, 2009b), they may not have been able to access more recalcitrant forms of N when the system became more N limited, while *P. arhizus* and *P. involutus* could and consequently became more enriched in ^{15}N. Support for this explanation comes from the higher enrichment factor $\varepsilon^{15}N$ of *P. arhizus* and *P. involutus* relative to their plant partner than that of the *Laccaria* species. A recent study has shown that *P. involutus* has the ability to liberate organic N from fungal necromass probably through enzymatic degradation of chitin (Takebayashi et al., 2010). *Paxillus involutus* is also known to be able to liberate N through an oxidative Fenton reaction similar to its brown rot saprotrophic cousins (Hobbie et al., 2012). *Pisolitus arhizus* is from a similar evolutionary lineage and may possibly be using similar mechanisms (Molina & Palmer, 1982).

5. Conclusion

This study sought to investigate the N dynamics between soil, ECM fungi, and ECM-associated plants and to establish whether differences in decomposition capability of the fungi translated to a difference in isotopic signature of the fungal and plant tissues. This study suggests that decomposition capabilities differ significantly between ECM species and that the species of associated ECM fungi may affect plant growth. Experiments tracing different isotopically-labelled N substrates from soil to fungus to plant could further elucidate this matter by demonstrating what substrates the different fungi use and quantifying the amount transferred to the plant partner. While microcosm studies are limited in their applicability to ecosystems as a whole, they can provide valuable insights into the mechanisms that play a key role in ecosystem processes such as N cycling.

Acknowledgements

We would like to thank the German Research Foundation for funding (PA2377/2-1, GU1309/5-1). Ilse Thaufelder and Angelika Mergner, technicians in the Department of Agroecology at the University of Bayreuth, provided a great deal of help in the laboratory work and in procuring all the materials for this experiment.

References

Abuzinadah, R., & Read, D. (1986). The role of proteins in the nitrogen nutrition of ectomycorrhizal plants: I. Utilization of peptides and proteins by ectomycorrhizal fungi. *New Phytologist*, *103*(3), 481-493.

Adams, T. S., McCormack, M. L., & Eissenstat, D. M. (2013). Foraging strategies in trees of different root morphology: the role of root lifespan. *Tree Physiology*, *33*(9), 940-948.

Agerer, R. (2001). Exploration types of ectomycorrhizae. *Mycorrhiza*, *11*(2), 107-114.

Akroume, E., Maillard, F., Bach, C., Hossann, C., Brechet, C., Angeli, N., Zeller, B., Saint-André, L., & Buée, M. (2019). First evidences that the ectomycorrhizal fungus *Paxillus involutus* mobilizes nitrogen and carbon from saprotrophic fungus necromass. *Environmental microbiology*, *21*(1), 197-208.

Allen, M., Swenson, W., Querejeta, J., Egerton-Warburton, L., & Treseder, K. (2003). Ecology of mycorrhizae: a conceptual framework for complex interactions among plants and fungi. *Annual Review of Phytopathology*, *41*(1), 271-303.

Attiwill, P. M., & Adams, M. A. (1993). Nutrient cycling in forests. *New Phytologist*, *124*(4), 561-582.

Averill, C., Bhatnagar, J. M., Dietze, M. C., Pearse, W. D., & Kivlin, S. N. (2019). Global imprint of mycorrhizal fungi on whole-plant nutrient economics. *Proceedings of the National Academy of Sciences*, *116*(46), 23163-23168.

Averill, C., Turner, B. L., & Finzi, A. C. (2014). Mycorrhiza-mediated competition between plants and decomposers drives soil carbon storage. *Nature*, *505*(7484), 543-545.

Cairney, J., & Chambers, S. (1997). Interactions between *Pisolithus tinctorius* and its hosts: a review of current knowledge. *Mycorrhiza*, *7*(3), 117-131.

Chen, J., Heikkinen, J., Hobbie, E., Rinne-Garmston, K., Penttilä, R., & Mäkipää, R. (2019). Strategies of carbon and nitrogen acquisition by saprotrophic and ectomycorrhizal fungi in Finnish boreal *Picea abies*-dominated forests. *Fungal biology*, *123*(6), 456-464.

Clemmensen, K., Bahr, A., Ovaskainen, O., Dahlberg, A., Ekblad, A., Wallander, H., Stenlid, J., Finlay, R. D., Wardle, D. A., & Lindahl, B. (2013). Roots and associated fungi drive long-term carbon sequestration in boreal forest. *Science*, *339*(6127), 1615-1618.

Du, E., Terrer, C., Pellegrini, A. F., Ahlström, A., van Lissa, C. J., Zhao, X., Xia, N., Wu, X., & Jackson, R. B. (2020). Global patterns of terrestrial nitrogen and phosphorus limitation. *Nature Geoscience*, *13*(3), 221-226.

Elser, J. J., Bracken, M. E., Cleland, E. E., Gruner, D. S., Harpole, W. S., Hillebrand, H., Ngai, J. T., Seabloom, E. W.; Shurin, J. B., & Smith, J. E. (2007). Global analysis of nitrogen

and phosphorus limitation of primary producers in freshwater, marine and terrestrial ecosystems. *Ecology letters*, *10*(12), 1135-1142.

Fry, B. (2006). *Stable isotope ecology* (Vol. 521). Springer.

Gebauer, G., & Taylor, A. (1999). ^{15}N natural abundance in fruit bodies of different functional groups of fungi in relation to substrate utilization. *The New Phytologist*, *142*(1), 93-101.

Grelet, G. A., Johnson, D., Paterson, E., Anderson, I. C., & Alexander, I. J. (2009). Reciprocal carbon and nitrogen transfer between an ericaceous dwarf shrub and fungi isolated from *Piceirhiza bicolorata* ectomycorrhizas. *New Phytologist*, *182*(2), 359-366.

Henn, M. R., & Chapela, I. H. (2001). Ecophysiology of ^{13}C and ^{15}N isotopic fractionation in forest fungi and the roots of the saprotrophic-mycorrhizal divide. *Oecologia*, *128*(4), 480-487.

Hibbett, D. S., Gilbert, L.-B., & Donoghue, M. J. (2000). Evolutionary instability of ectomycorrhizal symbioses in basidiomycetes. *Nature*, *407*(6803), 506-508.

Hobbie, E. A., & Hobbie, J. E. (2008). Natural abundance of ^{15}N in nitrogen-limited forests and tundra can estimate nitrogen cycling through mycorrhizal fungi: a review. *Ecosystems*, *11*(5), 815-830.

Hobbie, E. A., & Högberg, P. (2012). Nitrogen isotopes link mycorrhizal fungi and plants to nitrogen dynamics. *New Phytologist*, *196*(2), 367-382.

Hobbie, E. A., & Ouimette, A. P. (2009a). Controls of nitrogen isotope patterns in soil profiles. *Biogeochemistry*, *95*(2), 355-371.

Hobbie, E. A., & Ouimette, A. P. (2009b). Controls of nitrogen isotope patterns in soil profiles. *Biogeochemistry*, *95*(2-3), 355-371.

Hobbie, E. A., Sánchez, F. S., & Rygiewicz, P. T. (2012). Controls of isotopic patterns in saprotrophic and ectomycorrhizal fungi. *Soil Biology and Biochemistry*, *48*, 60-68.

Hobbie, J. E., & Hobbie, E. A. (2006). ^{15}N in symbiotic fungi and plants estimates nitrogen and carbon flux rates in Arctic tundra. *Ecology*, *87*(4), 816-822.

Hodge, A., Robinson, D., & Fitter, A. (2000). Are microorganisms more effective than plants at competing for nitrogen? *Trends in plant science*, *5*(7), 304-308.

Högberg, M. N., & Högberg, P. (2002). Extramatrical ectomycorrhizal mycelium contributes one-third of microbial biomass and produces, together with associated roots, half the dissolved organic carbon in a forest soil. *New Phytologist*, *154*(3), 791-795.

Jones, D. L., Healey, J. R., Willett, V. B., Farrar, J. F., & Hodge, A. (2005). Dissolved organic nitrogen uptake by plants—an important N uptake pathway? *Soil Biology and Biochemistry*, *37*(3), 413-423.

Kohler, A., Kuo, A., Nagy, L. G., Morin, E., Barry, K. W., Buscot, F., Canbäck, B., Choi, C., Cichocki, N., Clum, A., *et al*. (2015). Convergent losses of decay mechanisms and rapid turnover of symbiosis genes in mycorrhizal mutualists. *Nature genetics*, *47*(4), 410-415.

Koide, R. T., & Kabir, Z. (2001). Nutrient economy of red pine is affected by interactions between *Pisolithus tinctorius* and other forest-floor microbes. *New Phytologist*, *150*(1), 179-188.

Lal, R. (2004). Soil carbon sequestration impacts on global climate change and food security. *science*, *304*(5677), 1623-1627.

LeBauer, D. S., & Treseder, K. K. (2008). Nitrogen limitation of net primary productivity in terrestrial ecosystems is globally distributed. *Ecology*, *89*(2), 371-379.

Li, W., Jin, C., Guan, D., Wang, Q., Wang, A., Yuan, F., & Wu, J. (2015). The effects of simulated nitrogen deposition on plant root traits: a meta-analysis. *Soil Biology and Biochemistry*, *82*, 112-118.

Lilleskov, E., Hobbie, E. A., & Horton, T. (2011). Conservation of ectomycorrhizal fungi: exploring the linkages between functional and taxonomic responses to anthropogenic N deposition. *fungal ecology*, *4*(2), 174-183.

Lindahl, B. D., & Tunlid, A. (2015). Ectomycorrhizal fungi–potential organic matter decomposers, yet not saprotrophs. *New Phytologist*, *205*(4), 1443-1447.

Martin, F., & Selosse, M.-A. (2008). The *Laccaria* genome: a symbiont blueprint decoded. *New Phytologist*, 296-310.

Molina, R., & Palmer, J. (1982). Isolation, maintenance, and pure culture manipulation of ectomycorrhizal fungi.

Orwin, K. H., Kirschbaum, M. U., St John, M. G., & Dickie, I. A. (2011). Organic nutrient uptake by mycorrhizal fungi enhances ecosystem carbon storage: a model-based assessment. *Ecology Letters*, *14*(5), 493-502.

Pellitier, P. T., & Zak, D. R. (2018). Ectomycorrhizal fungi and the enzymatic liberation of nitrogen from soil organic matter: why evolutionary history matters. *New Phytologist*, *217*(1), 68-73.

Phillips, R. P., Brzostek, E., & Midgley, M. G. (2013). The mycorrhizal-associated nutrient economy: a new framework for predicting carbon–nutrient couplings in temperate forests. *New Phytologist*, *199*(1), 41-51.

Post, W. M., Pastor, J., Zinke, P. J., & Stangenberger, A. G. (1985). Global patterns of soil nitrogen storage. *Nature*, *317*(6038), 613-616.

Preiss, K., & Gebauer, G. (2008). A methodological approach to improve estimates of nutrient gains by partially myco-heterotrophic plants. *Isotopes in Environmental and Health Studies*, *44*(4), 393-401.

Rineau, F., Roth, D., Shah, F., Smits, M., Johansson, T., Canbäck, B., Olsen, P. B., Persson, P., Grell, M. N., Lindquist, E., Grigoriev, I. V., Lange, L., Tunlid, A. (2012). The ectomycorrhizal fungus *Paxillus involutus* converts organic matter in plant litter using a trimmed brown-rot mechanism involving Fenton chemistry. *Environmental Microbiology*, *14*(6), 1477-1487.

Rineau, F., Shah, F., Smits, M., Persson, P., Johansson, T., Carleer, R., Troein, C., & Tunlid, A. (2013). Carbon availability triggers the decomposition of plant litter and assimilation of nitrogen by an ectomycorrhizal fungus. *The ISME journal*, *7*(10), 2010-2022.

Ritz, K., & Young, I. M. (2004). Interactions between soil structure and fungi. *Mycologist*, *18*(2), 52-59.

Schack-Kirchner, H., Wilpert, K. V., & Hildebrand, E. E. (2000). The spatial distribution of soil hyphae in structured spruce-forest soils. *Plant and Soil*, *224*(2), 195-205.

Shah, F., Nicolás, C., Bentzer, J., Ellström, M., Smits, M., Rineau, F., Canbäck, B., Floudas, D., Carleer, R., Lackner, G., *et al*. (2016). Ectomycorrhizal fungi decompose soil organic matter using oxidative mechanisms adapted from saprotrophic ancestors. *New Phytologist*, *209*(4), 1705-1719.

Smith, S. E., & Read, D. J. (2010). *Mycorrhizal symbiosis*. Academic press.

Takebayashi, Y., Koba, K., Sasaki, Y., Fang, Y., & Yoh, M. (2010). The natural abundance of ^{15}N in plant and soil-available N indicates a shift of main plant N resources to NO from NH along the N leaching gradient. *Rapid Communications in Mass Spectrometry: An International Journal Devoted to the Rapid Dissemination of Up-to-the-Minute Research in Mass Spectrometry*, *24*(7), 1001-1008.

Talbot, J. M., Martin, F., Kohler, A., Henrissat, B., & Peay, K. G. (2015). Functional guild classification predicts the enzymatic role of fungi in litter and soil biogeochemistry. *Soil Biology and Biochemistry*, *88*, 441-456.

Wallander, H. (2006). External mycorrhizal mycelia: the importance of quantification in natural ecosystems. *The New Phytologist*, *171*(2), 240-242.

Wang, B., & Qiu, Y.-L. (2006). Phylogenetic distribution and evolution of mycorrhizas in land plants. *Mycorrhiza*, *16*(5), 299-363.

Wang, W., Wang, Y., Hoch, G., Wang, Z., & Gu, J. (2018). Linkage of root morphology to anatomy with increasing nitrogen availability in six temperate tree species. *Plant and soil*, *425*(1), 189-200.

Zijlstra, J. D., Van't Hof, P., Baar, J., Verkley, G. J., Summerbell, R. C., Paradi, I., Braakhekke, W. G., & Berendse, F. (2005). Diversity of symbiotic root endophytes of the Helotiales in ericaceous plants and the grass, *Deschampsia flexuosa*. *Studies in Mycology*, *53*, 147-162.

Supporting Information

Nitrogen fluxes between *Pinus sylvestris* and ectomycorrhizal fungi with different decomposition abilities – an *in vitro* stable isotope approach

Authors: Cara I. Meyer, **Saskia Klink**, Johanna Pausch, Matthias Gube

The following Supporting Information is available for this article:

Methods S1 Protocol for Modified Melin-Norkans Medium

Fig. S1: Total biomass (root and shoot combined) in g of Pinus sylvestris without fungal association (plant only) and with the association to one of the four ECM species.

Fig. S2: Relative proportion of root diameters as percentage of total root length for roots of Pinus sylvestris alone (plant only) and with fungal association.

Fig. S3: Specific root length (cm/g) of Pinus sylvestris roots without fungal association (plant only) or with association to one of the four ECM species.

Methods S1

Protocol for Modified Melin-Norkans Medium

Trace Element Solution:

3.728g KCl,

1.546g H_3BO_3,

0.845g $MgSO_4 + 7\ H_2O$,

0.575g $ZnSO_4 + 7\ H_2O$ and

0.125g $CuSO_4$ + 5 H2O were dissolved in 1L of distilled, deionized water. This solution was autoclaved and stored in the refrigerator.

0.066g $CaCl + 2\ H_2O$,

0.025g NaCl,

0.5 g KH_2PO_4,

0.05g $(NH_4)_2HPO_4$,

1µg $FeCl_3 + 6\ H_2O$ (used one small grain of powder),

0.15g $MgSO_4 + 7\ H_2O$,

83µL Thiamine hydrochloride solution (1.2mg/mL),

10mL Trace Element Solution (above), and

20g agar were dissolved in 1L of distilled, deionized water before autoclaving and pouring into petri dishes in laminar flow hood.

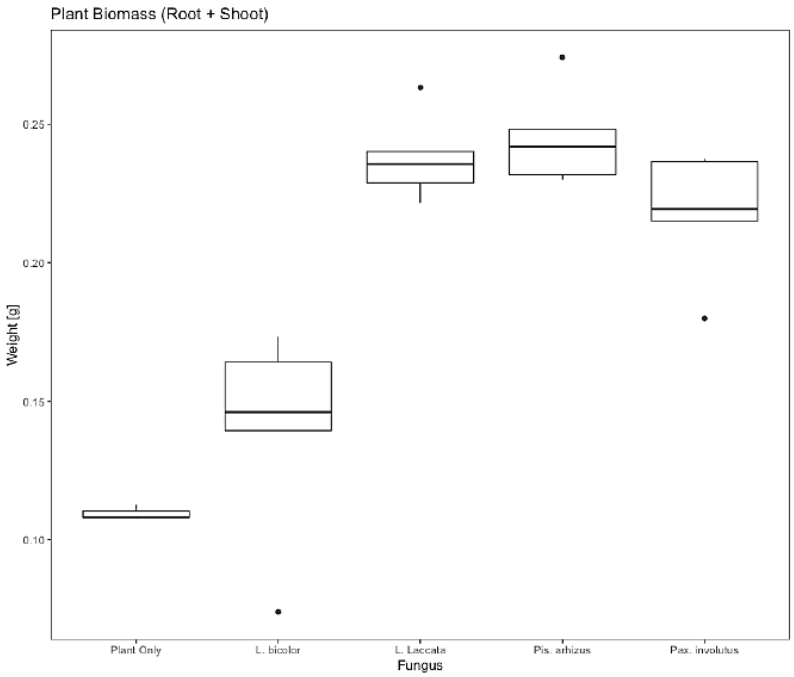

Fig. S 1: Total biomass (root and shoot combined) in g of Pinus sylvestris without fungal association (plant only) and with the association to one of the four ECM species. The length of the box of the boxplots represents the interquartile range (IQR) with the lower margin being the 25th and the upper margin the 75th percentile. The black line in the centre of the box indicates the median, whiskers indicate the minimum (25th percentile – 1.5 x IQR) or the maximum (75th percentile + 1.5 x IQR). Outliers are given by small dots above or below the boxes.

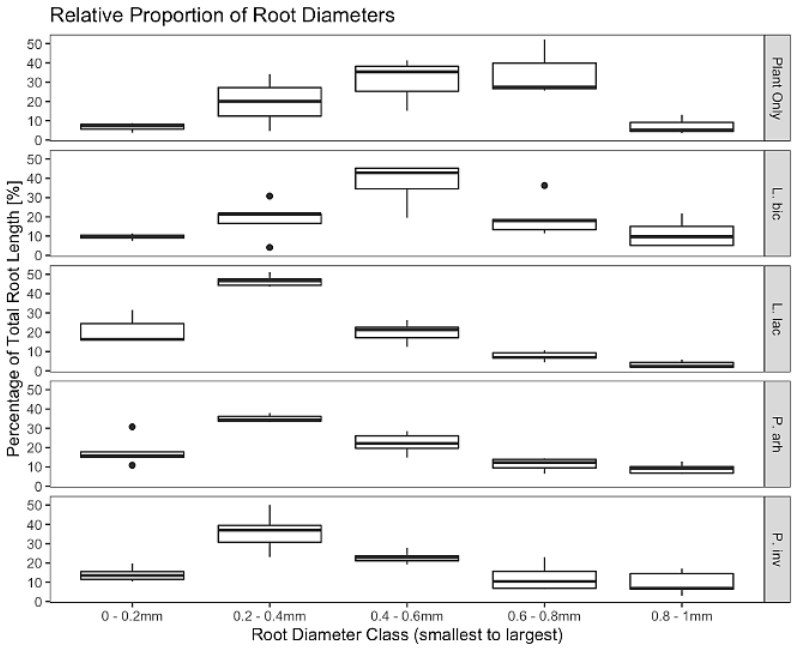

Fig. S 2: Relative proportion of root diameters as percentage of total root length for roots of Pinus sylvestris alone (plant only) and with fungal association. Root diameter was separated into five diameter classes: 0-0.2mm, 0.2-0.4mm, 0.4-0.6mm, 0.6-0.8mm and 0.8-1mm. The black line in the centre of the box indicates the median, whiskers indicate the minimum (25th percentile – 1.5 x IQR) or the maximum (75th percentile + 1.5 x IQR). Outliers are given by small dots above or below the boxes. The length of the box of the boxplots represents the interquartile range (IQR) with the lower margin being the 25th and the upper margin the 75th percentile.

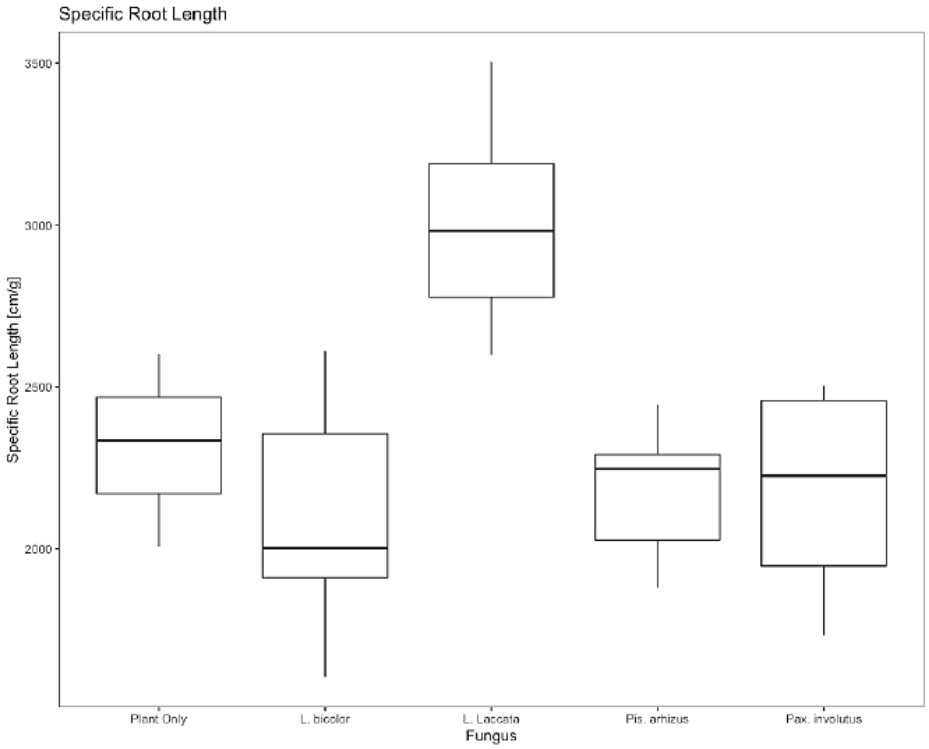

Fig. S3: Specific root length (cm/g) of Pinus sylvestris roots without fungal association (plant only) or with association to one of the four ECM species. The black line in the centre of the box indicates the median, whiskers indicate the minimum (25th percentile – 1.5 x IQR) or the maximum (75th percentile + 1.5 x IQR). Outliers are given by small dots above or below the boxes. The length of the box of the boxplots represents the interquartile range (IQR) with the lower margin being the 25th and the upper margin the 75th percentile.

Manuscript 4

Organic matter priming by invasive plants depends on dominant mycorrhizal association

Amit Kumar[1], Richard P. Phillips[2], Andrea Scheibe[2], **Saskia Klink[1]**, Johanna Pausch[1]

Soil Biology and Biochemisty 140: 107645 (2020), doi: 10.1016/j.soilbio.2019

[1]Department of Agroecology, Bayreuth Center of Ecology and Environmental Research (BayCEER), University of Bayreuth, 95440 Bayreuth, Germany

[2]Department of Biology, Indiana University Bloomington, IN 47405, USA

Key words: ^{13}C natural abundance, CO_2 emission, Flux partitioning, Microbial activation, Rhizosphere priming effects, Mycorrhizal-associated nutrient economy (MANE)

Received: 27 June 2019; Accepted: 29 October 2019; Published online: 1 November 2019

Soil Biology and Biochemistry 140 (2020) 107645

Contents lists available at ScienceDirect

Soil Biology and Biochemistry

journal homepage: http://www.elsevier.com/locate/soilbio

Short Communication

Organic matter priming by invasive plants depends on dominant mycorrhizal association

Amit Kumar [a,*,1], Richard P. Phillips [b], Andrea Scheibe [b], Saskia Klink [a], Johanna Pausch [a]

[a] Department of Agroecology, University of Bayreuth, Universitätsstr. 30, 95440, Bayreuth, Germany
[b] Department of Biology, Indiana University, 1001 E Third St, Bloomington, IN, 47403, USA

ARTICLE INFO

Keywords:
^{13}C natural abundance
CO_2 emission
Flux partitioning
Microbial activation
Rhizosphere priming effects
Mycorrhizal-associated nutrient economy (MANE)

ABSTRACT

While it has long been held that invasive plants alter ecosystem processes, the magnitude and direction of these effects have rarely been quantified *in situ*. We measured the effects of an invasive C_4 grass (*Microstegium vimineum*) on soil organic matter (SOM) decomposition in a deciduous forest in south-central Indiana, USA. The unique ^{13}C signature of the C_4 grass relative to the C_3 trees allowed us to partition soil CO_2 fluxes and estimate *M. vimineum* effects on decomposition. The magnitude and direction of priming effects hinged on the soil characteristics, which related to the mycorrhizal association of dominant trees. In forest plots dominated by ectomycorrhizal trees, with low nitrogen availability and most SOM in particulate (i.e., unprotected) forms, *M. vimineum* increased SOM decomposition by 58%. In contrast, in plots dominated by arbuscular mycorrhizal trees, characterized by high nitrogen availability and most SOM in mineral-associated (i.e., protected) forms, *M. vimineum* decreased decomposition by 14%. Collectively, our results demonstrate that invasive species can play a large role in altering ecosystem processes and suggest that the magnitude and direction of such effects depend on the dominant trees and edaphic characteristics of the stand.

Understanding the sensitivity of soil organic matter (SOM) decomposition to environmental change is critical given the massive stores of carbon (C) in soils globally (Lal, 2008). While numerous studies have examined the sensitivity of SOM decomposition to warming, nitrogen (N) deposition, elevated CO_2 and precipitation change (Song et al., 2019), far fewer have investigated the role of invasive plants in altering SOM dynamics. Plant invasions can have strong effects on soil C and N cycling (Liao et al., 2008) and there is a need to quantify and better understand how and why invaders impact SOM within and across ecosystems (Parker et al., 1999; Strayer, 2012; Vilà et al., 2011; Hulme et al., 2013).

Many invasive plants produce fast-decaying litter (Jo et al., 2017) and root-derived products (Bradford et al., 2012; Morris et al., 2016) that are presumed to accelerate SOM decomposition via 'priming effects'. Priming effects occur when soil microbes use energy from leaf (Chao et al., 2019) or root (Pausch et al., 2013; Kumar et al., 2016) inputs to synthesize extracellular enzymes in order to mine N from indigenous SOM, resulting in SOM decay (Cheng and Kuzyakov, 2005). While numerous studies have reported smaller SOM stocks in invaded soils vs. uninvaded soils (Peltzer et al., 2010), direct field measurements of priming based on soil CO_2 emissions are exceedingly rare given the challenges of quantifying SOM decomposition *in situ*.

Microstegium vimineum (Japanese stiltgrass) is a non-native C_4 grass that invades forest understories throughout the eastern U.S (Flory and Clay, 2010) and is known to accelerate C and N cycling (Ehrenfeld et al., 2001; Lee et al., 2012; Shannon-Firestone et al., 2015). Several studies have reported lower SOM in *M. vimineum*-invaded soils relative to adjacent uninvaded plots (Strickland et al., 2010; Craig and Fraterrigo, 2017; Craig et al., 2019), leading to speculation that the invader may activate microbes to decay SOM (Sokol et al., 2019). Nevertheless, there is no direct evidence of C fluxes resulting from priming by *M. vimineum* and the role of tree species and edaphic factors in shaping the magnitude and direction of invader-induced priming effects has not yet been investigated.

The Mycorrhizal-Associated Nutrient Economy (MANE) hypothesis (Phillips et al., 2013) provides a framework for considering variability in invader impacts on SOM dynamics. Forest plots dominated by arbuscular mycorrhizal (AM) trees typically have fast-decaying litters

* Corresponding author.
E-mail addresses: kumar@leuphana.de, akumar4@gwdg.de (A. Kumar).
[1] Current address: Chair of Ecosystem Functioning and Services, Institute of Ecology, Leuphana University of Lüneburg, Universitätsallee 1, 21335, Lüneburg, Germany.

https://doi.org/10.1016/j.soilbio.2019.107645
Received 27 June 2019; Received in revised form 23 October 2019; Accepted 29 October 2019
Available online 1 November 2019
0038-0717/

Table 1
Soil properties in uninvaded EcM and AM stands in Moore's creek forest reserve (Phillips et al., 2013; Craig et al., 2019).

Soil properties	EcM soil	AM soil
Soil pH	4.27 ± 0.09	5.23 ± 0.24
DOC	0.64 ± 0.06	0.32 ± 0.04
Organic N/Inorganic N	255 ± 50	159 ± 28
Nitrification rates	<0.001	1.05 ± 0.21
Decomposition rates	9.8 ± 1.6	17.7 ± 2.8
POM-N: MAOM-N	1.57 ± 0.76	0.96 ± 0.38
POM-C: MAOM-C	2.16 ± 0.93	1.36 ± 0.50

DOC: mg organic C g^{-1} soil; nitrification rates: μg NO^{3-} N g^{-1} soil d^{-1}; decomposition rates: % litter mass loss; POM-N (C): particulate organic matter-nitrogen (carbon); MAOM-N (C): mineral associated organic matter-nitrogen (carbon).

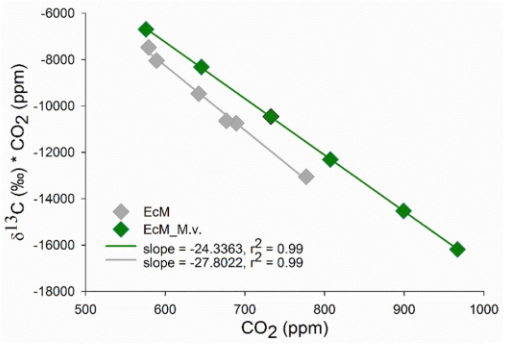

Fig. 1. Miller/Tans model for purification of the $\delta^{13}C$ value of soil CO_2 from atmospheric admixture. The slope of the regression line (OLS) represents the isotopic composition of pure soil CO_2. A reference plot without invasion (grey diamonds) and a plot with *M. vimineum* invasion (green diamonds) are shown exemplarily. With invasion, soil CO_2 shifts towards more positive $\delta^{13}C$ values due to an influence of the C_4-signal from *M. vimineum*. EcM represents uninvaded plots whereas EcM_Mv represents the plots invaded by *M. vimineum*. (For interpretation of the references to colour in this figure legend, the reader is referred to the Web version of this article.)

(Midgley et al., 2015; Keller and Phillips, 2019), high inorganic N availability (Midgley and Phillips, 2016; Mushinski et al., 2019), lower standing fungal biomass and fungal to bacterial ratio (Cheeke et al., 2017), and large stocks of mineral-associated (i.e., protected) organic matter (Craig et al., 2018, 2019). In contrast, plots dominated by ectomycorrhizal (EcM) trees have slow-decaying litters, low inorganic N availability, and large stocks of particulate (i.e. unprotected) organic matter. Given that priming depends on the chemical quality of plant inputs, nutrient availability, structure and functioning of microbial communities, and the degree to which the SOM is protected from decay (Cheng et al., 2014), priming effects are believed to be greater in EcM-dominated plots relative to AM-dominated plots (Fontaine and Barot, 2005; Brzostek et al., 2015; Sulman et al., 2017). However, the degree to which priming by invasive plants differs between AM- and EcM-dominated plots is unknown.

We quantified invader-induced SOM priming effects in adjacent AM- and EcM-dominated plots at Indiana University's Moores Creek Research and Teaching preserve in the south-central Indiana, USA. The forest plots are classified into AM- and EcM-plots based on known mycorrhizal associations of dominant tree species, in which, trees associated with dominant mycorrhizal type represented more than 80% of the basal area of the plot. The AM plots mainly contained a mixture of tulip poplar (*Liriodendron tulipifera*), sugar maple (*Acer saccharum*), and

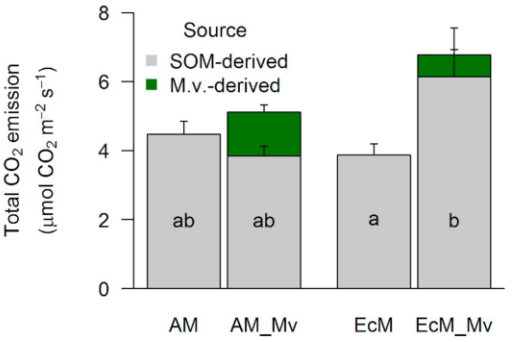

Fig. 2. Total CO_2 emission (μmol CO_2 m^{-2} s^{-1} ±SE) from AM and EcM plots. AM and EcM represents uninvaded plots whereas AM_Mv and EcM_Mv represents plots invaded by *M. vimineum*. Total CO_2 emission was partitioned into SOM-derived and *M. vimineum*-derived (M.v.-derived). Different letters indicate significant differences (Tukey's post-hoc test, $P < 0.05$) of total CO_2 emission between invasion and type of mycorrhizal association.

sassafras (*Sassafras albidum*), whereas, American beech (*Fagus grandifolia*), pignut hickory (*Carya glabra*), black oak (*Quercus velutina*), white oak (*Q. alba*), and red oak (*Q. rubra*) are the predominant species at the EcM plots (see Phillips et al., 2013; Mushinski et al., 2019 for detailed site description). Four *M. vimineum*-invaded and four uninvaded plots (80 × 80 cm) within EcM- and AM-dominated plots were identified and trenched to a depth of 30–35 cm. After trenching, three PVC collars (inner diameter 5 cm) were installed randomly to a depth of 3 cm within each plot. Extra care was taken during trenching and PVC collar installation to minimize the soil disturbance and allowed to establish for *c.* 3 weeks. Both the plots had similar abundances of *M. vimineum,* but differed in a number of soil characteristics (Table 1).

We hypothesized that *M. vimineum* accelerates SOM decomposition in EcM-dominated plots more than AM-dominated plots owing to the lower N availability and greater fraction of unprotected SOM in the EcM- relative to the AM-dominated plots. To test our hypothesis, we took advantage of differences in the ^{13}C natural abundance between sources of soil CO_2 emission (native SOM-derived vs. *M. vimineum*-derived) as a proxy for SOM decomposition. Trees with C_3 photosynthetic pathways have unique $\delta^{13}C$ values (−27.6‰ in EcM trees and −27.1‰ in AM trees) relative to the $\delta^{13}C$ signature of the C_4 grass *M. vimineum* (−14.39‰). This enabled us to partition the source of soil CO_2 emission and to calculate SOM priming under natural conditions. The $\delta^{13}C$ of pure soil CO_2 efflux was calculated after correcting the measured $\delta^{13}C$ value for the atmospheric CO_2 admixture based on the Miller/Tans model (Miller and Tans, 2003; Pausch and Kuzyakov, 2012) (Fig. 1). Priming effects (PE) were calculated as the difference of SOM-derived CO_2 between *M. vimineum*-invaded ($C_{s\ (M.vimineum\text{-invaded})}$) and uninvaded plots ($C_{s\ (uninvaded)}$):

$$PE = C_{s\ (M.vimineum\text{-invaded})} - C_{s\ (uninvaded)}$$

Where $C_{s\ (uninvaded)}$ is the total CO_2 efflux from the uninvaded plots (see supplementary material for detailed site description, measurements and calculations).

Rates of soil CO_2 emission between the uninvaded AM and EcM plots remained similar whereas recent invasion by *M. vimineum* resulted in increased rates of soil CO_2 emission in EcM plots only (Fig. 2). On average, *M. vimineum* increased rates of CO_2 emission by 41% compared to uninvaded plots. In invaded plots, a linear two-source isotopic mixing model was used to partition the total CO_2 to its sources (SOM-derived and *M. vimineum*-derived CO_2). *M. vimineum* resulted in a net positive SOM priming in EcM plots of 2.26 μmol CO_2 m^{-2} s^{-1} - a 58% increase

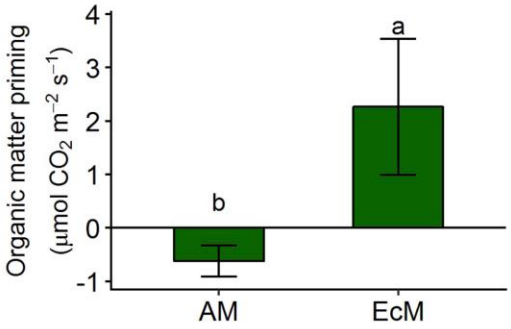

Fig. 3. Priming effect of *M. vimineum* on SOM decomposition in arbuscular (AM) and ectomycorrhizal (EcM) dominated plots. Letters indicates significant differences ($P < 0.05$, *t*-test).

compared to uninvaded plots (Fig. 3). In contrast, invasion resulted in 14% reduction in SOM-derived CO_2 in AM plots resulting in a negative SOM priming (Fig. 3).

Previous studies have reported links between invasive plants, microbial activities and accelerated SOM loss (Strickland et al., 2010; Bradford et al., 2012; Sokol et al., 2019; Craig et al., 2019); however, direct measurements of invader-induced priming effects *in situ* are rare. Our results showed that invader-induced priming can be appreciable (58% increase in SOM loss), and that site level factors (overstory community and edaphic characteristics) mediate this effect. Trace amounts of exudates can boost microbial metabolism and activity (De Nobili et al., 2001). Given the strong competition for N in EcM plots at this site (Midgley and Phillips, 2016), microbes stimulated by invader inputs may need to mine SOM for N (Craine et al., 2007). Moreover, higher fungal to bacterial ratios, and a shift in enzymatic stoichiometry to higher investment in extracellular enzyme production for nutrient rather than C acquisition in EcM than AM plots (Cheeke et al., 2017), can be directly linked to accelerated SOM decomposition through nutrient mining (Fontaine and Barot, 2005). This finding highlights the role of soil microbial communities as drivers of priming effects (McGuire et al., 2010; Taylor et al., 2016; Cheeke et al., 2017). In AM-dominated plots where N is abundant and competition for N is reduced (Midgley and Phillips, 2016), microbes may preferentially use C exuded by the invaders, resulting in reduced metabolic costs and less SOM decomposition leading to negative priming effects. Additionally, the accumulation of unprotected SOM in EcM soils owing to the slow decomposition of EcM tree litter was likely more vulnerable to priming than the protected SOM in AM soils that was formed from fast-decaying litter (Cotrufo et al., 2013; Averill and Hawkes, 2016; Sulman et al., 2017). Furthermore, recent studies that have tracked the flow of *M. vimineum* litter into soil pools have found that as particulate organic matter decays, it leads to more mineral-associated OM formation (Sokol et al., 2019; Craig et al., 2019). Thus, it is important to consider that while our study focused on priming effects, some fraction of fast-decaying litter from the invader likely moved into the mineral-associated SOM pool (Sokol et al., 2019; Craig et al., 2019). This could offset some of the losses from priming, though more work is needed to better evaluate the net effects of invaders on SOM pools.

Collectively, our results demonstrate that the impact of fast-growing invasive species on priming effects depends on the edaphic characteristics and highlight the importance of considering invasive plants as drivers of SOM change. Future studies should also consider soil mineralogy as a mediator of invasion-induced organic matter priming effects.

Acknowledgements

The authors would like to thank Robin Johnson, Elizabeth Huenupi, and Katie Beidler for their field assistance. Elizabeth Huenupi's help is laboratory analyses is highly appreciated. We would also like to thank Peter E. Sauer at the Stable Isotope Research Facility (SIRF) in the Department of Geological Sciences, Indiana University, Bloomington, U. S.A. for isotopic analyses. Authors would like to thank Andreas Fichtner and Benjamin M. Delory at the Institute of Ecology, Leuphana University Lüneburg, Germany for statistical consultancy. Authors gratefully acknowledge the German Academic Exchange Service (DAAD) for scholarship award (PPP-7020289). This study was supported by the German Research Foundation (DFG) within the project PA2377/2-1. We would like to thank the editor and two anonymous reviewers whose comments significantly improved the quality of this publication.

Appendix A. Supplementary data

Supplementary data to this article can be found online at https://doi.org/10.1016/j.soilbio.2019.107645.

References

Averill, C., Hawkes, C.V., 2016. Ectomycorrhizal fungi slow soil carbon cycling. Ecology Letters 19, 937–947.
Bradford, M.A., Strickland, M.S., DeVore, J.L., Maerz, J.C., 2012. Root carbon flow from an invasive plant to belowground foodwebs. Plant and Soil 359, 233–244.
Brzostek, E.R., Dragoni, D., Brown, Z.A., Phillips, R.P., 2015. Mycorrhizal type determines the magnitude and direction of root-induced changes in decomposition in a temperate forest. New Phytologist 206, 1274–1282.
Chao, L., Liu, Y., Freschet, G.T., Zhang, W., Yu, X., Zheng, W., Guan, X., Yang, Q., Chen, L., Dijkstra, F.A., Wang, S., 2019. Litter carbon and nutrient chemistry control the magnitude of soil priming effect. Functional Ecology 33, 876–888.
Cheeke, T.E., Phillips, R.P., Brzostek, E.R., Rosling, A., Bever, J.D., Fransson, P., 2017. Dominant mycorrhizal association of trees alters carbon and nutrient cycling by selecting for microbial groups with distinct enzyme function. New Phytologist 214, 432–442.
Cheng, W., Kuzyakov, Y., 2005. Root effects on soil organic matter decomposition. Agronomy 119–144. https://doi.org/10.2134/agronmonogr48.c7.
Cheng, W., Parton, W.J., Gonzalez-Meler, M.A., Phillips, R., Asao, S., McNickle, G.G., Brzostek, E., Jastrow, J.D., 2014. Synthesis and modeling perspectives of rhizosphere priming. New Phytologist 201, 31–44.
Cotrufo, M.F., Wallenstein, M.D., Boot, C.M., Denef, K., Paul, E., 2013. The Microbial Efficiency-Matrix Stabilization (MEMS) framework integrates plant litter decomposition with soil organic matter stabilization: do labile plant inputs form stable soil organic matter? Global Change Biology 19, 988–995.
Craig, M.E., Fraterrigo, J.M., 2017. Plant–microbial competition for nitrogen increases microbial activities and carbon loss in invaded soils. Oecologia 184, 583–596.
Craig, M.E., Lovko, N., Flory, S.L., Wright, J.P., Phillips, R.P., 2019. Impacts of an invasive grass on soil organic matter pools vary across a tree-mycorrhizal gradient. Biogeochemistry 144, 149–164.
Craig, M.E., Turner, B.L., Liang, C., Clay, K., Johnson, D.J., Phillips, R.P., 2018. Tree mycorrhizal type predicts within-site variability in the storage and distribution of soil organic matter. Global Change Biology 24, 3317–3330.
Craine, J.M., Morrow, C., Fierer, N., 2007. Microbial nitrogen limitation increases decomposition. Ecology 88, 2105–2113.
De Nobili, M., Contin, M., Mondini, C., Brookes, P.C., 2001. Soil microbial biomass is triggered into activity by trace amounts of substrate. Soil Biology and Biochemistry 33, 1163–1170.
Ehrenfeld, J.G., Kourtev, P., Huang, W., 2001. Changes in soil functions following invasions of exotic understory plants in deciduous forests. Ecological Applications 11, 1287–1300.
Flory, S.L., Clay, K., 2010. Non-native grass invasion suppresses forest succession. Oecologia 164, 1029–1038.
Fontaine, S., Barot, S., 2005. Size and functional diversity of microbe populations control plant persistence and long-term soil carbon accumulation. Ecology Letters 8, 1075–1087.
Hulme, P.E., Pyšek, P., Jarošík, V., Pergl, J., Schaffner, U., Vilà, M., 2013. Bias and error in understanding plant invasion impacts. Trends in Ecology & Evolution 28, 212–218.
Jo, I., Fridley, J.D., Frank, D.A., 2017. Invasive plants accelerate nitrogen cycling: evidence from experimental woody monocultures. Journal of Ecology 105, 1105–1110.
Keller, A.B., Phillips, R.P., 2019. Leaf litter decay rates differ between mycorrhizal groups in temperate, but not tropical, forests. New Phytologist 222, 556–564.
Kumar, A., Kuzyakov, Y., Pausch, J., 2016. Maize rhizosphere priming: field estimates using 13C natural abundance. Plant and Soil 409, 87–97.
Lal, R., 2008. Sequestration of atmospheric CO2 in global carbon pools. Energy & Environmental Science 1, 86–100.

Lee, M.R., Flory, S.L., Phillips, R.P., 2012. Positive feedbacks to growth of an invasive grass through alteration of nitrogen cycling. Oecologia 170, 457–465.
Liao, C., Peng, R., Luo, Y., Zhou, X., Wu, X., Fang, C., Chen, J., Li, B., 2008. Altered ecosystem carbon and nitrogen cycles by plant invasion: a meta-analysis. New Phytologist 177, 706–714.
McGuire, K.L., Zak, D.R., Edwards, I.P., Blackwood, C.B., Upchurch, R., 2010. Slowed decomposition is biotically mediated in an ectomycorrhizal, tropical rain forest. Oecologia 164, 785–795.
Midgley, M.G., Brzostek, E., Phillips, R.P., 2015. Decay rates of leaf litters from arbuscular mycorrhizal trees are more sensitive to soil effects than litters from ectomycorrhizal trees. Journal of Ecology 103, 1454–1463.
Midgley, M.G., Phillips, R.P., 2016. Resource stoichiometry and the biogeochemical consequences of nitrogen deposition in a mixed deciduous forest. Ecology 97, 3369–3378.
Miller, J.B., Tans, P.P., 2003. Calculating isotopic fractionation from atmospheric measurements at various scales. Tellus 55B, 207–214.
Morris, K.A., Stark, J.M., Bugbee, B., Norton, J.M., 2016. The invasive annual cheat grass releases more nitrogen than crested wheatgrass through root exudation and senescence. Oecologia 181, 971–983.
Mushinski, R.M., Phillips, R.P., Payne, Z.C., Abney, R.B., Jo, I., Fei, S., Pusede, S.E., White, J.R., Rusch, D.B., Raff, J.D., 2019. Microbial mechanisms and ecosystem flux estimation for aerobic NOy emissions from deciduous forest soils. Proceedings of the National Academy of Sciences 116, 2138–2145.
Parker, I.M., Simberloff, D., Lonsdale, W.M., Goodell, K., Wonham, M., Kareiva, P.M., Williamson, M.H., Holle, B.V., Moyle, P.B., Byers, J.E., Goldwasser, L., 1999. Impact: toward a Framework for Understanding the Ecological Effects of Invaders 17. n.d.
Pausch, J., Kuzyakov, Y., 2012. Soil organic carbon decomposition from recently added and older sources estimated by δ13C values of CO2 and organic matter. Soil Biology and Biochemistry 55, 40–47.
Pausch, J., Zhu, B., Kuzyakov, Y., Cheng, W., 2013. Plant inter-species effects on rhizosphere priming of soil organic matter decomposition. Soil Biology and Biochemistry 57, 91–99.
Peltzer, D.A., Allen, R.B., Lovett, G.M., Whitehead, D., Wardle, D.A., 2010. Effects of biological invasions on forest carbon sequestration. Global Change Biology 16, 732–746.
Phillips, R.P., Brzostek, E., Midgley, M.G., 2013. The mycorrhizal-associated nutrient economy: a new framework for predicting carbon-nutrient couplings in temperate forests. New Phytologist 199, 41–51.
Shannon-Firestone, S., Reynolds, H.L., Phillips, R.P., Flory, S.L., Yannarell, A., 2015. The role of ammonium oxidizing communities in mediating effects of an invasive plant on soil nitrification. Soil Biology and Biochemistry 90, 266–274.
Sokol, N.W., Kuebbing, S.E., Karlsen-Ayala, E., Bradford, M.A., 2019. Evidence for the primacy of living root inputs, not root or shoot litter, in forming soil organic carbon. New Phytologist 221, 233–246.
Song, J., Wan, S., Piao, S., Knapp, A.K., Classen, A.T., Vicca, S., Ciais, P., Hovenden, M.J., Leuzinger, S., Beier, C., Kardol, P., Xia, J., Liu, Q., Ru, J., Zhou, Z., Luo, D., Langley, J.A., Zscheischler, J., Dukes, J.S., Tang, J., Chen, J., Hofmockel, K.S., Kueppers, L.M., Rustad, L., Liu, L., Smith, M.D., Templer, P.H., Thomas, R.Q., Norby, R.J., Phillips, R.P., Niu, S., Fatichi, S., Wang, Y., Shao, P., Han, H., Wang, D., Lei, L., Wang, J., Li, X., Zhang, Q., Li, X., Su, F., Liu, B., Yang, F., Ma, G., Li, G., Liu, Y., Liu, Y., Yang, Z., Zhang, K., Miao, Y., Hu, M., Yan, C., Zhang, A., Zhong, M., Hui, Y., Zheng, M., 2019. A meta-analysis of 1119 manipulative experiments on terrestrial carbon-cycling responses to global change. Nature Ecology & Evolution 3, 1309–1320.
Strayer, D.L., 2012. Eight questions about invasions and ecosystem functioning. Ecology Letters 15, 1199–1210.
Strickland, M.S., Devore, J.L., Maerz, J.C., Bradford, M.A., 2010. Grass invasion of a hardwood forest is associated with declines in belowground carbon pools. Global Change Biology 16, 1338–1350.
Sulman, B.N., Brzostek, E.R., Medici, C., Shevliakova, E., Menge, D.N.L., Phillips, R.P., 2017. Feedbacks between plant N demand and rhizosphere priming depend on type of mycorrhizal association. Ecology Letters 20, 1043–1053.
Taylor, M.K., Lankau, R.A., Wurzburger, N., 2016. Mycorrhizal associations of trees have different indirect effects on organic matter decomposition. Journal of Ecology 104, 1576–1584.
Vilà, M., Espinar, J.L., Hejda, M., Hulme, P.E., Jarošík, V., Maron, J.L., Pergl, J., Schaffner, U., Sun, Y., Pyšek, P., 2011. Ecological impacts of invasive alien plants: a meta-analysis of their effects on species, communities and ecosystems. Ecology Letters 14, 702–708.

Supporting Information

Organic matter priming by invasive plants depends on dominant mycorrhizal association

Authors: Amit Kumar, Richard P. Phillips, Andrea Scheibe, **Saskia Klink**, Johanna Pausch

The following Supporting Information is available for this article:

Materials and methods

- Site description
- Soil CO_2 emission
- Miller/Tans model and CO_2 flux partitioning
- Statistics

Materials and methods:

Site description:

The present study was conducted in a *c.* 80 year-old temperate deciduous forest at Moores Creek, which is part of Indiana University's Research and Teaching Preserve (39°05'N, 86°27'W). Two field sites were identified as dominated either by AM or by EcM-trees. A detailed site description of Moores Creek can be found elsewhere (Phillips et al. 2013, Midgley et al. 2015). Mycorrhizal association (EcM or AM) was assigned when a tree from the respective mycorrhizal type contributed to more than 80% of the basal area of that plot (Phillips et al. 2013). We located patches of *M. vimineum* invasion in AM and EcM stands throughout the sites. Soil samples were analyzed for $\delta^{13}C$ to characterize the plots where the C_4-signal from *M. vimineum* in the SOM was weak or absent. Plots with *M. vimineum* close to the uninvaded plots, were taken as recently invaded plots depending on soil $\delta^{13}C$ signature. Notably, we found no differences in the biomass of *M. vimineum* in AM vs. EcM-dominated stands. Four recently *M. vimineum*-invaded and four uninvaded plots (80 x 80 cm) within EcM- and AM-dominated stands were identified and trenched to a depth of 30-35 cm. After trenching, three PVC collars (inner diameter 5 cm) were installed randomly to a depth of 3 cm within each plot and allowed to establish for *c.* 3 weeks.

Soil CO_2 emission

Once the plots were established, soil CO_2 emissions were measured in the field both in *M. vimineum*-invaded and uninvaded plots (in EcM- and AM-stands) at 3 time intervals (18th August, T1; 6th September, T2; and 20th September, T3) in 2017 using an infra-red gas analyzer (IRGA; Li-Cor, Biosciences, Lincoln, NE, USA, Model LI-8100). Within each plot, CO_2 efflux was measured for 4 min from 2 out of 3 PVC collars yielding a total of 32 measurement points for each sampling time. Soil respiration (C_t) was calculated using SoilFluxPro^{TM} (ver.4.0). Six gas samples with 3 min intervals (0, 3, 6, 9, 12, and 15 min) were collected from the third PVC collar from each plot at each sampling time. An air-tight chamber was installed on top of the collar, gas samples were taken with a syringe through a septum in the chamber lid and transferred to vacuum vials. The CO_2 concentrations and $\delta^{13}C$ values of the gas samples were determined at the Stable Isotope Research Facility (SIRF) of Indiana University, Bloomington, using a Thermo Delta Plus XP isotope ratio mass spectrometer (IRMS) with a Thermo Gas Bench II as inlet. Concentrations were calculated using dry air and a 1% CO_2 / He mixture. Stable C isotopic compositions were calibrated to the VPDB scale using NBS19 and three internal lab standards that have been calibrated to NBS19, NBS20, and LSVEC.

Miller/Tans model and CO_2 flux partitioning

The $\delta^{13}C$ of pure soil CO_2 efflux was calculated after correcting the measured $\delta^{13}C$ value for the atmospheric CO_2 admixture based on the Miller/Tans model (Miller and Tans, 2003; Pausch and Kuzyakov, 2012). For the Miller/Tans model, measured $\delta^{13}C$ values multiplied by the respective CO_2 concentrations were plotted against the CO_2 concentrations. The slope of the regression line is equivalent to the $\delta^{13}C$ value of soil CO_2 efflux purified from atmospheric CO_2 (Miller and Tans, 2003). For each sampling time, the slope and the standard error of the slope ($\delta^{13}C$ of soil CO_2 ± SE) were obtained for each replicate.

Total CO_2 efflux (C_t) was partitioned into root-derived CO_2 (C_r) and SOM-derived CO_2 (C_s) using a linear two-source mixing model (Pausch & Kuzyakov, 2012):

$$C_{s(M.vimineum\text{-invaded})} = C_t (\delta^{13}C_t - \delta^{13}C_r) / (\delta^{13}C_{s(uninvaded)} - \delta^{13}C_r)$$

$$C_r = C_t - C_{s(M.vimineum\text{-invaded})}$$

Where $\delta^{13}C_t$, $\delta^{13}C_r$, and $\delta^{13}C_s$ are the isotopic composition of total-, root-derived-, and SOM-derived $CO_{2(uninvaded)}$, respectively. $\delta^{13}C_s$ was taken from the uninvaded plots. The isotopic composition of *M. vimineum* roots were taken as a measure for root-derived CO_2 ($\delta^{13}C_r$). C_t, C_r, and C_s are the CO_2 concentrations of total-, root-derived-, and SOM-derived CO_2, respectively.

Priming effects (PE) were calculated as the difference of SOM-derived CO_2 between *M. vimineum*-invaded ($C_{s\ (M.vimineum\text{-invaded})}$) and uninvaded plots ($C_{s\ (uninvaded)}$):

$$PE = C_{s\ (M.vimineum\text{-invaded})} - C_{s\ (uninvaded)}$$

Where $C_{s\ (uninvaded)}$ is the total CO_2 efflux from the uninvaded plots.

Statistics

The values presented in graphs and tables are a mean of four field replicates ± standard errors (SE) at each sampling time. We applied statistics to assess the effects of mycorrhizal association and invasion on soil CO_2 emissions and t-test for assessing mycorrhizal association effects on priming effects. To account for temporal pseudo-replication (i.e. CO_2 emissions were measured at three time intervals), models were fitted using a generalized least square approach with a compound symmetry covariance structure (*corCompSymm(form =~Time|Plot)*) using *nlme* package (Pinheiro & Bates, 2009; Pinheiro et al. 2017). Multiple comparisons were tested (as for total CO_2 emission) for significance using generalized linear hypotheses with Tukey's HSD test using *lsmeans* (Lenth, 2016) and *multicomp* (Hothorn et al. 2008) packages. We used $P < 0.05$ as statistically significant difference if not specially mentioned elsewhere. All the statistical analyses were performed using R 3.5.0 (R Core Team, 2018).

Manuscript 5

Plants benefit more from elevated CO_2 in terms of nutrient acquisition than microbes despite different plant-microbial interactions

Saskia Klink[1], Adrienne B. Keller[2a], Richard P. Phillips[2], Matthias Gube[3], Johanna Pausch[1]

In preparation

[1]Department of Agroecology, Bayreuth Center of Ecology and Environmental Research (BayCEER), University of Bayreuth, 95440 Bayreuth, Germany

[2]Department of Biology, Indiana University Bloomington, IN 47405, USA

[3]Soil Science of Temperate Ecosystems, Büsgen Institute, Georg-August University Göttingen, 37077 Göttingen, Germany

[a]Current address: Department of Ecology, Evolution, and Behavior, University of Minnesota, Saint Paul, 55108, USA

Key words: Competition, Elevated CO_2, mycorrhizal dependency, microbial interaction, Progressive N limitation (PNL) hypothesis

Abstract

Effects of elevated atmospheric carbon dioxide (CO_2) concentrations attributed to climate change are frequently assumed to provide a benefit to plant and microbe growth and biomass production. Nevertheless, an increased CO_2 supply for photosynthesis and biomass production concomitantly causes a higher demand for nitrogen (N), especially on the plant's site. Still, how plants with different microbial interactions respond to elevated CO_2 in terms of N acquisition remains understudied.

We conducted a climate control chamber experiment in which three plant species with different nutrient acquisition strategies were grown at ambient (400 ppm) and elevated (700 ppm) atmospheric CO_2 conditions. The grass *Festuca ovina* represents a mycorrhizal associated species, legume *Medicago sativa* a mycorrhizal plant with N-fixing capabilities, and the cushion plant *Silene acaulis* represents a weakly mycorrhizal species. Plants were inoculated with the AM fungus *Rhizophagus irregularis* and a native soil community and planted in pots with an inserted ^{15}N-labeled litter containing mesh bag. Transfer of C and N was traced *via* stable isotopes.

Despite different microbial interactions, all three plant species benefitted more from soil N than microbes under elevated CO_2 conditions. While under ambient CO_2 nutrient cycling was accelerated, it was decelerated for microbes in the elevated treatment as visualized by a widening of the microbial biomass C:N ratio and higher ^{15}N remaining in the mesh bag at the end of the experiment under elevated *vs.* ambient CO_2. In contrast to soil microbes, intraradical mycorrhizal hyphae were not affected by N-limitation, as shown by an increased hyphal N-content under elevated CO_2 while MBN generally decreased. Plants N budget differed depending on plant species, with more total N in *Festuca* roots and *Silene* shoots under elevated CO_2, but less in *Medicago* shoots and roots.

These results highlight the ability of plants to successfully compete for soil N with soil microbes, while associated microbes/AM fungi likely act as an elongation of the root to support N acquisition. Concerning climate change scenarios, our findings demonstrate the need to consider effects on all members of an ecosystem. Even if plants and mycorrhizal fungi benefit via an increase in biomass and yield, other members necessary for the system's functioning may suffer and diminish, which also has an influence on the plants in the long term.

Introduction

CO_2 and climate change

Climate change threatens the functioning of the world's ecosystems, and rising atmospheric carbon dioxide (CO_2) concentrations represent a prominent factor aggravating the predicted impacts of climate change (e.g., increasing temperatures, prolonged drought periods) (Lindner *et al.*, 2010; Pecl *et al.*, 2017). While the current atmospheric CO_2 concentrations level is around 413 ppm (NOAA, 2021), a doubling of these concentrations by the year 2100 is predicted (UKCIP, 2011; Szulejko *et al.*, 2017), meaning additional 3 Pg carbon (C) is added to the atmosphere per year (Deeb *et al.*, 2011). Consequences of this drastic increase in atmospheric CO_2 levels comprise, among other effects, scarcity in food and water, desertification, biodiversity loss, and exacerbated CO_2 level increase due to the release of carbon bound in vegetation and soils (Lindner *et al.*, 2010; Pecl *et al.*, 2017).

Plants-soil-microorganism system and [e]CO_2

The storage of CO_2 in vegetation and soil holds as an effective mechanism to remove CO_2 from the atmosphere, with soils representing a major C sink (Dixon *et al.*, 1994; Ainsworth & Long, 2005; Kuzyakov *et al.*, 2019). However, the efficiency of this CO_2 removal strongly depends on the trade-off between C inputs from primary production and SOM decomposition-driven C release to the atmosphere (Treseder, 2004; Cheng *et al.*, 2012; Phillips *et al.*, 2012).

For plants and microbes, an increased atmospheric CO_2 level was frequently reported to result in increased growth and yield (Treseder, 2004; Alberton *et al.*, 2005; Drigo *et al.*, 2010), as more CO_2 is available for photosynthesis, and C exudation can promote microbial activity (e.g. Cheng *et al.*, 2012). Nevertheless, increased photosynthetic activity in response to increased CO_2 levels necessitates a sufficient nutrient availability to maintain effective photosynthesis and growth and frequently results in nutrient limitation on plants' site (Oren *et al.*, 2001; Schlesinger & Lichter, 2001; Finzi *et al.*, 2002; Norby *et al.*, 2009). Aiming to prevent nutrient scarcity, a majority of plant species are associated with microorganisms supporting the nutrient acquisition, e.g., symbiotic fungi or rhizobacteria (Arnone & Gordon, 1990; Jumpponen, 2001; Temperton *et al.*, 2003; Smith & Read, 2010). An option for ameliorating nutrient supply is the association with symbiotic fungi, for example in the form of a mycorrhiza (Smith & Read, 2010). For a mycorrhizal association under increased CO_2 conditions it is assumed that the surplus of carbohydrates from photosynthesis is transferred to the fungal partner (Treseder, 2004; Drigo *et al.*, 2010). The fungal partner uses this carbon for increased growth and nutrient acquisition – the latter is assumed to be beneficial for the associated plant partner as nutrients shared can be utilized to maintain photosynthesis and carbon

supply (e.g. Smith & Read, 2010). However, this scenario with benefits on both the plant and the fungal site was questioned by the progressive nutrient limitation hypothesis (PNL) (Luo *et al.*, 2004; Johnson, 2006). The PNL hypothesis argues that with an incremental duration of increased carbon supply to fungi, the fungi become a sink for nutrients accumulated in their tissues and soil pools due to fungal tissue turnover (Luo *et al.*, 2004; Fransson *et al.*, 2005; Johnson, 2006). Thereby, the plant becomes more and more nutrient-limited, despite increased CO_2 conditions and carbon supply to the mycorrhizal partner. Consequently, photosynthetic activity may be reduced, despite elevated CO_2 levels (Alberton *et al.*, 2005). Nevertheless, a range of studies analyzing plant-microbe responses to elevated CO_2 reported increased nutrient uptake of plants with increasing CO_2 (Johnson, 2006 and literature therein), suggesting for nutrient acquisition strategies proving themselves as beneficial under elevated CO_2.

Plant-microbial interactions to acquire nutrients

Plants execute a variety of different strategies to acquire nutrients from the soil. A plant-trait related strategy is the creation of a rooting architecture beneficial for nutrient acquisition, e.g., via the increase of fine roots or root tips (Yanai *et al.*, 1995; Pritchard *et al.*, 2008; Jackson *et al.*, 2009; Iversen, 2010; Nie *et al.*, 2013; Piñeiro *et al.*, 2017). Further, plant roots produce a mixture of exudates including organic acids to directly access soil nutrients (Dakora & Phillips, 2002) or to facilitate the activation of soil microbial nutrient mining (Dakora & Phillips, 2002; Phillips *et al.*, 2012; Verbruggen *et al.*, 2017; Frey, 2019) and take advantage of nutrients released to soil from soil organic matter (SOM) decomposition. Finally, the option of an association with microorganisms supporting nutrient supply in exchange for carbohydrate supply represents a successful nutrient acquisition strategy (Arnone & Gordon, 1990; Jumpponen, 2001; Temperton *et al.*, 2003; Smith & Read, 2010). Still, it remains unclear how plants with different microbial interactions to gain nutrients respond to elevated CO_2 conditions and how the association with microorganisms alleviates or aggravates nutrient limitation.

We sought to investigate how plants with varying microbial interactions respond to elevated [e] atmospheric CO_2 concentrations and whether the PNL hypothesis seems plausible under the given nutrient acquisition strategy. Further, we aimed to analyze the effect of [e]CO_2 on the corresponding microorganisms and their response with a view on plant partners' nutrient acquisition strategies. Therefore, we tested the response of plant species with well-developed mycorrhiza, with weak mycorrhiza, and with rhizobia-association to [e]CO_2 conditions. We hypothesize that

(I) Plant growth will be increased under elevated CO_2 levels due to an increased nutrient supply by associated microorganisms.

(II) A higher amount of nutrients will be transferred to the plant with well-developed mycorrhiza relative to the plant with weakly-developed mycorrhiza.

(III) The plant with rhizobia association will switch to a greater reliance on less cost-intense soil microorganisms than rhizobia under elevated CO_2 conditions.

(IV) Microorganisms will respond to elevated CO_2 with enhanced nutrient mining.

Materials and Methods

Pre-experiment preparation

For each of the two CO_2 concentrations, 42 pots (12 x 30 cm) were prepared from PVC pipes, and the bottom was closed with a PVC plug (DN 125). Two unplanted controls per CO_2 treatment were included with the same setup as for the planted pots to control for leaching from the mesh bag to bulk soil during watering. For the natural abundance controls, two replicates per plant species were prepared without an inner mesh bag.

Soil (sandy clay loam, upper 10 cm) from a C3-plant-covered location at the landwirtschaftliche Lehranstalten Bayreuth (49°55'42.618"N, 11°33'2.8656"E) was air-dried for two weeks to guarantee similar starting conditions. The soil 2 mm-sieved and mixed with sand (1:1; sand from BSR Bayreuth, 0 – 4 mm cover sand) to reduce the soil N content as high N availability was shown to result in low root colonization by mycorrhizal fungi (Treseder, 2004). The soil-sand mixture contained 0.1% nitrogen, 1.0% carbon, and had a pH of 5.3

Ingrowth cores were prepared from PVC tubes (3 x 10 cm) in which holes were drilled all over to allow hyphal ingrowth and covered with either a 30 µm or 1 µm mesh bag (Sefar Nitex, Switzerland). The 30 µm mesh should avoid root ingrowth into the cores but allow hyphal ingrowth (most hyphae < 5 µm), while the 1 µm mesh should avoid both root and hyphal ingrowth, to account for effects of diffusion. Nevertheless, our data did not reveal statistically significant differences between treatments with 1 µm or 30 µm meshes. This holds for all plant species; slight differences occurred only for isolated hyphae. Similar issues with a lack of distinction between hyphal-exclusion and hyphal-access meshes were described by Paterson *et al.* (2016) and Cheeke *et al.* (2021). Thus, in this study, the 1 µm and 30 µm mesh treatments were combined within a CO_2 treatment and plant species due to the lack of difference.

Each ingrowth core was filled with a mixture of 1 g isotopically labeled litter (*Leymus chinensis* (Trin.) Tzvelev, Poaceae; ^{15}N enrichment mean: 886.32‰) and 80 g of the soil-sand mixture, and the mesh

bag opening was sealed by flipping the upper end of the mesh bag around a cord and closing it with tape and a stapler. The cord was taped to the pots with the ingrowth core in the middle of the pots and in equal height for each of the pots. To ensure sufficient aeration of the soil a sandbag prepared from a nylon sock filled with 1.1 kg sand per pot was placed at the bottom of each pot. On top of each sandbag 2.5 kg of the soil-sand mix mixed with 0.4 g spores of *Rhizophagus irregularis* (Blaszk, Wubert, Renker & Buscot) (Schussler & Walker, 2010) (formerly *Glomus intraradices*) (AMM 6080001, BioFa AG, Münsingen, Germany) were filled and watered to a field capacity of 60 %.

Three plant species with different microbial interactions to acquire nutrients were chosen: sheep fescue (*Festuca ovina* L.), alfalfa (*Medicago sativa* L.) and moss campion (Silene acaulis (L.) Jacq.). For F. ovina and M. sativa, six replicates per mesh size (1 µm and 30 µm) were prepared per CO_2 concentration, while for S. acaulis five replicates were present due to dieback of plants. Seeds of the three plant species, all from Jelitto Staudensamen, were germinated one week prior to the experiment on sterilized, moist filter paper in Petri dishes. On the day of planting, seedlings a primary root and cotyledons were visible. Per experimental pot, three seedlings were planted to ensure plant growth if some of the seedlings died back. Daily watering of plants to a soil field capacity of 60% ensured plant growth. Weeds were removed from pots regularly to ensure growth and mycorrhization of target species only.

Experimental set up

The experiment was set up in climate control chambers (ThermoTEC, Rochlitz, Germany; Adaptis A1000, China, for ambient CO_2 natural abundance plants) for which temperature, day/night rhythm, light intensity, and CO_2 concentration was controlled. A day/night rhythm of 14 hours light with a temperature of 20 °C and 10 hours dark with a temperature of 18 °C was set. Light intensity was adjusted to ~ 760 µmol photons m^{-1} s^{-1} within the climate chamber, and CO_2 concentrations were set to 400 ppm for the ambient CO_2 treatment and 700 ppm for the elevated CO_2 treatment. The CO_2 concentration in the chamber was monitored with a LiCOR and kept constant via a computer-controlled system (for more detail see Pausch *et al.*, 2013; Pausch *et al.*, 2016). The CO_2 gas bottle (Rießer-Gase, Lichtenfels/Michelau, Germany) opened as soon as the [CO_2] dropped by 5 ppm to adjust the CO_2 levels. Inside the climate control chamber, the ^{13}C isotopic signature evened out around -19.38 ± 0.63‰.

Pots were rotated randomly after daily watering. The night rhythm was set during daytime to allow for watering in the night period so that an impact by respiratory CO_2 from the experimenter was minimized/neglectable. Pots were fertilized three times during the experiment for each CO_2 concentration with 1mL fertilizer (Wuxal Super, Hauert Manna, Nuremberg) per 1L water. The fertilizer contained 100g N/L, 100g P_2O_5/L, 75g K_2O/L, < 1g/L boron, copper, iron, manganese,

molybdenum, zinc and Cu, Fe, Mn and Zn are fully chelated. The experiment was run for 16 weeks for each of the two CO_2 concentrations to allow sufficient establishment of mycorrhizal networks (Johnson et al. 2001) and to circumvent artifacts caused by the carbon drain effect (cf. Rouhier & Read, 1998; Fitter *et al.*, 2000).

Harvest

After 120 days, pots were destructively harvested. Plant aboveground biomass was cut shortly above the soil, dried in an oven at 60 °C for 48 hours before dry weight of biomass was measured.

Roots were cleaned from soil by several washing steps with deionized water and cleaned from fine debris with tweezers. They were then subsampled for stable isotope analyses, colonization rate estimates, and hyphae isolation. From stable isotope root subsamples, fresh and dry weight was determined for biomass estimates. Afterward, subsamples for stable isotope analyses were dried at 60 °C for 48 hours in paper bags, subsamples for colonization rates were stored in 70% ethanol until staining.

Soil comprised the mesh bag soil from within the ingrowth core and the bulk soil around the ingrowth core. Subsamples were prepared for stable isotope measurements (dried at 60 °C for 48 hours), soil hyphae extraction (fresh soil, stored at 4 °C, no longer than 14 hours), and determination of microbial biomass C and N (fresh soil, stored at 4 °C, no longer than 48 hours). Soil hyphae isolation was performed according to Brundrett *et al.* (1994), and root hyphae were isolated following Klink *et al.* (2020), with the modification from Brundrett *et al.* (1994) that hyphae were not stained after isolation but collected in Eppendorf tubes and dried to constant weight at 60 °C in an oven.

Stable isotope analyses

Dried samples, except hyphae, were homogeneously ground in a ball mill (MM2, RETSCH, Haan, Germany) and stored in desiccators until being weighed into tin capsules. Hyphae were pipetted into silver capsules after diluting them in 100 µL deionized water and dried at 60 °C. Determination of $^{13}C/^{12}C$, $^{15}N/^{14}N$, and C- and N-content was done with an elemental analyzer isotope ratio mass spectrometer (Elemental analyzer NC2500, ThermoQuest, Milan, Italy; mass spectrometer Deltaplus, ThermoQuest, Germany; ConFlo II, ThermoQuest, Germany). An µEA-IRMS specialized on small samples was chosen for the determination of hyphal isotopic signatures.

The stable isotope natural abundances are expressed as δ-values relative to international standards. Delta-values were calculated according to equation 1, whereby R describes the heavy to the light isotope ratio.

$$\delta^{13}C \text{ or } \delta\,^{15}N = (R_{sample}/R_{standard} - 1) \times 1000\ (‰) \quad (1)$$

The standard for C was Vienna-Pee Dee Belemnite (V-PDB; $R_{standard} = 0.0111802$), the standard for N was air ($R_{standard} = 0.0036765$). By calibrating with acetanilide ($C_6H_5NH(COCH_3)$) C- and N-concentrations were calculated. Quantification of the incorporation of ^{15}N label from litter in the mesh bag into shoots, roots, and soil was performed following the equations given in Keller & Phillips (2019), with equation 2 for atom %:

$$\text{Atom \%} = (100 * STND * (\delta/1000 + 1))/(1 + STND * (\delta/1000 + 1)) \quad (2)$$

With STND being the V-PDB standard value (0.0111802) and atmospheric N_2 standard value (0.0036765) for ^{13}C and ^{15}N, respectively. Following, excess ^{15}N were calculated (equation 3) as

$$\text{Excess } ^{15}N \text{ (ng)} = (atom\%_L - atom\%_{UL})/100 * DW * (\%N)/100 * 10^6 \quad (3)$$

With $atom\%_L$ representing the atom% of the labelled litter and $atom\%_{UL}$ the atom% of the natural abundance material. The dry weight of the plant material (mg) is DW and the N composition of the respective tissue/compartment is %N.

Recovery of ^{15}N label in the samples was calculated according to equation 4:

$$\text{Recovery (\% of input)} = (\text{total } ^{15}N \text{ in shoots/roots/soil [mg]} / \text{total } ^{15}N \text{ tracer}) * 100 \quad (4)$$

The distribution of ^{15}N to the individual N-pools was calculated as % of the sum of all ^{15}N recovered at the sampling according to equation 5:

$$^{15}N \text{ distribution (\% recovered)} = 100/\text{sum } ^{15}N \text{ recovered [g } ^{15}N \text{ per pot]} * ^{15}N \text{ content [g } ^{15}N \text{ per pot]} \quad (5)$$

Microbial biomass C and N

Determination of microbial biomass C (MBC) and N (MBN) was conducted by applying the chloroform fumigation extraction (CFE) method following Vance *et al.* (1987), Jenkinson (1988), and Jenkinson & Powlson (1976). Thereby, a fumigated sample of fresh soil is related to a non-fumigated sample, and the difference between the fumigated and the non-fumigated sample represents the MBC or MBN. For the non-fumigated soil, C and N were extracted from 10 g fresh soil with 40 mL 0.05 K_2SO_4 by shaking for 1 hour on a laboratory shaker (GFL 3016, 150 rpm). The suspension was filtered through Ahlstrom-Munktell filters (grade: 3 hw, 110 mm diameter) and filtrates analyzed for organic C and N content at a multi-C/N analyzer (2100S, Analytik Jena). For fumigated samples, the soil was fumigated in a desiccator with 80 mL ethanol-free chloroform for 24 hours at room temperature. After fumigation, C and N were extracted by the same procedure as for the non-fumigated samples. For calculating MBC and MBN, conversion factors of 0.45 for

K_{EC} and 0.54 for K_{EN} were applied following Joergensen (1996) to allow for comparisons with other studies. MBC or MBN were calculated as the difference of fumigated and non-fumigated samples, the N content of the unfumigated samples represented dissolved N (DN).

Fungal colonization (AM)

Staining of root samples of *Festuca ovina*, *Medicago sativa*, and *Silene acaulis* was conducted according to the protocol of Phillips & Hayman (1970) and Vierheilig *et al.* (2005). Briefly, roots were washed three times with deionized water before being cleared with 10 % KOH (w/v) in a water bath (W760, Memmert GmbH, Schwabach, Germany) for 30 min at 70 °C. Pigmented roots of *Festuca ovina* were bleached in a solution of 5% (v/v) H_2O_2 and 0.5% (v/v) NH3 for 10-30 min (depending on pigmentation) at room temperature. After clearing and bleaching, root samples were washed with deionized water three times. Roots were acidified with 1% (v/v) HCL for 5 min before staining in a trypan blue (0.05%, v/v), acidic acid (33%, v/v), lactic acid (33%, v/v) and deionized water (33%) staining solution at room temperature overnight. Storage of stained roots was performed in a glycine-lactic acid-deionized water solution (3:1:3) in the refrigerator.
Colonization of roots with AM fungi was estimated by the hair-cross intersect method (Brundrett *et al.*, 1996) at a BA210LED trino microscope (Motic, Wetzlar, Germany). The colonization rate was calculated by relating the number of fields of view with fungal structures intersecting with the hair-cross to the total number of fields of view observed. Per plant species, individual 100 fields of view were observed. Apart from AM fungal structures such as hyaline, non-septate hyphae, arbuscules and vesicles also other fungi were present inside the roots. Most frequently, dark septate endophyte (DSE) fungi were observed with dark pigmented, septate hyphae or microsclerotia structures.

Statistical analyses and data evaluation

Figures were created with Software SigmaPlot (version 11.0, 2008), and statistical analyses were performed with SigmaPlot or Software R (version 3.6.1, 2019). Data were tested for normal distribution via Shapiro Wilk's test and homogeneity in variance via Levene's test. For parametric data, *t*-test (two-group comparison) was performed. For non-parametric data, Mann-Whitney *U* tests (two-group comparison) or Kruskal-Wallis (*H*) rank-sum tests (multiple group comparison) were conducted. Pairwise post hoc tests followed Kruskal-Wallis tests with Dunn's method given unequal sample size or Tukey method given equal sample sizes. P-values were adjusted with Holm-Bonferroni correction, and an $\alpha = 0.05$ was set as the significance level. Significant differences between ambient and elevated CO_2 treatments of shoots, roots, mesh bag, and bulk soil of the three plants for ^{15}N label and recovery in compartments, as well as for microbial biomass and colonization rates, were evaluated with t-test or Mann-Whitney *U* test. Differences between hyphae

in [a] *vs.* [e]CO_2 were assessed *via* the Kruskal-Wallis rank-sum test. For calculations of recovery and N budget negative values were set as zero and values over 100% were excluded.

Results

Aiming to identify the impact of elevated [e] CO_2 conditions on plants with varying microbial interactions to improve nutrient acquisition, we traced the transfer of ^{15}N labeled litter to plant (roots, leaves), fungal (root hyphae, soil hyphae), and soil compartments of *Silene acaulis*, *Medicago sativa* and *Festuca ovina* grown under ambient [a] and elevated [e] atmospheric CO_2.

Plant biomass, C- and N-contents and C:N ratio

The N- and C-content and the C:N ratio differed for all three plant species between plant organs (shoots, roots) and soils (bulk soil, mesh bag soil).

Festuca ovina had higher C- and N-content for shoots and roots under [a]CO_2, while for soils under [e]CO_2 conditions (Fig. S 3). The C:N ratio was higher under [a]CO_2 for roots and soils but similar for shoots under [a] and [e]CO_2 (Fig. S 3). Both root and shoot biomass increased under [e]CO_2 conditions, with about a doubling in root biomass under [e]CO_2 relative to [a]CO_2. Further, the root-to-shoot ratio of *F. ovina* increased under [e]CO_2 relative to [a]CO_2 levels (Fig. 1a).

Medicago sativa had higher C content for shoots and roots under [a]CO_2, while for soils it was higher under [e]CO_2 conditions (Fig. S 4). N content was higher under [a]CO_2 for shoots and tendentially for roots, while for soils it was higher under [e]CO_2. The C:N ratio tended to be higher for roots under [a]CO_2, for shoots under [e]CO_2, and for soils under [a]CO_2 conditions (Fig. S 4). Shoot biomass slightly increased under [e]CO_2 conditions, while root biomass was higher under [a]CO_2 relative to [e]CO_2 levels (Fig. 1b). Root-to-shoot ratio was higher under [a]CO_2 than under [e]CO_2 conditions (Fig. 1b). Further, it was observed that the number of nodules remained relatively constant under [a] and [e]CO_2, with slightly bigger nodules under [e]CO_2 (observation, no data). All nodules of *M. sativa* were active at the point of harvest, as indicated by the presence of leghaemoglobin.

Silene acaulis had a higher C content in roots under [a]CO_2 and tendentially for shoots (Fig. S 5). Conversely, C contents of soils were higher under [e]CO_2. N content was similar for roots, shoots, and bulk soil under [a] and [e] CO_2; only in the mesh bag soil it was higher under [e]CO_2 conditions. The C:N ratio was similar under [a] and [e] CO_2 (Fig. S 5). Shoot biomass of *S. acaulis* was slightly increased under [e]CO_2, while root biomass remained similar between [a] and [e]CO_2 levels (Fig. 1c). Further, no significant effect to root-to-shoot ratio was observed between [a] and [e]CO_2 conditions for *S. acaulis* (Fig. 1c).

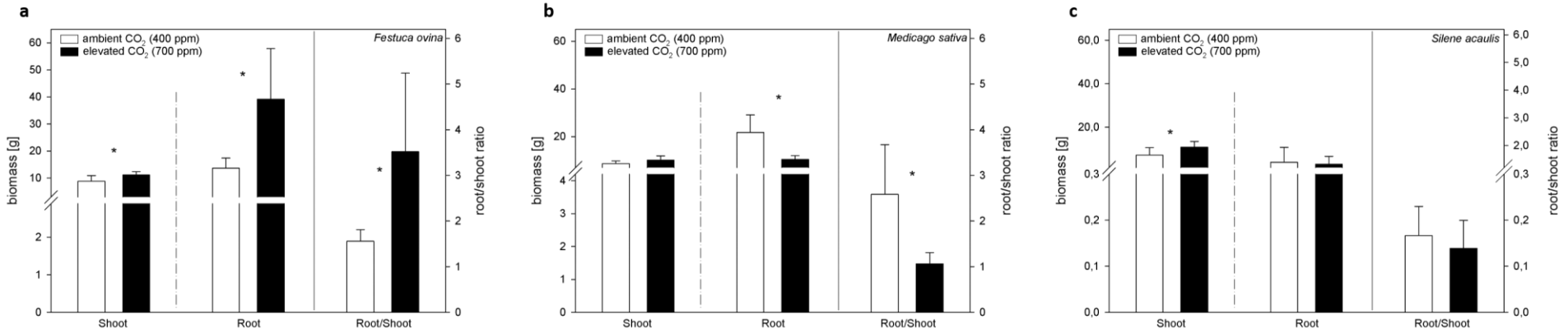

*Figure 1: Plant above- and belowground biomass [g]and root/ shoot ratio for Festuca ovina (a), Medicago sativa (b), and Silene acaulis (c), each with standard deviation. Significant differences between the ambient (white) and the elevated (black) CO_2 treatment are indicated by an asterisk *.*

Transfer and recovery of ^{15}N label and total N budgets

Label from the organic material in the mesh bag was detected in shoots and roots of all three plant species, with a trend of more ^{15}N label in shoots and roots under [e]CO_2 conditions (Fig. S 1). Total ^{15}N recovery was significantly higher under [e]CO_2 relative to [a]CO_2 for all three plant species (Table 1).

Table 1: Total ^{15}N recovered as percent (%) of input, given with standard deviation, for Festuca ovina, Medicago sativa, and Silene acaulis. Significant differences between the [a] and the [e]CO_2 conditions for the respective plant species are indicated by different superscripted small letters.

Festuca ovina		*Medicago sativa*		*Silene acaulis*	
Ambient CO_2	Elevated CO_2	Ambient CO_2	Elevated CO_2	Ambient CO_2	Elevated CO_2
48.8±7^{a}	71.0±16^{b}	40.1±10^{a}	80.8±8^{b}	57.6±8^{a}	77.5±10^{b}

Under [a]CO_2, more ^{15}N was recovered in shoots (~ 7%; $t = 2.35$, df = 22, $P = 0.028$), roots (~5%; $U = 33$, $P = 0.026$), and mesh bag soil (~ 87%; n.s.) than under [e]CO_2 for mycorrhizal *Festuca ovina* (shoot ~5%, root ~2%, mesh bag soil ~70%). For bulk soil, more ^{15}N was recovered under [e]CO2 (~23%; $U = 32.5$, $P = 0.019$) (Fig. 2a). For facultative mycorrhizal *Medicago sativa* more ^{15}N was recovered at harvest under [e]CO_2 in shoots (~4%; $t = -3.505$, df = 22, $P = 0.002$), roots (~5%; $U = 31$, $P = 0.017$) and bulk soil (~15%; $U = 13$, $P < 0.001$) than under ambient CO_2 (shoots ~2%, roots ~2%, bulk soil ~3%). For mesh bag soil, more ^{15}N was recovered at [a]CO_2 (~92%) than at [e]CO_2 (~78%; $U = 15$, $P = 0.001$) (Fig. 2 b). For weakly-mycorrhizal *Silene acaulis*, shoot (~ 16%; n.s.), root (~ 0.2) and bulk soil (~ 19%; $U = 21$, $P = 0.031$) had more ^{15}N recovered under [e]CO_2 relative to [a]CO_2 (shoot ~13%, root 0%, bulk soil ~6%) (Fig. 2c). Mesh bag soil had more ^{15}N recovered under [a]CO_2 (~81%; $t = 3.350$, df = 18, $P = 0.004$) than under [e]CO_2 (~65%).

Plants showed different patterns in total N budget in shoots and roots, while most total N was present in the bulk soil. *Festuca ovina* had equal amounts of total N in shoots (~ 1.6%; n.s.) under [a] and [e]CO_2, but more total N in roots (~4.3%; $U = 20$, $P = 0.003$), mesh bag soil (~ 2.6%; $t = -5.653$, $P < 0.001$), and bulk soil (~71%; $t = -5.799$, $P < 0.001$) under [e]CO_2 than under [a]CO_2 (roots ~ 2.6%, mesh bag soil ~2.1%, bulk soil ~45%) (Fig. 3a). *Medicago sativa* had more total N in shoots (~6%; $U = 6$, $P < 0.001$) and roots (~16%; $U = 0$, $P < 0.001$) under [a] then under [e]CO_2 (shoots ~4%, roots ~7%), while it was opposite for mesh bag ([a] ~ 2%, [e] ~3%; $t = -5.480$, $P < 0.001$) and bulk soil ([a] ~50% [e] ~76%; $t = 5.192$, $P < 0.001$) (Fig. 3b). *Silene acaulis* had more total N under [e] relative to [a]CO_2 levels for shoots ([a] ~ 3.9%, [e] ~5.2%; $U = 23$, $P = 0.045$), roots ([a] ~0.45%, [e] ~0.48%; n.s.), mesh bag soil ([a] ~2.2%, [e] ~ 2.4%; $t = -3.263$, $P = 0.004$) and bulk soil ([a] ~62%, [e] ~ 69%; n.s.) (Fig. 3c). As total N values were rather small for MBN and dissolved nitrogen (DN), these are given in Fig. S 2.

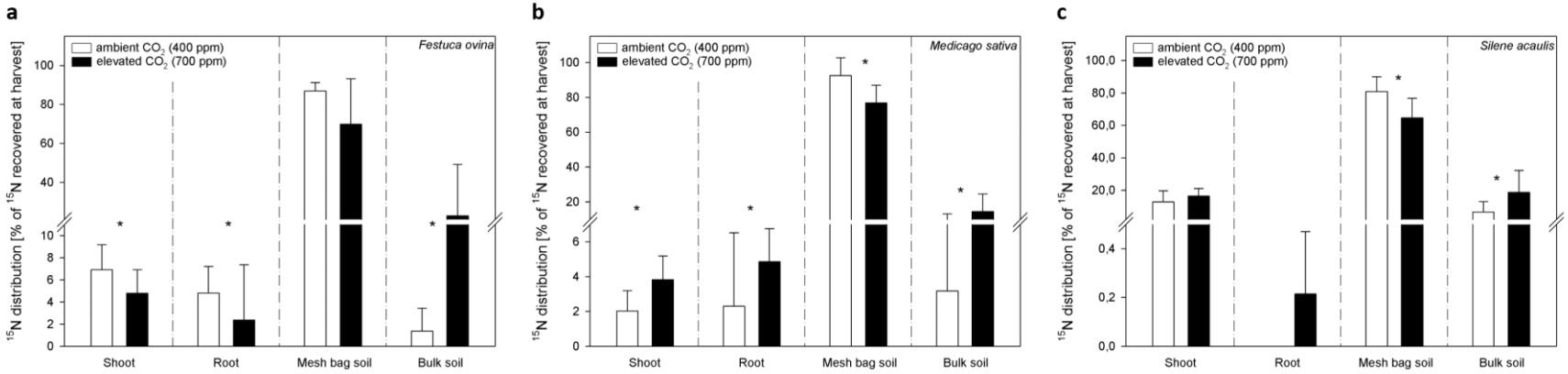

Figure 2: Recovery of total ^{15}N at harvest (% recovered) for shoots, roots, mesh bag soil and bulk soil of (a) Festuca ovina, (b) Medicago sativa, and (c) Silene acaulis, each with standard deviation. Significant differences between ambient (white, 400 ppm) and elevated (black, 700 ppm) CO_2 conditions are indicated by an asterisk.*

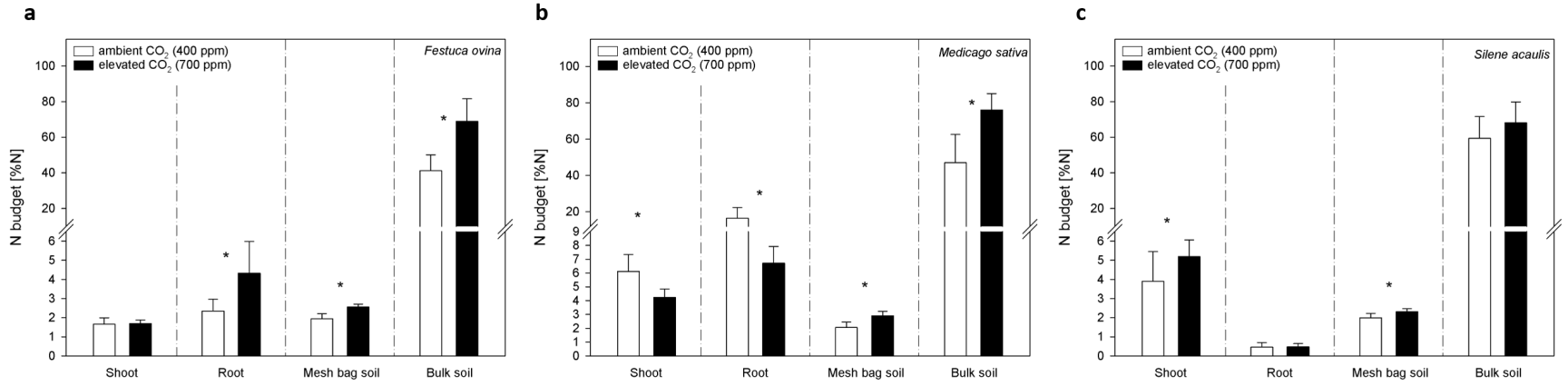

Figure 3: N budget [% total N] related to the unplanted controls for Festuca ovina (a), Medicago sativa (b), and Silene acaulis (c) shoots, roots, mesh bag soil, and bulk soil, each with standard deviation. Significant differences between [a]CO_2 (white) and [e]CO_2 (black) are indicated by an asterisk.*

Stable isotope patterns

Plant leaves were more $\delta^{13}C$-depleted under elevated CO_2 than under ambient CO_2 (Fig. S 6) for all three plant species. Patterns of $\delta^{15}N$ were relatively constant between ambient and elevated CO_2. *Medicago sativa* had lower $\delta^{15}N$ values (between ~5 to 10‰) than *Festuca ovina* and *Silene acaulis* (between 20 to 40‰). The same holds for plant roots, which were also more $\delta^{13}C$-depleted under elevated CO_2 than under ambient CO_2 (Figure S 7).

For soils, both bulk soil and mesh bag soil were more $\delta^{13}C$-depleted under elevated CO_2 than under ambient CO_2 (*F. ovina* bulk soil: $t = 6.137$, $df = 22$; $P < 0.001$; mesh bag soil: $U = 31.5$, $P = 0.021$; *M. sativa* bulk soil: t = 5.672, df = 22; $P < 0.001$; mesh bag soil: $U = 35.5$, $P = 0.04$; *S. acaulis* bulk soil: $U = 10$, $P = 0.003$; mesh bag soil: $t = 8.476$, $df = 18$, $P < 0.001$).

Hyphae isolated from *F. ovina roots* were mostly similarly ^{15}N-enriched between [a] and [e]CO_2 conditions, with highest values ~ 50‰ enrichment in $\delta^{15}N$ (Fig. 4a). Soil hyphae were more enriched in $\delta^{15}N$ under [a]CO_2 (~ 200‰) than under [e]CO_2 conditions ($H = 42.2$, $df = 7$, $P < 0.001$; Fig. 4d). Hyphae isolated from *Medicago sativa* roots had similar $\delta^{15}N$ values under [a] and [e]CO_2 conditions with highest values ~ 18‰ (Fig. 4b). Soil hyphae were more ^{15}N-enriched under [a]CO_2 (~ 195‰) than [e]CO_2 conditions ($H = 35.3$, $df = 7$, $P < 0.001$; Fig. 4e). Hyphae isolated from *S. acaulis* roots showed similar $\delta^{15}N$ values under [a] and [e]CO_2 conditions with highest values of ~ 22‰ and hyphae under elevated conditions showing a trend for higher ^{15}N-enrichment relative to ambient CO_2 conditions (Fig. 4c). The ^{13}C-enrichment of root hyphae was tendentially a little higher under [a]CO_2. Soil hyphae were more ^{15}N-enriched under [a]CO_2 (~ 180‰) than under [e]CO_2 conditions ($H = 34.6$, $df = 7$, $P < 0.001$; Fig. 4f). N-content of root and soil hyphae tended to be higher under [e]CO_2 concentrations than under [a]CO_2 concentrations (Fig. S 8), and root hyphae always had higher N-content relative to roots of all three plant species (Fig. S 9).

Microbial biomass C and N

A broadening of the MBC:MBN ratio with increasing CO_2 was visible for all three plant species microbial biomass in bulk and mesh bag soil.

Festuca ovina had lower MBC under [e]CO_2 in mesh bag soil ($t = 5.592$, $df = 22$, $P < 0.001$) and similar content for bulk soil under [a] and [e]CO_2. For MBN content this was higher under [a]CO_2 than under [e]CO_2 for both bulk ($t = 9.166$, $df = 22$, $P < 0.001$) and mesh bag soil ($U = 2.0$, $P < 0.001$), while MBC:MBN was higher under [e]CO_2 for bulk soil ($U = 0$; $P < 0.001$) and for mesh bag soil ($t = -2.853$, $df = 22$, $P = 0.009$; Fig. 5a).

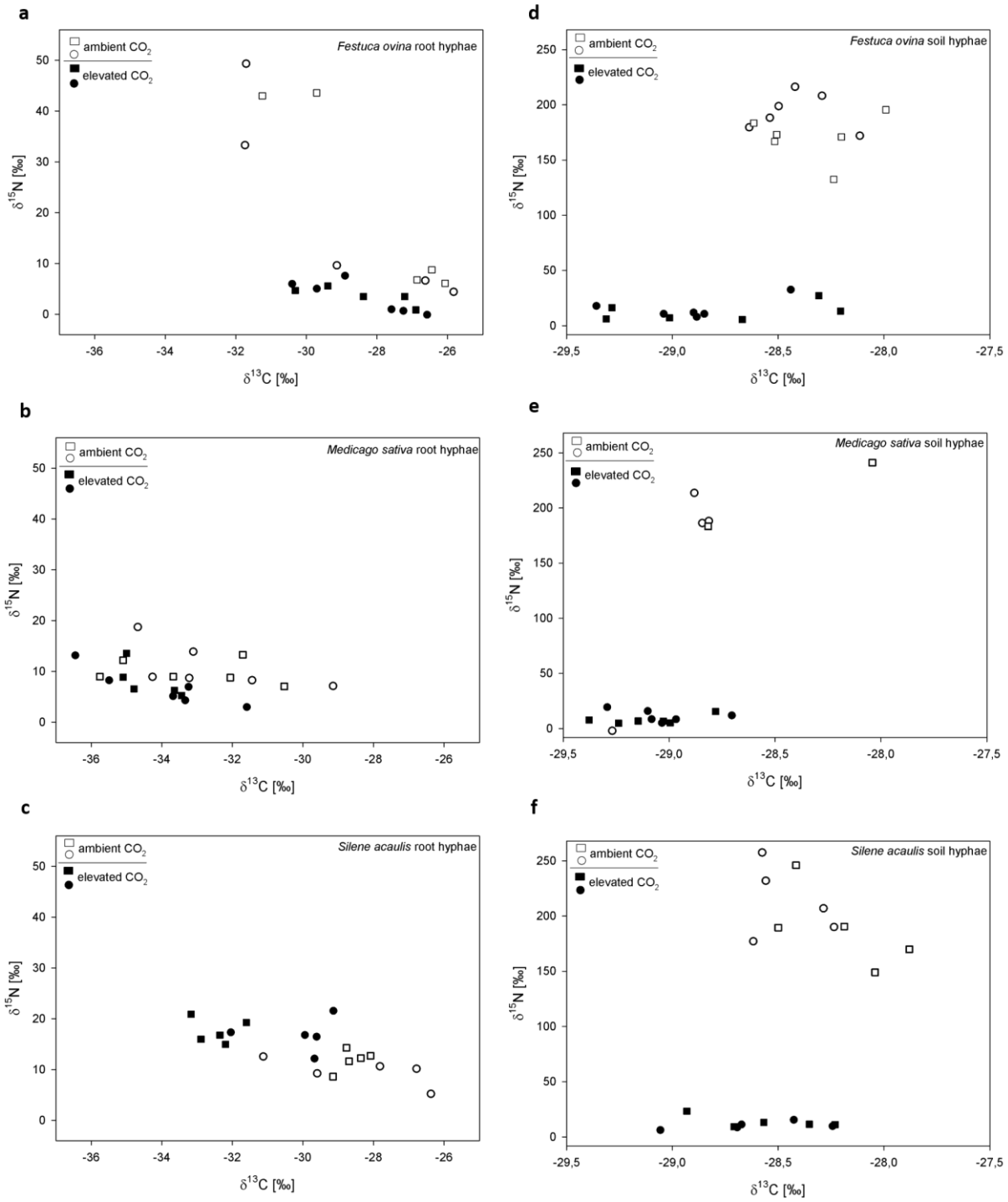

Figure 4: Dual isotope scatter plot of ^{15}N and ^{13}C values of root and soil hyphae of Festuca ovina (a, d), Medicago sativa (b, e), and Silene acaulis (c, f). White symbols indicate ambient CO_2 conditions (400 ppm), black symbols indicate elevated CO_2 conditions (700 ppm). Squares depict treatments with hyphal access to labeled litter, while circles depict treatments with hyphal exclusion from labeled litter.

Medicago sativa had similar MBC contents under [a] and [e]CO_2 for mesh bag soil, while higher MBC under [a]CO_2 for both bulk soil (t = 2.469, df = 22, P = 0.022; Fig. 5b). Microbial biomass N was higher for the [a]CO_2 treatment for both bulk soil (t = 5.978, df = 22; P < 0.001) and mesh bag soil relative to the [e]CO_2 treatment (t = 2.112, df = 22, P = 0.046). The MBC:MBN ratio was higher under [e]CO_2 conditions for bulk soil (t = -3.488, df = 22; P = 0.002) and for mesh bag soil (U = 23.0; P = 0.005; Fig. 5b).

Silene acaulis had higher MBC and MBN contents under [a]CO_2 than under [e]CO_2 for bulk (MBC: U = 0; P < 0.001; MNB: U = 6.0, P = 0.002) and mostly mesh bag soil (MBC: t = 3.597, df = 18, P = 0.002; Fig. 5c). Conversely, the MBC:MBN ratio was higher under [e]CO_2 for bulk soil (U = 11.0, P = 0.006) and by trend also for mesh bag soil (Fig. 5c).

Mycorrhizal colonization

Mycorrhizal colonization measured in terms of the presence of AM fungal structures (arbuscules, hyphae, vesicles) increased under [e]CO_2 conditions in roots of all three plant species. Mycorrhizal *F. ovina* increased its colonization rate from 79% ± 17 under [a]CO_2 to 85% ± 11 under [e]CO_2, while facultative mycorrhizal *M. sativa* increased from 57% ± 12 under [a]CO_2 to 60% ± 14 under [e]CO_2 conditions. Under [a]CO_2 conditions, weakly-mycorrhizal *S. acaulis* had a colonization rate of 13% ± 5, which increased statistically significant (t = -2.567, df = 18, P = 0.019) to 21% ± 9 under [e]CO_2.

Biomass of soil hyphae measured as dry weight after isolation from soil slightly increased under [e]CO_2 for *F. ovina* (from 0.1 to 0.2 mg/g soil). At the same time, it decreased slightly under [e]CO_2 relative to [a]CO_2 for *M. sativa* (from 0.2 to 0.1 mg/g soil). Soil hyphae biomass remained relatively similar under [a] and [e]CO_2 conditions for *S. acaulis* (both 0.2 mg/g soil).

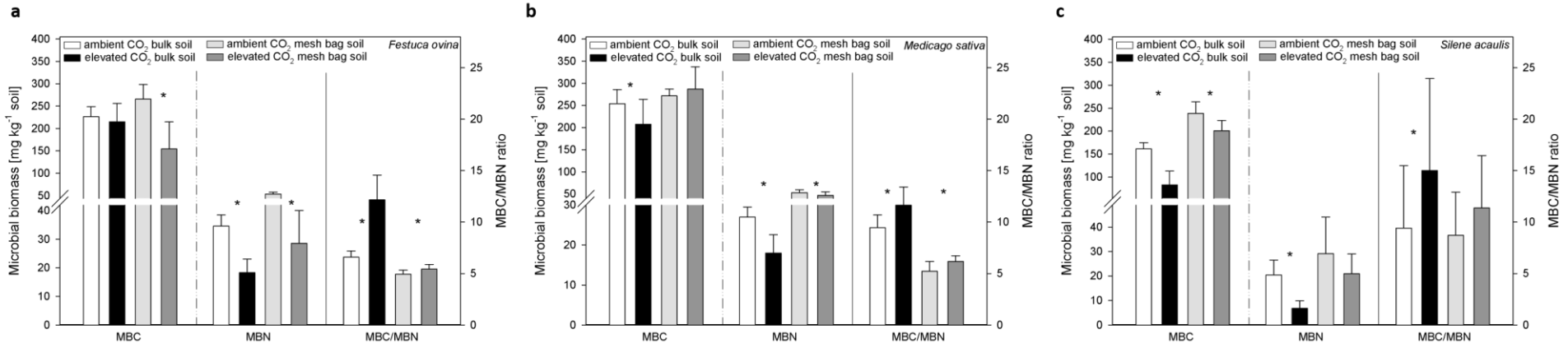

*Figure 5: Microbial biomass carbon (MBC), microbial biomass nitrogen (MBN), and MBC/MBN ratio of bulk soil and mesh bag soil of Festuca ovina (a), Medicago sativa (b), and Silene acaulis (c), each with standard deviation. Statistically significant differences between the ambient CO_2 treatment (white for bulk soil, light grey for mesh bag soil) and the elevated CO_2 treatment (black for bulk soil, dark grey for mesh bag soil) are indicated by an asterisk *.*

Discussion

We analyzed the response of plants with different nutrient microbial interactions to acquire nutrients to elevated CO_2 conditions. Despite different nutrient acquisition strategies, the response of plants remained remarkably similar, benefitting more from soil nutrients than soil microorganisms. Thus, a progressive nutrient limitation was not confirmed for plants, but soil microorganisms suffered from nutrient scarcity. These results highlight the need to account for all (eco)system constituents when addressing the effects of [e]CO_2 and climate change.

Response of soil microorganisms

Soil microorganisms were found N-limited under [e]CO_2 conditions and slowed down their activity and decomposition processes as visible in decreasing MBN values and a widening of the MBC:MBN ratio. The higher remains of labeled litter in the mesh bag soil further support this deceleration of microbial activity under [e]CO_2 conditions. Considered together with a higher ^{15}N label in bulk soil under [e]CO_2, it appears that at elevated CO_2 conditions, immobilization of N in soil occurs, as Johnson (2006) described for forest systems in which N becomes accumulated in the soil and the forest floor (see also Graaff *et al.*, 2007). Manzoni *et al.* (2010) further described an initial nutrient immobilization in litters by microorganisms in nutrient-poor systems accompanied by a reduced C use efficiency of the decomposers. This nutrient immobilization prevails until a critical value of the nutrient concentrations is reached (Manzoni *et al.*, 2010). Additionally, elevated CO_2 frequently results in a reduction of inorganic N due to altered activity of microbes, causing increased C losses (Manzoni *et al.*, 2010) and likely a reduced availability of NH_4^+ for plants, which was found a preferred plant N-source under elevated CO_2 (Cheng *et al.*, 2012).

Thus, while the accumulation and/or immobilization of nutrients in microbial tissues and soil under [e]CO_2 conforms with the PNL hypothesis (Luo *et al.*, 2004; Johnson, 2006), the three plant species of our study were not yet found to suffer from nutrient limitation severely. While this effect might occur after a longer duration of the experiment (see Johnson, 2006), we suppose that the spatial limitation in our pot experiment likely accelerated the reaching of the reversal point from nutrient gain benefit to PNL-driven nutrient limitation (cf. Johnson, 2006).

Response of plant species

As frequently described in the literature (Zak *et al.*, 2000; Ainsworth & Long, 2005; Johnson, 2006), exposure to [e]CO_2 resulted in a positive effect on plant biomass (shoots, roots variable), likely attributed to a kind of CO_2 fertilization effect (Norby *et al.*, 2009; Zhu *et al.*, 2017). Interestingly, all three plant species appeared to invest the surplus in C into plant-own nutrient acquisition from soil and out-competed microorganisms. This finding contrasts with the PNL hypothesis and the

assumption of plants being the losers in the competition with microbes for soil nutrients (Luo *et al.*, 2004; Johnson, 2006). The ability of plants to out-compete soil microorganisms for nutrients was described by Schimel & Bennett (2004), who highlighted the association with mycorrhizal fungi and access to microsites as prominent reasons for plants' success over microbes (see also McClain *et al.*, 2003). The colonization with AM fungi tended to increase for all plant species under [e]CO_2, and hyphae likely serve as an elongation of plant roots to support nutrient access. Thereby, they contribute to plants' out-competition of soil microbes (Schimel & Bennett, 2004). This finding agrees with (Zhu *et al.*, 2017), whose model estimates taking enzyme-substrate relations into account predict the ability of plants to out-compete microbes and suppress microbial nutrient acquisition in topsoils.
Alternatively, microbial immobilization of N under [e]CO_2 (cf. Johnson, 2006; Graaff *et al.*, 2007, for wheat) may be a trial of microbes to protect N from plants and AMF. Both plants and AMF mainly rely on the uptake of N from the soil solution. Thus immobile N would accumulate and starve the microbial biomass with time, as plants and/or AMF rapidly take up every N released to the soil solution.

The finding of a decrease in root biomass of legume *Medicago sativa* under [e]CO_2 was surprising, as frequently positive responses of legumes towards [e]CO_2 were reported (e.g. Temperton *et al.*, 2003; Karthikeyan, 2017). However, Arnone (1999) described that this positive response of legumes towards [e]CO_2 is not always consistent. Thus, despite showing similar patterns in out-competing soil microbes for soil nutrients, the benefit to the three different plant species appears variable, with *Festuca ovina* showing the highest benefit in biomass growth, followed by *Silene acaulis* and *Medicago sativa.*

All three plant species showed a decrease in biomass C- and N-content with [e]CO_2, despite a trend to positive responses of biomass yield. Johnson (2006) described the presence of lower tissue N for forest trees exposed to elevated CO_2 levels while establishing greater biomass or an increase in N uptake. Further, Taub & Wang (2008) found a decreased plant tissue N-content under [e]CO_2 due to dilution by biomass increase, decreases in transpiration, changes in root architecture, and an increase in N losses. They described that under [e]CO_2 an improved photosynthetic N use efficiency together with the downregulation of photosynthetic enzymes reduces the plant N demand and thus root N uptake (Taub & Wang, 2008). In addition, increasing concentrations of photosynthesis-derived compounds and increased C assimilation cause an N dilution in plant tissues (Long *et al.*, 2004; Norby & Iversen, 2006; Taub & Wang, 2008), which often results in reduced plant tissue N-contents under [e]CO_2.

An efficiently functioning photosynthesis is supported by stable isotope patterns of leaves and roots. While ^{15}N values remained relatively constant, the more depleted ^{13}C values under [e]CO_2 indicate open stomata (Dawson *et al.*, 2002; Fry, 2008) and utilization of CO_2 available in the atmosphere. The lower ^{15}N values found for the legume *Medicago sativa* suit patterns typically described for legumes performing N-fixation of atmospheric air (Fry, 2008; Peoples *et al.*, 2015), with likely some additional N gain from the soil.

Response of associated microorganisms/mycorrhizal fungi

Other than soil microorganisms, root-associated mycorrhizal fungi did not suffer from N-limitation, as indicated by an increasing N-content of hyphae under [e]CO_2, while MBN generally decreased. Hyphae appear to function as elongation of the plant root, while priming of soil microorganisms seems to be negligible. This finding of plants' support of associated mycorrhizal fungi agrees with Drigo *et al.* (2010), who described a rapid transfer of photosynthetically processed C to arbuscular mycorrhizal fungi. Whether a gradual liberation of C via priming of soil microorganisms (cf. Drigo *et al.*, 2010) occurs cannot be conclusively stated but seems to be of a relatively minor extent. Thus, it appears that the association with mycorrhizal fungi supports the competitive advantage of plants over soil microbes under [e]CO_2 in our study and conforms with Schimel & Bennett (2004) and McClain *et al.* (2003).

Contrary to root-associated, mycorrhizal fungi, the community of soil fungi appeared to suffer from N-limitation similarly to the other soil microbes under [e]CO_2 concentrations, as indicated by lower $\delta^{15}N$ values under [e]CO_2 than under [a]CO_2 concentrations. Thus, the activity of soil fungi appears to decelerate with [e]CO_2 relative to [a]CO_2, likely resulting in limited inorganic N availability and a subsequent reduction of the C use efficiency of decomposing microorganisms (cf. Manzoni *et al.*, 2010).

Conclusion

Our results provide clear evidence for plants' greater nutritional benefit under [e]CO_2 conditions compared to soil microorganisms, while associated mycorrhizal fungi are not affected. This highlights the need to consider all constituents of a system in predictions for climate change scenarios, as a positive effect on plant yield or mycorrhizal growth may conversely cause soil microorganisms' restrictions by nutrient limitation.

Acknowledgements

We thank Ilse Thaufelder for technical support with the climate control chamber. Many thans to the BayCEER Laboratory of Isotope Biogeochemistry (University of Bayreuth, Germany) for stable isotope analyses. This project was funded by the German Research Foundation (DFG): PA 2377/2-1GU 1309/5-1 "Towards a predictive understanding on how mycorrhizal types influence the decomposition of soil organic matter".

References

Ainsworth EA, Long SP. 2005. What have we learned from 15 years of free-air CO_2 enrichment (FACE)? A meta-analytic review of the responses of photosynthesis, canopy properties and plant production to rising CO_2. *New Phytologist* **165**: 351–371.

Alberton O, Kuyper TW, Gorissen A. 2005. Taking mycocentrism seriously: mycorrhizal fungal and plant responses to elevated CO_2. *New Phytologist* **167**: 859–868.

Arnone JA. 1999. Symbiotic N_2 fixation in a high Alpine grassland: effects of four growing seasons of elevated CO_2. *Functional Ecology* **13**: 383–387.

Arnone JA, Gordon JC. 1990. Effect of nodulation, nitrogen fixation and CO_2 enrichment on the physiology, growth and dry mass allocation of seedlings of *Alnus rubra* Bong. *New Phytologist* **116**: 55–66.

Brundrett M, Bougher N, Dell B, Grove T, Malajczuk N. 1996. Working with Mycorrhizas in Forestry and Agriculture. *ACIAR Monograph 32. Australian Centre for International Agricultural Research, Canberra*.

Brundrett M, Melville L, Peterson L. 1994. Extraction and staining of hyphae from soil. In: Brundrett M, ed. *Practical methods in mycorrhizal research*. Waterloo: Mycologue Publications, 71–80.

Cheeke TE, Phillips RP, Kuhn A, Rosling A, Fransson P. 2021. Variation in hyphal production rather than turnover regulates standing fungal biomass in temperate hardwood forests. *Ecology* **102**: e03260.

Cheng L, Booker FL, Tu C, Burkey KO, Zhou L, Shew HD, Rufty TW, Hu S. 2012. Arbuscular mycorrhizal fungi increase organic carbon decomposition under elevated CO_2. *Science (New York, N.Y.)* **337**: 1084–1087.

Dakora FD, Phillips DA. 2002. Root exudates as mediators of mineral acquisition in low-nutrient environments. In: Adu-Gyamfi JJ, ed. *Food Security in Nutrient-Stressed Environments: Exploiting Plants' Genetic Capabilities*. Dordrecht: Springer Netherlands, 201–213.

Dawson TE, Mambelli S, Plamboeck AH, Templer PH, Tu KP. 2002. Stable Isotopes in Plant Ecology. *Annual Review of Ecology and Systematics* **33**: 507–559.

Deeb A, French A, Heiss J, Jabbour, J., LaRochelle, D., Levintanus A, Kontorov A, Markku R, Sanchez Martinez G, McKeown R, Paus N *et al.* 2011. Climate Change Starter's Guidebook: An Issues Guide for Education Planners and Practitioners. *UNEP*.

Dixon RK, Solomon AM, Brown S, Houghton RA, Trexier MC, Wisniewski J. 1994. Carbon pools and flux of global forest ecosystems. *Science (New York, N.Y.)* **263**: 185–190.

Drigo B, Pijl AS, Duyts H, Kielak AM, Gamper HA, Houtekamer MJ, Boschker HTS, Bodelier PLE, Whiteley AS, van Veen JA *et al.* 2010. Shifting carbon flow from roots into associated microbial communities in response to elevated atmospheric CO_2. *Proceedings of the National Academy of Sciences of the United States of America* **107**: 10938–10942.

Finzi AC, DeLucia EH, Hamilton JG, Richter DD, Schlesinger WH. 2002. The nitrogen budget of a pine forest under free air CO_2 enrichment. *Oecologia* **132**: 567–578.

Fitter AH, Heinemeyer A, Staddon PL. 2000. The impact of elevated CO_2 and global climate change on arbuscular mycorrhizas: a mycocentric approach. *New Phytologist* **147**: 179–187.

Fransson PMA, Taylor AFS, Finlay RD. 2005. Mycelial production, spread and root colonisation by the ectomycorrhizal fungi *Hebeloma crustuliniforme* and *Paxillus involutus* under elevated atmospheric CO_2. *Mycorrhiza* **15**: 25–31.

Frey SD. 2019. Mycorrhizal Fungi as Mediators of Soil Organic Matter Dynamics. *Annual Review of Ecology, Evolution, and Systematics* **50**: 237–259.

Fry B. 2008. Stable Isotope Ecology. New York: Springer.

Graaff M-A de, **Six J, van Kessel C. 2007.** Elevated CO_2 increases nitrogen rhizodeposition and microbial immobilization of root-derived nitrogen. *New Phytologist* **173**: 778–786.

Iversen CM. 2010. Digging deeper: fine-root responses to rising atmospheric CO concentration in forested ecosystems. *The New phytologist* **186**: 346–357.

Jackson RB, Cook CW, Pippen JS, Palmer SM. 2009. Increased belowground biomass and soil CO_2 fluxes after a decade of carbon dioxide enrichment in a warm-temperate forest. *Ecology* **90**: 3352–3366.

Jenkinson DS. 1988. Determination of microbial biomass carbon and nitrogen in soil. *Advances in nitrogen cycling*: 368–386.

Jenkinson DS, Powlson DS. 1976. The effects of biocidal treatments on metabolism in soil - V: a method for measuring soil biomass. *Soil Biology and Biochemistry* **8**: 209–213.

Joergensen RG. 1996. The fumigation-extraction method to estimate soil microbial biomass: Calibration of the kEC value. *Soil Biology and Biochemistry* **28**: 25–31.

Johnson DW. 2006. Progressive N limitation in forests: review and implications for long-term responses to elevated CO_2. *Ecology* **87**: 64–75.

Jumpponen A. 2001. Dark septate endophytes - are they mycorrhizal? *Mycorrhiza* **11**: 207–211.

Karthikeyan A. 2017. Impact of elevated CO_2 in *Casuarina equisetifolia* rooted stem cuttings inoculated with *Frankia*. *Symbiosis* **72**: 89–94.

Klink S, Giesemann P, Hubmann T, Pausch J. 2020. Stable C and N isotope natural abundances of intraradical hyphae of arbuscular mycorrhizal fungi. *Mycorrhiza* **30**: 773–780.

Kuzyakov Y, Horwath WR, Dorodnikov M, Blagodatskaya E. 2019. Review and synthesis of the effects of elevated atmospheric CO_2 on soil processes: No changes in pools, but increased fluxes and accelerated cycles. *Soil Biology and Biochemistry* **128**: 66–78.

Lindner M, Maroschek M, Netherer S, Kremer A, Barbati A, Garcia-Gonzalo J, Seidl R, Delzon S, Corona P, Kolström M *et al.* 2010. Climate change impacts, adaptive capacity, and vulnerability of European forest ecosystems. *Forest Ecology and Management* **259**: 698–709.

Long SP, Ainsworth EA, Rogers A, Ort DR. 2004. Rising atmospheric carbon dioxide: plants FACE the future. *Annual review of plant biology* **55**: 591–628.

Luo Y, Su BO, Currie WS, Dukes JS, Finzi A, Hartwig U, Hungate B, Mc Murtrie RE, Oren RA, Parton WJ *et al.* 2004. Progressive Nitrogen Limitation of Ecosystem Responses to Rising Atmospheric Carbon Dioxide. *BioScience* **54**: 731.

Manzoni S, Trofymow JA, Jackson RB, Porporato A. 2010. Stoichiometric controls on carbon, nitrogen, and phosphorus dynamics in decomposing litter. *Ecological Monographs* **80**: 89–106.

McClain ME, Boyer EW, Dent CL, Gergel SE, Grimm NB, Groffman PM, Hart SC, Harvey JW, Johnston CA, Mayorga E *et al.* 2003. Biogeochemical Hot Spots and Hot Moments at the Interface of Terrestrial and Aquatic Ecosystems. *Ecosystems* **6**: 301–312.

Nie M, Lu M, Bell J, Raut S, Pendall E. 2013. Altered root traits due to elevated CO_2: a meta-analysis. *Global Ecology and Biogeography* **22**: 1095–1105.

NOAA. 2021. National Oceanic and Atmospheric Administration report.

Norby R, Warren J, Iversen C, Garten C, Medlyn B, McMurtrie R. 2009. CO_2 Enhancement of Forest Productivity Constrained by Limited Nitrogen Availability. *Nature Precedings*: 1.

Norby RJ, Iversen CM. 2006. Nitrogen uptake, distribution, turnover, and efficiency of use in a CO_2-enriched sweetgum forest. *Ecology* **87**: 5–14.

Oren R, Ellsworth DS, Johnsen KH, Phillips N, Ewers BE, Maier C, Schäfer KV, McCarthy H, Hendrey G, McNulty SG *et al.* 2001. Soil fertility limits carbon sequestration by forest ecosystems in a CO_2-enriched atmosphere. *Nature* **411**: 469–472.

Paterson E, Sim A, Davidson J, Daniell TJ. 2016. Arbuscular mycorrhizal hyphae promote priming of native soil organic matter mineralisation. *Plant and Soil* **408**: 243–254.

Pausch J, Loeppmann S, Kühnel A, Forbush K, Kuzyakov Y, Cheng W. 2016. Rhizosphere priming of barley with and without root hairs. *Soil Biology and Biochemistry* **100**: 74–82.

Pausch J, Zhu B, Kuzyakov Y, Cheng W. 2013. Plant inter-species effects on rhizosphere priming of soil organic matter decomposition. *Soil Biology and Biochemistry* **57**: 91–99.

Pecl GT, Araújo MB, Bell JD, Blanchard J, Bonebrake TC, Chen I-C, Clark TD, Colwell RK, Danielsen F, Evengård B *et al.* 2017. Biodiversity redistribution under climate change: Impacts on ecosystems and human well-being. *Science (New York, N.Y.)* **355**.

Peoples MB, Chalk PM, Unkovich MJ, Boddey RM. 2015. Can differences in ^{15}N natural abundance be used to quantify the transfer of nitrogen from legumes to neighbouring non-legume plant species? *Soil Biology and Biochemistry* **87**: 97–109.

Phillips JM, Hayman DS. 1970. Improved procedures for clearing roots and staining parasitic and vesicular-arbuscular mycorrhizal fungi for rapid assessment of infection. *Transactions of the British mycological Society*: 158–161.

Phillips RP, Meier IC, Bernhardt ES, Grandy AS, Wickings K, Finzi AC. 2012. Roots and fungi accelerate carbon and nitrogen cycling in forests exposed to elevated CO_2. *Ecology letters* **15**: 1042–1049.

Piñeiro J, Ochoa-Hueso R, Delgado-Baquerizo M, Dobrick S, Reich PB, Pendall E, Power SA. 2017. Effects of elevated CO_2 on fine root biomass are reduced by aridity but enhanced by soil nitrogen: A global assessment. *Scientific reports* **7**: 15355.

Pritchard SG, Strand AE, McCormack ML, Davis MA, Oren R. 2008. Mycorrhizal and rhizomorph dynamics in a loblolly pine forest during 5 years of free-air-CO_2 -enrichment. *Global Change Biology* **14**: 1252–1264.

Rouhier H, Read DJ. 1998. The role of mycorrhiza in determining the response of *Plantago lanceolata* to CO_2 enrichment. *The New phytologist* **139**: 367–373.

Schimel JP, Bennett J. 2004. Nitrogen mineralization: Challenges of a changing paradigm. *Ecology* **85**: 591–602.

Schlesinger WH, Lichter J. 2001. Limited carbon storage in soil and litter of experimental forest plots under increased atmospheric CO_2. *Nature* **411**: 466–469.

Schussler A, Walker C. 2010. *The Glomeromycota* A species list with new families and new genera.

Smith SE, Read DJ. 2010. Mycorrhizal Symbiosis. Academic Press.

Szulejko JE, Kumar P, Deep A, Kim K-H. 2017. Global warming projections to 2100 using simple CO_2 greenhouse gas modeling and comments on CO_2 climate sensitivity factor. *Atmospheric Pollution Research* **8**: 136–140.

Taub DR, Wang X. 2008. Why are nitrogen concentrations in plant tissues lower under elevated CO_2? A critical examination of the hypotheses. *Journal of integrative plant biology* **50**: 1365–1374.

Temperton VM, Grayston SJ, Jackson G, Barton CVM, Millard P, Jarvis PG. 2003. Effects of elevated carbon dioxide concentration on growth and nitrogen fixation in *Alnus glutinosa* in a long-term field experiment. *Tree physiology* **23**: 1051–1059.

Treseder KK. 2004. A meta-analysis of mycorrhizal responses to nitrogen, phosphorus, and atmospheric CO_2 in field studies. *The New phytologist* **164**: 347–355.

UKCIP. 2011. Making progress. UKCIP and adaptation in the UK. *UK climate impacts programme*: 23–26.

Vance ED, Brookes PC, Jenkinson DS. 1987. An extraction method for measuring soil microbial biomass C. *Soil Biology and Biochemistry* **19**: 703–707.

Verbruggen E, Pena R, Fernandez CW, Soong JL. 2017. Mycorrhizal Interactions With Saprotrophs and Impact on Soil Carbon Storage. In: *Mycorrhizal Mediation of Soil*. Elsevier, 441–460.

Vierheilig H, Schweiger P, Brundrett M. 2005. An overview of methods for the detection and observation of arbuscular mycorrhizal fungi in roots+. *Physiologia Plantarum* **0**: 051021083431001-???

Yanai RD, Fahey TJ, Miller SL. 1995. Efficiency of Nutrient Acquisition by Fine Roots and Mycorrhizae. In: *Resource Physiology of Conifers, 1995*, 75–103.

Zak DR, Pregitzer KS, King JS, Holmes WE. 2000. Elevated atmospheric CO_2, fine roots and the response of soil microorganisms: a review and hypothesis. *New Phytologist* **147**: 201–222.

Zhu Q, Riley WJ, Tang J. 2017. A new theory of plant-microbe nutrient competition resolves inconsistencies between observations and model predictions. *Ecological applications : a publication of the Ecological Society of America* **27**: 875–886.

Supporting Information

Plants benefit more from elevated CO_2 in terms of nutrient acquisition than microbes despite different plant-microbial interactions

Authors: **Saskia Klink**, Adrienne B. Keller, Richard P. Phillips, Matthias Gube, Johanna Pausch

The following Supporting Information is available for this article:

Fig. S1: ^{15}N content (in mg ^{15}N per pot) in shoots, roots, mesh bag soil and bulk soil of *Festuca ovina* (a), *Medicago sativa* (b) and *Silene acaulis* (c), respectively.

Fig. S2: N budget [% total N] of MBN and dissolved nitrogen (DN) in mesh bag soil and bulk soil of *Festuca ovina* (a), *Medicago sativa* (b), and *Silene acaulis* (c).

Fig. S3: N-content [mmol g dwt^{-1}] (a), C- content [mmol g dwt^{-1}] (b) and C:N ratio (c) of *Festuca ovina* shoots, roots, mesh bag soil and bulk soil.

Fig. S4: N-content [mmol g dwt^{-1}] (a), C- content [mmol g dwt^{-1}] (b) and C:N ratio (c) of *Medicago sativa* shoots, roots, mesh bag soil and bulk soil.

Fig. S5: N-content [mmol g dwt^{-1}] (a), C- content [mmol g dwt^{-1}] (b) and C:N ratio (c) of *Silene acaulis* shoots, roots, mesh bag soil and bulk soil.

Fig. S6: Dual isotope scatter plot of stable isotope patterns of ^{13}C and ^{15}N for leaves of *Festuca ovina* (a), *Medicago sativa* (b) and *Silene acaulis* (c), respectively.

Fig. S7: Dual isotope scatter plot of stable isotope patterns of ^{13}C and ^{15}N for roots of *Festuca ovina* (a), *Medicago sativa* (b) and *Silene acaulis* (c), respectively.

Fig. S8: N-content [mmol g dwt^{-1}] of root and soil hyphae of *Festuca ovina* (a), *Medicago sativa* (b) and *Silene acaulis* (c), respectively.

Fig. S9: N-content [mmol g dwt^{-1}] of roots and root hyphae of *Festuca ovina* (a), *Medicago sativa* (b) and *Silene acaulis* (c), respectively.

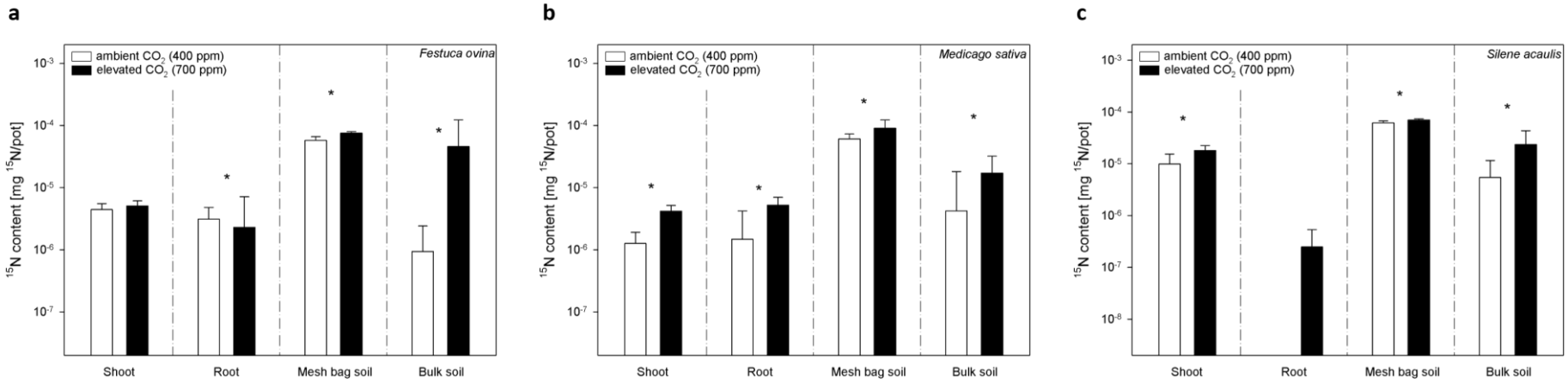

Fig. S1: ^{15}N content (in mg ^{15}N per pot) in shoots, roots, mesh bag soil and bulk soil of Festuca ovina (a), Medicago sativa (b) and Silene acaulis (c), respectively. Significant differences between ambient (white) and elevated CO_2 (black) treatments are indicated by an asterisk

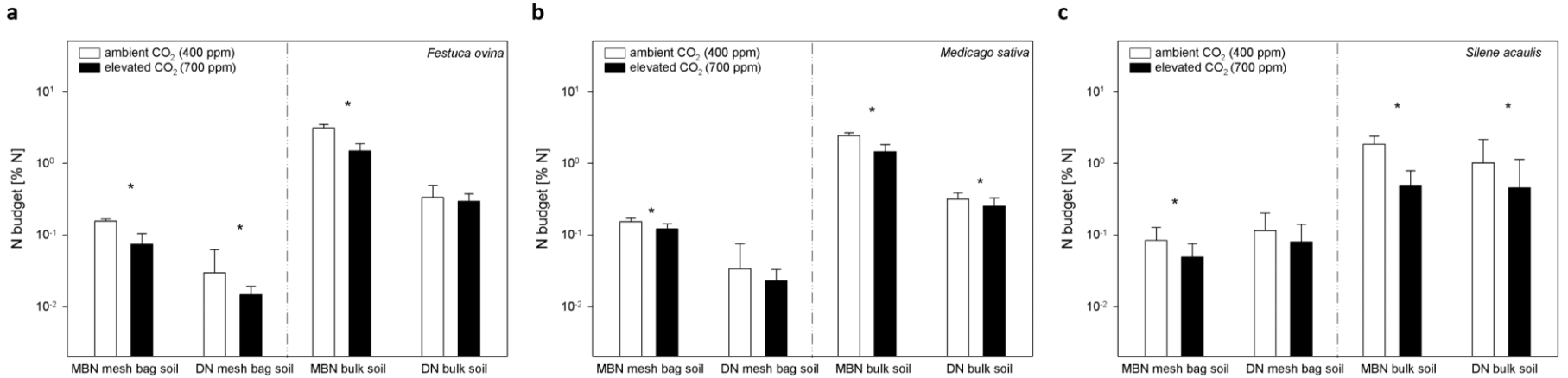

Fig. S2: N budget [% total N] of MBN and dissolved nitrogen (DN) in mesh bag soil and bulk soil of Festuca ovina (a), Medicago sativa (b), and Silene acaulis (c).Significant differences between ambient (white) and elevated (black) CO_2 levels are indicated by an asterisk.*

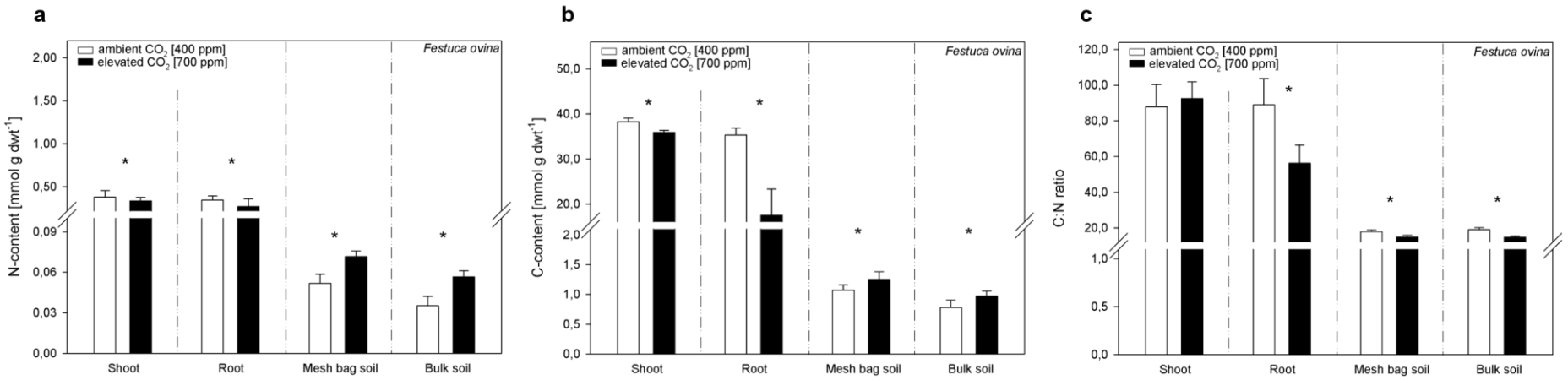

*Fig. S3: N-content [mmol g dwt^{-1}] (a), C- content [mmol g dwt^{-1}] (b) and C:N ratio (c) of Festuca ovina shoots, roots, mesh bag soil and bulk soil. Significant differences between the ambient CO_2 treatment (white) and the elevated CO_2 treatment (black) are indicated by an asteriks *.*

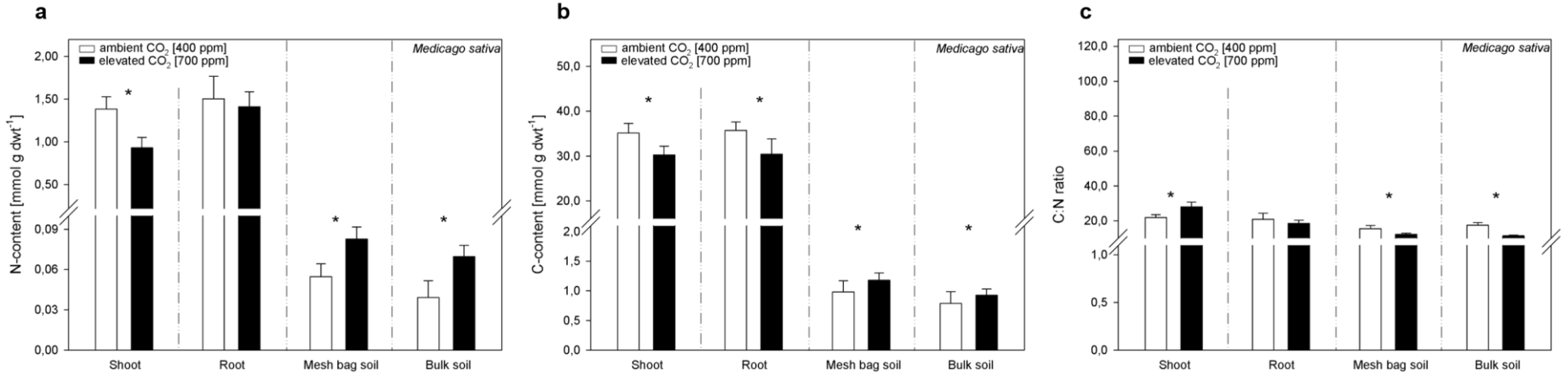

*Fig. S5: N-content [mmol g dwt^{-1}] (a), C- content [mmol g dwt^{-1}] (b) and C:N ratio (c) of Medicago sativa shoots, roots, mesh bag soil and bulk soil. Significant differences between the ambient CO_2 treatment (white) and the elevated CO_2 treatment (black) are indicated by an asteriks *.*

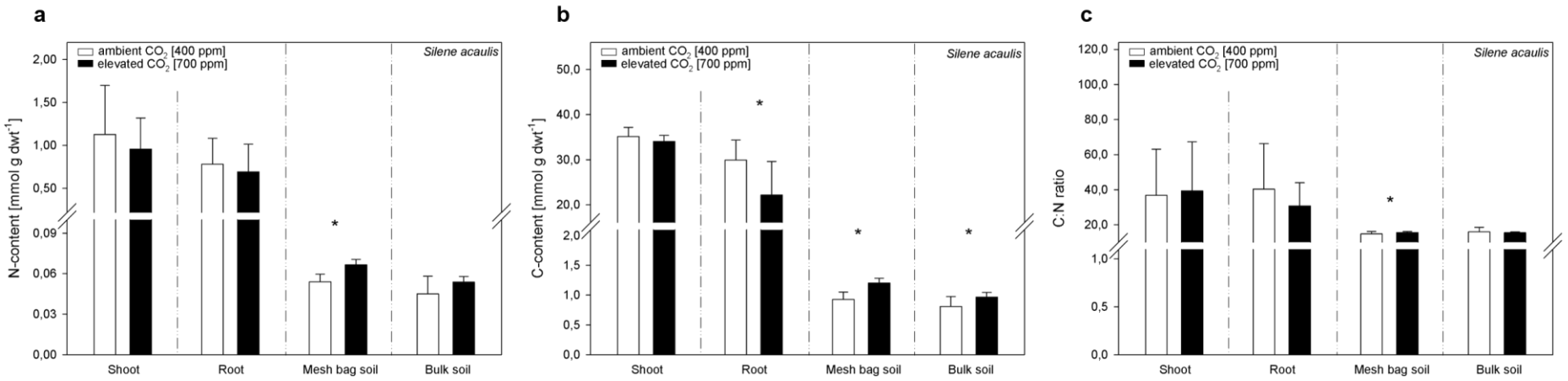

*Fig. S5: N-content [mmol g dwt^{-1}] (a), C- content [mmol g dwt^{-1}] (b) and C:N ratio (c) of Silene acaulis shoots, roots, mesh bag soil and bulk soil. Significant differences between the ambient CO_2 treatment (white) and the elevated CO_2 treatment (black) are indicated by an asteriks *.*

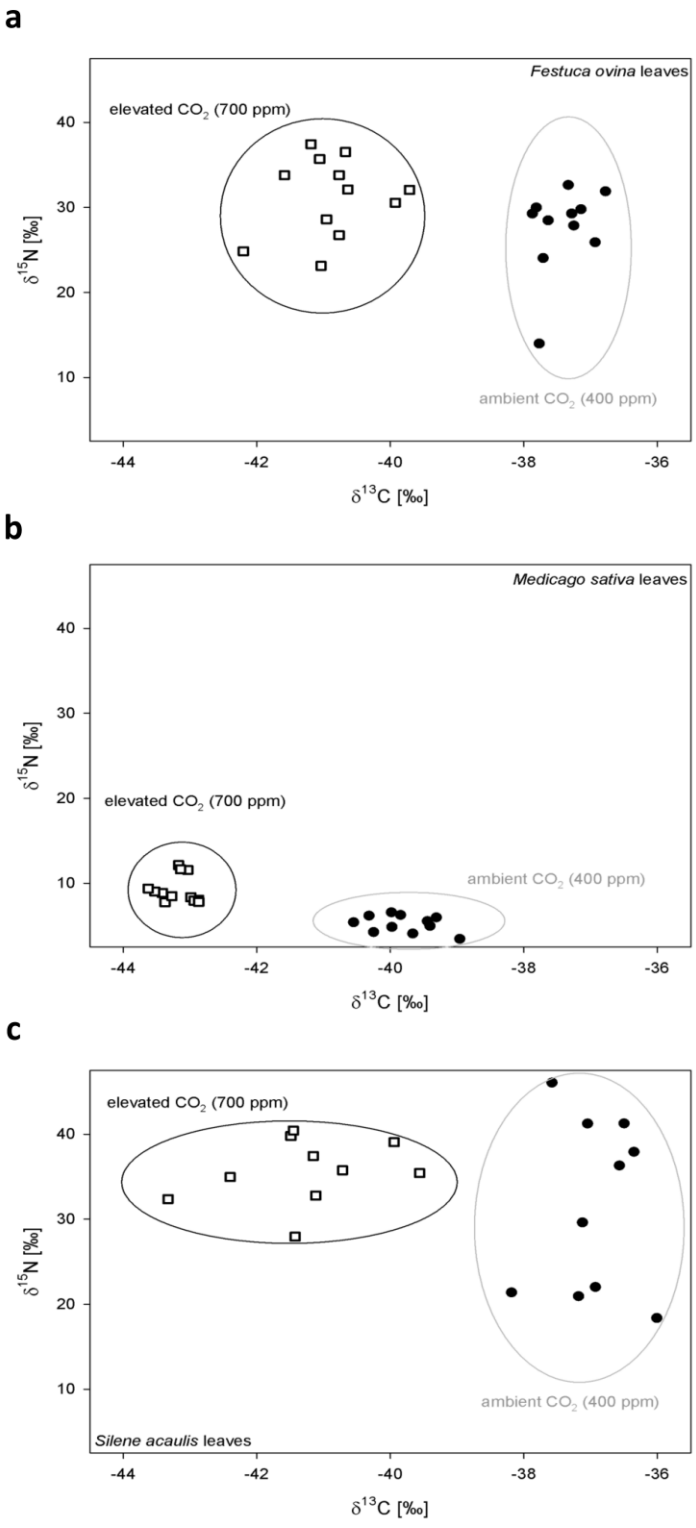

Fig. S6: Dual isotope scatter plot of stable isotope patterns of ^{13}C and ^{15}N for leaves of Festuca ovina (a), Medicago sativa (b) and Silene acaulis (c), respectively. Closed circles indicate leaves grown under ambient CO_2 treatment; open squares indicate leaves grown under elevated CO_2 treatment.

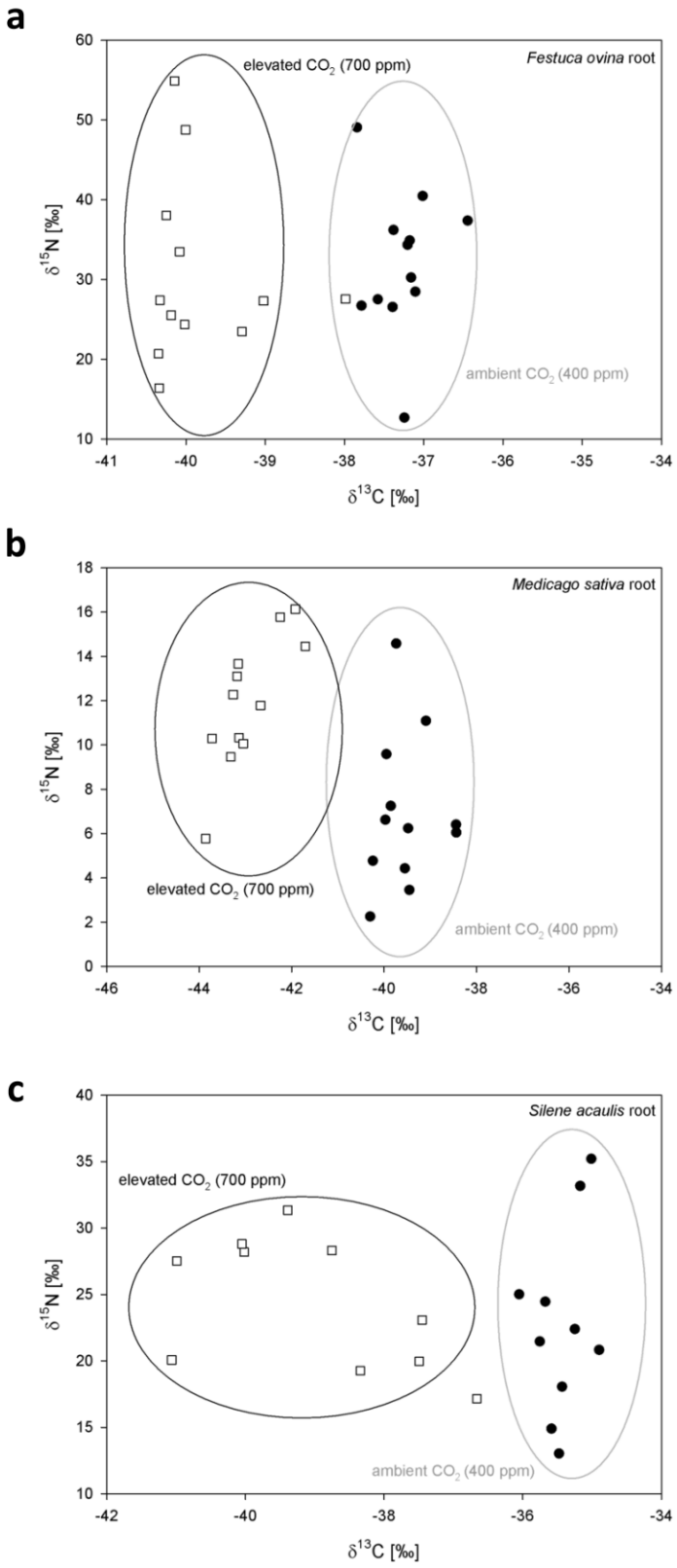

Fig. S7: Dual isotope scatter plot of stable isotope patterns of ^{13}C and ^{15}N for roots of Festuca ovina (a), Medicago sativa (b) and Silene acaulis (c), respectively. Closed circles indicate leaves grown under ambient CO_2 treatment; open squares indicate leaves grown under elevated CO_2 treatment.

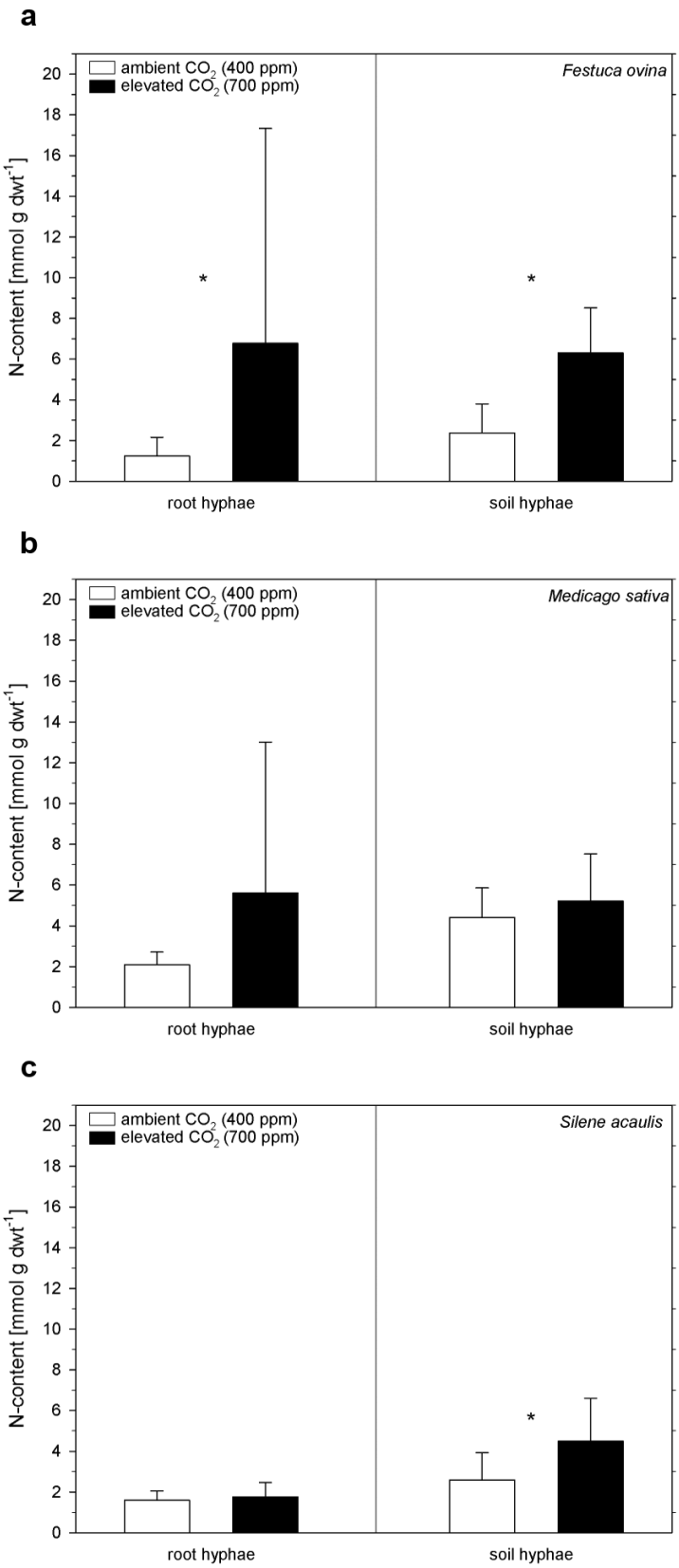

*Fig. S8: N-content [mmol g dwt^{-1}] of root and soil hyphae of Festuca ovina (a), Medicago sativa (b) and Silene acaulis (c), respectively. Significant differences between ambient CO_2 (white) and elevated CO_2 (black) treatments are indicated by an asterisk *.*

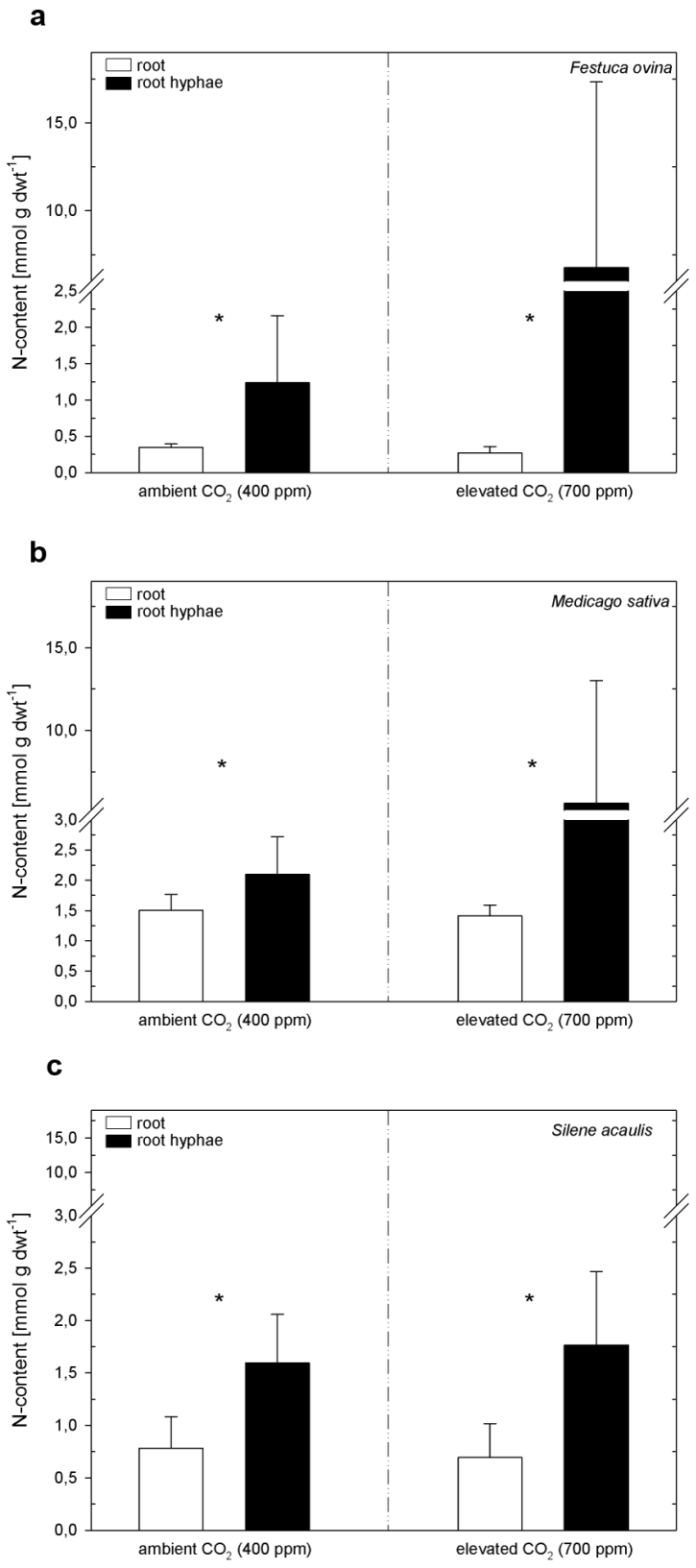

*Fig. S9: N-content [mmol g dwt^{-1}] of roots and root hyphae of Festuca ovina (a), Medicago sativa (b) and Silene acaulis (c), respectively. Significant differences between the ambient CO_2 (white) and the elevated CO_2 (black) treatment are indicated by an asterisk **

10 Declaration

(Eidesstattliche) Versicherungen und Erklärung

(§ 8 Satz 2 Nr. 3 PromO Fakultät)

Hiermit versichere ich eidesstattlich, dass ich die Arbeit selbstständig verfasst und keine anderen als die von mir angegebenen Quellen und Hilfsmittel benutzt habe (vgl. Art. 64 Abs. 1 Satz 6 BayHSchG).

(§ 8 Satz 2 Nr. 3 PromO Fakultät)

Hiermit erkläre ich, dass ich die Dissertation nicht bereits zur Erlangung eines akademischen Grades eingereicht habe und dass ich nicht bereits diese oder eine gleichartige Doktorprüfung endgültig nicht bestanden habe.

(§ 8 Satz 2 Nr. 4 PromO Fakultät)

Hiermit erkläre ich, dass ich Hilfe von gewerblichen Promotionsberatern bzw. –vermittlern oder ähnlichen Dienstleistern weder bisher in Anspruch genommen habe noch künftig in Anspruch nehmen werde.

(§ 8 Satz 2 Nr. 7 PromO Fakultät)

Hiermit erkläre ich mein Einverständnis, dass die elektronische Fassung der Dissertation unter Wahrung meiner Urheberrechte und des Datenschutzes einer gesonderten Überprüfung unterzogen werden kann.

(§ 8 Satz 2 Nr. 8 PromO Fakultät)

Hiermit erkläre ich mein Einverständnis, dass bei Verdacht wissenschaftlichen Fehlverhaltens Ermittlungen durch universitätsinterne Organe der wissenschaftlichen Selbstkontrolle stattfinden können.

Essen,

Ort, Datum, Unterschrift